



HAL
open science

Towards the Elucidation of Orphan Lysosomal Transporters

Quentin Verdon

► **To cite this version:**

Quentin Verdon. Towards the Elucidation of Orphan Lysosomal Transporters. Cancer. Université Paris Saclay (COMUE), 2016. English. NNT : 2016SACLS144 . tel-01827233

HAL Id: tel-01827233

<https://theses.hal.science/tel-01827233>

Submitted on 2 Jul 2018

HAL is a multi-disciplinary open access archive for the deposit and dissemination of scientific research documents, whether they are published or not. The documents may come from teaching and research institutions in France or abroad, or from public or private research centers.

L'archive ouverte pluridisciplinaire **HAL**, est destinée au dépôt et à la diffusion de documents scientifiques de niveau recherche, publiés ou non, émanant des établissements d'enseignement et de recherche français ou étrangers, des laboratoires publics ou privés.

NNT : 2016SACLS144

THESE DE DOCTORAT
DE
L'UNIVERSITE PARIS-SACLAY
PREPAREE A
L'UNIVERSITE PARIS-SUD

ECOLE DOCTORALE N°568
BIOSIGNE | Signalisations et réseaux intégratifs en biologie
Spécialité de doctorat : aspects moléculaires et cellulaires de la
biologie

Par

Mr Quentin Verdon

Towards the elucidation of orphan lysosomal transporters:
several shots on target and one goal

Thèse présentée et soutenue à Paris le 29/06/2016 » :

Composition du Jury :

Mr Le Maire Marc	Professeur, Université Paris-Sud	Président
Mr Birman Serge	Directeur de recherche, CNRS	Rapporteur
Mr Murray James	Assistant professor, Trinity college Dublin	Rapporteur
Mr Goud Bruno	Directeur de recherche, CNRS	Examineur
Mr Gasnier Bruno	Directeur de recherche, CNRS	Directeur de thèse
Mme Sagné Corinne	Chargée de recherche, INSERM	Co-directeur de thèse

Table of contents

Remerciements (acknowledgements)	6
Abbreviations	7
Abstracts	10
Introduction	12
1 Physiology of lysosomes	12
1.1 Discovery and generalities	12
1.2 Degradative function	13
1.3. Integral membrane proteins of lysosomes	14
1.4. Biogenesis of lysosomes	17
1.4.1. Formation of the compartment	17
1.4.2. Sorting and activation of lysosomal enzymes	19
1.4.3. Sorting of lysosomal membrane proteins.	20
1.5. Entry of macromolecules into lysosomes	21
1.5.1 Autophagies	21
1.5.2. Endocytosis and phagocytosis	23
1.5.3. Transport through the lysosomal membrane	24
1.6. Lysosomes and signaling pathways	24
2. Dysfunction of lysosomes: the lysosomal storage disorders (LSDs)	27
2.1. Generalities on LSDs	27
2.1.1 Types of LSDs	27
2.1.2. Treatments	28
2.2. LSDs due to a defective lysosomal membrane protein	29
2.2.1. Defect in ion transport	29
2.2.2. Defect in cholesterol trafficking	30
2.2.3. Defect in an enzyme/transporter	31
2.2.4. Defect in LAMP2	31
2.2.5. Defect in transport of catabolites	31
Chapter 1: functional study of putative lysosomal transporters	34
1. Introduction	34
2. How to screen for new lysosomal transporters	54

2.1. Step 1: is the candidate lysosomal?	54
2.2. Step 2: is it possible to express the candidate at plasma membrane?	55
2.3. Step 3: functional assays	56
2.4 Summary of the screening method	59
3. Study of five proteins of the lysosomal membrane: TMEM104, SLC37A2, TTYH3, MFSD1 and SPINSTER1	59
3.1. TTYH3, a chloride channel	59
3.1.1. Introduction	59
3.1.2. Screening of the putative lysosomal sorting motif	60
3.2. TMEM104, a putative amino acid transporter	60
3.2.1. Introduction	60
3.2.2. Screening of the putative lysosomal sorting motif	61
3.3. SLC37A2, a putative glucose-6-phosphate transporter?	62
3.3.1. Introduction and sorting motif	62
a- Former results on SLC37A2	62
b- A natural variant of SLC37A2 is sorted to lysosomes	63
3.3.2. Functional assays	64
3.3.3 Phosphoglycerate lysosomal transporters: a gap in the catabolism of lipids	66
3.4. hSPINSTER1, a putative transceptor	67
3.4.1 Introduction	67
3.4.2 Screening of the putative lysosomal sorting motif	69
3.5. MFSD1, a protein belonging to the major facilitator superfamily	72
3.5.1 Introduction	72
3.5.2. Topology issue and screening of the putative lysosomal motif	72
3.5.3 Functional assays on MFSD1	73
4. Conclusion	75
Chapter 2: study of two lysosomal membrane proteins implicated in neurodegenerative disorders: CLN3 and CLN7	77
1. Introduction	77
1.1 On neuronal ceroid lipofuscinosis	77
1.1.1 Generalities	77

1.1.2 Pattern of neurodegeneration in brain	78
1.1.3 Genetic determinants of NCLs	78
1.1.4 Therapies	79
1.2 CLN3	81
1.3 CLN7	82
2. Functional characterization of CLN7 by TEVC	83
2.1 Expression of human CLN7 at plasma membrane in <i>Xenopus</i> oocytes	83
2.2 Functional study of CLN7 using TEVC	85
3. Lysosomal proteolysis is impacted by CLN3 malfunction	89
3.1 Metabolomics of <i>Cln3</i> KI mice	89
3.2 Evaluation of proteolysis in neurons of CLN3 KI mice	94
3.3 Measure of long-lived protein degradation in CLN3 WT and KI primary fibroblasts	97
3.4 Rescue of lysosomal proteolysis by CLN3 overexpression	100
4. Conclusion	103
4.1 Other approaches to identify CLN7 substrate	103
4.1.1 Widening the electrophysiological screen	103
4.1.2 Checking for a non-electrogenic transport of amino acids	103
4.1.3 Enriching oocytes in CLN7 substrate	103
4.1.4 Metabolomic profiling of CLN7 KO mice	104
4.2 Relevance of the lack of lysosomal proteolysis in the context of CLN3 deficiency	104
4.2.1 Checking the selectivity of the proteolysis defect	105
4.2.2 A need for a better model to study CLN3 dysfunction	106
4.2.3 Generalization to other NCLs	107
4.2.4 Increasing lysosomal proteolysis: a potential therapeutic target	108
Chapter 3: Identification of SNAT7 as a lysosomal glutamine transporter essential to the opportunistic nutrition of cancer cells	109
1. Introduction	109
1.1 The SLC38 family	109
1.2 About SNAT7	112
1.2.1. Results from Hägglung et al	112
1.2.2. SNAT7 could still be a lysosomal transporter	112

2. SNAT7 is a lysosomal transporter for glutamine and asparagine	113
2.1 Radioactive uptake in <i>Xenopus</i> oocytes	113
2.2. Sorting of SNAT7	116
2.3 Sending SNAT7 to plasma membrane by activating lysosomal exocytosis	119
2.4 Confirming SNAT7 function as lysosomal transporter for glutamine by developing an indirect assay	122
2.4.1 Principle of the test	122
2.4.2 Quantification method and determination of the optimal ester concentration	123
2.4.3 Proof of principle	125
2.4.4 Application to SNAT7	126
2.4.5 Localization of endogenous SNAT7	127
2.4.6 Direct transport assay	131
2.4.7. Control experiment: are lysosomes from SNAT7 KO cells more fragile?	134
2.4.8 Further characterization of SNAT7 activity	135
3. Does SNAT7 play a role in the nutrition of cancer cells?	140
3.1 Glutamine and cancer cells	140
3.2 SNAT7 is necessary for cancer cells to obtain glutamine from extracellular proteins	142
3.2.1 BSA can be used as a source of glutamine	142
3.2.2. SNAT7 is critical to use BSA as a source of glutamine	143
3.2.3 Control experiment: is BSA degraded properly in SNAT7 deficient cells?	147
4. Conclusion	148
4.1. Function of SNAT7 as a lysosomal transporter for glutamine and asparagine	148
4.2. Role of SNAT7 in cancer cell nutrition	149
4.2.1 Role of SNAT7 in in vivo cancer models	149
4.2.2 Relevance of macropinocytosis in the nutrition of cancer cells	149
4.2.3 Advantages and development of a SNAT7-based anti-cancer therapy	150
4.3 Importance of SNAT7 in other mechanisms	151
Conclusion: emerging roles for lysosomal membrane proteins	153
Material and methods	157

DNA and RNA constructs	157
Antibodies	158
Expression of proteins in <i>Xenopus</i> oocytes	158
Uptake of glutamine in oocytes	159
Cell-surface biotinylation	159
Electrophysiological recordings	160
Cell culture and transfection	160
Western Blot	161
Immunofluorescence	161
TFEB test	162
CRISPR-Cas9	163
Sialic acid uptake	163
Mice models	163
Preparation of hippocampal neurons	163
DQ-red-BSA uptake	163
Flow cytometry	164
Lysosomal proteolysis measures in primary fibroblasts	165
Cellular fractionation	165
Transport assay on lysosomal preparations	165
Latency test	166
Growth assays	166
References	167

Remerciements

Je souhaite remercier Bruno Gasnier et Corinne Sagné pour m'avoir accueilli dans leur équipe et m'avoir confié ces projets. Je me sens exceptionnellement privilégié d'avoir pu compter en toutes circonstances sur deux encadrants aussi brillants que disponibles.

Je souhaite remercier particulièrement Cécile Jouffret et Christopher Ribes, qui ont participé avec beaucoup d'entrain et de disponibilité à la plupart des expériences décrites dans cette thèse. Mes plus vifs remerciements aux autres membres de l'équipe : Xavier Leray, Christine Anne et Seana O'Regan pour leur soutien, leur écoute, leur patience, mais aussi pour leurs dons désintéressés de calories et de caféine, sous des formes diverses.

Je souhaite également remercier les autres membres du laboratoire : Isabelle Fanget, Claire Desnos, Damien Carrel, Dany Khamsing et Solène Lebrun pour tous les bons moments passés ensemble.

Je remercie également particulièrement François Darchen et Valentina Emiliani, les deux directeurs successifs du laboratoire, pour m'avoir accueilli en thèse.

Je souhaite exprimer ma gratitude à l'Ecole Normale Supérieure et à Vaincre les maladies lysosomales qui ont successivement financé ma bourse de thèse, ainsi qu'à la Ligue contre le cancer qui a par ailleurs financé l'un de mes projets.

Je remercie également Marielle Boonen, Michel Jadot, Agnès Journet et Jérôme Garin pour des collaborations fructueuses. Je souhaite également remercier et recommander la plate-forme de cytométrie du site des Saints-Pères de l'université Paris-Descartes et remercier plus particulièrement Stéphane Dupuy, mon interlocutrice sur place, pour ses précieux conseils. Je remercie également la plate-forme LIMP, de l'UPMC, et sa responsable, Aurélie Prignon, pour l'aide apportée à nos expériences. Je remercie également le personnel de l'animalerie centrale des Saints-Pères pour les soins apportés à nos animaux.

Abbreviations

AP	adaptor protein
Atg	autophagy related
ATP	adenosine tri-phosphate
BSA	bovine serum albumine
CGN	cis-Golgi network
CLC	chloride voltage-gated channel
CMA	chaperone-mediated autophagy
CRISPR	cluster regularly interspaced palindromic repeats
CSPα	cysteine string protein alpha
CTS	cathepsin
DMEM	Dulbecco's Modified Eagle Medium
DNA	desoxyribonucleic acid
dsiRNA	double-strand small interfering RNA
EAAT	excitatory amino acid transporter
EGFP	enhanced green fluorescent protein
ENT	equilibrative nucleoside transporter
ER	endoplasmic reticulum
FCCP	Carbonyl cyanide-4-(trifluoromethoxy)phenylhydrazone
GABA	gamma aminobutyric acid
Gb3	globotriaosylceramide
GGA	Golgi-localized, gamma-ear-containing, Arf-binding protein
HGSNAT	Heparan-alpha-glucosamine N-acetyltransferase
HPLC	high performance liquid chromatography
HRS	hepatocyte growth factor regulated tyrosine kinase substrate
Hsp70	heat shock protein 70

ISSD	infantile sialic acid storage disease
KI	knock-in
KO	knock-out
LAMP	lysosomal associated membrane protein
LC3	light chain 3
LDL	low-density lipoprotein
LIMP	lysosomal integral membrane protein
LMBRD	LMBR1 domain containing
LSD	lysosomal storage disorder
LYAAT	lysosomal amino acid transporter
MAP	microtubule-associated protein
MAPK	mitogen-activated protein kinase
MEF	mouse embryonic fibroblast
MES	2-(N-morpholino)-ethanesulfonic acid
MFSD	major facilitator superfamily domain-containing
MOPS	3-(N-morpholino)-propanesulfonic acid
MPR	mannose-6-phosphate receptor
mTORC	mammalian target of rapamycin
NCL	neuronal ceroid lipofuscinosis
NMDA	N-methyl-D-aspartate
NPC	Niemann-Peak disease type C
OSTM	osteopetrosis associated transmembrane protein
PACS-1	phosphofurin acidic cluster sorting protein
PBS	phosphate-buffered saline
pH	hydrogen potential
Pi(3,5)P2	phosphatidyl-inositol-(3,5)-diphosphate
PPT	palmitoyl-protein thioesterase

PQLC	PQ-loop repeat containing
Ras	rat sarcoma
RFP	red fluorescent protein
Rheb	Rab homolog enriched in brain
RNA	ribonucleic acid
SDS	sodium dodecyl sulfate
SLC	solute carrier
SNAT	system N and A transporter
SNARE	soluble N-ethylmaleimide-sensitive-factor attachment protein receptor
TEVC	two-electrode voltage-clamp
TFE3	transcription factor binding to IGMH enhancer 3
TFEB	transcription factor EB
TFEB-AAE	TFEB amino acid ester (assay)
TGF	transforming growth factor
TGN	trans-Golgi network
TMEM	transmembrane protein
TNF-α	tumor necrosis factor alpha
TPC	two-pore channel
TPP	tripeptidyl peptidase
TRPML1	transient receptor potential cation channel, mucolipin orthologs
TTYH	tweety family member
ZNT	Zinc transporter

Abstract

Within lysosomes, about sixty different hydrolases degrade macromolecules. This degradation is dependent on the acidity of the lysosomal lumen, which pH ranges between 4.5 and 5.0. The lysosomal pH is maintained by the v-ATPase, a proton pump. Lysosomal degradation generates catabolites, which can be recycled to the cytosol by secondary active transporters: lysosomal transporters.

The dysfunction of lysosomal proteins leads to lysosomal storage disorders (LSDs), rare inherited metabolic diseases characterised by accumulation of material inside lysosomes. Depending on the mutated gene, symptoms of LSDs vary greatly, although about half of LSD patients display some kind of neurodegenerative symptoms. Studying the physiopathology of LSDs has led to a good understanding of the function of lysosomal enzymes, but the knowledge of lysosomal transporters remain poor, since only a few LSDs have been shown to be linked with a mutation in a lysosomal transporter gene.

I focused on two proteins whose dysfunction causes a special type of LSDs: CLN3 and CLN7. Mutations in *CLN3* and *CLN7* cause neuronal ceroid lipofuscinoses (NCLs), a special type of LSD which has mostly neurodegenerative symptoms and which is characterized by the accumulation of a specific pigment inside lysosomes: lipofuscin. There are fourteen NCL genes, but CLN3 and CLN7 are the two only proteins of the family which are resident proteins of the lysosomal membrane, suggesting they might be transporters.

Amino acids were screened as possible substrates for CLN7, but none could be shown to be transported. For CLN3, the content in metabolites of lysosomes from *Cln3*-deficient mice and from WT mice were compared by mass spectrometry, revealing a specific decrease in the amount of catabolites of proteins in lysosomes from *Cln3*-deficient mice. This suggested a lack of lysosomal proteolysis, which was checked in neurons, in primary fibroblasts and in immortalized fibroblasts. These results suggested that CLN proteins could take part to a metabolic pathway important for lysosomal proteolysis and, more generally, for neuronal health. These results could help improve the understanding of the early steps of NCL physiopathology.

To extend the number of candidates for lysosomal transporters, I took part to the validation step of an extensive proteomic study of the lysosomal membrane, which revealed forty-six new candidates for lysosomal transporters. I studied in more details TMEM104, SPINSTER, MFSD1, SLC37A2, TTYH3 and SNAT7. Proteins were overexpressed in HeLa cells to check for lysosomal localization. Then, their putative sorting motifs were mutated to misroute their expression to plasma membrane and to enable their functional study. No function could elucidate for the first five candidates.

SNAT7 could not be misrouted to plasma membrane, but, since it belonged to a family of transporters for glutamine, its function was studied by an indirect assay based on an artificial lysosomal overload in amino acids and a direct transport measure on lysosome-enriched cellular fractions, using radiolabelled substrates. Thus, SNAT7 was shown to be a lysosomal transporter selective for glutamine and asparagine.

The function of SNAT7 in the nutrition of cancer cells was then studied. Many cancer cells use glutamine as their main source of carbon, nitrogen and energy. Because of insufficient blood supply, they use macropinocytosis to uptake extracellular proteins, which degradation in lysosomes generates glutamine. Then, glutamine is recycled to the cytosol. SNAT7 was shown to be critical in this process: in glutamine-dependent cancer cells, when *SNAT7* expression is reduced, cells cannot obtain glutamine from extracellular proteins. Thus, blocking SNAT7 is a promising approach to target specifically the metabolism of cancer cells.

Résumé

Les lysosomes contiennent environ soixante hydrolases différentes, qui peuvent dégrader une grande variété de macromolécules. L'activité de ces enzymes est dépendante du pH, maintenu dans les lysosomes entre 4.5 et 5.0 par une pompe à protons : la v-ATPase. Les produits de dégradation sont recyclés dans le cytoplasme par des transporteurs actifs secondaires de la membrane des lysosomes.

Les maladies de surcharges lysosomales sont causées par des mutations de gènes codant pour des protéines lysosomales, souvent des enzymes. Elles sont caractérisées par un engorgement des lysosomes avec des agrégats ou des cristaux. Les symptômes associés à ces maladies sont variés, mais la moitié d'entre elles induisent des défauts neurologiques. L'étude de ces maladies a permis d'élucider la fonction de nombreuses enzymes, mais la connaissance des transporteurs lysosomaux reste parcellaire. Peu de ces transporteurs sont ainsi caractérisés au niveau moléculaire.

Je me suis intéressé à deux gènes dont la mutation provoque une maladie de surcharge particulière : *CLN3* et *CLN7*. Leur mutation provoque des céroïdes lipofuscinoses neuronales, des maladies de surcharge lysosomales caractérisées par une neurodégénérescence précoce et par l'accumulation dans les lysosomes d'un pigment autofluorescent, la lipofuscine. La mutation de 14 gènes différents cause une céroïde lipofuscinose neuronale. J'ai étudié *CLN3* et *CLN7* car ils codaient pour des protéines membranaires du lysosome, qui pourraient donc être des transporteurs.

Sur *CLN7*, j'ai effectué des tests de transport en utilisant les acides aminés comme substrats potentiels, sans résultats probants. Concernant *CLN3*, le contenu métabolique de lysosomes a été étudié par spectrométrie de masse dans des souris WT ou de souris où le gène *CLN3* était déficient. Les lysosomes des cellules déficientes contenaient moins de produits de la protéolyse, ce qui suggérerait que *CLN3* était important pour la protéolyse lysosomale. Cela a été confirmé par des mesures plus directes sur des neurones et des fibroblastes primaires, et sur des fibroblastes immortalisés. Ces résultats pourraient aider à comprendre les premières étapes de la physiopathologie dans les cellules où des gènes *CLN* sont déficients.

Pour accroître le nombre de transporteurs lysosomaux potentiels, j'ai participé à la finalisation d'une étude par protéomique de la membrane lysosomale. Elle a révélé 46 transporteurs potentiels de fonction encore inconnue. Dans cette liste, j'ai étudié *TMEM104*, *SPINSTER*, *MFSD1*, *SLC37A2*, *TTYH3* et *SNAT7*. Pour ce faire, j'ai d'abord muté les motifs d'adressage de ces protéines pour les rediriger, lors de leur synthèse, vers la membrane plasmique, afin de faciliter leur étude. Aucune fonction claire n'a pu être identifiée par cette approche.

SNAT7 appartenait cependant à une famille de transporteurs de glutamine, ce qui était suffisamment encourageant pour envisager d'autres approches. Sa fonction a ainsi été étudiée en développant un nouveau test indirect basé sur la détection d'une surcharge artificielle des lysosomes en acides aminés. Un test fonctionnel plus direct a ensuite été mis au point sur des fractions enrichies en lysosomes en utilisant des acides aminés radiomarqués. Ces deux tests ont montré que *SNAT7* était un transporteur spécifique de l'asparagine et de la glutamine.

J'ai enfin étudié l'hypothèse suggérant que *SNAT7* pourrait jouer dans la nutrition de cellules cancéreuses. En effet, certaines utilisent la glutamine comme nutriment principal à la place du glucose ; mais les apports sanguins en glutamine, dans les tumeurs, sont parfois insuffisants. La glutamine est donc obtenue par macropinocytose de protéines extracellulaires et dégradation lysosomale de ces protéines, avant un recyclage vers le cytoplasme. J'ai montré qu'en l'absence de *SNAT7*, ce phénomène était bloqué. *SNAT7* est donc une cible thérapeutique intéressante pour tenter de bloquer l'approvisionnement des cellules cancéreuses en glutamine.

Introduction

1. Physiology of lysosomes

1.1. Discovery and generalities

At the end of the 1940s, cellular fractionations had developed extensively owing to the invention of analytical and preparative ultracentrifuges along with tissue homogenizers. Organelles could thus be separated and followed by activity tests on marker enzymes. A popular animal tissue for such studies was rat liver. Authors could mainly discriminate between three fractions: a heavy nuclear fraction, an average mitochondrial fraction and a light microsomal fraction, corresponding to both ER and plasma-membrane-derived vesicles.

However, it was pointed out in 1951 ¹ that one enzyme, acid phosphatase, had an ambiguous distribution between microsomal and mitochondrial fractions. Appelmans, Wattiaux and de Duve ² adapted available fractionation protocol to discover that acid phosphatase was in fact mostly contained in a new compartment described as “a special class of granules, very few in proportion, entirely distinct from microsomes and comparable in size to small mitochondria” which ended up to be lysosomes.

Lysosomes are membrane-bound compartments that are present in almost all animal cell type, except for red blood cells. They are characterized by the presence within their lumen of active hydrolases. They typically account for about 5% of the whole cellular volume ³ (see Fig 1).

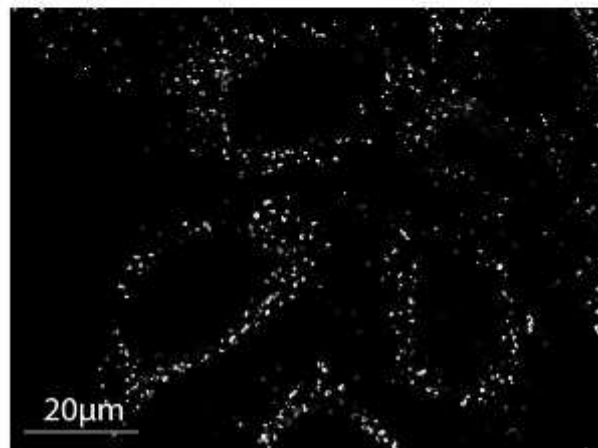
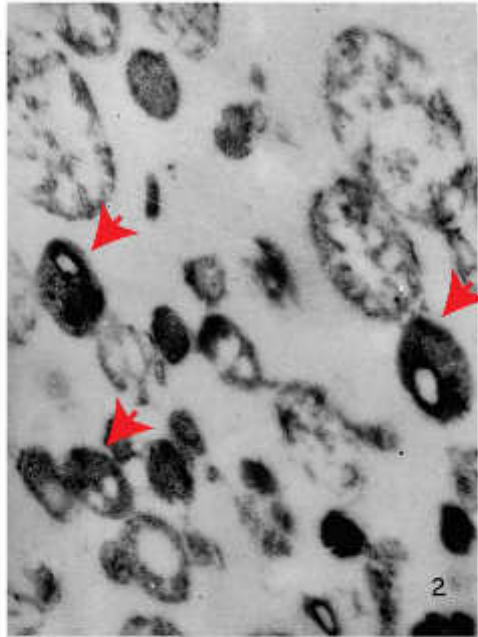


Fig 1: Visualization of lysosomes

Upper panel: first picture of lysosomes (red arrows) using electron microscopy on lysosome-enriched fractions from rat liver according to de Duve's team's protocol. In this paper, they were called "dense bodies" and were only hypothesized to be lysosomes (adapted from ⁴).

Lower panel: HeLa cells were fixed. LAMP-1, a resident protein of the lysosomal membrane, was revealed by immunofluorescence (picture taken in my host laboratory).

1.2. Degradative function

Lysosomes are the main compartment for the degradation of macromolecules, aside from the proteasome which degrades cytosolic short-lived proteins. They contain enzymes, which are able to hydrolyze most biological macromolecules such as proteins, sugars, nucleic acids or lipids. Many of these enzymes are as well able to remove or transfer phosphate or sulfate groups from proteins. To date, about 60 lysosomal enzymes have been characterized at the molecular level, but proteomic studies suggest there may be more ⁵.

Most lysosomal enzymes are soluble in the matrix of lysosomes, but a few of them are trans-membrane proteins, such as α -glucosamine N-acetyltransferase⁶.

In lysosomes, pH varies between 4.5 and 5. It is maintained by a proton pump, the vacuolar H⁺-ATPase⁷, and by ion channels which balance the charge of the protons to enable continuing proton pumping⁸⁻¹⁰. In addition to increasing the stability of lysosomal enzymes, this pH increases their activity, which generally peaks around pH 5.0¹¹. It has been recently suggested that lysosomal pH could be controlled more tightly than previously expected, thus controlling the activity of lysosomal enzymes¹².

In addition to enzymes, degradation sometimes requires activator proteins, such as saposins (A-D) or GM2 activator protein, activators of the degradation of sphingolipids¹³. These activators bind lipids and enable their solubilization and their interaction with lysosomal lipases.

Products of this degradation include amino acids, sugars, nucleobases, inorganic ions and lipid building blocks, such as glycerol or fatty acids. These products can be used again by cellular anabolic pathways to regenerate functional macromolecules. Some of them may be able to diffuse through the lysosomal membrane, but most of them are exported by membrane transporters. Like lysosomal enzymes, most of these transporters are driven by the proton gradient generated by the v-ATPase through a mechanism coupling the export of the degradation product with the one of luminal protons¹⁴. This coupling mechanism may thus coordinate the degradative and metabolite recycling activities of the lysosome. By keeping catabolites at levels below their cytosolic concentration in the lysosomal lumen, this could also reduce the increase in osmolarity caused by the fast degradation of macromolecules in a small organelle.

1.3. Integral membrane proteins of lysosomes

There are different types of protein within the lysosomal membrane. The most abundant ones are LIMPs and LAMPs, which roles are not clearly understood yet.

LAMPs are heavily glycosylated. Thus, they are believed to take part in coating the lysosomal membrane with a coat of glycans, called the lysosomal glycocalyx. This could play a role in protecting less abundant membrane proteins from lysosomal enzymes¹⁵. LAMP2 has as well been suggested to regulate fusion between lysosomes and autophagosomes and organelle motility¹⁶.

The splicing isoform LAMP2A of LAMP2 is known to form a selective pore for importing proteins into lysosomes for degradative purposes. This pathway is called CMA (chaperone-mediated autophagy, see p21). Although their function is poorly understood overall, LAMP proteins seem critical to the lysosomal function: LAMP-2 deficiency causes Danon disease, a fatal disease characterized by skeletal muscle weakness, cardiomyopathy and, in some cases, retinopathy and mental retardation. At the tissue level, the disease is characterized by accumulation of glycogen-containing autophagic vacuoles in muscles ¹⁷.

The role of LIMP1 is poorly understood as well, but LIMP-2 has been implicated in a sorting mechanism of soluble enzymes to lysosomes (see p20).

Apart from LIMPs and LAMPs, many proteins from the lysosomal membranes are transport proteins, which are separated in two classes: channels and transporters. Channels are proteins containing a hydrophilic pore that can open or close depending on stimuli, but create a full permeation pathway across the membrane in its open state. Permeant molecules are thus translocated according to their concentration gradient (if charged, their electrochemical gradient) at a very fast pace in a diffusive manner. On the lysosomal membrane, mostly ion channels (rather than porins) have been described, such TPC1 and TPC2 (two pore channels), which are selective for Ca^{2+} or Na^+ (debated issue) and activated by the endosomal lipid phosphatidylinositol-(3, 5)-diphosphate (Pi3,5P_2) ¹⁸; TMEM175, a potassium selective channel ¹⁰; or TRPML1, a ion channel selective mostly for divalent cations (calcium, iron, zinc) and also activated by Pi3,5P_2 ¹⁹.

In contrast to channels, transporters undergo cyclic conformational changes to trigger translocation of substrates through a biological membrane. They are thus much slower than channels. Two types of transporters can be distinguished: passive and active transporters. Passive transporters translocate substrates from the most concentrated compartment to the least, thus requiring no additional energy. On the other hand, active transporters can translocate substrates to the more concentrated of the two sides of the membrane (or uphill the electrochemical gradient if the substrate is electrically charged), thus requiring direct or indirect coupling with an energy source. When they are *directly* coupled to a source of chemical energy (ATP, mostly), they are called primary active transporters, or pumps. When they are *indirectly* coupled to a chemical energy source, i.e. when they use a transmembrane gradient established by a primary active transporter, they are called secondary active transporters, or merely 'transporters'. In the latter case, the source of energy used by the transporter is the dissipation of the 'motor ion' gradient (see Fig 2).

Within the lysosomal membranes, mostly two kinds of transporters have been described (see Fig 2). The v-ATPase is the main primary active lysosomal transporter. This pump hydrolyses ATP on its cytosolic side and translocates proton within lysosomes against their concentration gradient, thus creating both a pH gradient and an electric potential gradient between the two sides of the lysosomal membrane.

Next, secondary active lysosomal transporters use the proton gradient to export catabolites from the lysosomal lumen to the cytosol. The first lysosomal transporter, cystinosin, has been identified in a pathological context from patients with cystinosis, a disease in which lysosomes accumulate cystine to high levels, resulting in a renal disease and, at later stages, in multisystemic manifestations. It was shown by biochemical methods that the efflux of cystine was specifically defective in cystinotic patients' cells and that the activity of the v-ATPase was necessary for lysosomal cystine efflux ²⁰.

Other lysosomal transporter activities were biochemically studied on purified lysosomes in the 80s ^{21,22}. However, because these transporters are present on inner membranes, they are much more difficult to study than plasma membrane transporters, thus limiting their functional study and molecular identification.

Almost all small biological molecules can be transported by lysosomal transporters, amino acids or small peptides ^{23,24}, sugars ^{25,26}, ions ^{27,28}, nucleosides ²⁹, according to the variety of hydrolases present in lysosomes. However, there are still many substrates that are known to be transported at the lysosomal membrane but whose transporters are unknown, such as cysteine ³⁰ and many other amino acids, or inorganic phosphate ³¹.

The discovery of genes encoding new lysosomal transporters boomed thanks to the development in my host lab of a technique enabling the expression of lysosomal transporters at the plasma membrane, thus making it possible to apply classical transport assays to lysosomal transporters ^{23,25,32}. This approach will be further detailed below (p55).

The entry point for lysosomal transporter discovery has also recently evolved. Until recently, most lysosomal were identified by the genetic study of diseases. However, an increasing quantity of proteomics data now provides new possible candidates and helps fill the gap of knowledge in this area of cell biology (see p34).

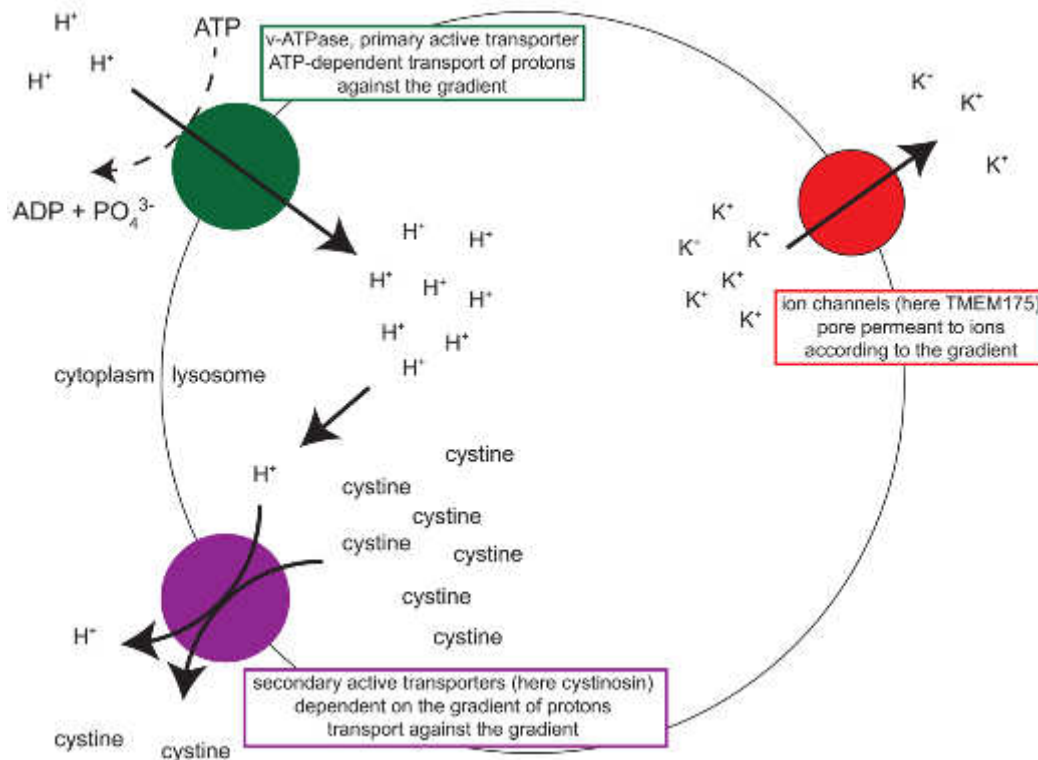


Fig 2: three main kinds of transport proteins at the lysosomal membrane. Channels let inorganic pass through in a very fast, electrodiffusive way (red, TMEM175 channel for potassium). Transporters undergo cyclic conformational changes for each transported molecule. This mechanism, known as the alternate access model, allows transporters of the lysosomal membrane to perform active transport: substrates are transported 'uphill' against their concentration (or electrochemical) gradients. They can be directly driven by ATP hydrolysis, in which case they are called primary active (V-type H⁺-pumping ATPase, green). Alternately, they can indirectly depend on the V-ATPase by using the H⁺ electrochemical gradient across the lysosomal membrane as a source of energy. These transporters are designated as secondary active (for instance, cystinosin, purple).

1.4. Biogenesis of lysosomes

1.4.1. Formation of the compartment

Lysosomes are the terminal compartment of the endocytic pathway. There is constant trafficking of membrane between the plasma membrane, endocytic compartments and the Trans-Golgi network (TGN).

Early endosomes are formed by the invagination of plasma membrane. They can then mature into late endosomes and eventually lysosomes. All these compartments are well identified by subsets of protein markers: Rab 5 for early endosomes; Rab 7 for late ones; presence of late endosome markers combined with an absence of mannose-6-phosphate-receptor for lysosomes. In addition, the luminal pH decreases along the endocytic pathway.

In both intracellular trafficking steps, the maturation process consists in (i) SNARE-dependent fusion with the next compartment (early endosomes fuse with late endosomes; late endosomes with lysosomes), and (ii) input of new material from vesicles secreted by the TGN³³ (see Fig 3). Every time, fusion is followed by (i) condensing of the resulting compartment and (ii) recycling of components from the donor compartment, including v-SNARE proteins.

In addition, lipids can be brought to the lysosomes from low-density lipoproteins, a lipid and glycoprotein small particle that is one of the way lipids are transported through blood. These lipoproteins can be degraded in lysosomes and their lipids released, thus bringing new membranes directly to the lysosomal compartment³⁴

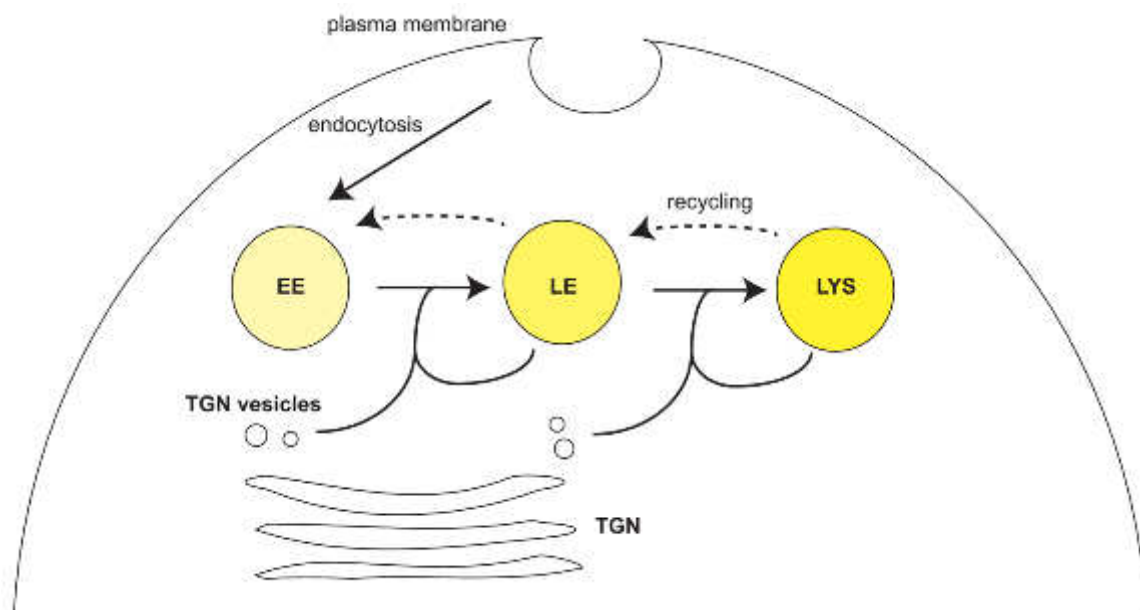


Fig 3: biogenesis of lysosomes.

Lysosomes are formed along the endocytic pathway. Early endosomes (EE) are derived from the internalization of plasma membrane vesicles. They mature into late endosomes (LE) by fusion with already existing LE and vesicles formed by the TGN. Similarly, lysosomes (LYS) are formed from LE by fusion with former lysosomes and TGN vesicles.

1.4.2. Sorting and activation of lysosomal enzymes

Because the biogenesis of lysosomes is complex, the sorting of soluble lysosomal proteins is very specific.

The most common pathway for the sorting of lysosomal enzymes uses a post-translational modification of proteins: a sugar added in the cis-Golgi network (CGN) onto preexisting glycosylations: mannose-6-phosphate. Next, in the trans-Golgi network,

lysosomal enzymes precursors are selected by the membrane-embedded mannose-6-phosphate receptor (MPR). MPR can be recognized thanks to its lysosomal sorting motifs (see next paragraph) exposed on the cytosolic side of the membrane. Recognition of these motifs is responsible for the segregation of mannose-6-phosphate-bearing lysosomal proteins into clathrin-coated vesicles that are targeted to late endosomes³⁵. The MPR is then recycled to the TGN by other vesicles. These trafficking pathways are regulated by membrane-associated complexes³⁶.

Other, less common pathways of lysosomal protein delivery have been described as well. For example, some enzymes, like beta-glucocerebrosidase, can be selected by LIMP-2 in the ER and thereby sorted to lysosomes³⁷. This mechanism is independent of MPR. Mice models deficient in LIMP-2 lack beta-cerebrosidase inside lysosomes. The enzyme is instead secreted, suggesting a lack of selection for sorting in the TGN and showing that the LIMP2 pathway is essential for its lysosomal delivery.

A small fraction of lysosomal enzymes are not selected in the TGN and are eventually secreted. However, a small population of MPRs can as well be found at the plasma membrane, allowing for the internalization of such 'escaping' lysosomal enzymes and delivery to lysosomes via the endocytic pathway. Such a phenomenon can occur between different cells, providing a pathway for intercellular cross-correction of lysosomal enzyme deficiencies. Delivering mannose-6-phosphate-bearing enzymes directly via blood is thus a therapeutic strategy known as enzyme replacement therapy for diverse lysosomal diseases.

^{38,39}

Cells are protected in two ways from unwanted activity of lysosomal enzymes. Firstly, these enzymes have a much better activity at acidic pH. Secondly, most of them are synthesized as inactive precursors. To become active, like extracellular proteases, they must be cleaved to release the propeptide blocking their active site. For instance, pre-pro-cathepsin D is processed by cathepsins B and L⁴⁰

1.4.3. Sorting of lysosomal membrane proteins.

The sorting of lysosomal membrane proteins occurs as well in the TGN, but they can be directly recognized thanks to small sorting motifs present in their amino acid sequence.

Similarly to MPR, these motifs are recognized by cytosolic adaptors and clustered in small trafficking vesicles which are targeted to endosomes.

Because adaptors are cytosolic, these motifs are localized in a cytosolic loop. There are two main types of motifs: tyrosine-based and dileucine-based. Tyrosine-based motifs are of the form: (G)YXXØ, with G being a glycine residue, Y a tyrosine one, X any residue and Ø a bulky hydrophobic one. The first glycine residue is not mandatory for sorting.

Dileucine-based motifs can have two forms: [D or E]XXXLL or DXXLL, in which D is an aspartate residue, E a glutamate, X any residue and L a leucine. The second leucine can be replaced by an isoleucine, more rarely by a valine or a methionine residue. The clustering of acidic residues close to the motifs can as well prove helpful ⁴¹.

Some proteins are however sorted to lysosomes with either no apparent motif or a non-canonical motif (see p 81 and 116).

These diverse motifs can be recognized by different adaptors in different compartments, leading to variable sorting processes. There are two main types of adaptors: APs (heterotetrameric adaptors) or GGAs (monomeric adaptors). These adaptors all trigger the formation of clathrin-coated vesicles that send lysosomal membrane proteins from one compartment to another.

In the TGN, [D/E]XXXLL and YXXØ can be recognized by AP1. AP1 can sort proteins either to early endosomes, late endosomes or sometimes even the plasma membrane. Thus, some proteins are not directly sorted to late endosomes. When they are sorted to plasma membrane, lysosomal membrane proteins can be internalized to early endosomes by AP2 proteins. When in early endosomes, they can be sorted to late endosomes by AP3. In some polarized cells, AP4 can as well recognize YXXØ and send the corresponding proteins from TGN to basolateral membranes. Finally, GGAs specifically recognize DXXLL motifs and select them for sorting to early endosomes.

Other adaptors have been suggested to interact with the clathrin network and potentially be implied in the sorting of lysosomal membrane proteins, for instance HRS in early endosomes or PACS-1 in late endosomes. Thus, the sorting process of lysosomal membrane proteins can vary greatly depending on the protein and on the cell type.

From a more practical point of view, two main types of sorting pathways are generally considered: direct sorting, directly from TGN to endosomes, or indirect sorting, from TGN to plasma membrane and then back to endosomes^{35,41}.

In addition, a recently published paper suggests that the sorting of lysosomal membrane proteins, here ZNT2, a zinc transporter, could be regulated in a breast cancer cell model by TNF- α ⁴². However, the fate of ZNT2 upon treatment with the TNF- α is unclear in this paper, and the cellular model was not very well adapted to localization studies, so these results should be considered with caution.

1.5. Entry of macromolecule cargoes into lysosomes

Cargos destined for degradation reach lysosomes mainly in three different ways: the autophagic pathways; the endocytic and phagocytic pathways; and via transport proteins.

1.5.1 Autophagies

Three types of autophagies can be distinguished: macroautophagy, microautophagy and chaperone-mediated autophagy (CMA) (see Fig 4)

During macroautophagy, a portion of the ER called phagophore engulfs parts of the cytosol, which can contain organelles. This forms an autophagosome, which can then fuse with lysosomes to form an autolysosome. Degradation is then performed by lysosomal enzymes. This mechanism is the main degradative process for old or damaged organelles and for aggregated material.

Autophagy occurs at basal rate under normal conditions but it is upregulated in most cellular responses to stress⁴³. In particular, it plays an important role in the cellular response to amino acid starvation and seems to be the main source of amino acids in this case. This cellular response is controlled by mTORC1 (see p 25 for more details on mTORC1)⁴⁴

Two main cellular complexes regulate macroautophagy. The early control is made by the Atg1 complex, comprising Atg1 itself in addition to Atg13 and several regulating subunits. This complex is necessary to the triggering steps of macroautophagy, which include the lipidation of LC3a into LC3b. This lipidation drives the association of LC3b with autophagic

membranes. LC3b is used as a general marker for autophagy. Then, another complex, associating with LC3b and comprising Atg5 and 7, is necessary for the maturation of the autophagosome and its fusion with lysosomes.

The regulation of autophagy varies depending on the engulfed material. In particular, specific pathways targeted to specific types of organelle have been described, such as “mitophagy”, macroautophagy of mitochondria ⁴⁵.

Microautophagy is a process during which the lysosomal membrane invaginates and engulfs a small portion of the cytoplasm into the lysosomal lumen, enabling its degradation ⁴⁶. Like all autophagic pathway, it is induced under starvation or stress.

Molecular mechanisms of microautophagy are still relatively unclear as compared to those of macroautophagy. It is in particular not clear how substrates are selected. Deformation of the lysosomal membrane is performed by a complex of Atg proteins, which associates with the lipids of the membrane ^{47,48}.

CMA is a very selective process by which proteins are unfolded in the cytosol and selectively imported into lysosomes via a pore⁴⁹. This process is as well upregulated in cases of stress or if other proteolytic pathways are defective ⁵⁰.

Substrates of CMA associate to Hsp70 and other chaperones via a KFERQ motif (lysine, phenylalanine, glutamate, arginine, glutamine), which triggers their unfolding. This complex then associates with LAMP2a at the surface of lysosomes. LAMP2a then forms homotetramers, which form a pore through which selected proteins are imported into lysosomes and degraded.

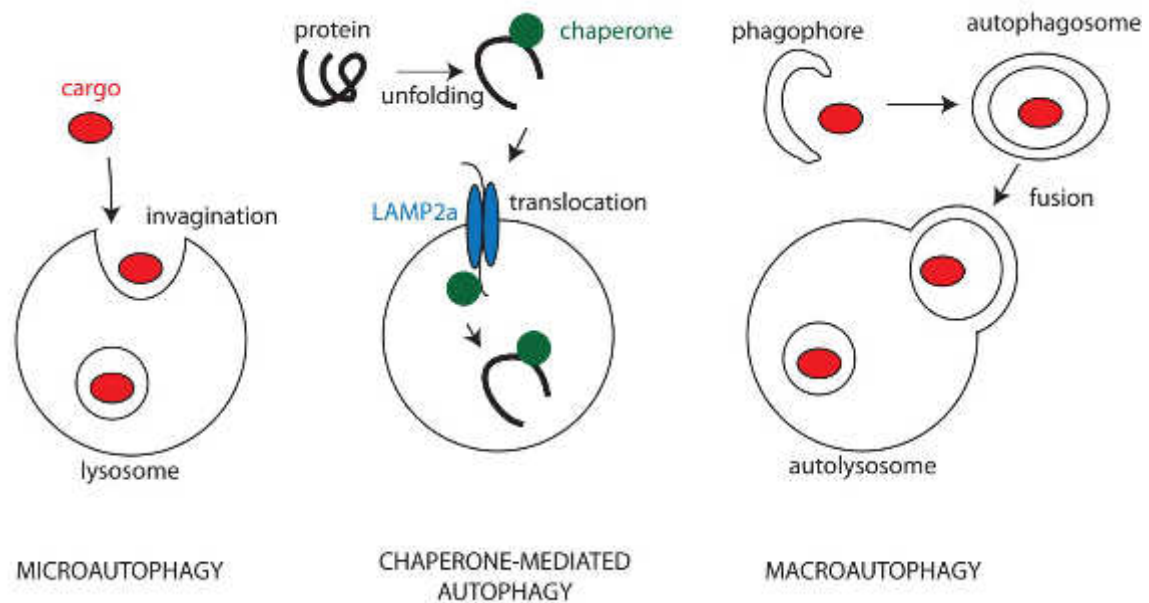


Fig 4: three types of autophagy

Left: microautophagy is characterized by the invagination of the lysosomal membrane. Middle: During CMA, proteins are unfolded in the cytosol and translocated through the lysosomal membrane. Right: During macroautophagy, portions of cytosol are engulfed by an ER-derived double membrane: the phagophore. After closure of the phagophore, an autophagosome is formed. It fuses with lysosome to enable the degradation of cargos.

1.5.2. Endocytosis and phagocytosis

During endocytosis, cargos from the extracellular medium or from the plasma membrane are internalized within vesicles which form the endosomal system. Some cargos then reach lysosomes by fusions of endosomes and lysosomes, in the same way as do lysosomal proteins (see p20). Other material can as well be recycled back via exocytosis. Endocytosis can be selective, but there is also a basal level of constitutive endocytosis which is believed to be less regulated.

Selective endocytosis and lysosomal degradation play a critical role in the control of signaling receptors of the cellular surface. Upon activation, some receptors can be internalized and sorted to lysosomes for degradation, thus avoiding overactivation of their signaling pathway. This is for example the case for tyrosine kinase receptors⁵¹.

In addition, selective endocytosis and lysosomal degradation are very important for the cellular supply in most of the nutrients that are tightly coupled to carrier proteins in blood. For example, vitamin B12 is quite a reactive molecule and a rare micronutrient. Hence, it is always coupled to proteins when transported during digestion or in blood. In blood, when it reaches cells, it is coupled to transcobalamin and cannot be internalized directly into the

cytosol. Transcobalamin is recognized by a specific receptor and endocytosed. Cobalamin is released upon the degradation of transcobalamin in lysosomes. It is then exported from the lysosomal lumen to the cytosol by a lysosomal transporter of discussed identity, where it can be used as an enzymatic cofactor⁵². Similar processes take place for the transport of other nutrients, such as cholesterol and other sterols, which transit through blood coupled to proteins in LDLs (low density lipoproteins).

Phagocytosis only occurs in specialized cells, in particular cells of the immune system. It enables them to internalize in phagosomes big particles, such as bacteria or apoptotic bodies. The formation of phagosomes is highly dependent on vast changes in the actin network of phagocytic cells. Phagosomes then fuse to lysosomes, where cargos can be degraded. Phagocytosis plays a particular role in innate immunity and many pathogens can induce phagocytosis-like mechanisms to trigger their entry in cells⁵³.

1.5.3. Transport through the lysosomal membrane

This process has only been described in very particular cases, as most lysosomal transporters typically catalyze export reactions from lysosomes. Yet, some metabolites have been shown to be able to enter lysosomes, which can act as storage compartments.

Polymannoses have been shown by biochemical approaches to be imported inside lysosomes. This activity is ATP-dependent, of high affinity and saturable, which suggests involvement of an active transporter⁵⁴.

Cysteine is the only amino acid which is imported into, rather than exported from, lysosomes³⁰. The transporter responsible for this import is still unknown and the function of the import of cysteine is not clear either. However, it has been hypothesized that lysosomes could be implied in the regulation of the redox state of the cell, and cysteine, as a thiol, could be important in keeping the lysosomal lumen reductive⁵⁵.

Zinc is as well transported inside lysosomes by ZNT2. Since the excess of zinc is highly toxic, it is believed that lysosomes act here as storage bodies to avoid zinc-induced cell death. In case of high zinc concentrations, lysosomes could even be exocytosed to remove some zinc out of the cell⁵⁶.

1.6. Lysosomes and signaling pathways

Homeostasis in amino acids is mostly controlled by a kinase complex: mTORC1. This kinase integrates signals from growth factor pathways, energy levels and levels of amino acids. This integration takes place at the lysosomal membrane, on which two main regulators are present: the Ragulator, a complex sensing the levels of amino acids and Rheb, which integrates signals from other pathways, such as growth factor signaling. mTORC1 regulates both anabolic and catabolic processes, such as translation of proteins, or, respectively, macroautophagy.

When energy levels or amino acid supplies are low or when there is no growth factor signaling, mTORC1 cannot bind to these regulators at the lysosomal membrane and is inactive, thus slowing down all anabolic processes and activating catabolism. However, when positive signals are present (more ATP, more amino acid, active growth factor pathways), mTORC1 associates to its regulators onto the lysosome and is activated⁵⁷.

Thus, the lysosomal membrane is the main place of control of the cellular metabolism. However, it is not only the support of mTORC1 regulation, but it plays an active role as well in the regulation itself. Lysosomes are indeed able to send signals to the Ragulator complex about the levels of catabolites, amino acids in particular, in the lysosomal lumen (see Fig 5). This takes place through interactions between lysosomal transporters and subunits of the Ragulator. So far, two lysosomal transporters have been described to be able to signal to mTORC1: SLC38A9⁵⁸ and cystinosin⁵⁹.

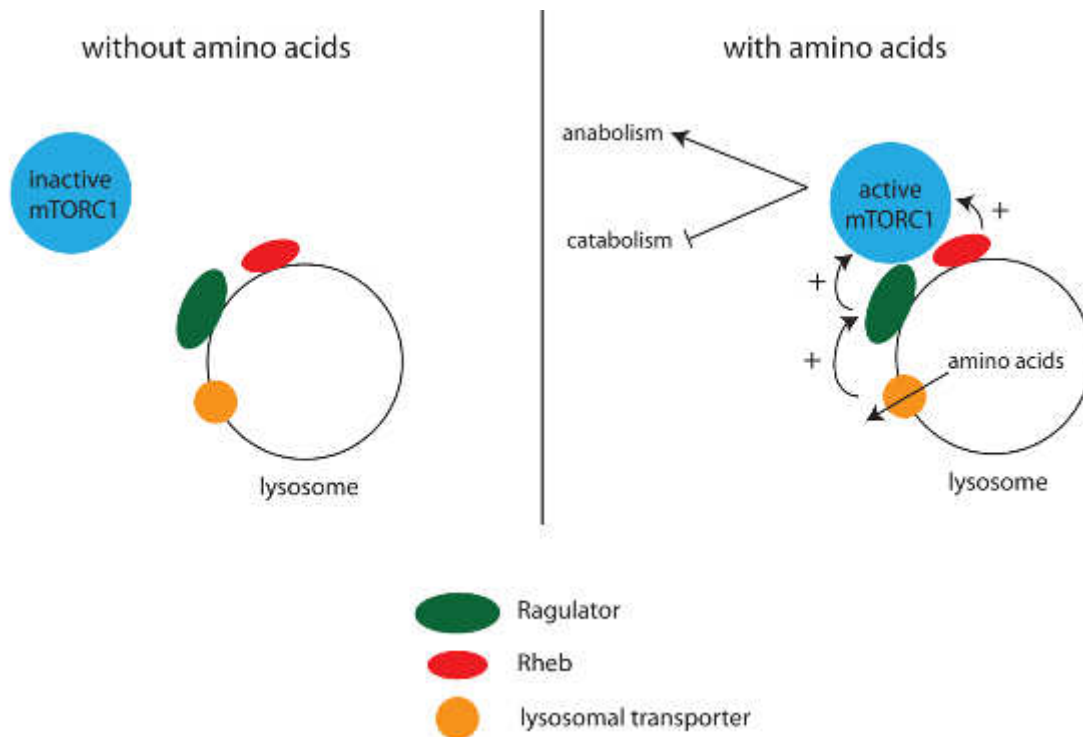


Figure 5: activation on mTOR on the lysosomal membrane. Without amino acids (left), mTORC1 does not bind its regulators on the lysosomal membrane and is inactive. The delivery of proteins to lysosomes activates some lysosomal transporters for amino acid such as SLC38A9 or cystinosin, which activate the Ragulator complex. This complex can now bind mTORC1 and activate it, thus activating anabolism and down-regulating catabolism.

Recently, a retroactive loop has been discovered in this mechanism. Downstream of mTOR lays a transcription factor, TFEB, which selectively controls the transcription of most lysosomal and autophagic genes. It is regulated by mTORC1 by phosphorylation. It is active when mTORC1 is not and vice-versa.

Thus, when amino acid levels are low, mTORC1 is inactive and TFEB active. Upon activation, TFEB is translocated to the nucleus, where it activates the transcription of autophagic and lysosomal genes. This increases lysosomal degradation and eventually replenishes the lysosomal pools of amino acids. TFEB is also activated by lysosomal storage of undegraded cargos, thus creating a feedback loop that adapts the pool of lysosomes to cellular degradative needs ⁶⁰.

Overall, the content in nutrients of lysosomes seems to be one of the most important parameters considered by the cell to adjust its metabolism.

2. Dysfunction of lysosomes: the lysosomal storage disorders (LSDs)

2.1. Generalities on LSDs

2.1.1 Types of LSDs

LSDs are inherited metabolic disorders characterized by the accumulation of material inside lysosomes of cells. The concept of LSDs has been first proposed in the case of Pompe disease, in which a lysosomal enzyme, alpha-glucosidase, is defective, leading to the accumulation of glycogen inside lysosomes. Today, more than 40 LSDs has been described, with subgroups within these different diseases.

LSDs often share common clinical features: fetal edema, spleno- and hepatomegaly, dysfunction of liver, kidney or heart. Most of them present as well neuronal symptoms, such as blindness, mental retardation or dementia. The gravity of LSDs usually correlates with the age of onset: the later the onset, the milder the symptoms. Consequently, infantile forms are usually very severe^{61,62}.

At the cellular level, most LSDs are caused by a mutation making a lysosomal enzyme inactive. Sometimes, the structure of enzymes is perturbed enough to impact on their sorting. In Gaucher disease, for example, all beta-glucocerebrosidase proteins are not well folded and some cannot pass through the ER quality control and are degraded there. However, other cellular defects than primary enzymatic defect have been documented in some LSDs:

- In multiple sulfatases deficiency syndrome, sulfatases are not well processed post-translation, due the defect of an enzyme in the ER, C α -formyl-glycine generating enzyme.
- In mucopolipidosis type 2, the sorting of lysosomal enzymes is affected by the mutation of an enzyme essential to add mannose-6-phosphate groups in the cis-Golgi network.
- In galactosialidosis, the deficiency of cathepsin A, a protease, impairs the activation of other lysosomal enzymes, such as beta-galactosidase.

- Lysosomal membrane proteins can be mutated (see below).

It should be pointed out that some LSDs may still not be well characterized, the vast range of symptoms making diagnosis without genetic analyses difficult. Since LSDs were first proposed as a disease due to the deficiency of an enzyme, this could explain why LSDs due to other problems remain relatively uncommon along with the lesser tractability of non-enzymatic assays.

2.1.2. Treatments

LSDs being genetic disorders, the development of treatment for LSDs is especially challenging. All therapies aim at clearing or reducing the accumulating material inside lysosomes. This can be done in several ways:

- Enzyme replacement therapies. Lysosomal enzymes can be taken up from the extracellular medium to lysosomes by plasma membrane MPRs. Injection or large quantities of enzymes can thus be curative in some LSDs. This has for instance been attempted for Fabry disease⁶³, but, because of their cost, the availability of these treatments is poor. However, since many LSDs show neurological symptoms, blood-brain barrier can prove troublesome for the efficacy of these therapies.
- Reduction of substrate. When the accumulated material is not of a complex chemical nature and is homogenous, its accumulation can be reduced with drugs inhibiting its biosynthesis. This has for example been attempted in Gaucher disease⁶⁴
- Bone marrow transplant. This approach is as well based on the idea that cells are able to take up lysosomal enzymes from the outer medium. The transplantation of bone marrow from a healthy donor can provide a permanent source of functional lysosomal enzymes⁶⁵.
- Supplementation of the lacking metabolite. This case is particular of the cblF cobalamin deficiency, where the pathology is caused by the shortage of cytosolic cobalamin consecutive to its accumulation in lysosomes rather than by a lysosomal storage effect *per se* (see p31 for more details).
- Alternative efflux. In the case of cystinosis, cystine accumulates in lysosomes. Patients are treated with cystagon, a thiol compound that can react with lysosomal cystine and form a disulfide that is able to be exported from lysosomes by another lysosomal transporter, PQLC2. This alternative efflux pathway partially clears lysosomes from the accumulated cystine.

2.2. LSDs due to a defective lysosomal membrane protein

LSDs have provided the base of the knowledge of the biology of lysosomal transporters. Thus, I will focus on LSDs due to the mutation of a lysosomal membrane protein in further details. I will treat the specific case of ceroid neuronal lipofuscinoses in a dedicated introduction in Chapter 2 (see p77)

2.2.1. Defect in ion transport

Two LSDs are due to a dysfunction in ion transport proteins. Mucopolisosis of type four is due to a mutation in *mcoln1*, a gene encoding a lysosomal ion channel: TRPML1. The main symptoms of this disease are anemia, neurological signs and an increase in gastric acid secretion. At the cellular level, the dysfunction of TRPML1 seems to affect the trafficking of lipids. The function of TRPML1 is not clear yet: it has been characterized as a lysosomal channel for divalent cations, but its gating mechanism and its selectivity remain debated⁶⁶. Recently, TRPML1 has been confirmed to play a role in the release of calcium from lysosomes⁶⁷ and in the regulation of autophagy. It had previously been implicated in the regulation of fusion between lysosomes and endosomes, in the regulation of lysosomal pH or in lysosomal iron homeostasis. As a result, the link between these putative molecular functions, the traffic of lipid and the lysosomal defaults are not clear yet.

Osteopetrosis, from greek “stone bone”, can be dominant or recessive. Recessive forms are due to the dysfunction of one of two genes, one encoding CLC7 and one encoding the CLC7 ancillary protein OSTM1. This disease is characterized by very fragile bones, visual and auditory defects, anemia and general neurological symptoms. CLC7 is a proton/chloride antiporter but it requires OSTM1 for its function.

CLC7 function is linked to the v-ATPase. The translocation of protons due to the activity of this pump results in both a concentration gradient and an electric gradient due to the positive charge of protons. CLC7 helps attenuating the electrical component of the proton gradient by exchanging luminal protons against cytosolic chloride, which balance the positive charges accumulated by the v-ATPase. This charge compensation mechanism allows continuing proton pumping into lysosomes, a requirement to substantially lower the luminal pH⁶⁸. CLC7 plays a similar role at the ruffled border membrane of osteoclast to help acidify

the bone resorption lacuna. As a result, it was hypothesized that the defect of CLC7 or OSTM1 would result in a defective lysosomal pH and a defective acidification of the outer medium of osteoclasts. This could be confirmed for osteoclasts ⁶⁹.

However, the comparison between CLC7 knock-out and knock-in mice models suggested that this hypothesis could not explain why CLC7 dysfunction resulted in neuronal death. The knock-in model expressed, instead of WT CLC7, a mutant CLC7 that only transports chloride and no longer protons. In this case, it was expected that CLC7 efficiency would be reduced but not abolished, yet neurodegenerescence was just as strong in this mouse model as in knock-out mice. This suggested that, in the brain, CLC7 plays another role, more important than the regulation of the lysosomal pH ⁷⁰. However, the role of CLC7 in lysosome acidification is still debated ^{8,28}.

2.2.2. Defect in cholesterol trafficking

Type C Niemann-Pick disease is a recessive LSD characterized by neurodegenerescence and hepatosplenomegaly. In patients' cells, cholesterol accumulates inside lysosomes, late endosomes and Golgi network ⁷¹. It can be due to the mutation of two genes encoding NPC1, a membrane protein, and NPC2, a lysosomal soluble protein, which play a role in cholesterol transport across the lysosomal membrane ⁷²⁻⁷⁴.

NPC1 and 2 have been extensively suggested to act together as a cholesterol transporter, although a few authors argue that glycosphingolipids are in fact the first lipids which trafficking would be impacted by a defect of NPC proteins, and that the accumulation of cholesterol is a secondary phenomenon.

2.2.3. Defect in a dual enzyme/transporter protein

Type 3 mucopolysaccharidosis is characterized by the accumulation in lysosomes of heparan sulfate, which mostly causes neurodegenerative symptoms. It is due to the mutation of a gene encoding HGSNAT (heparin acetyl coenzyme A alpha glucosamine N-acetyltransferase).

HGSNAT is a transmembrane enzyme able to use acetyl-co-A from the cytosol to acetylate alpha-glucosamine of heparan sulfate residues inside lysosomes. This enables the

subsequent cleavage of heparan sulfate by another lysosomal enzyme, alpha-N-acetylglucosamidase⁶.

2.2.4. Defect in LAMP2

Danon disease is due to the mutation of *lamp2*, which is X-linked. It is characterized by a hypertrophy of heart, skeletal abnormalities and mental retardation. Danon disease is particularly associated with a mutation in the gene making the production of one splicing variant, LAMP2b, impossible. At the cellular level, it is characterized by the accumulation of autophagic vacuoles within muscle fibers.

LAMP2b seems important for the maturation of autophagosomes, mostly because of a defect in the fusion between autophagosomes and lysosomes. However, most studies on Danon diseases have been performed in immune cells⁴⁴ and its precise molecular function remains unclear.

2.2.5. Defect in membrane transport of catabolites

Several diseases have been linked with a lack of export of catabolites from lysosomes: ISSD (infantile sialic acid storage disease), some histiocytosis, Salla disease, cystinosis and cblF.

Inherited disorder of vitamin B12 F (cblF) is due to the accumulation inside lysosome of vitamin B12, which suggests a defect in the transport of vitamin B12. Lysosome is the main pathway of entry for vitamin B12 into cells. Thus, the symptoms have been linked more to a deficiency in vitamin B12 in the cytosol than to the lysosomal accumulation per se. This vitamin is indeed necessary to the activity of two enzymes implied in the synthesis of fatty acid and methionine and in the methylation and synthesis of nucleobases⁷⁵. As a result, symptoms are similar to those of a deficiency in vitamin B12: serious neurological symptoms and anemia, mostly. This pathology can be treated by a large supplementation in vitamin B12, thus bypassing the defective lysosomal transport systems. In cblF patients, the gene *LMBRD1* is mutated, but it could not be shown to be a lysosomal transporter for vitamin B12⁷⁶. It could however be linked to the function of ABCD4, which mutation seems to cause a similar disease⁷⁷.

ISSD and Salla disease are both due to the mutation of the gene encoding sialin, but ISSD is more severe. Salla disease is a progressive disease caused by a specific hypomorphic mutation (R39C). Both diseases are essentially neurological. In patients, sialic acids accumulate inside lysosomes. Sialin is the secondary active lysosomal transporter for sialic acids. Its activity was characterized in my host laboratory²⁵. The link between the defect of sialin and the pathology is not well established. It is possible that the accumulation of sialic acids perturbs other lysosomal enzymes, thus leading to general lysosomal dysfunctions. Yet, since Salla disease is mostly neurological, it was proposed that the retention of sialic acids inside lysosomes would impact on downstream pathways. Sialic acids are especially important as precursors of myelin in maturing oligodendrocytes. A lack of sialic acid could lead to a defect in myelination of the CNS, thus explaining why symptoms are mostly neurological¹⁶.

Cystinosis is caused by the mutation of a gene encoding cystinosin. There are three different types of cystinosis. The juvenile and infantile forms are multisystemic diseases, but kidneys, eyes and central nervous system are especially impacted. In the adult forms, patients only have mostly ocular lesions. In all patients, cysteine crystals accumulate inside lysosomes. It seems clear that the pathology is not due to the accumulation of cystine itself, but rather to side effects on other compartments. It has been proposed, for instance, that cells lacked cysteine or that they were less sensitive to apoptosis¹⁶.

Cystinosin is another lysosomal transporter which was characterized in my host laboratory. It is an exporter of cystine³². A therapy has been developed for cystinosis. This strategy consists in the following: patients are treated with cysteamine, a thiol-based drug able to react with cystine and form a mixed disulfide, which can be exported by another lysosomal transporter, PQLC2²³.

Two types of histiocytosis (Faisalabad histiocytosis and sinus histiocytosis with massive lymphadenopathy) have been linked with the mutation of *SLC29A3*. These diseases are characterized by an abnormal production of histiocytes, a type of macrophage. Patients suffer from joint deformities, hearing loss and lymphadenopathy.

SLC29A3 codes for ENT3, a lysosomal exporter of nucleosides. The physiopathology of these diseases is unclear at the cellular level and no specific therapies exist⁷⁸.

A very recent study ⁷⁹ suggested that the mutation of *SLC17A4* could lead to carotid intima media thickness. However, their results on this very gene were only marginally significant. *SLC17A4* encodes for a lysosomal co-transporter of sodium and phosphate ⁸⁰.

Chapter 1: functional study of putative lysosomal transporters

1. Introduction

Degradation of macromolecules and transport of catabolites to cytosol by lysosomes have been studied by biochemists⁸¹⁻⁸³. Proteins implied in these mechanisms have mostly been characterized by studying the genetics of inherited disorders, which led to identify many lysosomal hydrolases at the molecular level.

The discovery of lysosomal membrane proteins was much slower due to the small number of inherited diseases that could be linked to the dysfunction of such proteins. In particular, only a few lysosomal transporters could be identified by genetic approaches⁸⁴.

However, improvements in proteomic techniques recently expanded the knowledge of both soluble and membrane proteins of lysosomes. Concerning soluble proteins, most studies were performed by isolating proteins modified with mannose-6-phosphate, which drives their sorting to lysosomes (see introduction). These studies resulted in a map containing about 60 luminal proteins, most of them being enzymes or putative enzymes⁸⁵.

Concerning lysosomal membrane proteins, two main studies had been published before the beginning of my PhD. In the first one⁸⁶ rats were treated with TritonWR1339, a detergent able to accumulate inside lysosomes and drastically change their density, which enabled an easier purification by differential centrifugations and isopycnic centrifugation on a discontinuous sucrose gradient. This study resulted in an extensive map of putative new proteins of the lysosomal membrane. However, authors made no comparative study between treated and untreated rats. Yet, some organelles had about the same density as Triton-treated lysosomes. This led to a strong contamination of fractions by other compartments such as mitochondria, ER, Golgi or plasma membrane, resulting in flawed mass-spectrometry data, limiting the scope of this study.

The second study by Schröder and colleagues⁸⁷ took advantage of a technique to purify lysosomes from human placenta previously developed in their lab. Authors separated

lysosomes from contaminants by another method of density shift. Lysosome-containing fractions were treated with methionine methyl-ester. Amino acid esters can diffuse through biological membranes. Lysosomes are the main compartments containing esterases, which generate the original amino acid, although the lysosomal pH could as well play a role⁸⁸. Such artificial delivery of amino acids into lysosomes is much faster than their efflux through transporters, resulting in a net influx. As a result, treating with esters results in the accumulation of amino acids in the lysosomal lumen, changing its density. Interestingly, in contrast to the previous study, Schröder and colleagues did perform a comparative analysis of ester-treated and untreated lysosomal fractions, which made it possible to discard from final results many proteins of mitochondrial origin. This study found many previously described lysosomal proteins and provided twelve new lysosomal proteins previously uncharacterized (“orphan” proteins).

I took part to the most recent proteomic study of the lysosomal membrane (see p37 below) extending the inventory of lysosomal membrane proteins, done in collaboration with Agnès Journet and Jérôme Garin (CEA Grenoble, France). In this study, lysosomes were purified according to classical protocols, from rat liver, by differential centrifugation and isopycnic centrifugation on a Nycodenz gradient. Like in the previous study, results were analysed by comparing lysosome-enriched and lysosome-depleted fractions.

An important change was introduced in this study. In most proteomic studies, samples are indeed usually directly loaded onto SDS-page to separate proteins by size, before being loaded onto an HPLC coupled to mass spectrometry. However, this method typically results in complex samples, which makes it difficult to identify low-abundance proteins by mass spectrometry. To extend the coverage of the membrane protein repertoire, sampled were, in this case, subjected to a first fractionation procedure. Hydrophobic proteins were extracted from samples using either methanol and chloroform or TritonX114. Since transport proteins are usually more hydrophobic than membrane-associated proteins or proteins with one or two transmembrane domains, this enabled the enrichment of putative transport proteins in less complex fractions, facilitating their detection by mass spectrometry.

This study greatly extended the previous map of the lysosomal membrane. In particular, 46 proteins of unknown function discovered in this study belonged to families or superfamilies containing transporters. I took part in the validation of this study by overexpressing a few of the newly discovered orphan proteins and comparing their subcellular distribution to the distribution of LAMP-1, a very abundant protein of the

lysosomal membrane. Out of twenty-two initial candidates, eleven seemed to be expressed in the ER. However, it was not possible to discriminate with this test between actual resident proteins from the ER and fusion proteins failing to pass the ER quality control, so we focused on the remaining eleven proteins. Nine proteins out of the eleven colocalized well with LAMP-1, strengthening the reliability of this study.

Among all the newly discovered proteins, PQLC2, was characterized as a lysosomal transporter for basic amino acids by a former PhD student of the lab, Adrien Jézégou,²³ in collaboration with Bruno André's laboratory (Université Libre de Bruxelles, Belgium). A competing study, published at the time, reported the same function for PQLC2⁸⁹. TMEM175 was as well identified thanks to this study as a lysosomal channel for potassium by the group of Deijan Ren (University of Pennsylvania, USA).¹⁰

In this chapter, following the proteomics paper, I will present my own attempts of functional characterization on other candidates for lysosomal transporters from this study: TMEM104, SLC37A2, TTYH3, MFSD1 and Spinster 1. In chapter 3, I will introduce a new lysosomal transporter for glutamine and asparagine, which was identified in this study.

An Extended Proteome Map of the Lysosomal Membrane Reveals Novel Potential Transporters*

Agnès Chapel[†], Sylvie Kieffer-Jaquinod[†], Corinne Sagné^{||}, Quentin Verdon^{||§§}, Corinne Ivaldi[†], Mourad Mellal[†], Jaqueline Thirion^{**}, Michel Jadot^{**}, Christophe Bruley[†], Jérôme Garin[†], Bruno Gasnier^{||}, and Agnès Journet^{††}

Lysosomes are membrane-bound endocytic organelles that play a major role in degrading cell macromolecules and recycling their building blocks. A comprehensive knowledge of the lysosome function requires an extensive description of its content, an issue partially addressed by previous proteomic analyses. However, the proteins underlying many lysosomal membrane functions, including numerous membrane transporters, remain unidentified. We performed a comparative, semi-quantitative proteomic analysis of rat liver lysosome-enriched and lysosome-nonenriched membranes and used spectral counts to evaluate the relative abundance of proteins. Among a total of 2,385 identified proteins, 734 proteins were significantly enriched in the lysosomal fraction, including 207 proteins already known or predicted as endo-lysosomal and 94 proteins without any known or predicted subcellular localization. The remaining 433 proteins had been previously assigned to other subcellular compartments but may in fact reside on lysosomes either predominantly or as a secondary location. Many membrane-associated complexes implicated in diverse processes such as degradation, membrane trafficking, lysosome biogenesis, lysosome acidification, signaling, and nutrient sensing were enriched in the lysosomal fraction. They were identified to an unprecedented extent as most, if not all, of their subunits were found and retained by our screen. Numerous transporters were also identified, including 46 novel potentially lysosomal proteins. We expressed 12 candidates in HeLa cells and observed that most of them colocalized with the lysosomal marker LAMP1, thus confirming their

lysosomal residency. This list of candidate lysosomal proteins substantially increases our knowledge of the lysosomal membrane and provides a basis for further characterization of lysosomal functions. *Molecular & Cellular Proteomics* 12: 10.1074/mcp.M112.021980, 1572–1588, 2013.

Lysosomes are membrane-bound intracellular organelles that are key players in the degradation and recycling of biological material. Their crucial role in cell physiology is underlined by the existence of ~50 lysosomal storage diseases caused by genetic defects in lysosomal proteins or proteins involved in lysosome biogenesis (1). The degradative function is carried out in the lysosomal lumen by the concerted action of over 60 hydrolases and accessory proteins (2). Although these soluble lysosomal proteins have been extensively studied, knowledge about membrane proteins remains rather limited, despite the multiple and crucial functions fulfilled by the membrane. It is indeed responsible for establishing and maintaining pH and ionic gradients, transporting degradation substrates and products from/into the cytosol, and maintaining lysosome integrity. Additionally, the lysosomal membrane is subjected to multiple fusion and fission events with other endocytic or biosynthetic compartments. Substrates for degradation are conveyed to lysosomes from the extracellular milieu, the plasma membrane, or the cytoplasm through the endocytic, phagocytic, and autophagic routes. Delivery of newly synthesized material to lysosomes requires exchanges between endocytic or biosynthetic organelles on the one hand and lysosomes on the other hand. These numerous trafficking events are supported by molecular machineries that associate with the lysosomal membrane (3).

In the last decade, large scale mass spectrometry-based approaches have been exploited to study the lysosome protein composition. The soluble content has first been analyzed by the use of an affinity purification protocol based on the mannose 6-phosphate modification (4–11) that is characteristic of soluble lysosomal proteins (12). This has resulted in the identification of about 60 known luminal lysosomal proteins, as well as of many mannose 6-phosphate-containing proteins that were not previously thought to carry out a lysosomal

From the [†]Commissariat à l'Energie Atomique, Institut de Recherches en Technologies et Sciences du Vivant, Laboratoire Biologie à Grande Echelle, F-38054 Grenoble, France, [§]INSERM, U1038, F-38054 Grenoble, France, the [¶]Université Joseph Fourier, Grenoble 1, F-38000, France, the ^{||}Université Paris Descartes, Sorbonne Paris Cité, CNRS, UMR 8192, Centre Universitaire des Saints-Pères, 45 Rue des Saints-Pères, F-75006 Paris, France, ^{§§}Graduate School ED 419, Université Paris-Sud 11, Hôpital Bicêtre, F-94276 Le Kremlin Bicêtre France, and the ^{**}Unité de Recherche en Physiologie Moléculaire, Namur Research Institute for Life Sciences, University of Namur (FUNDP), 61, Rue de Bruxelles B,-5000, Namur, Belgium

Received July 14, 2012, and in revised form, February 1, 2013
Published, MCP Papers in Press, February 24, 2013, DOI 10.1074/mcp.M112.021980

function (13). To gain insight into the membrane composition, several groups have used preparative subcellular fractionation to recover samples enriched in lysosomes (14–18). Despite the experimental limitations of the latter methods that are unable to completely separate organelles, the use of comparative strategies and statistical tools (14, 16, 17) allowed the identification of novel putative resident lysosomal membrane proteins, including a few potential transporters, such as SLC12A4, SLC44A2, C19ORF28 (MFSD12), SIDT2, and MFSD1 (14, 16). More recently, the coupling of selective lysosome density shift and MS quantification was shown to allow simultaneous identification and validation of lysosomal candidates (19). The efficiency of these various approaches in identifying candidates was highlighted by the demonstration of the effective lysosomal residency of several selected proteins (16, 20–29). Concerning membrane proteins, these studies have led to a list of about 45 integral membrane lysosomal proteins for which evidence of the lysosomal localization has been obtained by at least overexpression of epitope-tagged fusion proteins (30).

However, despite the expanded knowledge provided by these recent studies, many lysosomal actors are still missing. For instance, although more than 20 lysosomal transport activities have been biochemically described (31, 32), many of these transport functions remain orphans because the underlying proteins have not been identified yet (33). The aim of the present proteomic study was to gain deeper insight into the characterization of the lysosomal membrane and its associated proteins, with a particular interest in novel potential lysosomal transporters, given their major role in lysosomal physiology. Transporters are integral membrane proteins (IMPs)¹ displaying multiple transmembrane domains, and such IMPs are usually difficult to identify by mass spectrometry because of their high hydrophobicity and low abundance (34, 35). Therefore, to extend our protein identification capacities, we used a combination of subcellular and biochemical fractionations prior to MS analysis. We first established an overall list of 2,385 gene products from lysosome-enriched and lysosome-nonenriched fractions. Then, a comparative proteomics analysis based on spectral counts led to the selection of 734 candidate proteins. They included on the one hand 94 novel potentially lysosomal proteins and, on the other hand, 46 established or putative transporters for which lysosomal residency is suggested by this study. The lysosomal localization has been validated for nine candidates, including five transporters. Moreover, we recently showed elsewhere that another candidate identified during this proteomic study, PQLC2, is a novel lysosomal amino acid transporter (36).

¹ The abbreviations used are: IMP, integral membrane protein; CM, chloroform/methanol; Nsc, normalized spectral count; Spl, spectral index; PM, plasma membrane; EL, endo-lysosome; MFS, major facilitating superfamily; SLC, solute carrier; mTOR, mammalian target of rapamycin; CMI, CM-insoluble; CMS, CM-soluble; ER, endoplasmic reticulum; TGN, trans-Golgi network; L, light mitochondrial.

EXPERIMENTAL PROCEDURES

Subcellular Fractionation—All experiments involving rats were conducted in compliance with approved Institutional Animal Use Committee protocols. Livers were obtained from male Wistar rats. Each preparation was performed on four rat livers essentially as described previously (37). Briefly, fractionation of subcellular organelles by differential centrifugation produced nucleus and heavy mitochondrial (NM), light mitochondrial (L), and microsomal and soluble (PS) fractions. The L fraction was subjected to isopycnic centrifugation on a discontinuous Nycodenz density gradient. Conditions of the gradient were essentially the same as described in the original publication (37), except that Nycodenz[®] was used instead of metrizamide. The following density layers were successively loaded on top of the L fraction: 1.16 (7 ml), 1.145 (6 ml), 1.135 (7 ml), and 1.10 (7 ml). Centrifugation was performed at $83,000 \times g$ for 2 h 30 min in an SW26 Beckman rotor. Fraction 2 (the interface between the layers of respective densities, 1.10 and 1.135 g/ml) was recovered as the L+ (“lysosome-enriched”) fraction. Fractions 1, 3, and 4 (upper and lower fractions) were pooled as the L− (“lysosome-nonenriched”) fraction. Organelles from both L+ and L− fractions were separately diluted in 0.25 M sucrose, pelleted by ultracentrifugation ($100,000 \times g$, 4°C, 1 h), and subjected to a hypoosmotic shock in buffer A (10 mM Hepes, pH 7.8, supplemented with protease inhibitors (Complete, Roche Applied Science)). Membranes (M_BL+ and M_BL−) were recovered by ultracentrifugation ($100,000 \times g$, 4°C, 1 h), extensively washed in buffer A, and resuspended in 200 μ l of buffer A before storage at −80°C.

Recovery of lysosomes in the fractions resulting from differential centrifugation and from the Nycodenz gradient was followed by β -galactosidase activity measurement (38). These data along with the protein amounts recovered in each fraction allowed calculation of purification factors as compared with the initial homogenate. Protein concentration was evaluated using a Micro BCA[™] protein assay kit (Thermo Scientific).

Chloroform/Methanol Extraction—Chloroform/methanol (CM) fractionation of proteins was performed according to Salvi *et al.* (39). Briefly, 250 μ g of organelle membranes (1–10 mg/ml) in buffer A were sonicated, left for 15 min on ice, and ultracentrifuged for 40 min at $100,000 \times g$ and at 4°C. Membranes pellets were then gently resuspended in 100 μ l of buffer A and slowly diluted in 900 μ l of cold CM (5:4, v/v) on ice. The mixture was left 15 min on ice, with periodic agitation, and then centrifuged (15 min, $15,000 \times g$, 4°C) to produce a pellet (the CM-insoluble fraction, CMI) and a supernatant (the CM-soluble fraction, CMS, containing the most hydrophobic proteins). Solvent from the CMS fraction was evaporated under nitrogen, down to 100 μ l, and proteins were acetone-precipitated. Proteins from the CMI and CMS pellets were dissolved in Laemmli buffer for SDS-PAGE separation.

Triton X-114 Phase Separation—Triton X-114 phase separation was performed according to Donoghue *et al.* (40). Briefly, 250 μ g of organelle membranes (1–10 mg/ml) in buffer A were sonicated, left for 15 min on ice, and ultracentrifuged for 40 min, at $100,000 \times g$ and at 4°C. Membranes pellets were then gently resuspended in 800 μ l of cold PBS, and 200 μ l of 10% Triton X-114 (Sigma-Aldrich) was added. The mixture was gently agitated on a rotating wheel overnight at 4°C and cleared by centrifugation (30 min, $20,000 \times g$, 4°C). The supernatant was warmed at 37°C for 30 min and centrifuged (30 min, $5,000 \times g$, 25°C) for phase separation. The upper aqueous phase (AQ) and lower detergent phase (DT) were mixed, respectively, with 200 μ l of 10% Triton X-114 and 800 μ l of cold PBS, incubated for 15 min at 37°C, and centrifuged as described previously. This step was repeated three times, before recovering the final AQ and DT phases as well as a pellet present in the DT fraction (DTP). AQ and DT proteins were acetone-precipitated, and all samples were finally dissolved in Laemmli buffer for SDS-PAGE separation. AQ samples from the first replicate were not kept.

SDS-PAGE Protein Separation and Western Blots—For Western blots, proteins were separated by SDS-PAGE as described previously (41), transferred to PVDF membranes (Immobilon P, Millipore), and immunodetected with the following antibodies directed against subcellular organelles markers: monoclonal mouse anti-rat LAMP2, 1:5 (10D10; homemade); rabbit polyclonal anti-OSCP, 1:50,000 (kind gift from G. Brandolin); rabbit polyclonal anti-GRP78, 1:250 (BiP; Abcam, ab2902); mouse monoclonal anti-TGN38, 1:250 (Transduction Laboratories, T69020); rabbit polyclonal anti-58K protein, 1:500 (FTCD; Abcam, ab5820); rabbit polyclonal anti-Rab5, 1:2,000 (StressGen, KAP-GP006); and mouse monoclonal anti- α 1 sodium potassium ATPase, 1:5,000 (Abcam, ab7671). Proteins were revealed with the Western Lightning Plus-ECL reagent (PerkinElmer Life Sciences) and visualized on autoradiography films (Kodak Biomax XAR).

For MS analysis, SDS-PAGE separation of the reduced proteins was performed on 4–12% gradient acrylamide gels (NuPAGE, Invitrogen). Proteins were stained by Bio-Safe Coomassie stain or Coomassie Brilliant Blue R-250 (Bio-Rad). The amount of loaded proteins and the migration length were adapted to the protein sample complexity.

MS Sample Preparation—For protein digestion each SDS-polyacrylamide gel lane was systematically cut into 1-mm bands that were washed several times by successive incubations in 25 mM NH_4HCO_3 for 15 min and in 50% (v/v) acetonitrile, 25 mM NH_4HCO_3 for 15 min. Gel pieces were dehydrated by 100% acetonitrile and then incubated with 7% H_2O_2 for 15 min before being washed again with the destaining solutions described above. 0.15 μg of modified trypsin (Promega, sequencing grade) in 25 mM NH_4HCO_3 was added to the dehydrated gel pieces for an overnight incubation at 37°C. Peptides were extracted from gel pieces in three 15-min sequential extraction steps in 30 μl of 50% acetonitrile, 30 μl of 5% formic acid, and 30 μl of 100% acetonitrile. The pooled supernatants were finally dried under vacuum.

NanoLC-MS/MS Analysis—The dried extracted peptides were resuspended in 30 μl in 4% acetonitrile, 0.5% trifluoroacetic acid and analyzed by on-line nanoLC-MS/MS (Ultimate 3000 and LTQ-Orbitrap, Thermo Fisher Scientific). The nanoLC method consisted of a 40-min gradient ranging from 5 to 55% acetonitrile in 0.1% formic acid at a flow rate of 300 nL/min. Peptides were sampled on a 300- μm \times 5-mm PepMap C18 precolumn and separated on a 75- μm \times 150-mm C18 column (Gemini C18, Phenomenex). MS and MS/MS data were acquired using Xcalibur (Thermo Fischer Scientific) and processed automatically using Mascot Daemon software (version 2.1, Matrix Science).

Database Searching and Criteria for Protein Identification—Consecutive searches against the IPI_rat_decoy_database (based on the IPI-Rat version 3.48 database; 80,082 entries including the reverse ones) were performed for each sample using Mascot 2.1 (Matrix Science, London, UK). ESI-TRAP was chosen as the instrument and trypsin as the enzyme, and two missed cleavages were allowed. Precursor and fragment mass error tolerance were set respectively at 15 ppm and 1 Da. Peptide variable modifications allowed during the search were: acetyl (N-terminal), oxidation (M), dioxidation (M), and trioxidation (C). Proteins identified with a minimum of one unique peptide and with a score higher than the query threshold (for a p value of peptide <0.01) were automatically validated using IRMa (42). The filtered results were downloaded into an MS identification database, in which the peptide false discovery rate (FDR) was of 2.38%. (FDR = $2 \times \text{reverse}/(\text{reverse} + \text{forward})$). A homemade tool² was used for the compilation, grouping of proteins identified by a same set or subset of peptides (according to the principle of parsimony) and final comparison. Peptides shorter than hexamers were rejected at the grouping

step. A last filtering step retained only protein groups identified by at least two unique peptides. All keratin isoforms and trypsin were deleted from the results. All MS data are available on the Pride database site (43) as Pride project 22847.

Protein Annotation—Gene names were retrieved from the IPI-Rat or Uniprot databases. Uncharacterized proteins (IPI sequence set) underwent a Blastp process against the mammalian Uniprot database section (released February, 2011). Top protein hits with at least $10e-05$ e-value and a query coverage greater than 50% were kept and manually checked for relevance. The query coverage represents the percent of the query length that is included in the aligned segments and is calculated over all segments. When several protein groups corresponded to the same gene name, they were all kept.

The TMHMM version 2.0 server (Center for Biological sequence analysis, Lyngby, DK) was used for predictions of membrane-spanning regions (i.e. transmembrane domains). Protein functional annotation and subcellular localization information, either experimental or predicted, were collected from the IPI, Uniprot, or QuickGO sites and from the bibliography.

Spectral Counting and Semi-quantitative Analysis—For each identified protein p , the spectral count values ($sc_{p,s}$ = number of spectra assigned per protein in a given sample s) were determined with the homemade hEIDI software (supplemental Tables S1 and S2). All spectra pointing to a given protein after the filtering steps were considered. Spectra matching the protein isoforms were counted once for each protein group containing one or several of the isoforms. These spectral count values were then normalized to the equivalent amount (in micrograms) of total membrane protein prior to CM or Triton X-114 extraction (Fig. 1), which had been injected in the spectrometer. The normalized spectral count (Nsc) thus corresponds to a number of spectra per microgram of total MBL+ or MBL- proteins. For each identified protein p , the Nsc value was first calculated for each sample s ($Nsc_{p,s}$), then for each fraction f (MBL+ or MBL-; $Nsc_{p,f}$) in each replicate, as the sum of the $Nsc_{p,s}$ in the CMS, CMI, AQ, DTP, and DT samples and at last for each of the MBL+ or MBL- fractions by summing the $Nsc_{p,r}$ obtained for the three replicates. Evaluation of the relative abundance of a protein in a given sample or fraction was based on the label-free spectral counting method (44), and performed by dividing $Nsc_{p,s}$ or $Nsc_{p,f}$ by the total Nsc of the considered sample or fraction.

For each protein, a spectral index (SpI) comprising both relative protein abundance and number of samples containing this protein was then calculated as indicated in Fu *et al.* (45) to allow comparison between MBL- and MBL+ samples. Confidence intervals were established through permutation analysis (45) and used for determination of proteins significantly enriched in MBL+ (lysosomal protein candidates).

Molecular Cloning—IMAGE or ORFOME clones coding for the following proteins were obtained from Source Bioscience: LOH12CR1, MFSD1, PTTG1IP, SLC37A2, SLC38A7, SLC46A3, SLCO2B1, STARD10, TMEM104, TMEM175, TTYH2, and TTYH3. Inserts were amplified by PCR using the Phusion polymerase (New England Biolabs) and the commercial plasmids as template and cloned for heterologous expression of GFP or YFP fusion proteins. Original plasmids, DNA accession numbers, primers, and expression vectors are given in supplemental Table S3.

Cell Culture and Fluorescence Studies—HeLa cells were from the American Type Culture Collection (ATCC) and were grown in DMEM/GlutaMAXI supplemented with 10% FBS. Media and serum were from PAA Laboratories and Invitrogen, respectively. Cells were transiently transfected using electroporation or lipofection with Lipofectamine 2000 and processed for epifluorescence 2 days after transfection. Cells were fixed at room temperature in 4% paraformaldehyde. Antibodies were used at the following dilutions: mouse monoclonal anti-human LAMP1, 1:2,000 (H4A3, Developmental Studies Hy-

² hEIDI: Hesse, A.-H., Adam, A., Dupieris, V., Court, M., Barthe, D., Ernaldi, A., Masselon, C., Ferro, M., and Bruley C., manuscript in preparation.

bridoma Bank); Cy3-conjugated donkey anti-mouse, 1:1,000 (The Jackson Laboratory). Fluorescence was examined using a Nikon TE2000 epifluorescence microscope. Images were deconvoluted after acquisition with the PSF-based Iterative 3D Deconvolution module of Metamorph software (Universal Imaging Corp.).

RESULTS

To extend our knowledge of the lysosomal protein content, with a particular focus on membrane proteins and especially transporters, we performed a semi-quantitative and comparative proteomics analysis of membranes from rat liver fractions enriched and nonenriched in lysosomes. As novel proteins remaining to be discovered have a low abundance, we maximized protein resolution and coverage by analyzing several biological replicates and by reducing sample complexity using membrane protein subfractionation and SDS-PAGE. The label-free spectral counting method, based on the number of redundant peptides that identify a protein (44, 46), was used to evaluate the relative abundance of each protein. Further selection of lysosomal protein candidates resulted from a statistical comparison between lysosome-enriched and -nonenriched fractions (45). Finally, novel candidate lysosomal transporters were identified among the multipass transmembrane proteins.

Preparation of Samples from Lysosome-enriched and -non-enriched Fractions—We essentially followed the well established protocol of Wattiaux *et al.* (37) for preparation of lysosomal fractions (Fig. 1). Rat liver homogenates were first fractionated by differential centrifugation, and the primary lysosome-enriched fraction (fraction L) was further separated on a discontinuous Nycodenz density gradient (47), resulting in secondary L+ and L- fractions. Nycodenz is a gradient medium that displays very similar banding density for various organelles as the originally described metrizamide medium (48). Three independent preparations (biological replicates) were made. Our protocol aimed at improving the identification of IMPs, because their hydrophobicity and usually low abundance hinder their MS detection and identification in highly complex protein samples (34, 35). However, we also attempted to retain peripheral membrane associated proteins. These membrane associated proteins indeed include various trafficking machineries and cytoskeleton-associated proteins, which are crucial for the biogenesis and function of endo-lysosomes. We thus avoided harsh treatments that would have removed membrane-associated proteins, such as alkaline washes, to prepare L+ and L- membranes (respectively MbL+ and MbL- fractions). We then subfractionated both fractions according to protein hydrophobicity by two independent treatments, chloroform/methanol extraction (39) and Triton X-114 phase separation (Fig. 1) (40, 49). All resulting samples were finally separated by 1D electrophoresis, before being processed for MS analysis.

The β -galactosidase activity was measured to follow the recovery of lysosomes along the fractionation process, for the three replicates. These measurements indicated that the L,

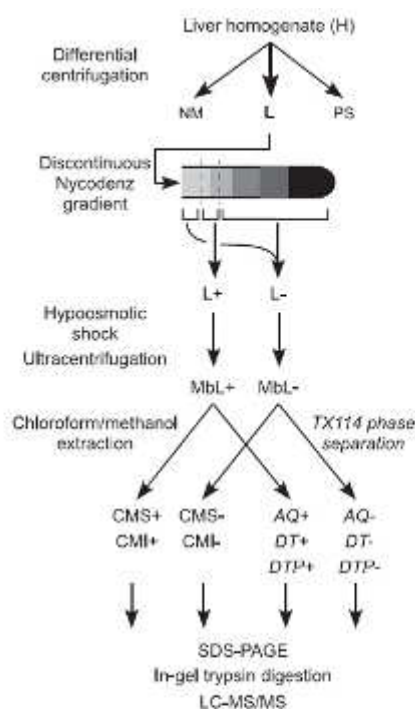


FIG. 1. Workflow of the sample preparation for MS analysis. Differential centrifugation of rat liver homogenates (*H*) produced a light mitochondrial fraction L, which was submitted to Nycodenz gradient centrifugation. This step allowed separation of a lysosome-enriched fraction (L+) from the rest of the gradient (L-). Organelles from L+ and L- were broken by hypoosmotic shock, and membranes were recovered by ultracentrifugation. Membrane pellets (MbL+ and MbL-) were split in two equal parts that were separately fractionated by independent methods based on protein hydrophobicity (chloroform/methanol extraction or Triton X-114 (TX114) phase separation). All resulting samples were subsequently separated by SDS-PAGE prior to LC-MS/MS analysis of in-gel digested samples.

L+, and L- fractions were enriched 9–13-, 65–75-, and 7–9.5-fold, respectively, in lysosomes relative to the initial liver homogenate. These values, consistent with published data (37, 47), demonstrated the enrichment and nonenrichment of L+ and L-, respectively, as compared with L, and the much higher concentration (~7–9-fold) of lysosomes in L+ as compared with L-. These fractions are thus described as lysosome-enriched and lysosome-nonenriched, respectively, and evaluation of "enrichment" will hereafter always be based on the comparison between L+ and L- fractions.

We then analyzed the enrichment of several subcellular compartments by immunodetection of organelle markers in the NM, L, and PS fractions resulting from differential centrifugation, as well as in the membranes of the L, L+, and L- fractions (Fig. 2). The lysosomal protein LAMP2 was the only protein that was strongly enriched in both L and MbL+ fractions. Rab5 (early endosome), the α 1 subunit of the sodium potassium ATPase (plasma membrane), TGN38 (TGN), and

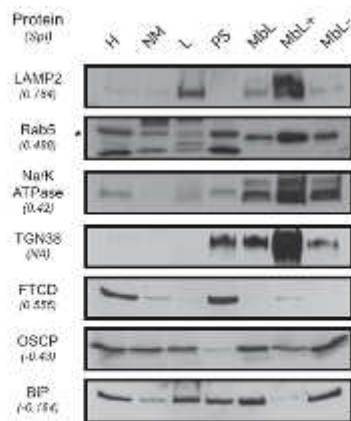


FIG. 2. Western blot analysis of subcellular fractions. The relative abundance of organelle protein markers was examined by Western blot analysis, in the differential centrifugation fractions (H, NM, L, and PS) and in the membranes recovered from the L fraction and the L+ and L- samples (respectively MbL, MbL+, and MbL-). Identical protein amounts (25 μ g) have been loaded for each sample. Subcellular markers are as follows: LAMP2, lysosomes; Rab5, early endosomes; α 1 subunit of the sodium potassium ATPase (Na/K-ATPase), plasma membrane; TGN38, trans-Golgi network; FTCD, Golgi; OSCP subunit of the ATP synthase, mitochondria; and BiP, endoplasmic reticulum. For each protein tested, the Spl (see "Results" and Fig. 4) is indicated in *italics*.

FTCD (Golgi) were depleted from L and enriched in PS to different extents. Although they all display some enrichment in MbL+, TGN38 is the only one for which this enrichment is comparable with that of LAMP2. Both the mitochondrial ATP synthase OSCP subunit and the endoplasmic reticulum BiP were depleted in MbL+.

Protein Identification—From the three biological replicates, we generated 959 MS analyses. After first pass filters, this resulted in 1,398,920 spectra, 368,147 of which could be assigned to 4,097 nonredundant rat gene products from the IPI-Rat database. According to the principle of parsimony, protein isoforms that could not be segregated by the identified peptides were counted as one unique gene product. The 4,097 gene products corresponded to 24,316 nonredundant peptide sequences. All corresponding protein and peptide information is available in the PrIDE database under project number 22847 and in supplemental Table S2. Further filtering excluding trypsin and keratins as contaminants and retaining proteins identified by at least two unique peptides led to a list of 2,385 nonredundant gene products, hereafter named the MbL2385 list. In this list, 528 proteins were present in the MbL+ fraction only, 157 in the MbL- fraction only, and 1,700 in both fractions (supplemental Tables S4a and S5a). Thus, most of the proteins were common to both MbL+ and MbL- fractions, in agreement with the limited resolution power of subcellular fractionation and the high sensitivity of mass spectrometers.

To evaluate the content in IMPs identified in our samples, transmembrane domains were predicted by use of the TMHMM

2.0 server (supplemental Table S4a). This led to the identification of 762 IMPs (32%), including 361 polytopic proteins (proteins with at least two transmembrane domains, 15.1%).

Extraction of Semi-quantitative Data—Despite the high enrichment factor obtained by the well established Nycodenz gradient method used in this study, cofractionation of other organelles, such as mitochondria, challenges the identification of true lysosomal residents, including proteins with dual or multiple localization. We thus compared the protein sets from lysosome-enriched and -nonenriched fractions to identify the subset associated with lysosomes. Because most proteins were common to both MbL+ and MbL- fractions, comparing their number was less informative and relevant than comparing their abundance (compare Fig. 3 with supplemental Fig. S1). Abundance information was extracted from spectral count data (supplemental Table S1), according to the spectral counting semi-quantitative approach (44, 46). The relative abundance for any given protein was derived from the Nsc calculated as indicated under "Experimental Procedures" using merged data issued from all MbL+ or MbL- samples (supplemental Table S1).

MbL+ and MbL- Fractions Display Different Organellar Profiles—We then analyzed the known or predicted subcellular localization of proteins from the MbL2385 list by manually collecting this information in protein databases (IPI, UniprotKB, and QuickGO) and bibliography. For IPI entries without any attributed gene name, homologs were previously searched in a mammalian subset of the Uniprot database using Blastp. This allowed comparison of protein abundances in MbL+ and MbL- according to the following subcellular categories: endo-lysosomes (EL), plasma membrane (PM), mitochondria, peroxisomes and nucleus (MPN), endoplasmic reticulum (ER), Golgi (G), cytoplasm (C), cytoskeleton (CS), secreted (S), miscellaneous (Misc; vesicles, granules, and multiple localizations) and Unknown. The comparison of protein abundances in MbL+ and MbL- according to the subcellular distribution showed striking differences (Fig. 3, *left panel*; supplemental Table S5c); EL and PM proteins were clearly enriched in MbL+, as they altogether accounted for 34% of the material, as compared with 4.7% only in MbL-. By contrast, proteins from the ER and MPN compartments were depleted from MbL+ relative to MbL- (34.2 and 73.7%, respectively). The similar behaviors of EL and PM proteins on the one hand and ER and MPN proteins on the other hand were systematically observed in subsequent analyses. Despite its slight enrichment in the MbL+ fraction (0.59% of the abundance in MbL+ versus 0.15% in MbL-), the small set of Golgi proteins ($n = 30$) has been ranked as "Contaminants," along with ER and MPN proteins, in subsequent quantitative analyses (see below). Except for the cytoplasm, the other subcellular constituents (CS, S, and Misc) were slightly enriched in the MbL+ fraction (15.6 versus 7.1%). Proteins of unknown localization represented 11.2 and 10.0% in number but 6.3 and 3.8% in abundance in MbL+ and MbL-, respec-

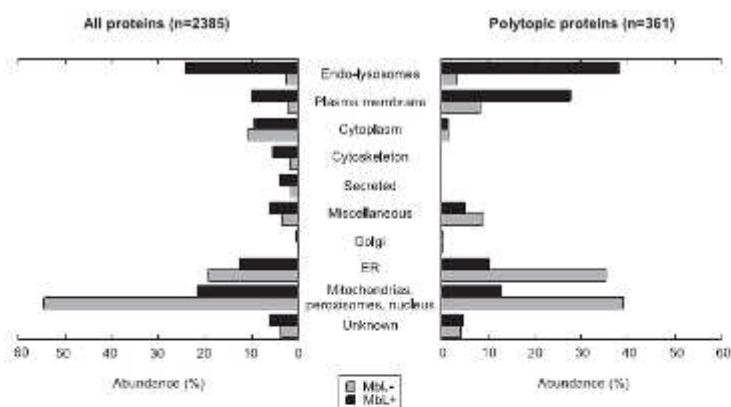


FIG. 3. Subcellular distribution of the proteins in MbL+ and MbL-. The relative abundance of proteins in MbL+ (black bars) or in MbL- (gray bars) is compared, according to their subcellular classification. Left panel, distribution of all proteins. Right panel, distribution of polytopic proteins (i.e. harboring at least two transmembrane domains).

tively, indicating that the average relative abundance of such proteins is low (Fig. 3, left panel, and supplemental Fig. S1 and supplemental Table S5c).

Thus, the subcellular distribution features that stem from our spectral count data were consistent with qualitative expectations based on a restricted set of organelle markers (Fig. 2) (37). The substantial presence of contaminant organelles in MbL+ was expected as a known characteristic of subcellular fractions. Our results therefore validate the use of the spectral count-based semi-quantitative method to describe and analyze these fractions.

Assignment of Proteins to Lysosomes—The next step in our study was to identify which proteins identified in MbL+ were indeed novel potential lysosomal proteins. We thus aimed at identifying those significantly enriched in MbL+ relative to MbL-, similarly, for instance, to the observed enrichment of the typical lysosomal marker β -galactosidase in L+ relative to L-. Proteins from the MbL+ fraction were either exclusively detected in MbL+ or common to both fractions (supplemental Table S4a). Among the 528 proteins exclusively present in MbL+, we chose to consider as potentially lysosomal only those present in at least two out of the three biological replicates and identified by at least five spectra (356 proteins; supplemental Table S4b). Among the proteins common to MbL+ and MbL-, lysosomal candidates were selected according to their S_{pl} (45), a parameter that takes into account both the relative protein abundance (estimated by normalized spectral counts) and the number of replicates in which the protein has been found (supplemental Tables S1 and S4a). S_{pl} values range from -1 to +1, the lower and upper extreme values corresponding to proteins almost exclusively detected in MbL- and MbL+ fractions, respectively. These values displayed a roughly bimodal distribution in the MbL2385 list, with a massive peak covering negative values and a second subset rising toward an S_{pl} of +1 (Fig. 4A). The S_{pl} analysis highlighted the different distributions between MbL+ and

MbL- of proteins from various annotated subcellular categories (Fig. 4B). Indeed, proteins from contaminants (essentially mitochondrial, ER and peroxisomal proteins) were the main contributors to the massive peak of negative S_{pl}, whereas EL and PM proteins demonstrated a strong tendency to score high S_{pl} values, with respective median values of 0.77 and 0.60. Confidence intervals were established through permutation analysis (45). Proteins were considered as significantly enriched in MbL+ when their S_{pl} was higher than the 95th percentile cutoff value (S_{pl} \geq 0.594), a level reached by 378 proteins out of 1,700 (supplemental Table S4b).

Altogether, our selection criteria for significant enrichment in MbL+ led us to sort 734 proteins (Lys-734 list; supplemental Table S4b) out of 2,385. This selection included 79.3% ($n = 207$) of the EL-annotated proteins, 56% ($n = 132$) of the PM-annotated ones, and only 3.2% ($n = 28$) of the contaminant proteins (Fig. 5A and supplemental Table S5d). The C, CS, S, and Misc categories were represented by a total of 273 proteins. To our knowledge, 38 of the 94 proteins without any subcellular localization annotation (Table I) were completely novel lysosomal candidates, because they have not been identified in previous proteomic studies of lysosomes (14–17, 19).

As it was recently shown that most known lysosomal genes exhibit a coordinated transcriptional behavior regulated by the transcription factor TFEB, we compared our Lys-734 list to the list of 291 genes up-regulated following TFEB overexpression in HeLa cells (50). This comparison pointed to 38 common proteins, among which 30 were EL-annotated proteins and one, the product of the *Wdr81* gene, was of unknown annotated localization.

Extraction from protein databases or bibliography, and analysis of known or predicted functional annotation showed that all defined functional processes were represented in the Lys-734 list, although only two "polypeptide transport" annotated proteins remained (Fig. 5B). Transporters, channels, and pumps of ions and small molecules represented the most

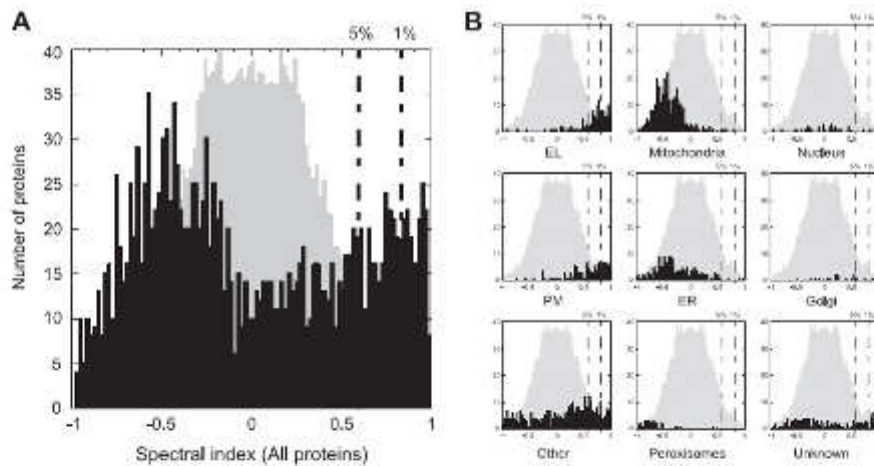


FIG. 4. Distribution of spectral indexes. The distribution of spectral indexes of identified proteins is represented (in black) along with a random distribution (light gray) derived from permutation analysis. Thresholds for the 5 and 1% confidence intervals (indicative of a significant enrichment in MbL+) are indicated by dotted lines. **A**, Spl distribution for all identified proteins common to MbL+ and MbL-. **B**, Spl distribution for proteins of specific subcellular annotation. The number of proteins in each category is as follows: All, $n = 1,700$; EL, $n = 160$; ER, $n = 228$; Golgi, $n = 19$; Mitochondria, $n = 419$; Nucleus, $n = 32$; other, $n = 467$; Peroxisomes, $n = 44$; PM, $n = 163$; Unknown, $n = 168$; x axis, Spl (range from -1 to $+1$); y axis, number of proteins.

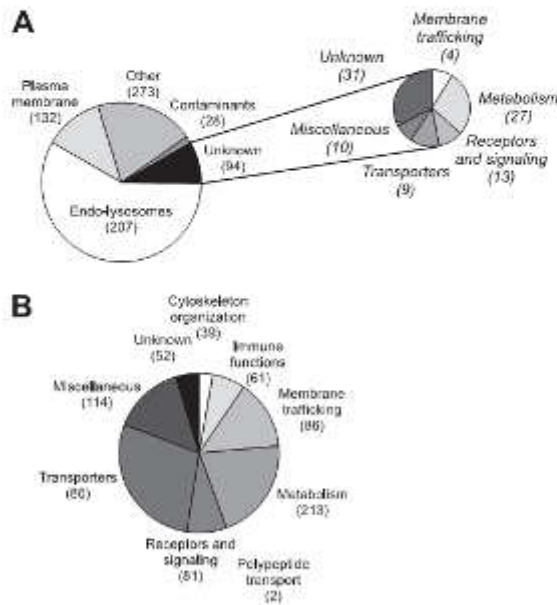


FIG. 5. Subcellular and functional distribution of the Lys-734 proteins. **A**, distribution of the proteins according to their subcellular annotation. The functional annotation of proteins of unknown localization is shown. "Cytoplasm," "cytoskeleton," "secreted," and "miscellaneous" are merged in the *Other* category. **B**, distribution of the proteins according to their functional annotation. Each pie section represents the relative abundance of proteins from the corresponding category. Numbers of proteins are indicated.

abundant functional class, despite its third position by protein number. Metabolism-associated proteins were the most numerous but ranked second in abundance (supplemental Table S5e). As for the 94 proteins without subcellular annotation, one-third had no functional annotation either; more than one-quarter were various metabolic enzymes; and the remaining were distributed between the "miscellaneous," "transporters, channels, and ion pumps," and "receptors and signaling" classes with rather similar abundances (Fig. 5A).

Identification of Novel Putative Lysosomal Transporters—In addition to extending the current list of known lysosomal proteins, our interest was focused on the discovery of potential novel lysosomal transporters. As transporters display multiple membrane spanning domains (35), we filtered the Lys-734 list for polytopic proteins. Among the 136 MbL+-enriched polytopic proteins, 10% ($n = 11$) had no attributed function and more than half ($n = 72$; 67.5% of the Lys-734 IMPs abundance) belonged to the transporters, channels, and ion pumps class. This protein set contains numerous subunits of ATPases (*v*-ATPase ($n = 6$); P-ATPases ($n = 5$)), ATP-binding cassette (ABC) transporters ($n = 9$), channels ($n = 10$), and secondary active transporters ($n = 42$). The latter include the recently discovered potential or effective lysosomal transporters C2ORF18 (21, 51), DIRC2 (27), LMBD1 (52), and MFSD8 (53) (Fig. 6). During the revision of our manuscript, the lysosomal localization of the ABC transporter ABCD4 was established (29), and we showed in a separate study the lysosomal localization and transport function of the PQLC2 protein (36).

Removal of the transporters already annotated as endo-lysosomal led to a set of 46 novel potentially lysosomal transporters that notably included 27 plasma membrane proteins

TABLE I
List of potential novel lysosomal proteins

Proteins from the Lys-734 list without any subcellular localization annotation are given. The functions are as follows: I, immune function; M, metabolism; Misc, miscellaneous; MT, membrane trafficking; R/S, receptors and signaling; T, transporters, channels, and ion pumps; U, unknown; TM, number of transmembrane domains; Spl, spectral index; NA, not applicable (protein identified in MBL+ exclusively). The lysosomal localization of MFSD1 has been shown during the course of this work (66).

Gene name	Description	Accession no.	TM	Function	Spl	No. of peptides	Coverage
<i>Abca6</i>	Abca6, similar to ATP-binding cassette, subfamily A (ABC1), member 6	IPI00762951	13	T	0.76	6	4.61
<i>Acp1</i>	Acp1, isoform 1 of low molecular weight phosphotyrosine protein phosphatase	IPI00206664	0	R/S	NA	2	12.66
<i>Afmid</i>	LOC688283, similar to kynurenine formamidase	IPI00882532	0	M	NA	7	27.45
<i>Ahcy</i>	Ahcy, adenosylhomocysteinase	IPI00476295	0	M	0.60	16	38.66
<i>Akr1c12/11</i>	RGD1559604, similar to protein RAKd	IPI00557070	0	M	NA	4	13.31
<i>Akr1c13</i>	LOC364773, 17 β -hydroxysteroid dehydrogenase	IPI00387641	0	M	NA	5	19.38
<i>Aox3</i>	Aox3, aldehyde oxidase 1	IPI00205560	0	M	0.88	26	25.11
<i>Ap5z1</i>	Kiaa0415, hypothetical protein LOC641386	IPI00363750	0	MT	NA	8	11.03
<i>Atp11c-ps1</i>	128-kDa protein	IPI00370178	8	T	0.63	25	27.32
<i>C10orf32</i>	RGD1311783, hypothetical protein	IPI00371685	0	U	NA	10	59.06
<i>C16orf62</i>	LOC361635, UPP0505 protein C16orf62 homolog	IPI00569226	0	U	0.80	5	5.61
<i>C17orf59</i>	LOC497934, uncharacterized protein C17orf59 homolog	IPI00188598	0	U	0.87	11	22.16
<i>C1galt1</i>	C1galt1, glycoprotein-N-acetylgalactosamine 3 β -galactosyltransferase 1	IPI00200858	1	M	NA	7	19.83
<i>C1galt1c1</i>	C1galt1c1, C1GALT1-specific chaperone 1	IPI00197034	1	Misc	NA	3	11.08
<i>C2orf72</i>	18-kDa protein	IPI00188569	0	U	NA	4	36.9
<i>C6orf58</i>	RGD1311933, hypothetical protein	IPI00358842	0	U	0.95	9	29.97
<i>C9orf91</i>	RGD1304595, hypothetical protein LOC298104	IPI00357901	2	U	NA	7	22.51
<i>Ca2</i>	Ca2, carbonic anhydrase 2	IPI00230787	0	M	NA	2	8.85
<i>Cacfd1</i>	RGD1311501, hypothetical protein LOC296599	IPI00363948	3	T	NA	2	14.62
<i>Ccdc22</i>	Ccdc22, similar to coiled-coil domain containing 22	IPI00362580	0	U	NA	11	23.6
<i>Ccdc93</i>	Ccdc93, coiled-coil domain-containing protein 93	IPI00371846	0	U	NA	10	18.28
<i>Cd302</i>	Cd302, CD302 antigen	IPI00372762	1	R/S	NA	4	15.79
<i>Clec4f</i>	Clec4f, C-type lectin domain family 4 member F	IPI00193212	1	R/S	0.98	20	33.64
<i>Clec4g</i>	Clec4g, similar to C-type lectin domain family 4, member g	IPI00764324	1	U	NA	4	14.65
<i>Cnp</i>	Cnp, 2',3'-cyclic-nucleotide 3'-phosphodiesterase	IPI00199394	0	M	0.78	5	13.81
<i>Comm10</i>	Comm10, COMM domain containing 10	IPI00365123	0	U	NA	8	36.63
<i>Comm2</i>	Comm2, COMM domain containing 2	IPI00372217	0	U	NA	2	8.54
<i>Comm3</i>	Comm3, COMM domain-containing protein 3	IPI00400613	0	U	NA	6	36.92
<i>Comm7</i>	Comm7, COMM domain containing 7	IPI00373166	0	Misc	NA	5	31
<i>Comm9</i>	Comm9, COMM domain containing 9	IPI00210812	0	U	NA	8	58.59
<i>Cpne5</i>	Cpne5, copine V	IPI00360489	0	MT	0.60	2	3.04
<i>Crip2</i>	Crip2, cysteine-rich protein 2	IPI00200352	0	Misc	NA	3	33.65
<i>Csad</i>	Csad, cysteine sulfonic acid decarboxylase	IPI00214394	0	M	0.74	12	32.86
<i>Csnk2a1</i>	Csnk2a1, casein kinase II subunit α	IPI00192586	0	R/S	NA	4	10.23
<i>Dak</i>	Dak, dihydroxyacetone kinase	IPI00372498	0	M	0.81	22	46.71
<i>Dnajc13</i>	Dnajc13, 108-kDa protein	IPI00366703	0	U	NA	3	5.59
<i>Dnajc13</i>	Dnajc13, DnaJ (Hsp40) homolog, subfamily C, member 13	IPI00870706	0	U	NA	6	4.14
<i>Dnajc5</i>	Dnajc5, DnaJ homolog subfamily C member 5	IPI00210881	0	Misc	0.63	6	31.31
<i>Enpp4</i>	Enpp4, ectonucleotide pyrophosphatase/phosphodiesterase 4	IPI00371761	1	M	0.89	5	11.07
<i>Eprs</i>	Eprs, LRRGT00050	IPI00476855	0	M	NA	4	2.76
<i>Fth1</i>	Fth1, ferritin heavy chain	IPI00777061	0	Misc	0.70	14	59.34
<i>Gna11</i>	Gna11, guanine nucleotide-binding protein α -11 subunit	IPI00200437	0	R/S	0.86	13	36.21
<i>Gna13</i>	Gna13, G α 13	IPI00422053	0	R/S	0.79	13	34.22
<i>Gna14</i>	Gna14, guanine nucleotide-binding protein, α 14	IPI00360645	0	R/S	0.86	3	12.68

Table I—continued

Gene name	Description	Accession no.	TM	Function	Spl	No. of peptides	Coverage
<i>Gnai3</i>	Gnai3, guanine nucleotide-binding protein G(k) subunit α	IP100231726	0	R/S	0.88	12	43.22
<i>Gpr155</i>	Gpr155 G protein-coupled receptor 155	IP100365274	17	R/S	0.89	9	14.29
<i>Grhpr</i>	Grhpr, Grhpr protein	IP100767591	0	M	0.87	7	24.18
<i>Haao</i>	Haao 3-hydroxyanthranilate 3,4-dioxygenase	IP100339188	0	M	NA	9	22.03
<i>Iah1</i>	Iah1, isoamyl acetate-hydrolyzing esterase 1 homolog	IP100421610	0	M	NA	5	16.47
<i>Igtp</i>	Igtp Ac2-233	IP100369234	0	M	NA	5	5.73
<i>Itfg3</i>	Itfg3 protein ITFG3	IP100372350	1	U	NA	5	11.78
<i>Jak1</i>	Jak1, similar to tyrosine-protein kinase JAK1	IP100212981	0	R/S	0.75	3	2.84
<i>Kctd12</i>	Kctd12, similar to potassium channel tetramerization domain-containing protein 12	IP100767085	0	Misc	NA	3	9.77
<i>Kxd1</i>	LOC498606, UPF0459 protein C19orf50 homolog	IP100197953	0	U	NA	7	28.25
<i>Lgals5</i>	Lgals5, galectin-5	IP100231663	0	Misc	0.94	8	55.17
<i>Loh12cr1</i>	Loh12cr1, loss of heterozygosity, 12, chromosomal region 1 homolog	IP100189639	0	U	0.94	22	80.51
<i>Mef2bnb</i>	LOC684626, similar to K11B4.2	IP100364627	0	U	0.97	6	38.66
<i>Mfsd1</i>	Mfsd1, similar to major facilitator superfamily domain-containing 1	IP100373212	11	T	NA	6	18.75
<i>Mic1</i>	RGD1311805, similar to RIKEN cDNA 2400010D15	IP100363472	0	U	NA	25	41.55
<i>Mios</i>	RGD1308432, similar to missing oocyte CG7074-PA	IP100199953	0	U	NA	7	8.11
<i>Mon1b</i>	Mon1b, MON1 homolog b	IP100359673	0	MT	0.93	23	53.86
<i>Mpeg1</i>	Mpeg1, macrophage-expressed gene 1 protein	IP100204417	1	U	0.80	18	39.92
<i>Myadm</i>	Myadm, myeloid-associated differentiation marker	IP100339007	8	U	0.76	2	8.49
<i>Napg</i>	LOC682827, 35-kDa protein	IP100367524	0	MT	0.92	28	52.24
<i>Oplah</i>	Oplah, 5-oxoprolinase	IP100326436	0	M	NA	5	5.05
<i>Pah</i>	Pah, phenylalanine-4-hydroxylase	IP100193258	0	M	0.66	11	36.64
<i>Pbld</i>	Pbld, phenazine biosynthesis-like domain-containing protein	IP100200041	0	M	NA	6	32.64
<i>Pebp1</i>	Pebp1, phosphatidylethanolamine-binding protein 1	IP100230937	0	Misc	0.68	5	43.85
<i>Plk3ca</i>	Plk3ca, similar to phosphatidylinositol-4,5-bisphosphate 3-kinase catalytic subunit α isoform	IP100955176	0	R/S	0.64	2	2.06
<i>Pk</i>	Similar to pyruvate kinase 3	IP100561880	0	M	NA	18	35.78
<i>Pklr</i>	Pklr, isoform R-type of pyruvate kinase isozymes R/L	IP100202549	0	M	0.86	18	43.55
<i>Pla2g2a</i>	Pla2g2a, phospholipase A2, membrane-associated	IP100205248	1	M	NA	3	28.08
<i>Ppa1</i>	Ppa1, similar to pyrophosphatase	IP100371957	0	M	NA	3	11.63
<i>Prkag1</i>	Prkag1, 5'-AMP-activated protein kinase subunit γ -1	IP100196645	0	R/S	0.72	5	20
<i>Rbp1</i>	Rbp1, retinol-binding protein 1	IP100231825	0	T	NA	5	29.63
<i>RGD1308461</i>	RGD1308461, similar to CG5149-PA	IP100359821	0	U	NA	9	24.35
<i>Sec14f4</i>	Sec14f4, SEC14-like 4	IP100204634	0	Misc	0.66	11	31.07
<i>Slc38a7</i>	Slc38a7, putative sodium-coupled neutral amino acid transporter 7	IP100421684	11	T	NA	7	10.8
<i>Slc46a3</i>	Slc46a3, solute carrier family 46 member 3	IP100364398	11	T	NA	2	5.86
<i>Slco2b1</i>	Slco2b1, solute carrier organic anion transporter family member 2B1	IP100230858	12	T	0.75	3	5.56
<i>Sord</i>	Sord, sorbitol dehydrogenase	IP100760137	0	M	0.68	16	45.1
<i>Stard10</i>	Stard10, START domain containing 10	IP100555188	0	U	NA	5	16.21
<i>Tagln3</i>	Tagln3, transgelin-3	IP100210532	0	U	NA	5	11.47
<i>Tgm2</i>	Tgm2, transglutaminase 2, C polypeptide	IP100205135	0	M	NA	6	11.81
<i>Tm9sf4</i>	Tm9sf4, transmembrane 9 superfamily member 4	IP100373155	9	Misc	NA	9	13.84
<i>Tmem104</i>	Tmem104, similar to CG5262-PA	IP100778760	11	T	NA	6	11.29
<i>Tmem144</i>	Tmem144, transmembrane protein 144	IP100373219	10	U	0.95	5	23.85
<i>Tmem175</i>	Tmem175, transmembrane protein 175	IP100211068	9	U	NA	5	18.44

Table I—continued

Gene name	Description	Accession no.	TM	Function	Spl	No. of peptides	Coverage
<i>UBB</i>	LOC679594;LOC682397 similar to polyubiquitin	IP100763565	0	M	0.88	3	38.96
<i>Ubi3</i>	Ubi3, ubiquitin-like protein 3	IP100358637	0	U	NA	6	47.01
<i>Uroc1</i>	Uroc1, similar to urocanase domain containing 1	IP100388707	0	M	NA	8	14.35
<i>UST4r</i>	UST4r, putative integral membrane transport protein	IP100202688	7	T	0.89	6	10.33
<i>Vsig4</i>	Vsig4, V-set and immunoglobulin domain-containing 4	IP100372986	1	R/S	NA	5	17.19
<i>Wdr81</i>	Wdr81, similar to α 2-plasmin inhibitor	IP100370309	0	U	0.65	6	3.58
<i>Wdr91</i>	Wdr91, Wdr91 protein	IP100373314	0	U	NA	4	7.62

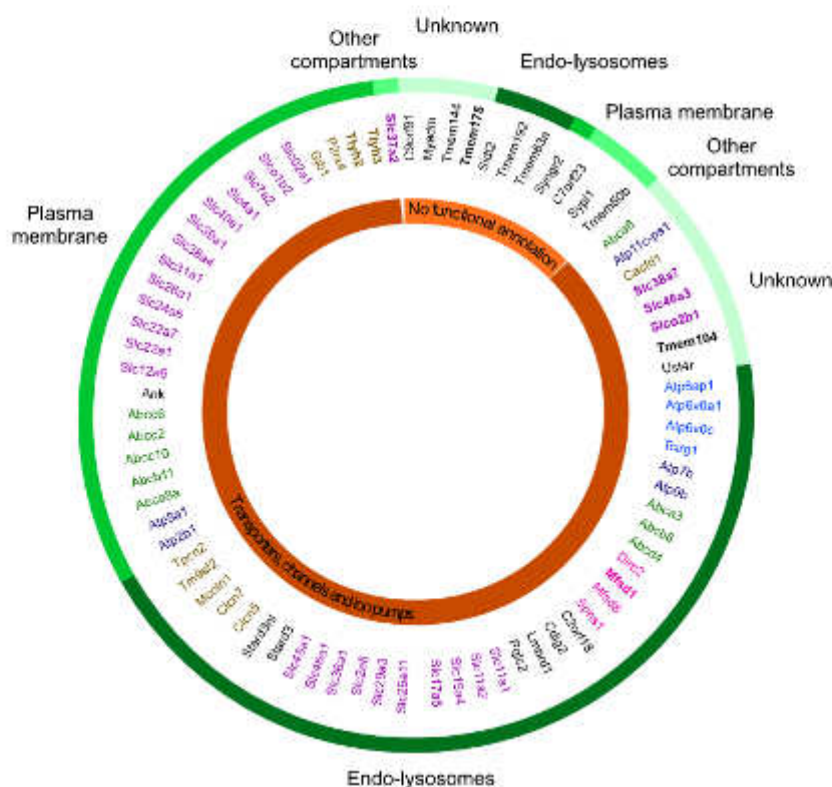


Fig. 6. **Lysosomal transportome.** All known and potential transporters or channels retained as selectively enriched in MbL+ are represented. These proteins display at least two transmembrane domains, they either belong to the functional class "transporters, channels, and ion pumps" or have no functional annotation. They are classified according to their functional and subcellular annotations. Different categories of transporters are depicted by different colors (ABC transporters, green; MFS transporters, pink; SLC family members, purple; ATPases, deep blue; V-ATPase subunits, light blue; channels, brown; miscellaneous, black). Validated candidates are in boldface.

and 12 proteins of unknown localization (Table II). To our knowledge, 9 out of these 46 proteins (ABCA6, C9ORF23, C9ORF91, CACFD1, SLC26A1, SLC38A7, SLC40A1, SLC46A3, and TMEM50b) have not been identified in previous proteomic analyses of mammalian lysosomes, phagosomes, or lysosome-related organelles (14–17, 19, 54–61).

Validation of Selected Candidates—Twelve candidates, LOH12CR1, STARD10, PTTG1IP, MFSD1, SLC37A2, SLC38A7, SLC46A3, SLCO2B1, TMEM104, TMEM175, TTYH2 and

TTYH3, were chosen to validate independently the proteomic data. Peptides allowing their identification are given in [supplemental Table S6](#). LOH12CR1 and STARD10 are putative cytosolic proteins. PTTG1IP is predicted to be an integral membrane protein with a role in cellular trafficking. Its subcellular localization is unclear as it has been observed in cytosol and nucleus by some authors (62) and in late endosomes by others (63). All other candidates are multispanning transmembrane proteins. TMEM175 has no homology with

TABLE II
List of potential novel lysosomal transporters

Candidates with two TM or more, of unknown function or with an attributed transport function, are shown. The localizations are as follows: ER, endoplasmic reticulum, Golgi; EL, endo-lysosomes; Misc, miscellaneous; PM, plasma membrane; U, unknown. The functions are as follows: T, transporters, channels, and ion pumps; U, unknown; TM, number of transmembrane domains; Spl, spectral index; NA, not applicable (proteins identified in MBL⁻ exclusively). The lysosomal localization of MFSD1 has been shown during the course of this (66).

Gene name	Description	Accession no.	TM	Localization	Function	Spl	No. of peptides	Coverage
<i>Abca6</i>	<i>Abca6</i> , similar to ATP-binding cassette, subfamily A (ABC1), member 6	IPI00762951	13	U	T	0.76	6	4.61
<i>Abca8a</i>	<i>Abca8a</i> , similar to ATP-binding cassette, subfamily A (ABC1), member 8a	IPI00763783	11	PM	T	NA	4	1.18
<i>Abcb11</i>	<i>Abcb11</i> , bile salt export pump	IPI00195615	9	PM	T	0.90	15	14.76
<i>Abcc10</i>	<i>Abcc10</i> , ATP-binding cassette, subfamily C (CFTR/MRP), member 10	IPI00371742	14	PM	T	0.84	15	10.85
<i>Abcc2</i>	<i>Abcc2</i> , canalicular multispecific organic anion transporter 1	IPI00205806	14	PM	T	0.94	28	24.08
<i>Abcc6</i>	<i>Abcc6</i> , multidrug resistance-associated protein 6	IPI00207513	12	PM	T	0.97	17	17.58
<i>Ank</i>	<i>Ank</i> , progressive ankylosis protein homolog	IPI00765376	8	PM	T	NA	2	6.63
<i>Atp11c-ps1</i>	128-kDa protein	IPI00370178	8	U	T	0.63	25	27.32
<i>Atp2b1</i>	<i>Atp2b1</i> , isoform D of plasma membrane calcium-transporting ATPase 1	IPI00231268	7	PM	T	NA	5	4.26
<i>Atp8a1</i>	<i>Atp8a1</i> , similar to ATPase, aminophospholipid transporter (APLT), class I, type 8A, member 1	IPI00952342	8	PM	T	NA	10	9.08
<i>C7orf23</i>	RGD1562351, hypothetical protein LOC499990	IPI00565669	3	MPN	U	0.60	4	23.73
<i>C9orf91</i>	RGD1304595, hypothetical protein LOC298104	IPI00357901	2	U	U	NA	7	22.51
<i>Cacfd1</i>	RGD1311501, hypothetical protein LOC296599	IPI00363948	3	U	T	NA	2	14.62
<i>Gjb1</i>	<i>Gjb1</i> , Gap junction β -1 protein	IPI00207191	4	PM	T	NA	4	15.19
<i>Mfsd1</i>	<i>Mfsd1</i> , similar to major facilitator superfamily domain containing 1	IPI00373212	11	U	T	NA	6	18.75
<i>Myadm</i>	<i>Myadm</i> , myeloid-associated differentiation marker	IPI00339007	8	U	U	0.76	2	8.49
<i>P2rx4</i>	<i>P2rx4</i> , P2X purinoceptor 4	IPI00324987	2	PM	T	0.87	13	38.4
<i>Sid2</i>	<i>Sid2</i> , SID1 transmembrane family, member 2	IPI00369576	9	EL	U	0.82	4	6.23
<i>Slc12a9</i>	<i>Slc12a9</i> , solute carrier family 12 member 9	IPI00198772	11	PM	T	NA	6	9.85
<i>Slc22a1</i>	<i>Slc22a1</i> , isoform 1 of solute carrier family 22 member 1	IPI00213324	10	PM	T	0.77	6	15.81
<i>Slc22a7</i>	<i>Slc22a7</i> , solute carrier family 22 member 7	IPI00203971	11	PM	T	0.83	12	25.23
<i>Slc24a6</i>	<i>Slc24a6</i> , sodium/potassium/calcium exchanger 6	IPI00464527	12	PM	T	0.92	5	12.27
<i>Slc26a1</i>	<i>Slc26a1</i> , sulfate anion transporter 1	IPI00207298	9	PM	T	0.74	10	25.6
<i>Slc31a1</i>	<i>Slc31a1</i> , high affinity copper uptake protein 1	IPI00231403	3	PM	T	0.79	5	16.58
<i>Slc37a2</i>	<i>Slc37a2</i> , similar to solute carrier family 37 (glycerol 3-phosphate transporter), member 2	IPI00569704	12	ER	T	0.98	5	16.4
<i>Slc38a4</i>	<i>Slc38a4</i> , sodium-coupled neutral amino acid transporter 4	IPI00189469	11	PM	T	0.95	7	14.63
<i>Slc38a7</i>	<i>Slc38a7</i> , putative sodium-coupled neutral amino acid transporter 7	IPI00421684	11	U	T	NA	7	10.8
<i>Slc39a1</i>	<i>Slc39a1</i> , similar to zinc transporter ZIP1	IPI00373235	6	PM	T	0.96	6	19.75
<i>Slc40a1</i>	<i>Slc40a1</i> , solute carrier family 40 member 1	IPI00326002	10	PM	T	NA	2	5.61
<i>Slc46a3</i>	<i>Slc46a3</i> , solute carrier family 46 member 3	IPI00364398	11	U	T	NA	2	5.86
<i>Slc4a1</i>	<i>Slc4a1</i> , solute carrier family 4, member 1	IPI00231379	10	PM	T	NA	6	8.41
<i>Slc7a2</i>	<i>Slc7a2</i> , cationic amino acid transporter-2	IPI00608159	16	PM	T	0.92	9	14.63
<i>Slc7a2</i>	<i>Slc7a2</i> , cationic amino acid transporter-2A	IPI00206144	14	PM	T	0.95	6	8.98
<i>Slco1b2</i>	<i>Slco1b2</i> , isoform 1 of solute carrier organic anion transporter family member 1B2	IPI00215390	11	PM	T	0.73	14	27.91
<i>Slco2a1</i>	<i>Slco2a1</i> , solute carrier organic anion transporter family member 2A1	IPI00231272	11	PM	T	0.76	3	5.13
<i>Slco2b1</i>	<i>Slco2b1</i> , solute carrier organic anion transporter family member 2B1	IPI00230858	12	U	T	0.75	3	5.56
<i>Syng2</i>	<i>Syng2</i> , synaptogyrin 2	IPI00200093	4	PM	U	0.72	2	4.7
<i>Sypl1</i>	<i>Sypl1</i> , synaptophysin-like protein	IPI00471762	3	Misc	U	0.95	4	20.16
<i>Tmem104</i>	<i>Tmem104</i> similar to CG5262-PA	IPI00778760	11	U	T	NA	6	11.29
<i>Tmem144</i>	<i>Tmem144</i> , transmembrane protein 144	IPI00373219	10	U	U	0.95	5	23.85

Table II—continued

Gene name	Description	Accession no.	TM	Localization	Function	Spl	No. of peptides	Coverage
<i>Tmem175</i>	Tmem175, transmembrane protein 175	IP100211068	9	U	U	NA	5	18.44
<i>Tmem192</i>	Tmem192, transmembrane protein 192	IP100364640	4	EL	U	NA	4	12.78
<i>Tmem50b</i>	Tmem50b, transmembrane protein 50B	IP100373040	4	ER	U	NA	2	12.03
<i>Tmem63a</i>	Tmem63a, similar to transmembrane protein 63a	IP100363369	11	EL	U	NA	4	5.1
<i>Ttyh2</i>	Ttyh2, similar to tweety 2	IP100763162	6	PM	T	NA	5	4.81
<i>Ttyh3</i>	Ttyh3, tweety homolog 3	IP100363776	5	PM	T	NA	4	7.44
<i>UST4r</i>	UST4r, putative integral membrane transport protein	IP100202688	7	U	T	0.89	6	10.33

functionally known proteins, and there is no other clue about its function. TTYH2 and TTYH3 may represent large conductance anion channels (64). The remaining candidates correspond to orphan members from distinct transporter families.

SLC46A3 (SoLute Carrier family 46 member 3), SLC37A2 (SoLute Carrier 37 family member 2), and MFSD1 (Major Facilitator Superfamily Domain-containing protein 1) belong to distant families within the Major Facilitator Superfamily of secondary transporters (65). MFSD1, which has previously been identified in proteomics analyses of lysosomes and phagosomes (14, 16, 19, 54, 59, 60), is responsive to the transcription factor TFEB, and it was considered as a promising lysosomal protein candidate (16, 50). Its lysosomal localization has been confirmed independently during the course of our study (66). SLC37A2 mediates sugar-phosphate/phosphate and phosphate/phosphate exchange in proteoliposomes (67).

SLC38A7 (SoLute Carrier family 38 member 7) belongs to the amino acid/polyamine/organocation superfamily (68). It has been reported to transport neutral and cationic amino acids at the plasma membrane during the course of this study (69), but signal-to-noise ratios were intriguingly low, suggesting that the actual role of SLC38A7 deserves further investigation. SLCO2B1/SLC21A9/OATP2B1 is an organic anion transporter that is stimulated at acidic pH (70). TMEM104 is an orphan member of the amino acid and auxin permease transporter family.

These candidates were transiently expressed as GFP or YFP fusion proteins in HeLa cells, and their intracellular distribution was compared with the lysosomal/late endosomal marker LAMP1. Interestingly, only three candidates did not overlap with LAMP1 but localized instead at the plasma membrane (STARD10 and SLCO2B1) or in LAMP1-negative puncta (LOH12CR1; data not shown). By contrast, the distribution of the nine other candidates extensively overlapped with LAMP1 (Fig. 7), thus confirming that they reside in lysosomes and validating the predictive value of the Lys-734 list.

DISCUSSION

The main concern in lysosome-oriented proteomic studies based on subcellular fractionation is the identification of true lysosomal residents, because of cofractionation of other organelles (37, 71). Thus, identification of lysosomal candidates

requires comparison of lysosome-enriched and -nonenriched fractions. A pioneer study performed by Callaghan and co-workers (15) aimed at identifying lysosomal membrane proteins from Triton WR1339 density-shifted lysosomes, also referred to as tritosomes. However, the actual lysosomal residency of several proteins identified in this study could not be established, because of the lack of comparative approach. Later on, a study of placental lysosomal proteins took advantage of the comparison between successive steps of the preparation and used a semi-quantitative label-free spectral counting method to select 86 lysosomal candidates (16). More recently, Lobel and co-workers (19) demonstrated the potential of coupling the selective lysosome density shift induced by Triton WR-1339 injection in rats with MS quantification by isobaric peptide labeling, for simultaneous identification and validation of lysosomal candidates. In this work, we compared lysosome-enriched and -non-enriched fractions obtained from rat liver by differential centrifugation and isopycnic density gradient centrifugation, followed by detergent or organic solvent extraction steps to reduce sample complexity prior to MS analysis. Our spectral count-based analysis provided us with an extensive list of 2,385 proteins (Mbl2385 list), including 32% of IMPs. Among these proteins, 734 were selected as significantly enriched in the lysosomal fraction (Lys-734 list).

To our knowledge, the Mbl2385 list is the most extensive published to date for lysosomes (15–17, 19, 72), phagosomes (54–56, 59, 60, 73, 74), or lysosome-related organelles (57, 58, 75–78). Its IMP content (32%) is much higher than that commonly obtained if no specific subfractionation treatment is performed (5–15% IMPs (34)), but it is very similar to that obtained in a study of placental lysosomal membranes that also used an organic solvent treatment (16). Because of our preparation protocol, we identified altogether IMPs and membrane-associated proteins, but soluble proteins as well, such as luminal lysosomal hydrolases. Indeed, centrifugation of the lysosomal membranes leads to sedimentation of aggregated inclusions from the lysosomal matrix and thus induces the presence of soluble lysosomal enzymes and of proteins being degraded (30). Moreover, soluble proteins might also be retained as entrapped in membrane fragments generated upon hypotonic lysis and subsequent resealing of the organelles. The Lys-734 list is also longer than those pre-

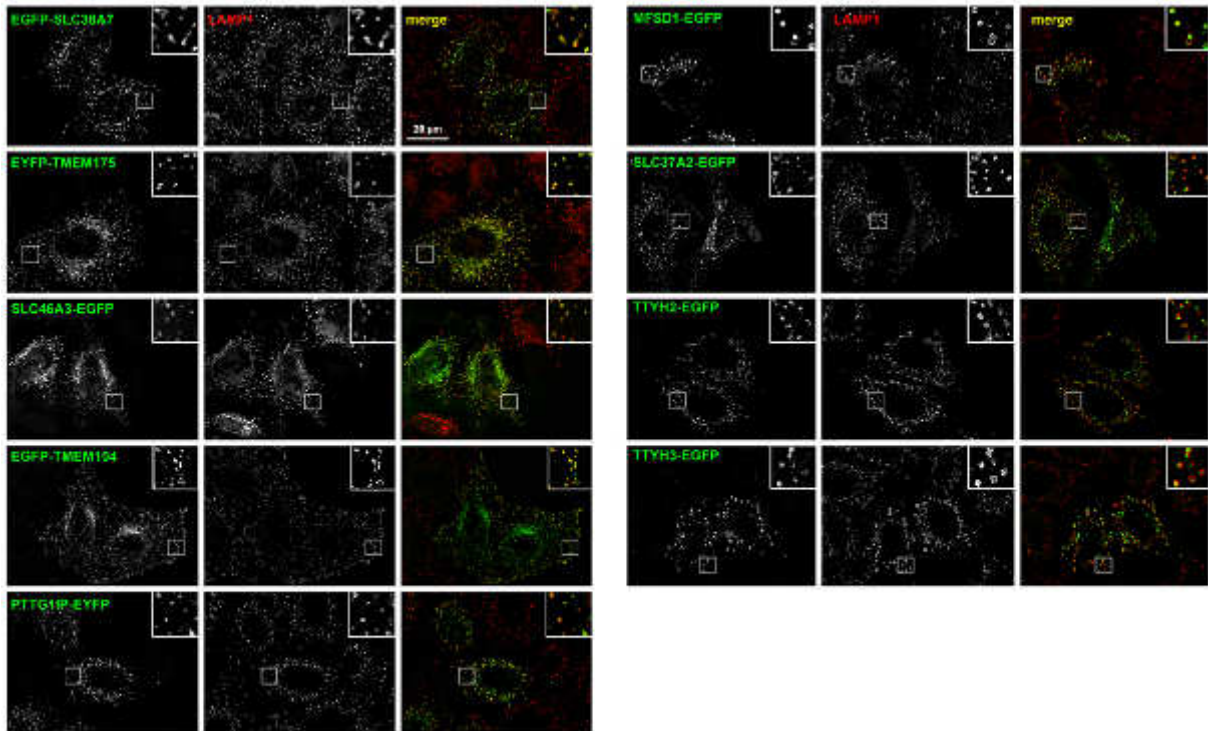


FIG. 7. **Subcellular localization of candidates in HeLa cells.** HeLa cells transiently expressing GFP- or YFP-tagged candidates were fixed, immunostained with an antibody directed against LAMP1, a late endosome and lysosome marker, and imaged by epifluorescence followed by deconvolution. Fluorescent protein-associated fluorescence, LAMP1 immunostaining, and merged images are shown from left to right. Insets are $\times 3$ magnification of the squared area. Scale bar, 20 μm .

sented in other comparative proteomic studies (124 proteins in Ref. 16 and 76 in Ref. 19). Comparison of these datasets indicates nevertheless rather important overlaps of 69 and 51 proteins, respectively.

As $\sim 80\%$ of the EL-annotated proteins but only 3.2% of contaminant proteins were recovered in the Lys-734 list, our semi-quantitative approach was able to strongly discriminate endo-lysosomal proteins from those of recognized contaminating organelles, such as mitochondria or endoplasmic reticulum. Nevertheless, the presence of proteins annotated as non-endo-lysosomal questions the significance of their selection, beside the possibility of false-positive retention. Additionally, among the EL proteins themselves, lysosomal proteins are not distinguished from proteins from other endocytic compartments (early or late endosomes).

The presence of proteins annotated to other compartments than lysosomes may represent true lysosomal residents with multiple subcellular locations, the lysosomal residency being either predominant or secondary. Indeed, as our data were restricted to fractions issued from the isopycnic density gradient, we do not know if the "lysosome-like" behavior observed for a given protein is representative of the whole cellular pool of protein or restricted to a small, specific subset.

For instance, the TGN marker TGN38 is depleted from the L fraction and mainly recovered in the PS fraction after differential centrifugation (Fig. 2). However, the minority of TGN38 proteins that cosegregated with lysosomes during differential centrifugation was concentrated in the MbL+ fraction after the subsequent centrifugation on a Nycodenz gradient (Fig. 2). A surprisingly high number of PM proteins (56%) was retained in the Lys-734 list. The presence of PM in the lysosome-enriched fraction has been discussed previously (37); it was shown that the small amount of PM proteins recovered in the L fraction ($\sim 5\%$) behaves like lysosomes on a metrizamide gradient, either as true PM residents or as lysosomal proteins. Migration of PM proteins between PM and lysosomes is conceivable. Indeed, the endocytic pathway constitutes a link between these two compartments, as numerous fusion/fission events occur between the various entities of the pathway (PM, endocytic vesicles, early and late endosomes, and lysosomes). Moreover, lysosomes are known to directly fuse with the PM in given circumstances (3). Such a dual localization has been suggested by observations of 5'-nucleotidase reactivity on the cytoplasmic face of lysosomes (37). This protein, which is considered as a PM marker, is notably present in the Lys-734 list.

in proteomic studies of phagosomes (54), lysosome-related organelles (57), or *Arabidopsis thaliana* vacuoles.³

Biogenesis of the lysosomes and delivery of endocytic cargo to these organelles involve numerous and highly dynamic membrane fusion and fission events between compartments of the endocytic pathway and with the secretory pathway, thus allowing protein import to, or retrieval from, lysosomes (3, 85). All complexes involved in these processes were present in the Lys-734 list (Fig. 8). Whereas numerous components of the ESCRT-III (Endosomal Sorting Complex Required for Transport-III) complex, which mediates the abscission of the newly forming intraluminal vesicles (86), were selected, none of the components of the ESCRT-0, -I, or -II complexes was identified. This was already the case in our recent proteomic analysis of the endocytic pathway of *Dictpostellum discoideum* (87) or in studies performed on the vacuolar membrane of *Arabidopsis thaliana*.³ The origin of this apparently "tighter" association of ESCRT-III with endo-lysosomal membranes (in contrast, ESCRT-0 and -I were detected in phagosomes (54)) deserves further investigation. As for the process of homo- or heterotypic fusion between late endosomes and lysosomes, it implies an initial tethering step mediated by the HOPS (homotypic fusion and vacuole protein sorting) complex (88). Very similarly, tethering in early endosomes homotypic fusion is performed by the CORVET (class C core vacuole-endosome transport) complex, which shares four subunits with HOPS (89). Interestingly, all HOPS components were present in the Lys-734 list, although none of the specific CORVET subunits could be detected. This is similar to what was observed in a proteomic study of the yeast vacuolar membrane (90).

Similarly to endosomes (91), lysosomes are now emerging as signaling platforms with the capability to detect modifications of the cell environment, such as energy, growth factors, and nutrient levels (92). Accordingly, many actors of signaling processes were enriched in the MbL+ fraction, such as receptors, α subunits of the heterotrimeric G proteins, protein kinases and a few Ras-related proteins. As half of these signaling proteins were PM-annotated, their additional endocytic localization might have been ignored until now. A key signaling pathway in nutrient sensing involves the master cell growth regulator mTOR that controls autophagy in response to a wide range of signals, including amino acid availability (93). Recent studies showed that the lysosome acts as an assembly site for a sensing device, the "nutrisome," which is composed of the RagA/B-RagC/D heterodimer, the Ragulator and mTORC1 complexes, the Rheb GTPase, and the V-ATPase (92, 94). Most proteins from this pathway were present in the Lys-734 list (Fig. 8).

Conclusions and Perspectives—Almost a hundred proteins, in which subcellular localization had never been described nor predicted, were sorted out as novel putative lysosomal proteins

³ N. Jamo and M. Jaquinod, personal communication.

in this study. Concerning molecular transporters, 46 candidates were selected, most of which were either devoid of subcellular annotation or annotated as plasma membrane proteins, suggesting a dual localization for the latter. The lysosomal subcellular localization was validated for nine candidates, including five secondary transporters, further supporting the relevance of our list of candidate lysosomal proteins. The numerous novel candidates revealed by this work should promote new research and help with understanding the cell biology, physiology, and pathophysiology of this important organelle.

Acknowledgments—We thank L. Aubry and G. Klein for their stimulating support and L. Aubry for critical reading of the manuscript. We thank A. Kraut for technical help; C. Adam, D. Barthe, and V. Dupieris for the homemade software support, and Y. Vandembrouck for Blast searches. We also thank M. Court and C. Masselon for writing the Spl analysis script. Author contributions: J.G., B.G., M.J., and A.J. conceived the project. J.T. and A.C. prepared samples for proteomics analysis. S.K.J. performed the mass spectrometry analysis. A.J. analyzed proteomic data. M.M. and A.J. performed statistical analysis. A.J., C.S., C.I., and Q.V. performed molecular biology experiments and subcellular localization analyses. C.B. supervised software developments for protein identification and parsimony analysis. A.J., B.G., M.J., and J.G. wrote the manuscript.

* This work was supported by Fonds de la Recherche Scientifique Grant 2.4543.08 and a grant from the Cystinosis Research Foundation (to B.G.).

§ This article contains supplemental material.

¶ To whom correspondence should be addressed: IRTSV/BGE/ODYCell, CEA-Grenoble, 17, Rue des Martyrs, 38054 Grenoble Cedex 9, France. Tel.: 33-438-785-419; Fax: 33-438-783-065; E-mail: ajournet@cea.fr.

REFERENCES

1. Scriver, C. R., Beaudet, A. L., Sly, W. S., Valle, D., and Childs, B. (eds) (2001) *The Metabolic and Molecular Basis of Inherited Disease*, 8th Ed., McGraw-Hill Inc., New York
2. Lübke, T., Lobel, P., and Sleat, D. (2009) Proteomics of the lysosome. *Biochim. Biophys. Acta* **1793**, 625–635
3. Luzio, J. P., Pryor, P. R., and Bright, N. A. (2007) Lysosomes: fusion and function. *Nat. Rev. Mol. Cell Biol.* **8**, 622–632
4. Jaquinod, S. K., Chapel, A., Garin, J., and Journet, A. (2008) Affinity purification of soluble lysosomal proteins for mass spectrometric identification. *Methods Mol. Biol.* **432**, 243–258
5. Sleat, D. E., Della Valle, M. C., Zheng, H., Moore, D. F., and Lobel, P. (2008) The Mannose 6-phosphate glycoprotein proteome. *J. Proteome Res.* **7**, 3010–3021
6. Sleat, D. E., Zheng, H., Qian, M., and Lobel, P. (2006) Identification of sites of mannose 6-phosphorylation on lysosomal proteins. *Mol. Cell. Proteomics* **5**, 696–701
7. Czupalla, C., Mansukoski, H., Riedl, T., Thiel, D., Krause, E., and Hofflack, B. (2006) Proteomic analysis of lysosomal acid hydrolases secreted by osteoclasts: implications for lytic enzyme transport and bone metabolism. *Mol. Cell. Proteomics* **5**, 134–143
8. Sleat, D. E., Lackland, H., Wang, Y., Sohar, I., Xiao, G., Li, H., and Lobel, P. (2005) The human brain mannose 6-phosphate glycoproteome: A complex mixture composed of multiple isoforms of many soluble lysosomal proteins. *Proteomics* **5**, 1520–1532
9. Kollmann, K., Mutenda, K. E., Balleininger, M., Eckermann, E., von Figura, K., Schmidt, B., and Lübke, T. (2005) Identification of novel lysosomal matrix proteins by proteome analysis. *Proteomics* **5**, 3966–3978
10. Journet, A., Chapel, A., Kieffer, S., Roux, F., and Garin, J. (2002) Proteomic analysis of human lysosomes: Application to monocytic and breast cancer cells. *Proteomics* **2**, 1026–1040
11. Journet, A., Chapel, A., Kieffer, S., Louwagie, M., Luche, S., and Garin, J.

- (2000) Towards human repertoire of monocytic lysosomal proteins. *Electrophoresis* **21**, 3411–3419
12. Kornfeld, S. (1986) Trafficking of lysosomal enzymes in normal and disease states. *J. Clin. Invest.* **77**, 1–6
 13. Sleat, D. E., Jadot, M., and Lobel, P. (2007) Lysosomal proteomics and disease. *Proteomics Clin. Appl.* **1**, 1134–1146
 14. Zhang, H., Fan, X., Bagshaw, R. D., Zhang, L., Mahuran, D. J., and Callahan, J. W. (2007) Lysosomal membranes from beige mice contain higher than normal levels of endoplasmic reticulum proteins. *J. Proteome Res.* **6**, 240–249
 15. Bagshaw, R. D., Mahuran, D. J., and Callahan, J. W. (2005) A proteomic analysis of lysosomal integral membrane proteins reveals the diverse composition of the organelle. *Mol. Cell. Proteomics* **4**, 133–143
 16. Schröder, B., Wrocklage, C., Pan, C., Jäger, R., Kösters, B., Schäfer, H., Elässer, H. P., Mann, M., and Hasilik, A. (2007) Integral and associated lysosomal membrane proteins. *Traffic* **8**, 1676–1686
 17. Duclos, S., Clavirho, G., Rousserie, G., Goyette, G., Boulais, J., Camossetto, V., Gatti, E., LaBrosse, S., Pierre, P., and Desjardins, M. (2011) The endosomal proteome of macrophage and dendritic cells. *Proteomics* **11**, 854–864
 18. Stahl, S., Reinders, Y., Asan, E., Mothes, W., Conzelmann, E., Sickmann, A., and Felber, U. (2007) Proteomic analysis of cathepsin B- and L-deficient mouse brain lysosomes. *Biochim. Biophys. Acta* **1774**, 1237–1246
 19. Della Valle, M. C., Sleat, D. E., Zheng, H., Moore, D. F., Jadot, M., and Lobel, P. (2011) Classification of subcellular location by comparative proteomic analysis of native and density-shifted lysosomes. *Mol. Cell. Proteomics* **10**, M110.006403
 20. Jensen, A. G., Chemali, M., Chapel, A., Kieffer-Jaquinod, S., Jadot, M., Garin, J., and Journet, A. (2007) Biochemical characterization and lysosomal localization of the mannose 6-phosphate protein p76 (hypothetical protein LOC196463). *Biochem. J.* **402**, 449–456
 21. Boonen, M., Hamer, I., Bouessac, M., Delsaute, A. F., Flamion, B., Garin, J., and Jadot, M. (2006) Intracellular localization of p40, a protein identified in a preparation of lysosomal membranes. *Biochem. J.* **395**, 39–47
 22. Deuschl, F., Kollmann, K., von Figura, K., and Lübke, T. (2006) Molecular characterization of the hypothetical 66.3-kDa protein in mouse: Lysosomal targeting, glycosylation, processing and tissue distribution. *FEBS Lett.* **580**, 5747–5752
 23. Della Valle, M. C., Sleat, D. E., Sohar, I., Wen, T., Pintar, J. E., Jadot, M., and Lobel, P. (2006) Demonstration of lysosomal localization for the mammalian ependymin-related protein using classical approaches combined with a novel density-shift method. *J. Biol. Chem.* **281**, 35436–35445
 24. Campomenosi, P., Salls, S., Lindqvist, C., Mariani, D., Nordström, T., Acquati, F., and Taramelli, R. (2006) Characterization of RNASET2, the first human member of the RH/T2/S family of glycoproteins. *Arch. Biochem. Biophys.* **449**, 17–26
 25. Jialin, G., Xuefan, G., and Huiwen, Z. (2010) SID1 transmembrane family, member 2 (Sid12): a novel lysosomal membrane protein. *Biochem. Biophys. Res. Commun.* **402**, 588–594
 26. Schieweck, O., Damme, M., Schröder, B., Hasilik, A., Schmidt, B., and Lübke, T. (2009) NCU-G1 is a highly glycosylated integral membrane protein of the lysosome. *Biochem. J.* **422**, 83–90
 27. Savalas, L. R., Gasnier, B., Damme, M., Lübke, T., Wrocklage, C., Debecker, C., Jézégou, A., Reinheckel, T., Hasilik, A., Saftig, P., and Schröder, B. (2011) Disrupted in renal carcinoma 2 (DIRC2), a novel transporter of the lysosomal membrane, is proteolytically processed by cathepsin L. *Biochem. J.* **439**, 113–128
 28. Lang, C. M., Fellerer, K., Schwenk, B. M., Kuhn, P. H., Kremmer, E., Edbauer, D., Capell, A., and Haass, C. (2012) Membrane orientation and subcellular localization of transmembrane protein 106B (TMEM106B), a major risk factor for frontotemporal lobar degeneration. *J. Biol. Chem.* **287**, 19355–19365
 29. Coelho, D., Kim, J. C., Mousse, I. R., Fung, S., du Moulin, M., Buers, I., Suormala, T., Burda, P., Frapoll, M., Stucki, M., Nürnberg, P., Thiele, H., Robenek, H., Höhne, W., Longo, N., Pasquali, M., Mengel, E., Watkins, D., Shoubbridge, E. A., Majewski, J., Rosenblatt, D. S., Fowler, B., Rutsch, F., and Baumgartner, M. R. (2012) Mutations in ABCD4 cause a new inborn error of vitamin B12 metabolism. *Nat. Genet.* **44**, 1152–1155
 30. Schröder, B. A., Wrocklage, C., Hasilik, A., and Saftig, P. (2010) The proteome of lysosomes. *Proteomics* **10**, 4053–4076
 31. Pisoni, R. L., and Thoens, J. G. (1991) The transport systems of mammalian lysosomes. *Biochim. Biophys. Acta* **1071**, 351–373
 32. Mancini, G. M., Havelaar, A. C., and Verheijen, F. W. (2000) Lysosomal transport disorders. *J. Inher. Metab. Dis.* **23**, 278–292
 33. Sagné, C., and Gasnier, B. (2008) Molecular physiology and pathophysiology of lysosomal membrane transporters. *J. Inher. Metab. Dis.* **31**, 258–266
 34. Speers, A. E., and Wu, C. C. (2007) Proteomics of integral membrane proteins—theory and application. *Chem. Rev.* **107**, 3667–3714
 35. Tan, S., Tan, H. T., and Chung, M. C. (2008) Membrane proteins and membrane proteomics. *Proteomics* **8**, 3924–3932
 36. Jézégou, A., Linares, E., Anne, C., Kieffer-Jaquinod, S., O'Regan, S., Aupetit, J., Chabli, A., Sagné, C., Debecker, C., Chadefaux-Vekemans, B., Journet, A., André, B., and Gasnier, B. (2012) Heptahelical protein PQLC2 is a lysosomal cationic amino acid exporter underlying the action of cysteamine in cystinosis therapy. *Proc. Natl. Acad. Sci. U.S.A.* **109**, E3434–E3443
 37. Wattiaux, R., Wattiaux-De Coninck, S., Romeaux-dupul, M. F., and Dubois, F. (1978) Isolation of rat liver lysosomes by isopycnic centrifugation in a metrizamide gradient. *J. Cell Biol.* **78**, 349–368
 38. Peters, T. J., Müller, M., and De Duve, C. (1972) Lysosomes of the arterial wall. I. Isolation and subcellular fractionation of cells from normal rabbit aorta. *J. Exp. Med.* **136**, 1117–1139
 39. Salvi, D., Rolland, N., Joyard, J., and Ferro, M. (2008) Purification and proteomic analysis of chloroplasts and their sub-organelle compartments. *Methods Mol. Biol.* **432**, 19–36
 40. Donoghue, P. M., Hughes, C., Vissers, J. P., Langridge, J. I., and Dunn, M. J. (2008) Nonionic detergent phase extraction for the proteomic analysis of heart membrane proteins using label-free LC-MS. *Proteomics* **8**, 3895–3905
 41. Laemmli, U. K. (1970) Cleavage of structural proteins during the assembly of the head of bacteriophage T4. *Nature* **227**, 680–685
 42. Duperris, V., Masselon, C., Court, M., Kieffer-Jaquinod, S., and Bruley, C. (2009) A toolbox for validation of mass spectrometry peptides identification and generation of database: IRMA. *Bioinformatics* **25**, 1980–1981
 43. Vizcaino, J. A., Côté, R., Reisinger, F., Foster, J. M., Mueller, M., Rameseder, J., Hermjakob, H., and Martens, L. (2009) A guide to the Proteomics Identifications Database proteomics data repository. *Proteomics* **9**, 4276–4283
 44. Liu, H., Sadygov, R. G., and Yates, J. R., 3rd (2004) A model for random sampling and estimation of relative protein abundance in shotgun proteomics. *Anal. Chem.* **76**, 4193–4201
 45. Fu, X., Gharib, S. A., Green, P. S., Aitken, M. L., Frazer, D. A., Park, D. R., Vaisar, T., and Heinecke, J. W. (2008) Spectral index for assessment of differential protein expression in shotgun proteomics. *J. Proteome Res.* **7**, 845–854
 46. Gilchrist, A., Au, C. E., Hiding, J., Bell, A. W., Fernandez-Rodriguez, J., Lesimple, S., Nagaya, H., Roy, L., Gosline, S. J., Hallett, M., Paiement, J., Kearney, R. E., Nilsson, T., and Bergeron, J. J. (2006) Quantitative proteomics analysis of the secretory pathway. *Cell* **127**, 1265–1281
 47. Olsson, G. M., Svensson, I., Zdzolek, J. M., and Brunk, U. T. (1989) Lysosomal enzyme leakage during the hypoxanthine/xanthine oxidase reaction. *Virchows Arch. B Cell Pathol. Incl. Mol. Pathol.* **56**, 385–391
 48. Ford, T., Rickwood, D., and Graham, J. (1983) Buoyant densities of macromolecules, macromolecular complexes, and cell organelles in Nycodenz gradients. *Anal. Biochem.* **128**, 232–239
 49. Bordier, C. (1981) Phase separation of integral membrane proteins in Triton X-114 solution. *J. Biol. Chem.* **256**, 1604–1607
 50. Sardiello, M., Palmieri, M., di Ronza, A., Medina, D. L., Valenza, M., Genarino, V. A., Di Malta, C., Donaudy, F., Embrione, V., Polishchuk, R. S., Banfi, S., Parenti, G., Cattaneo, E., and Ballabio, A. (2009) A gene network regulating lysosomal biogenesis and function. *Science* **325**, 473–477
 51. Boonen, M., Rezen de Castro, R., Cuvelier, G., Hamer, I., and Jadot, M. (2008) A dileucine signal situated in the C-terminal tail of the lysosomal membrane protein p40 is responsible for its targeting to lysosomes. *Biochem. J.* **414**, 431–440
 52. Rutsch, F., Gallus, S., Mousse, I., Suormala, T., Sagné, C., Toliat, M. R., Nürnberg, G., Wittkamp, T., Buers, I., Shariff, A., Stucki, M., Becker, C., Baumgartner, M., Robenek, H., Marquardt, T., Höhne, W., Gasnier, B., Rosenblatt, D. S., Fowler, B., and Nürnberg, P. (2009) Identification of a putative lysosomal cobalamin exporter altered in the cbf1 defect of

- vitamin B₁₂ metabolism. *Nat. Genet.* **41**, 234–239
53. Siintola, E., Topcu, M., Aula, N., Lohi, H., Minassian, B. A., Paterson, A. D., Liu, X. Q., Wilson, C., Lahtinen, U., Anttonen, A. K., and Lehesjoki, A. E. (2007) The novel neuronal ceroid lipofuscinosis gene *MFSD8* encodes a putative lysosomal transporter. *Am. J. Hum. Genet.* **81**, 136–146
 54. Boulais, J., Trost, M., Landry, C. R., Dieckmann, R., Levy, E. D., Soldati, T., Michnick, S. W., Thibault, P., and Desjardins, M. (2010) Molecular characterization of the evolution of phagosomes. *Mol. Syst. Biol.* **6**, 423
 55. Buschow, S. I., Lasonder, E., Szklarczyk, R., Oud, M. M., de Vries, I. J., and Figdor, C. G. (2012) Unraveling the human dendritic cell phagosome proteome by organellar enrichment ranking. *J. Proteomics* **75**, 1547–1562
 56. Li, Q., Singh, C. R., Ma, S., Price, N. D., and Jagannath, C. (2011) Label-free proteomics and systems biology analysis of mycobacterial phagosomes in dendritic cells and macrophages. *J. Proteome Res.* **10**, 2425–2439
 57. Raymond, A. A., Gonzalez de Peredo, A., Stella, A., Ishida-Yamamoto, A., Bouyssié, D., Serré, G., Monsarrat, B., and Simon, M. (2008) Lamellar bodies of human epididymis: proteomics characterization by high throughput mass spectrometry and possible involvement of CLIP-170 in their trafficking/secretion. *Mol. Cell. Proteomics* **7**, 2151–2175
 58. Schmidt, H., Gelhaus, C., Nebendahl, M., Lettau, M., Lucius, R., Leippe, M., Kabelitz, D., and Janssen, O. (2011) Effector granules in human T lymphocytes: proteomic evidence for two distinct species of cytotoxic effector vesicles. *J. Proteome Res.* **10**, 1603–1620
 59. Shui, W., Sheu, L., Liu, J., Smart, B., Petzold, C. J., Hsieh, T. Y., Pletcher, A., Keasling, J. D., and Bertozzi, C. R. (2008) Membrane proteomics of phagosomes suggests a connection to autophagy. *Proc. Natl. Acad. Sci. U.S.A.* **105**, 16952–16957
 60. Shui, W., Petzold, C. J., Redding, A., Liu, J., Pletcher, A., Sheu, L., Hsieh, T. Y., Keasling, J. D., and Bertozzi, C. R. (2011) Organelle membrane proteomics reveals differential influence of mycobacterial lipoglycans on macrophage phagosome maturation and autophagosome accumulation. *J. Proteome Res.* **10**, 339–348
 61. Trost, M., English, L., Lemieux, S., Courcelles, M., Desjardins, M., and Thibault, P. (2009) The phagosomal proteome in interferon-gamma-activated macrophages. *Immunity* **30**, 143–154
 62. Chien, W., and Pei, L. (2000) A novel binding factor facilitates nuclear translocation and transcriptional activation function of the pituitary tumor-transforming gene product. *J. Biol. Chem.* **275**, 19422–19427
 63. Smith, V. E., Read, M. L., Turnell, A. S., Sharma, N., Lewy, G. D., Fong, J. C., Seed, R. I., Kwan, P., Ryan, G., Mehanna, H., Chan, S. Y., Darras, V. M., Boelsert, K., Franklyn, J. A., and McCabe, C. J. (2012) PTTG-binding factor (PBF) is a novel regulator of the thyroid hormone transporter MCT8. *Endocrinology* **153**, 3526–3536
 64. Suzuki, M., and Mizuno, A. (2004) A novel human Cl⁻ channel family related to *Drosophila* flightless locus. *J. Biol. Chem.* **279**, 22461–22466
 65. Pao, S. S., Paulsen, I. T., and Saier, M. H., Jr. (1998) Major facilitator superfamily. *Microbiol. Mol. Biol. Rev.* **62**, 1–34
 66. Palmieri, M., Impey, S., Kang, H., di Ronza, A., Pelz, C., Sardiello, M., and Ballabio, A. (2011) Characterization of the CLEAR network reveals an integrated control of cellular clearance pathways. *Hum. Mol. Genet.* **20**, 3852–3866
 67. Pan, C. J., Chen, S. Y., Jun, H. S., Lin, S. R., Mansfield, B. C., and Chou, J. Y. (2011) SLC37A1 and SLC37A2 are phosphate-linked, glucose 6-phosphate antiporters. *PLoS ONE* **6**, e23157
 68. Jack, D. L., Paulsen, I. T., and Saier, M. H. (2000) The amino acid/polyamine/organocation (APC) superfamily of transporters specific for amino acids, polyamines, and organocations. *Microbiology* **146**, 1797–1814
 69. Häggglund, M. G., Sreedharan, S., Nilsson, V. C., Shaik, J. H., Almkvist, I. M., Bäcklin, S., Wrangé, O., and Fredrikson, R. (2011) Identification of SLC36A7 (SNAT7) protein as a glutamine transporter expressed in neurons. *J. Biol. Chem.* **286**, 20500–20511
 70. Kobayashi, D., Nozawa, T., Imai, K., Nezu, J., Tsuji, A., and Tamai, I. (2003) Involvement of human organic anion transporting polypeptide OATP-B (SLC21A9) in pH-dependent transport across intestinal apical membrane. *J. Pharmacol. Exp. Ther.* **306**, 703–708
 71. Bergeron, J. J., Au, C. E., Desjardins, M., McPherson, P. S., and Nilsson, T. (2010) Cell biology through proteomics—ad astra per astra porci. *Trends Cell Biol.* **20**, 337–345
 72. Nylandsted, J., Becker, A. C., Bunkenborg, J., Andersen, J. S., Dengjel, J., and Jäätelä, M. (2011) ErbB2-associated changes in the lysosomal proteome. *Proteomics* **11**, 2830–2838
 73. Garin, J., Diez, R., Kieffer, S., Dermine, J. F., Duclos, S., Gagnon, E., Sadoul, R., Rondeau, C., and Desjardins, M. (2001) The phagosome proteome: insight into phagosome functions. *J. Cell Biol.* **152**, 165–180
 74. Rogers, L. D., and Foster, L. J. (2007) The dynamic phagosomal proteome and the contribution of the endoplasmic reticulum. *Proc. Natl. Acad. Sci. U.S.A.* **104**, 18520–18525
 75. Schmidt, H., Gelhaus, C., Nebendahl, M., Lettau, M., Lucius, R., Leippe, M., Kabelitz, D., and Janssen, O. (2011) Effector granules in human T lymphocytes: the luminal proteome of secretory lysosomes from human T cells. *Cell Commun. Signal.* **9**, 4
 76. Ridsdale, R., Na, C. L., Xu, Y., Greis, K. D., and Weaver, T. (2011) Comparative proteomic analysis of lung lamellar bodies and lysosome-related organelles. *PLoS ONE* **6**, e16482
 77. Lominadze, G., Powell, D. W., Luerman, G. C., Link, A. J., Ward, R. A., and McLeish, K. R. (2005) Proteomic analysis of human neutrophil granules. *Mol. Cell. Proteomics* **4**, 1503–1521
 78. Basur, V., Yang, F., Kushimoto, T., Higashimoto, Y., Yasumoto, K., Valencia, J., Muller, J., Vieira, W. D., Watabe, H., Shabanowitz, J., Hearing, V. J., Hunt, D. F., and Appella, E. (2003) Proteomic analysis of early melanosomes: identification of novel melanosomal proteins. *J. Proteome Res.* **2**, 69–79
 79. Caviston, J. P., and Holzbaur, E. L. (2006) Microtubule motors at the intersection of trafficking and transport. *Trends Cell Biol.* **16**, 530–537
 80. Krendel, M., and Mooseker, M. S. (2005) Myosins: tails (and heads) of functional diversity. *Physiology* **20**, 239–251
 81. Sorkin, A., and von Zastrow, M. (2009) Endocytosis and signalling: intertwining molecular networks. *Nat. Rev. Mol. Cell Biol.* **10**, 609–622
 82. Melman, L., Geuze, H. J., Li, Y., McCormick, L. M., Van Kerkhof, P., Strous, G. J., Schwartz, A. L., and Bu, G. (2002) Proteasome regulates the delivery of LDL receptor-related protein into the degradation pathway. *Mol. Biol. Cell* **13**, 3325–3335
 83. Longva, K. E., Blystad, F. D., Stang, E., Larsen, A. M., Johannessen, L. E., and Madhus, I. H. (2002) Ubiquitination and proteasomal activity is required for transport of the EGF receptor to inner membranes of multivesicular bodies. *J. Cell Biol.* **156**, 843–854
 84. Dong, J., Chen, W., Welford, A., and Wandinger-Ness, A. (2004) The proteasome α -subunit XAPC7 interacts specifically with Rab7 and late endosomes. *J. Biol. Chem.* **279**, 21334–21342
 85. McGough, I. J., and Cullen, P. J. (2011) Recent advances in retromer biology. *Traffic* **12**, 963–971
 86. Adell, M. A., and Tels, D. (2011) Assembly and disassembly of the ESCRT-III membrane scission complex. *FEBS Lett.* **585**, 3191–3196
 87. Journet, A., Klein, G., Brugière, S., Vandenbergue, Y., Chapel, A., Kieffer, S., Bruley, C., Masselon, C., and Aubry, L. (2012) Investigating the macrophagocytic proteome of *Dictyostellum amoebae* by high-resolution mass spectrometry. *Proteomics* **12**, 241–245
 88. Pryor, P. R., and Luzio, J. P. (2009) Delivery of endocytosed membrane proteins to the lysosome. *Biochim. Biophys. Acta* **1793**, 615–624
 89. Epp, N., Rethmeier, R., Krämer, L., and Ungermann, C. (2011) Membrane dynamics and fusion at late endosomes and vacuoles—Rab regulation, multisubunit tethering complexes and SNAREs. *Eur. J. Cell Biol.* **90**, 779–785
 90. Wiederhold, E., Gandhi, T., Permentier, H. P., Breiting, R., Poolman, B., and Slotboom, D. J. (2009) The yeast vacuolar membrane proteome. *Mol. Cell. Proteomics* **8**, 380–392
 91. Scita, G., and Di Fiore, P. P. (2010) The endocytic matrix. *Nature* **463**, 464–473
 92. Sancak, Y., Bar-Peled, L., Zoncu, R., Markhard, A. L., Nada, S., and Sabatini, D. M. (2010) Regulator-Rag complex targets mTORC1 to the lysosomal surface and is necessary for its activation by amino acids. *Cell* **141**, 290–303
 93. Sengupta, S., Peterson, T. R., and Sabatini, D. M. (2010) Regulation of the mTOR complex 1 pathway by nutrients, growth factors, and stress. *Mol. Cell* **40**, 310–322
 94. Zoncu, R., Bar-Peled, L., Efeyan, A., Wang, S., Sancak, Y., and Sabatini, D. M. (2011) mTORC1 senses lysosomal amino acids through an inside-out mechanism that requires the vacuolar H⁺-ATPase. *Science* **334**, 678–683

2. How to screen for new lysosomal transporters

Our proteomic study identified 46 new putative lysosomal transporters. I screened several of them using a systematic methodology to try to identify their molecular function. Another candidate, SPINSTER, although identified in the proteomic screen, was first identified as a potential target from genetic studies on *D. melanogaster*.

This methodology consists in:

- 1) expressing a fusion with EGFP to check for lysosomal localization;
- 2) expressing candidates at plasma membrane by mutating their lysosomal sorting motif;
- 3) screening substrates using radioactive uptake measurements and electrophysiology

2.1. Step 1: is the candidate lysosomal?

The first step in our screen was to generate a plasmid encoding a fusion between our protein of interest and EGFP. However, some transmembrane proteins have a tail in the lysosomal lumen, which contains active proteases. This could result in cleaving the bond between EGFP and our protein, or EGFP itself.

To avoid this, the topology of the protein of interest was first predicted using TMHMM server v2.0 (<http://www.cbs.dtu.dk/services/TMHMM/>). We then selected for fusion a cytosolic end of the putative transporter polypeptide and generated a plasmid encoding the EGFP-fused protein.

Proteins of interest fused to EGFP were overexpressed in HeLa cells using electroporation, which resulted in milder expression levels and thus reduced localization artefacts. HeLa cells are helpful as well to assess the localization of proteins, since, contrary to HEK-293T or Cos-7, they cannot replicate plasmid with a SV40 origin, which keeps the overexpression at mild levels. It should indeed be pointed out that overexpression might result in slight artefacts of localisation and lifespan of proteins. These modifications can be due to the saturation of synthesis and maturation machineries or to an activation of degradation machineries, such as autophagy pathways or proteasome-mediated degradation.

Eleven out of the 25 tested proteins remained in the ER even after 48 hours of expression. As ER was a significant contaminant of lysosomal fractions during our proteomic study, some of them could indeed have been resident proteins of the ER. Yet, most of them were probably unable to go through quality control in the ER. These proteins were thus not studied further. This showed that going through quality control in the ER was the most critical milestone to be reached when it came to appropriate overexpression of fusion proteins.

After 48 hours of expression, cells were fixed and the subcellular localisation of LAMP1 was revealed by immunofluorescence. LAMP-1 is one of the most abundant membrane proteins in late endosomes and lysosomes. Comparing the subcellular localisation of a protein of interest with LAMP1 distribution is an easy method to determine whether a protein is expressed in lysosomes or late endosomes. Proteins of interest were taken to the next step only if colocalization with LAMP-1 was satisfactory.

2.2. Step 2: is it possible to express the candidate at plasma membrane?

Lysosomal transporters are more challenging to study than plasma membrane transporters because of their localization on endomembranes. To bypass this difficulty, lysosomal transporters can be misrouted to plasma membrane by mutating their sorting motif. Lysosomal transporters are normally selected by adaptors either in the Golgi or, after secretion, at the plasma membrane, to be sorted to endosomes and then lysosomes. On the other hand, mutated proteins lacking the sorting motif(s) undergo synthesis in the ER, maturation in the Golgi and are sent by default to the plasma membrane via the secretory pathway (see Fig 6).

Because membrane topology is conserved during intracellular trafficking, the cellular model expressing the lysosomal transporter of interest at its surface is equivalent to a giant, inside-out lysosome. Lysosomal export is thus replaced by an easily tractable cellular uptake (see Fig 6). This approach has been developed by my host laboratory (Kalatzis EMBO J 2001) and successfully applied to diverse transporters.

Primary sequences of proteins of interest were thus screened for putative sorting motifs. We tried to identify three types of motifs:

- tyrosine-based: YXXØ (X being any amino acid and Ø a big and non polar one), and
- dileucine-based:
 - * DXLL,
 - * [D/E]XXXLL (X being any amino acid).

Using the former TMHMM topology prediction, we firstly focused on motifs predicted in cytosolic loops of proteins of interest and mutated them. Sorting motifs have indeed been shown to be recognized by cytosolic adaptors to trigger sorting from the Golgi to endosomes.

Then, mutated proteins fused to EGFP were overexpressed in HeLa cells. We selected for functional assays the mutated proteins that showed significant localisation at the plasma membrane.

2.3. Step 3: functional assays

Most functional assays were performed in *Xenopus* oocytes, because they have very few transporters of sugars or amino acids in their plasma membrane, contrary to mammalian cells. In addition, the transporter candidate can be expressed at very high levels (up to 10^{11} molecules per oocyte)⁸³. Thus, it is much easier to detect transport signals in this expression system. To express misrouted lysosomal transporter fused to EGFP in *Xenopus* oocytes, specific expression plasmids were designed (pOX(+)-vector), which enables in vitro transcription of synthetic mRNAs, stabilized by both 5' and 3' UTR of a very abundant protein of *Xenopus* oocytes, beta globin. These mRNA were capped in vitro prior to injection.

Mainly two techniques were used for functional assays. Both have technical limitations, so they were used complementarily:

Radioactivity uptake: *Xenopus* oocytes expressing the protein of interest at the plasma membrane were incubated in buffers containing radiolabelled putative substrates. Oocytes were then washed and accumulated radioactivity quantified. Lysosomal transporters will mediate an influx into oocytes if, like most lysosomal transporters, they naturally mediate an export from lysosomes.

The pH gradient between lysosomes and the cytosol is critical for the activity of lysosomal transporters. To mimic it, a gradient between cytosol and extracellular medium was artificially created by using pH 5.0 transport buffers.

Radioactivity uptake assays are quite quick and easy. However, radioactive molecules are quite pricy and not always commercially available, which limited the use of this technique. Moreover, variability between oocytes of the same batch can be quite high.

Two-electrode voltage clamp (TEVC): For this technique *Xenopus* oocytes expressing the protein of interest at the plasma membrane were impaled with two electrodes: one to measure electric potential and the other to inject an automatically adjusted current which maintains the potential at a fixed level chosen by the operator (voltage “clamp”). This current reflects fluxes of ions across the membrane and is used as read-out to measure the activity of electrogenic transporters. In our experiment, oocytes were clamped at -40mV and the baseline current was monitored in substrate-free pH 5.0 buffer. Oocytes are then perfused with the same buffer, but containing the putative substrate. If substrates are transported in an electrogenic manner, inward or outward currents should be observed, depending on the charge of the substrate. An inward current corresponds to the entry of positive charges or the exit of negative ones. An outward current corresponds to the entry of negative charges or the efflux of positive ones.

This assay is less quick than the previous one, but it enables to screen potentially any available substrate. The ability to clamp the membrane potential and the fact that test measurements and negative controls are recorded on a single oocyte limits the impact of the aforementioned inter-oocyte variability. A few substrates can even be screened on the same oocyte, thus facilitating accurate comparison between them. This technique has essentially one limitation: transport reactions must be electrogenic to trigger a current signal.

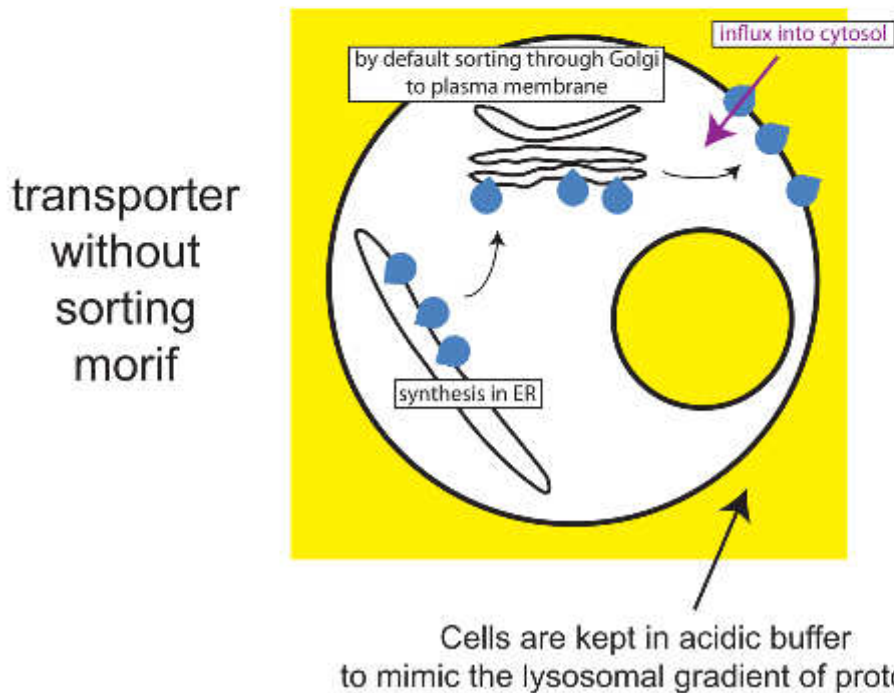
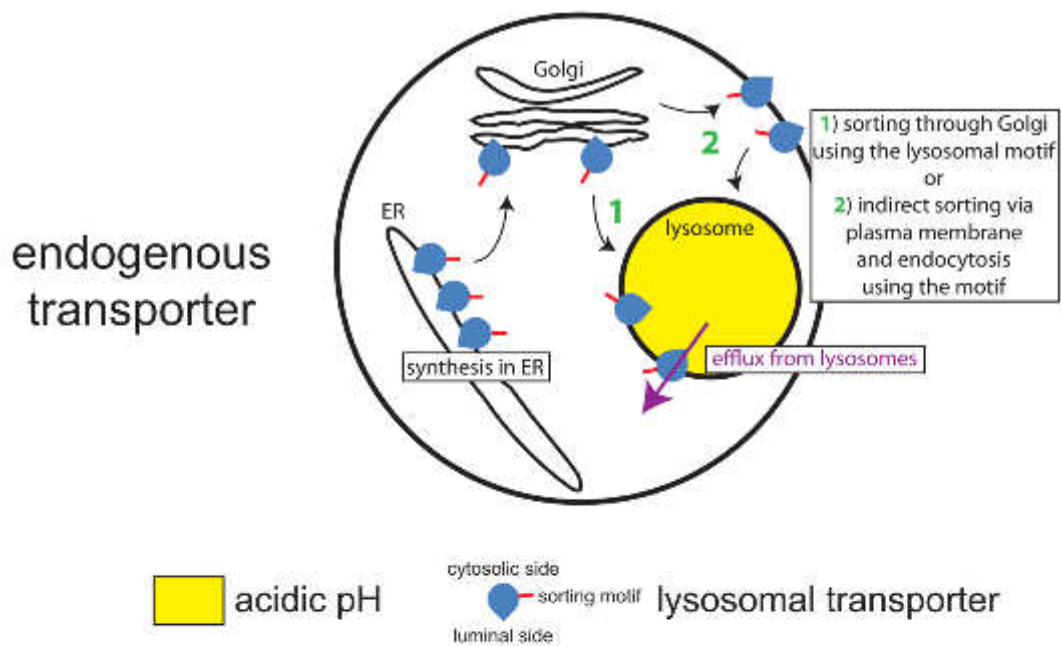


Figure 6: Lysosomal transporter misrouting as an approach to facilitate their functional study. Upper panel: lysosomal transporters are synthesized in the ER and transported to the Golgi. Some transporters are directly selected there by adaptor proteins and are sent to late endosomes, which fuse with lysosomes. Others reach lysosomes indirectly: there are delivered to the plasma membrane and selected there for endocytosis by adaptors. In lysosomes, most transporters mediate an efflux of lysosomal catabolites generated in the lumen (amino acids, sugars, etc). Similarly to lysosomal enzymes, this efflux activity is usually activated at low luminal pH and often actively driven through a proton cotransport process. Lower panel: when the sorting motif of lysosomal transporters is mutated, they are often sorted by default to the plasma membrane. In this approach, the lysosomal export of these transporters is replaced by a cellular influx. To study this influx, the acidity of the lysosomal lumen is mimicked by incubating cells in an acidic buffer.

2.4 Summary of the screening method

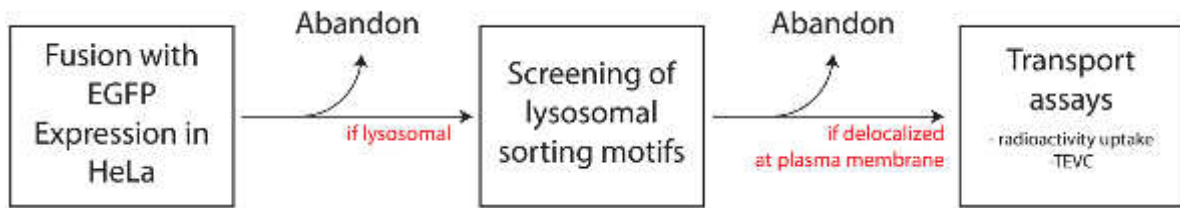


Figure 7: Workflow used to characterize orphan lysosomal transporters.

3. Study of five proteins of the lysosomal membrane:

TMEM104, SLC37A2, TTYH3, MFSD1 and SPINSTER1

3.1. TTYH3, a chloride channel

3.1.1. Introduction

Human *Ttyh3* is homologous to *tweety*, a *D.melanogaster* gene adjacent to the flightless gene. Flies mutated for *tweety* only display no phenotype. When mutated for the other genes of the locus (*dodo* and *penguin*), they only have a slightly reduced viability⁹⁰. In mammals, *ttyh3* is widely expressed in excitable tissues.

The corresponding protein and other TTYH isoforms have been described as a large conductance chloride channel activated by intracellular Ca²⁺ or cell swelling in a patch-clamp study⁹¹. However, subsequent studies of TTYH have failed to reproduce these data⁹². On the other hand, Ca²⁺-activated Cl⁻ channels have been identified to bestrophin and TMEM16 gene families, while volume-regulated anion channels have recently been identified to LRRC8 heteromers⁹³. The molecular function of TTYH proteins, including TTYH3, thus remained an open question.

TTYH3 has 5 or 6 transmembrane domains, depending on the prediction algorithm. Until the release of our proteomic study, its subcellular localisation was not precisely documented, although patch-clamp studies suggested that at least a fraction of proteins were present at plasma membrane.

3.1.2. Screening of the putative lysosomal sorting motif

TTYH3 has one putative sorting motif: 486ENTPLI, localized in the C-terminal tail.

A plasmid encoding the double mutant TTYH3 L491A/I492A EGFP was generated and overexpressed in HeLa cells. WT and LI/AA proteins had comparable subcellular distributions. In particular, TTYH3-LIAA-EGFP displayed no detectable expression at plasma membrane (see Fig 8). This suggested that TTYH3 depends on non-canonical motifs for its sorting to the lysosome. However, due to its localization on lysosomes, further studies were impossible.

New techniques such as patch-clamp of lysosomes or endosomes artificially enlarged using drugs (vacuoline) or recombinant proteins (Rab5-Q79L), could prove useful to study lysosomal transporters than cannot be sent to the plasma membrane⁹⁴.



Figure 8: Subcellular localisation of human TTYH3-EGFP and human TTYH3-LIAA-EGFP, overexpressed in HeLa cells. Mutant TTYH3 is not expressed at plasma membrane. Bar: 10µm.

3.2. TMEM104, a putative amino acid transporter

3.2.1. Introduction

No study has been published specifically on TMEM104. It belongs to the AAAP family (amino acid and auxin permease), like several transporters, including LYAAT-1, a lysosomal transporter for small neutral amino acids⁹⁵. This could be consistent with a role of amino acid transporter. In this study, for availability reasons, the mouse homolog was used. It has 11 predicted transmembrane domains.

3.2.2. Screening of the putative lysosomal sorting motif

There was no obvious region in TMEM104 possibly involved in its sorting to lysosomes. This protein has only one putative lysosomal sorting motif: 95 DSDLL, located in the second cytosolic loop. It is conserved between mice and rats, but not other animal species. In humans, chickens or zebrafishes, another type of motif is present at the same location (DXXXLL); however these motifs are selected by AP adaptors instead of GGA adaptors (see p20), which does not suggest a strong conservation of its function. This variability suggested that this motif might not be critical for the sorting of mTMEM104, but we still tried to mutate it in case hTMEM104 and mTMEM104 had different sorting mechanisms.

A plasmid encoding double mutant TMEM104 L95A/L96A EGFP was generated and overexpressed in HeLa cells. WT and LL/AA proteins had comparable subcellular distributions. In particular, TMEM104-LIAA-EGFP displayed no detectable expression at plasma membrane (see Fig 9)

Since TMEM104 belongs to a superfamily that contains amino acid transporters, it could be an interesting target for our amino acid lysosomal transporter screening test based on the transcription factor TFEB which will be introduced in Chapter 3, p122.

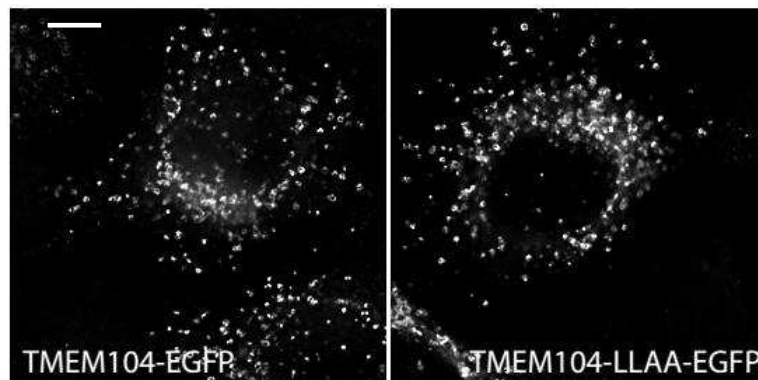


Figure 9: Subcellular localisation of mouse EGFP-TMEM104 and mouse EGFP-TMEM104-LLAA, overexpressed in HeLa cells. Mutant TMEM104 is not expressed at the plasma membrane. Bar: 10 μ m

3.3. SLC37A2, a putative glucose-6-phosphate transporter?

3.3.1. Introduction and sorting motif

a- Former results on SLC37A2

SLC37A2 has already been described as an ER antiporter of inorganic phosphate and glucose-6-phosphate. Transport assays were performed in proteoliposomes.⁹⁶

The description of SLC37A2 in the ER could look surprising considering it was found in our proteomic screen of lysosomal membranes. Localisation data in this article were performed using a fusion protein Flag-SLC37A2. This paper provides no information about how long the linker between Flag and SLC7A2 was. However, the length of linker is critical for correct folding of recently synthesized proteins in the ER. Localisation in the ER of integral membrane proteins fused with EGFP is not unusual, as our proteomic screen has shown (see Fig 10), but it is hard to discriminate between resident proteins of the ER and fusion proteins failing to pass through quality control. In our proteomic paper, EmGFP-fused human SLC37A2 was sorted to lysosomes. Fused of SLC37A2 was done at its C-terminus, whereas Flag was fused at the N-terminus in Pan et al. study. In addition, we designed a linker which was 15 amino acid-long, which is usually enough to provide satisfactory flexibility between both components of the fusion protein.

In addition, Pan et al. fixed their cells only 24h after infection with viruses. However, synthesis and sorting of lysosomal membrane consistently requires 48 hours to go through synthesis, glycosylations, sorting to the TGN, sorting to endosomes and eventually maturation of endosomes into lysosomes in systems routinely used in my host laboratory. 24 hours after transfection, fusion proteins are usually still under synthesis and sorting in the ER or Golgi apparatus. This difference in protocols could explain the difference between our study and the latter.

Thus, we decided to investigate in more detail the intracellular distribution of SLC37A2.

b- A natural variant of SLC37A2 is sorted to lysosomes

To address the intracellular distribution of SLC37A2, the existence of natural isoforms of this protein proved very informative. Human SLC37A2 has four different documented splicing isoforms. Isoform 1 has a lysosomal sorting motif in its cytosolic tail (496YKEI), which is present in all species, contrary to isoform 2 (496 SSMVLTHQ), only present in mouse and human. Isoforms 3 and 4 are truncated forms. In principle, isoforms 1 and 2 could have different localizations: at the lysosomal membrane for isoform 1, due to the sorting motif; and at plasma membrane for isoform 2, due to the absence of motif. We thus focused on these two isoforms. The plasmid was designed in the same way for both constructs, with the same linker.

They were both expressed mainly in lysosomes. However, SLC37A2-iso2-EmGFP was as well partially expressed at the plasma membrane (see Fig 10), possibly sufficiently to study SLC37A2 at this location. This alternative localisation is probably due to the lack of lysosomal sorting motif at the C-terminus of SLC37A2. Other putative lysosomal sorting motifs, such as 482 YKEI, were not studied. They may however be responsible for the partially lysosomal localisation of SLC37A2-iso2-EmGFP.

Altogether, these data:

- Invalidate the localization in the ER documented by Pan and colleagues and confirms that SLC37A2 is expressed at the lysosomal membrane.
- Suggest that a natural splicing variant, partially expressed at plasma membrane, could be suitable for functional studies.

SLC37A2 (isoform 2) was expressed in *Xenopus* oocytes by injections of mRNA. In oocytes, the protein was mainly expressed inside the oocyte, but as well partially at the plasma membrane, which suggested this model could be suitable to elucidate SLC37A2 function.

In addition to a possible function of transporter for phosphate sugars as reported by Pan et al 2011, we also investigated the possibility that SLC37A2 could be a transporter of phosphoglycerates for two reasons: firstly, because of the chemical similarity between these compounds and phosphate sugars; secondly, because phosphoglycerates are likely generated in lysosomes by phospholipid hydrolysis. It should indeed be pointed out that phosphoglycerates, for example glycerophosphocholine, share a phosphate group with

glycerol-6-phosphate and have similar molecular masses. In addition, a bacterial homolog of SLC37A2 has been documented to transport glycerol-3-phosphate⁹⁷. We thus hypothesised that SLC37A2 could export lysosomal catabolites of lipids to the cytosol.

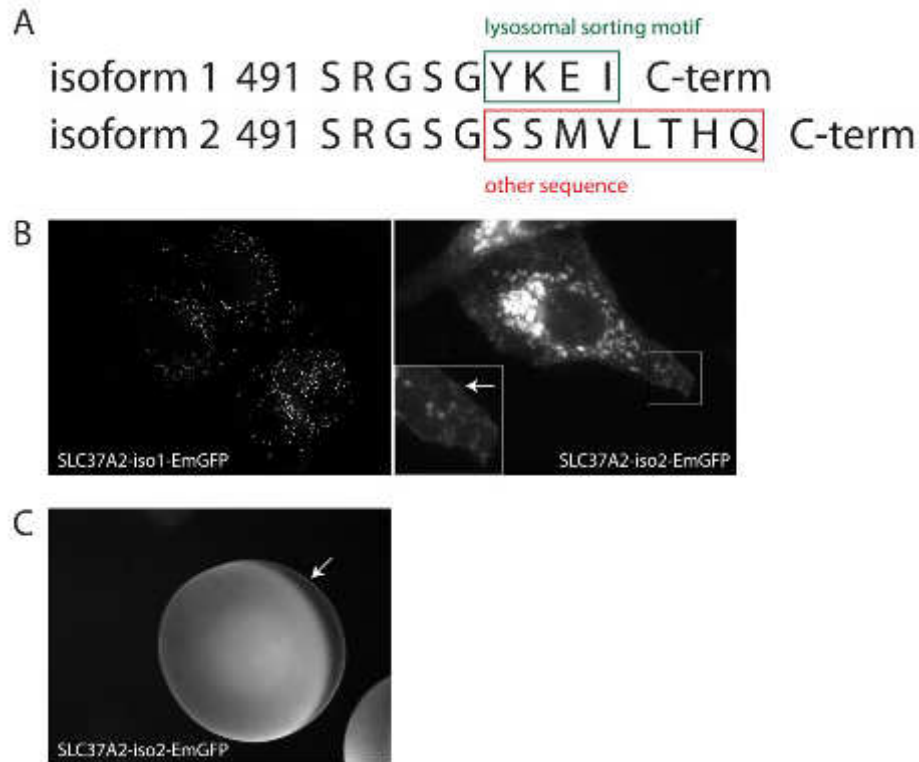


Figure 10: subcellular localisation of two splicing isoforms of SLC37A2.
A: C-terminal tail primary sequences of isoform 1 and 2 of human SLC27A2. The alternative C-terminus of isoform 1 is a lysosomal sorting motif.
B: Subcellular localisation of both isoforms. Cells were transfected to express SLC37A2-isoform1-EmGFP (left panel) or SLC37A2-isoform2-EmGFP (right panel). Cells were fixed after 48hours. For isoform 1, pictures were deconvoluted from stack of epifluorescence images acquired at different depths. SLC37A2-iso1 is expressed in lysosomes, whereas iso2is expressed in lysosomes and at the plasma membrane (see arrow). Bar: 10µm
C: Xenopus oocytes were injected with mRNA encoding SLC37A2-iso2-EmGFP. Like in mammalian cells, some fluorescent protein can be noticed at or near the plasma membrane (see arrow), enabling functional experiments. Bar: 0.25mm.

3.3.2. Functional assays

5 putative substrates were tested using TEVC on SLC37A2 iso2 expressed in Xenopus oocytes (see summary, Fig 11). No specific transport signal was found in these experiments, thus failing to confirm the role of SLC37A2 in transport of glucose-6-phosphate, nor unveiling a possible role in the recycling of lipid catabolites from lysosomes.

However, as glucose-6-phosphate carries one negative charge, it was much possible that SLC37A2 transport activity was overall electroneutral, and therefore undetectable in our

TEVC assay, if this activity was coupled with proton transport as observed for most lysosomal transporters.

To address this possibility, radioactivity uptake was used to test the role of SLC37A2 as glucose-6-phosphate and phosphate lysosomal antiporter. Oocytes were injected with potassium phosphate a few minutes before uptake to reach an intracellular concentration of 0, 20 or 50 mM. They were then incubated in a pH 5.0 buffer containing ^{14}C -glucose-6-phosphate (see Fig 11). No significant uptake was observed, nor in control oocytes, nor in oocytes expressing SLC37A2, thus failing again to reproduce the functional data reported by Pan et al 2011.

A

substrate	concentration	method	
		radioactivity	TEVC
phosphate	10mM		X
Mannose-6-phosphate	10mM		X
Glycerophosphocholine	1mM		X
Glycerol-3-phosphate	10mM		X
Glucose-6-phosphate	10mM	X	X

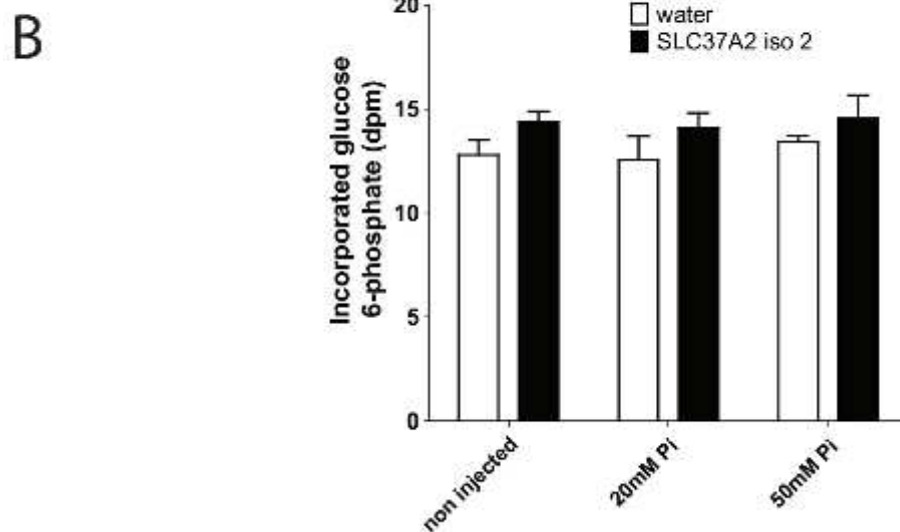


Figure 11: summary of functional experiments performed on SLC37A2.

A: summary of substrates screened, concentrations of screening and methods used.

B: experiment done using the radioactivity method on *Xenopus* oocytes. Oocytes were injected with mRNA encoding SLC37A2-EmGFP or water 48h before experiment. Prior to incubation, oocytes were injected with 50nL of phosphate buffer to increase intracellular concentrations to 20 or 50mM. Oocytes were then incubated for 20 min in ND100 buffer at pH 5 containing 10 mM of glucose-6-phosphate and 1 μ Ci of [14 C]-glucose-6-phosphate. . Then, oocytes were washed in cold pH 7 buffer and radioactivity counted. Data are means \pm s.e.m of 5 oocytes. No uptake was observed.

3.3.3 Phosphoglycerate lysosomal transporters: a gap in the catabolism of lipids

Transport of glucose-6-phosphate by SLC37A2 was studied, but this function could not be confirmed. However, its putative function as transporter for phosphoglycerates was only tested in TEVC and using only two candidate compounds. It is still possible that SLC37A2 is a transporter for other phosphoglycerates, or that its activity is electroneutral.

Discovering transporters for phosphoglycerates in the lysosomal membrane could fill an important gap in our knowledge of lipid catabolism.

Lipases have been described in lysosomal lumen⁹⁸, and in particular phospholipases, which catalyse cleavage of phosphoglycerolipids into 1) fatty acids and 2) other catabolites comprising glycerol, a phosphate group and various other groups, such as ethanolamine or choline. The fate of these second catabolites is unknown, although bacteria transporters of phosphoglycerates, such as glycerol-3-phosphate, have been described within the Major Facilitator Superfamily⁹⁹. SLC37A2 could fill this gap in the knowledge of phospholipid catabolism by being a transporter for phosphoglycerates.

3.4. hSPINSTER1, a putative transceptor

3.4.1 Introduction

SPINSTER1 is a mammalian homolog of *D. melanogaster* *Spinster*. The corresponding protein has been documented as a late endosomal and lysosomal protein with 12 trans-membrane segments. It belongs to the Major Facilitator Superfamily (MFS), which contains many established or putative transporters.

In flies, the mutation of *spinster* drives a very strong and specific change in the behaviour of female flies: they reject male courtship (see Fig 12). In addition, they experiment a slight decrease in their lifespan. *Spinster* was as well characterized as important for the survival of neurons and oocytes: its mutation in *D. melanogaster* leads to neurodegeneration and degeneration of oocytes. Interestingly, neurons from the CNS of *spinster* mutant flies accumulate autofluorescent pigments^{91,100}, in a similar fashion as observed in some human genetic neurodegenerative disorders such as neuronal ceroid lipofuscinoses (see Chapter 2) It was shown as well that *SPINSTER* was important for the establishment of neuromuscular synapses in flies. Interaction with the TGF- β signalling pathway seems relevant for this role, which is not incompatible with the hypothesis of a lysosomal exporter¹⁰¹.

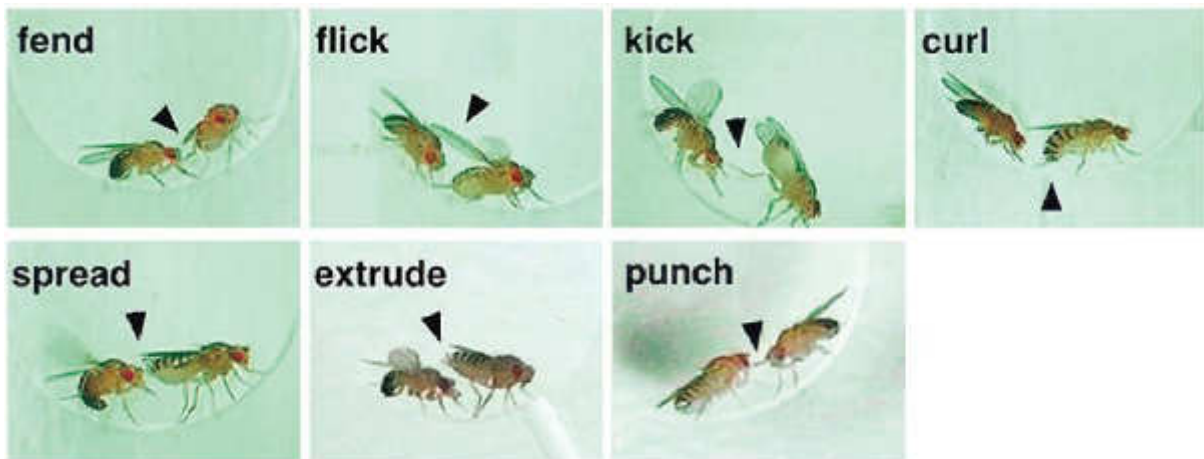


Figure 12: *spinster* female flies reject male courtship. See Nakano et al *Mol Cell Biol.* 2001, 21:3775-88.

Autofluorescent deposits have been shown to be carbohydrates in two independent studies ^{102,103}, suggesting an important role of SPINSTER in the lysosomal efflux of sugars, although no direct evidence of SPINSTER sugar transport activity has ever been presented.

Spinster1 was as well shown to be implicated in lysosome reformation following macroautophagy activation by signalling to mTORC1 ¹⁰³. Besides, when *Spinster1* is repressed with small RNAs, material accumulates inside enlarged lysosomes of mammalian cells. Displaying both transport and signalling activity, it could be described as a putative lysosomal transceptor which activity is critical in neurons especially. The concept of transceptor (transporter/receptor), initially developed in studies of nutrient sensing in yeast, designates transporter-like proteins in which the conformational changes characteristic of transporters has evolved to fulfil a signalling role rather than a substrate translocation role ¹⁰⁴.

Why lysosomal sugar efflux could be critical in neurons in flies remains unclear. Since no human natural mutant of SPINSTER has been described, no comparison with human pathology can be made. However, it could be hypothesised either that:

- SPINSTER is responsible for the export of a few sugars which are used in a particular manner by neuronal metabolism,
- or that all cells are flawed when SPINSTER is inactive, but neurons are more fragile.

3.4.2 Screening of the putative lysosomal sorting motif

Spinster1 has one putative lysosomal sorting motif: 408 YVVI, in the sixth cytosolic domain. This motif is conserved in mouse, rat, zebrafish and *X. laevis*. In *D. melanogaster*, there is another tyrosine-based motif at a comparable localisation (451 YVVV) when all hSPINSTER1 orthologs are aligned.

A plasmid encoding mutant SPINSTER1-Y408A-EmGFP was generated and overexpressed in HeLa cells. WT and Y408A proteins had comparable subcellular distributions. In particular, SPINSTER1-Y408A-EmGFP displayed no detectable expression at the plasma membrane (see Fig 12)

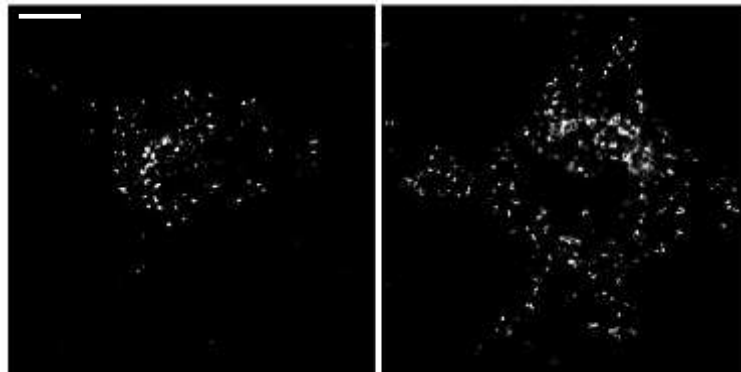


Figure 12: Subcellular localisation of human SPINSTER1-EmGFP and human hSPINSTER1-Y408A-EmGFP, overexpressed in HeLa cells. Mutant SPINSTER1 is not expressed at plasma membrane. Bar: 10µm.

Since it was impossible to express hSPINSTER at the plasma membrane, no direct functional assay was performed. However, SPINSTER was one of the candidates that were screened in our amino acid transporter screen based on TFEB localization.

The principle of this test will be detailed in Chapter 3 (p123). Briefly, this test is based on an indirect way to measure of lysosomal overload using the transcription factor TFEB (see Introduction). HeLa cells are treated with an amino acid ester, which can diffuse through membranes, to artificially overload their lysosomes with a specific amino acid. Overexpression of a lysosomal transporter able to export this amino acid from lysosomes should reduce this overload, a response detectable using the level of TFEB translocation to nucleus.

As mentioned earlier (Introduction), TFEB is a transcription factor sensitive to lysosomal stress. In case of stress, it is translocated to nucleus to activate transcription of lysosomal genes, degrade intra-lysosomal cargos and thereby reduce lysosomal stress.

Thus, lysosomal overload of a specific amino acid induces the translocation of TFEB to the nucleus, whereas overexpression of a transporter that exports this amino acid from lysosomes reduces the overload and restores the basal, cytosolic localization of TFEB.

In this experiment, HeLa cells transiently expressing (i) TFEB and (ii) SPINSTER1 or PQLC2, a lysosomal transporter for lysine, were treated with a range of amino acid esters. TFEB localization was measured by dividing 50 cells per condition in three categories depending of TFEB localization: C: TFEB in the cytosol; N, in the nucleus; M: mixed localization.

Had SPINSTER1 been a lysosomal transporter of amino acids, resistance to amino acid esters of SPINSTER1-transfected cells compared to control cells (mock transfection) should have been expected. Surprisingly, we observe opposite results. When compared to PQLC2-expressing cells, SPINSTER1-expressing cells display “oversensitivity” of the TFEB pathway to lysosomal overload with the following amino acids: glutamic acid, asparagine, serine, tryptophan and a slight oversensitivity to overload in leucine and methionine (see Fig 13A).

These results could be explained in two ways. First, SPINSTER could be an importer of amino acids inside lysosomes. Second, SPINSTER1 has been linked to signalling networks. Overexpression of SPINSTER1 could over signal to mTORC1 pathway and, indirectly, interfere with TFEB localisation and activation regulation. To test this hypothesis, we repeated the previous experiment using as a control a mutant of SPINSTER1 which has been suggested to be inactive by fly genetic studies: SPINSTER1 E164K (164 in human protein, equivalent of glutamate 217 in *D.melanogaster* when aligned). This mutant is indeed unable to functionally complement the accumulation of sugars in vacuoles of *spin* flies¹⁰³.

However, results were exactly the same between cells expressing both proteins (see Fig 13B), as we observe the same oversensitivity to the same esters between WT and mutant SPINSTER1, suggesting the paradoxical behaviour of SPINSTER1 in our TFEB/amino acid ester assay does not depend on the molecular activity of the protein. SPINSTER1 may thus not be a lysosomal importer of amino acids, nor a putative transceptor of amino acids in this organelle. However, it is possible that overexpression of a signalling protein, even in a theoretically inactive form, could cause dysfunction of cellular signalling pathways and lead to unexpected responses. The transceptor hypothesis thus cannot be fully excluded.

It would be interesting to use a similar approach to test a potential sugar transport function or sugar-sensing function (sugar transceptor) of SPINSTER1. However the ester precursor trick used in our TFEB assay cannot be trivially implemented to overload sugars in lysosomes because they are overall more polar than amino acids.

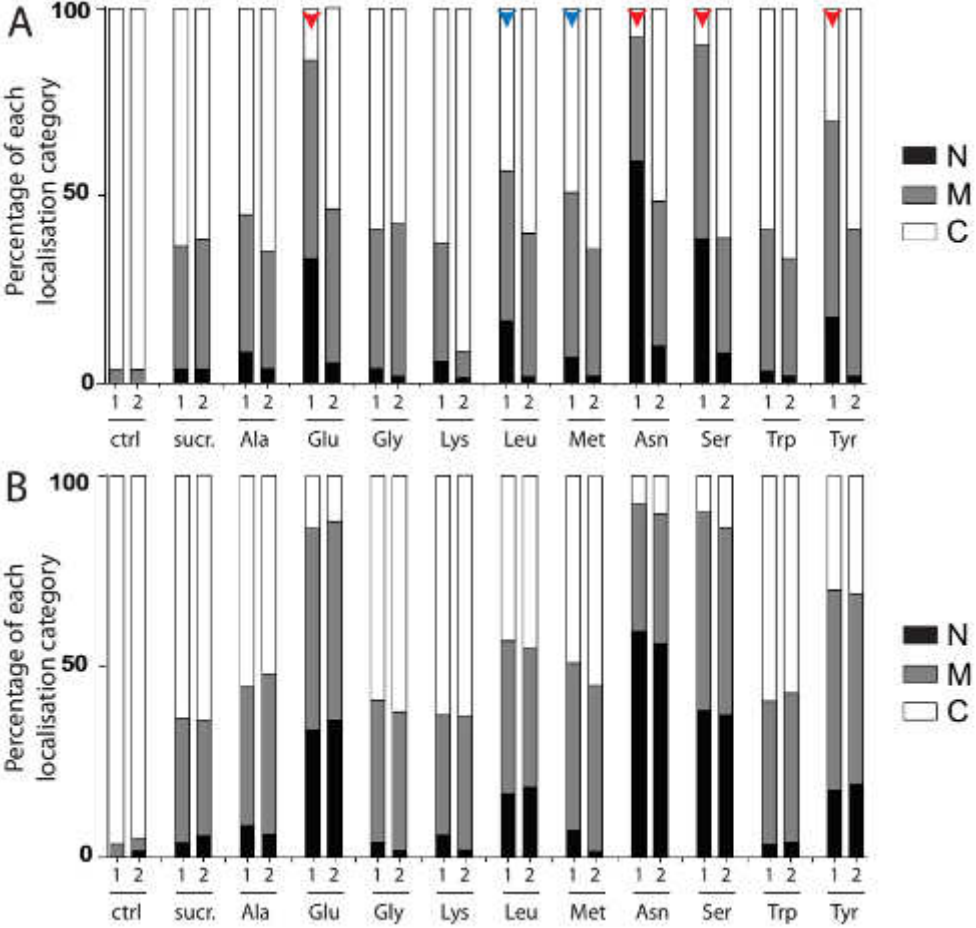


Figure 13: SPINSTER1 overexpression causes over reactivity of the TFEB pathway to amino acid esters. A: HeLa cells were transfected with the following constructs and mRFP-TFEB 48h before being tested in the TFEB assay. Column 1: SPINSTER1-EmGFP or column 2: PQLC2-EGFP. They were incubated for 2h with sucrose or amino acid esters (of alanine, glutamate, glycine, lysine, leucine, methionine, asparagine, serine, tryptophan or tyrosine) and fixed. mRFP-TFEB localisation was measured as presented previously. In cells overexpressing SPINSTER1, TFEB nuclear translocation is stronger when cells are challenged with esters of glutamate; leucine, methionine, asparagine, serine and tryptophan (see arrows, red, strong difference, blue, weaker difference). B: same experiment with HeLa cells transfected with: column1: SPINSTER1-EmGFP, column2: SPINSTER1-E164K-EmGFP. Both overexpressed proteins induce oversensibility to the same esters as previously. This oversensibility to specific amino acid esters is thus probably not due to SPINSTER1 molecular function.

3.5. MFSD1, a protein belonging to the major facilitator superfamily

3.5.1 Introduction

MFSD1 belongs to the MFS superfamily. This superfamily contains many permeases and secondary active transporters, often coupled to ions, thus supporting a role as a lysosomal transporter. However, no work has been published on MFSD1 and it has not been implicated in any pathologies.

3.5.2. Topology issue and screening of the putative lysosomal motif

MFSD1 was predicted to have eleven transmembrane segments, contrary to most MFS members who typically have twelve of them. The N-terminus was predicted to be luminal, which is uncommon for lysosomal proteins. In addition, the predictions were not bright clear: another possible transmembrane segment could barely be detected but was hardly statistically significant.

With the eleven-transmembrane prediction, no lysosomal motif was predicted to be in a cytosolic loop of MFSD1. However, when we added the additional helix, a very clear motif was predicted as cytosolic, in the N-terminal loop. This motif was: 7EDRALL. Thus, we considered this last hypothesis to try and delocalize MFSD1.

Mutated (LL(12/13)AA) MFSD1 had a subcellular localization that was dramatically different to the one of WT MFSD-EGFP. Instead of being localized to lysosomes, the protein is expressed at the plasma membrane (see fig 14). The same could be observed when expressed in *Xenopus* oocytes (see fig 14).

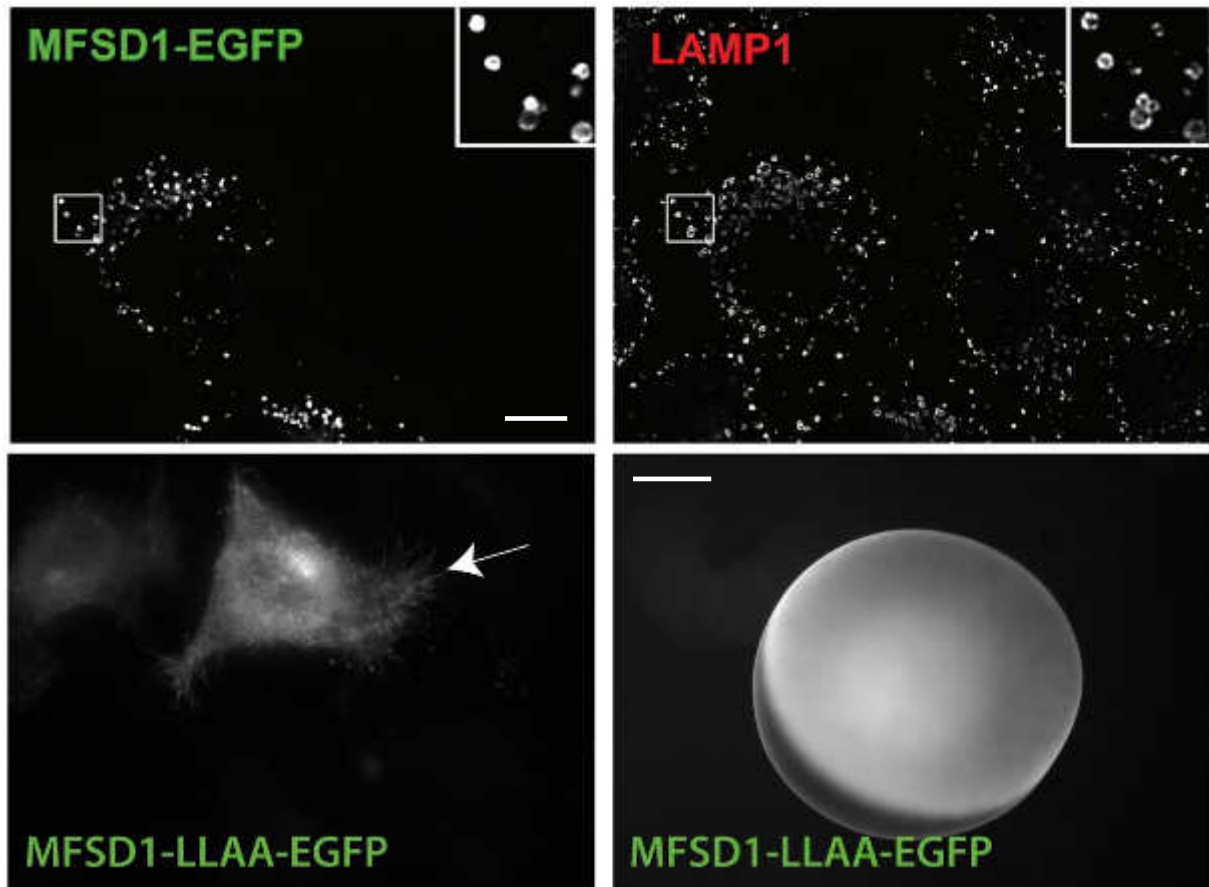


Figure 14: MFSD1 is sorted to lysosomes thanks to a canonical di-leucine motif in its N-terminus. Upper panels: Subcellular localizations of MFSD1-EGFP transiently expressed in HeLa cells (left). MFSD1-EGFP is sorted to lysosomes (LAMP-1 revealed by immunofluorescence, right). Lower panels: Subcellular localization of MFSD1-LLAA-EGFP in HeLa cells (left) and *Xenopus* oocytes (right). In both cases, MFSD1 is partially expressed at the plasma membrane. Scale bar for mammalian cells: 10 μ m; for oocyte: 0.25mm.

These results suggest that MFSD1 has an additional transmembrane domain compared to the original prediction, since lysosomal sorting motifs have to be exposed to cytosolic adaptors to be active. MFSD1-LLAA expressed in oocytes was used as our model for functional studies.

3.5.3 Functional assays on MFSD1

Since there was no particular hypothesis on MFSD1 substrate, a variety of substrates was screened in TEVC, including amino acids and sugars.

Amino acids were tested in mixes and applied onto oocytes. In mixes, each amino acid was at 1mM in NFD100 at pH 5.0.

No amino acid mix evoked any MFSD1-specific current (see fig 15). A strong, yet quite variable cysteine-evoked current was observed. However, such currents are not specific for MFSD1 and may correspond to an artefact induced in oocytes by overexpression of several proteins (see chapter2 p86 for more detail). These results suggested that either MFSD1 is not an amino acid transporter, or that its activity is electroneutral.

The same experiment was repeated with sugars, which were applied individually. Comparable results were obtained. In these experiments, glucose, mannose, mannose- and glucose-6-phosphate were applied. Myo-inositol, although not a sugar, was tested as well and had no effect (data not shown).

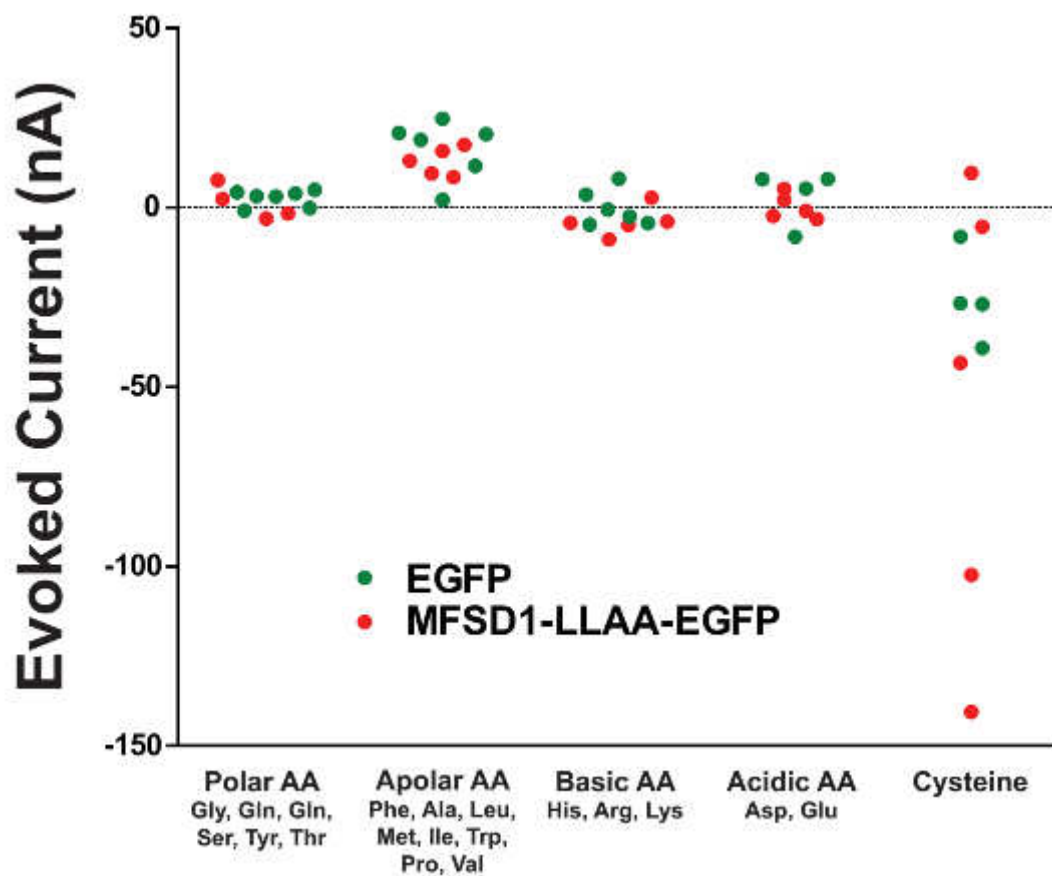


Fig 15: MFSD1 is not an electrogenic transporter of amino acids. Amino acids in acidic buffer at 1mM each were applied to *Xenopus* oocytes in TEVC and induced current measured. EGFP-expressing oocytes were compared with MFSD1-LLAA-EGFP expressing oocytes. Apart from cysteine, which induces an artefact, no MFSD1-specific current could be observed.

Since there was no particular hypothesis on MFSD1 potential substrate, no further experiments were performed. It is still possible that it is an electroneutral transporter.

Wide screenings such as the one developed using TFEB (see chapter 3 p122) could prove interesting to try and narrow down hypotheses about MFSD1 function.

4. Conclusion

Our proteomic study provided a great number of putative lysosomal transporters. In this chapter, five of them were studied. Three of them could not be sent to plasma membrane by mutating their sorting motif, showing that the sorting of lysosomal proteins sometimes depends on either several motifs or uncanonical motifs.

For example, this has been well described in the case of CLN3 (see p81 chapter 2), which sorting relies on two motifs. Because proteomic studies provided so many candidates, extensive studies to try and impact the traffic of putative lysosomal transporters were not performed, but they could be an axis of research for candidates with an interesting putative substrate, like TMEM104.

However, studying lysosomal transporters in situ could as well be done in certain conditions:

- a screening test for amino acid transporters was developed without the need to express candidate proteins at plasma membrane (see chapter 3 p122). In particular, it was applied to SPINSTER.

- A recent technique is based on in situ lysosome enlargement using vacuoline or recombinant proteins to enable patch-clamp measurements at the lysosomal membrane directly. A few labs in the world master this technique and one of them has already characterized a new lysosomal channel from our proteomic study this way ¹⁰.

These methods could be applied for more extensive study of our candidates, although it seems less sensitive than current transport assays.

One transporter, SLC37A2, could be expressed at plasma membrane by taking advantage of a splicing variant. It seems to have a different function to other members of its family (phosphate/phosphate-sugars antiporters). Our hypothesis of a putative role in the transport of lipid catabolites could not be confirmed by the use of radiolabelled compounds. Another transporter, MFSD1, was delocalized successfully, thus infirming its predicted

secondary structure, but the lack of data on its putative function or biological significance gives little clue on putative substrates.

This study provided as well another candidate, SNAT7, which was successfully characterized as a lysosomal transporter for glutamine and asparagine. This characterization along with the biological role of SNAT7 in cancer cells will be presented in Chapter 3.

Chapter 2: study of two lysosomal membrane proteins implicated in neurodegenerative disorders: CLN3 and CLN7

1. Introduction

1.1 On neuronal ceroid lipofuscinoses

1.1.1 Generalities

Neuronal ceroid lipofuscinoses (NCL) are a family of inherited lysosomal storage disorders (LSDs), characterized by neurodegeneration in the central nervous system and the retina. NCL patients typically display a combination of blindness, epilepsy, motor decline and dementia, although the onset and the gravity of symptoms greatly vary from one NCL genetic form to the other and from one patient to the other.

NCLs are the most common cause for neurodegeneration in children, having an incidence of 1:100000 globally. In some populations, this incidence can however be much higher (for instance 1:12500 in Finland). NCL patients display accumulations of lipofuscin in lysosomes of diverse organs, including brain.

Although NCLs were firstly clinically described in Norway in 1826¹⁰⁵, the term “NCL” was proposed in 1969 based on histological hallmarks of several patients. Patients affected by NCL present indeed accumulation of autofluorescent material inside lysosomes that shares common properties in EM. Patients can display accumulation with granular, curvilinear or rectilinear patterns. In some cases, the accumulated material is as well shaped like fingerprints (see Fig 15).

Later, the accumulated material was identified as lipofuscin, although a different kind from what accumulates naturally during ageing^{106,107}. Lipofuscin is composed of undegraded and oxidized proteins, lipids and sugars. Iron can be found as well in the accumulation

bodies¹⁰⁸. In the case of NCLs, the accumulation of lipofuscin begins early, at different ages depending on the disease, and is correlated with neurodegeneration.

Two kinds of NCLs can indeed be distinguished based on the most abundant protein composing lipofuscin: either the c subunit of the mitochondrial ATPase, or saposins A or D. This can be correlated with the pattern of accumulation within lysosomes: accumulation of saposins leads to granular pattern of accumulation within lysosomes, whereas the accumulation of the c subunit of the mitochondrial ATPases can lead to variable patterns of accumulation¹⁰⁹.

1.1.2 Pattern of neurodegeneration in brain

Post-mortem analyses of patients' brains have been performed and these results have been refined by the analysis of animal models. The regions that are mostly affected by neurodegenerescence vary from one NCL to the other, although, overall, cortex, thalamus and hippocampus seem to be the most prone to neurodegeneration¹¹⁰. Similarly, in these tissues, all neurons are not affected in the same way depending on their function.

For instance, in the cerebral cortex, sensory regions seem more affected than motor ones. GABAergic neurons overall seem more sensitive to neurodegeneration in this region in a *Ppt1* mouse KO model¹¹¹. This suggests that depending on their morphology, their activity and their metabolism, CLN proteins are more or less critical for neuronal survival.

In addition, neurodegeneration is associated with astrogliosis and microgliosis in patients' brains.

1.1.3 Genetic determinants of NCLs

Most LSDs are caused by the deficiency of either an enzyme or a transporter, leading to the accumulation of respectively one type of undegraded material or of the product of degradation. For instance, Fabry disease is caused by the mutation of α -galactosidase A, which causes the accumulation of globotriaosylceramide (Gb3), the substrate of this enzyme. NCLs are a different kind of LSDs: 14 genes have been involved in NCLs, yet the accumulated material within lysosomes is comparable in each form and composed of lipofuscin, despite some variation of its composition.

Most NCLs are autosomal and recessive, with the exception of the one caused by the mutation of *cln4*. Mutation of CLN4/CSP α causes Parry disease, an adult onset form of NCL which is dominant ¹¹².

Even with a mutation in the same gene, symptoms can vary greatly. For instance, mutations in CLN10 can lead from a late infantile form of NCL to an adult form ¹¹². In the same way, similar pathologies such as late infantile NCLs can be due to mutations in different NCL genes ¹¹³. Thus, the former classification of NCLs based on how early the first symptoms appear tends to be overcome by a genetic classification. ¹¹²

How mutations in NCL genes lead to similar pathologies is not very well understood at the cellular level. Many NCL proteins seem related to the lysosomal function. They can be enzymes, lysosomal soluble proteins or lysosomal membrane proteins. Yet, some of them are resident proteins of the ER membrane, cytosolic or even secreted (see Table 15) ¹¹⁴.

Despite a tendency to play a role in the function of lysosomes, it remains unclear why the mutation of very different proteins can lead to the same cellular defect, and even more how it can lead to similar clinical features. Since neurons are the main cell type that is affected by the dysfunction of NCL genes, it could be hypothesized that NCL proteins play a role in a common pathway that implies lysosomes and that this pathway is especially important for neuronal survival. This pathway has been hypothesized to play a role in autophagy, trafficking or synapse maintenance, but without very conclusive experimental evidence ^{107,115,116}

1.1.4 Therapies

So far, there is no specific treatment for NCLs. Patients are treated to palliate symptoms. Enzyme-delivery is being considered as well for *CLN1* mutations, which encodes a lysosomal enzyme, PPT1, similarly to what has been developed by other LSDs implying lysosomal enzymes, in addition to a substrate reduction strategy ¹¹⁷.

Several clinical trials are currently run, mostly focusing on gene-replacement therapies for *CLN1* and *CLN2*, which encode two lysosomal enzymes: respectively PPT1 and TPP1, similarly to what has already been tried for disease with mutation in enzyme genes, like Gaucher disease.

Since the immune system has been shown to play a particular role in Batten disease (mutation of *cln3*, see below), a treatment with immunosuppressors is currently under tests (<http://www.ucl.ac.uk/ncl/SummaryofHumanClinicalTrialsforNCL.htm>).

Gene	Clinical onset	Accumulation pattern	Protein	localization	function
<i>CLN1</i>	infantile	granular	PPT1	lysosomal (soluble)	thioesterase
<i>CLN2</i>	late infantile	curvilinear / fingerprints / granular	TPP1	lysosomal (soluble)	peptidase
<i>CLN3</i>	juvenile	curvilinear / fingerprints / rectilinear	CLN3	lysosomal (membrane)	?
<i>CLN4</i>	adult	curvilinear / fingerprints / rectilinear	CSP α	cytosolic	chaperone
<i>CLN5</i>	late infantile	curvilinear / fingerprints / rectilinear	CLN5	lysosomal (soluble)	?
<i>CLN6</i>	late infantile	curvilinear / fingerprints / rectilinear	CLN6	ER (membrane)	?
<i>CLN7</i>	late infantile	curvilinear / fingerprints / rectilinear	CLN7	lysosomal (membrane)	?
<i>CLN8</i>	late infantile	curvilinear / fingerprints	TPP1	ER (membrane)	?
<i>CLN9</i>	late infantile	curvilinear / fingerprints / granular	CLN9	lysosomal (membrane)	?
<i>CLN10</i>	congenital	granular	CTSD	lysosomal (soluble)	protease
<i>CLN11</i>	adult	rectilinear	progranulin	extracellular	?
<i>CLN12</i>	juvenile	rectilinear	ATP13A2	lysosomal (membrane)	?
<i>CLN13</i>	adult	rectilinear	CTSF	lysosomal (soluble)	protease
<i>CLN14</i>	infantile	granules / fingerprints / rectilinear	KCTD7	intracellular/ plasma membrane (membrane)	putative potassium channel

Table 15: summary of a few characteristics of the different NCL types and function of the corresponding mutated proteins.

Among the 14 CLN proteins, two of them are localized in the membrane of lysosomes: CLN3 and CLN7. They were studied in my host laboratory, both by former members and myself during my PhD.

1.2 CLN3

The mutation of *CLN3* is the most frequent of all NCLs in Northern Europe. It causes a juvenile form of NCL called Batten disease (although “Batten disease” may also be used for all NCLs). Symptoms begin around the age of 5 by impairment of vision, followed by a delay, then a regression in cognitive developmental milestones. Epilepsy and dementia usually appear after the age of 10. ¹⁰⁹.

Neurodegeneration is especially rapid in both cortices (cerebellum and brain), which thin down as the disease progresses. Before cell death, neurons characterized by inflated cell bodies can be observed. Batten disease is as well characterized by the presence of large vacuoles within the cytoplasm of lymphocytes¹¹⁸. Pathogenesis in Batten disease seems to have an early and important auto-immune component, with the production of antibodies against brain proteins¹⁰⁷.

CLN3 protein is a transmembrane protein of the lysosomal membrane¹¹⁹. It is predicted to have six transmembrane domains. Its sorting to lysosomal depends on two atypical signals: a dileucine-like motif between the fourth and the fifth transmembrane domains and two amino acids: a methionine and a glycine, separated by nine amino acids, in the C-terminus. Both motifs must be mutated for CLN to be partially expressed at the plasma membrane^{120,121}.

There are only a few cellular processes in which CLN3 has not been implicated. This vast amount of results is possibly due to the impossibility to decipher between the initial consequences of a dysfunction of CLN3 and its long-term consequences¹²². Interestingly, CLN3 ortholog in yeast, Btn1p was described as a lysosomal transporter for arginine¹²³ and this proposed function was later extended to the human protein by the same lab¹²⁴. However, this function was not confirmed in my host lab. A more general hypothesis of a lysosomal transporter was also investigated, with many substrates tested, but no transport activity of CLN3 could be observed (unpublished data).

Three murine models of Batten disease have currently been developed since no spontaneous model was available¹²⁵. One of them reproduces the most common mutation, observed in 85% of the patients (a large deletion). Although symptoms are milder than in humans, mice do display both:

- cellular signs of NCLs: neuronal death, fingerprint inclusion in lysosomes and elevated levels of lysosomal enzymes in tissues,
- NCL-like symptoms, in particular loss of activity and impairment of motor functions

^{126,127}.

This model, a kind gift from Susan Cotman at Harvard Medical School, was used in the present chapter.

1.3 CLN7

CLN7 has only been discovered in 2007¹²⁸ although clinicians had already characterized an atypical form of NCL from a population of Turkish patients that corresponded to mutations of *CLN7*¹²⁹. The form of NCL caused by the mutation of *CLN7* is late infantile and resembles NCLs due to the mutation of *CLN5* or *CLN6*, although clinical features are especially variable from one patient to another. One particularity of this form of the disease is the sensitivity of the granular layer of the cerebellum to the neurodegeneration¹³⁰.

The *CLN7* gene encodes for a protein called either CLN7 or MFSD8 because of its belonging to the major facilitator superfamily¹³¹, which contains many permeases and ion-coupled secondary active transporters, suggesting CLN7 could be a lysosomal transporter. CLN7 is localized at the lysosomal membrane thanks to a dileucine sorting motif previously identified in my host laboratory¹³⁰ and another group (Storch, Pohl, and Braulke 2010). Yet, so far, no functional data are available on CLN7.

2. Functional characterization of CLN7 by TEVC

2.1 Expression of human CLN7 at the plasma membrane in *Xenopus* oocytes

To study CLN7, we used the misrouting approach developed in my host laboratory. This method, introduced in Chapter 1, takes advantage of the sorting process of lysosomal membranes proteins. When their sorting motif is mutated, lysosomal membrane proteins are misrouted to the plasma membrane, making them amenable to techniques used to study plasma membrane transporters, such as electrophysiology or radioactive uptake (see p56).

CLN7 is sorted to lysosomes thanks to a dileucine motif (9EQEPLL) which was previously characterized in my host laboratory¹³⁰. Mutation of this motif (LL->AA) led to CLN7 being expressed at the plasma membrane in HeLa cells, thus greatly facilitating functional studies.

To enable functional study of CLN7, an expression plasmid for *Xenopus* oocytes encoding a fusion protein between EGFP and human CLN7 carrying the LL->AA mutation was designed. mRNA was produced in vitro from the plasmid and was injected into oocytes. Analysis of expression was performed 48h later using epifluorescence microscopy and surface biotinylation.

Xenopus oocytes clearly showed under epifluorescence microscopy a distribution suggesting partial expression of EGFP-CLN7 at the plasma membrane (see Fig 16). Design of the plasmid and expression were already established when I arrived in my host laboratory

I confirmed the conclusion suggested by these epifluorescence data using a surface biotinylation assay. Oocytes were treated with sulfoNHS-SS-biotin, which reacts with free amine groups of proteins and enables their labelling with biotin. However, this compound is not permeable, so, when *Xenopus* oocytes are treated with this form of biotin, only plasma membrane proteins are labelled. Oocytes were then lysed and lysates loaded onto streptavidin-coupled beads to separate plasma membrane proteins from others. Total lysates, non-retained fractions and retained fractions were analyzed by Western Blot against EGFP. While no WT CLN7 was retained by streptavidin-beads, a significant amount of EGFP-CLN7 LLAA was retained, showing that the mutation triggers partial expression at plasma membrane (see Fig 16).

As a result, *Xenopus* oocytes were a suitable model to screen for potential CLN7 substrates using techniques for plasma membrane transporters.

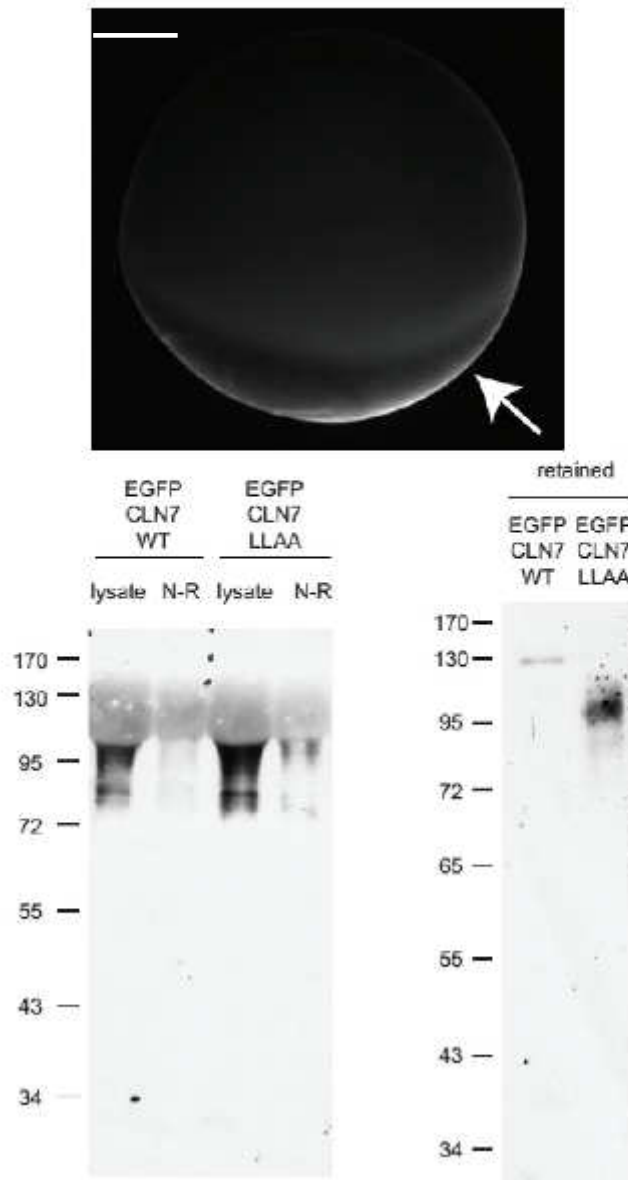


Figure 16: EGFP CLN7 LLAA is sorted to the plasma membrane in *Xenopus* oocytes. Upper panel: epifluorescence picture of an oocyte injected with EGFP-CLN7-LLAA-encoding mRNA 48h prior to imaging. The arrow indicates visible expression at or near the plasma membrane. Bar: 0.25mm. Lower panel: Surface biotinylation was performed on EGFP-CLN7-WT and EGFP-CLN7-LLAA-expressing oocytes 48h after injection. Lysates of oocytes, streptavidin-retained fractions and non-retained fractions were analyzed by Western Blot using an anti-EGFP antibody. Only EGFP-CLN7-LLAA is significantly biotinylated, confirming it is expressed at the plasma membrane.

2.2 Functional study of CLN7 using TEVC

We decided to screen very for a large set of potential substrates of CLN7, since it is not clear with which biochemical pathways CNL proteins could interact. Some of them are lysosomal proteases, but patients' lysosomes accumulate lipofuscin, which contains oxidized lipids and sugars ¹¹⁴.

Many MFS members are known to be coupled to ions. Besides, lysosomal transporters are often coupled to protons, which suggested CLN7 may be an electrogenic transporter. Thus, TEVC seemed the best method to screen a large set of putative substrates quite rapidly (see page 57 for more details on TEVC).

Many substrates were screened in my host laboratory before my arrival. In particular, Anna Norton screened for amino acids. She applied mixtures of amino acids of the same chemical family on oocytes in acidic buffer, to mimic the lysosomal proton gradient, and checked for amino acid-evoked currents. Since lysosomal transporters are typically coupled to protons, inward currents were expected. That is to say that, to keep potential at -40mV, more electrons would have to be injected into the oocytes to compensate for protons entry.

Interestingly, the polar amino acids mix did trigger a strong inward current (see Fig 17), although it was very variable from one oocyte to the other. Anna Norton then repeated the experiment splitting the mix to apply each constitutive amino acid separately and found out that cysteine was responsible for this inward current. It was absent from the negative control used at this time: oocytes expressing human sialin LLGG. Sialin is a lysosomal transporter which specificity is very well known and rather narrow: it only transports sialic acids. A study suggesting another transport function, namely aspartate loading into synaptic vesicles ¹³², has been subsequently invalidated by two other labs ^{133,134}. Sialin thus appeared as an appropriate negative control in amino acid transport measurements. The LLGG mutation triggers its misrouting to plasma membrane ²⁵.

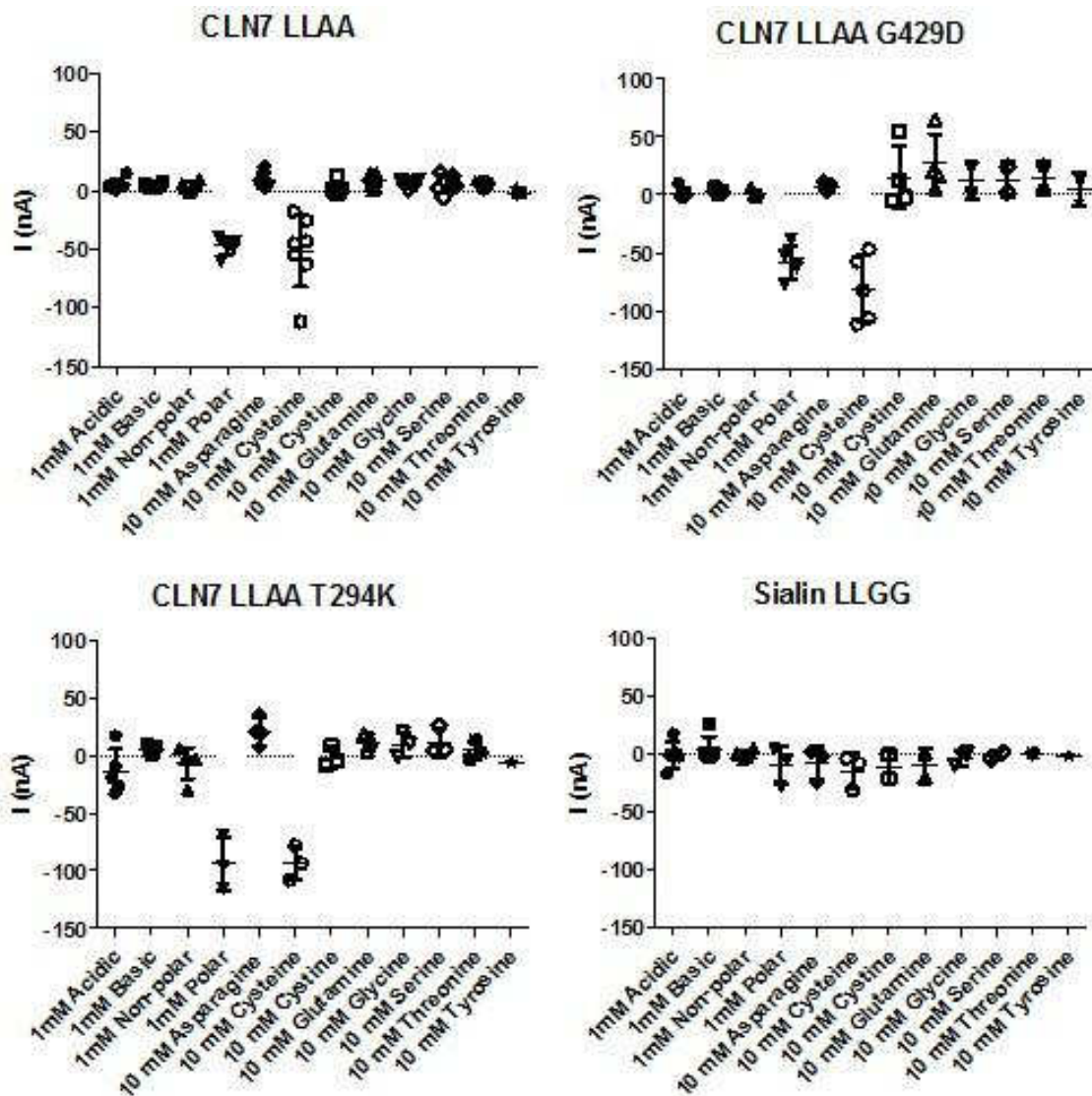


Figure 17 (adapted from A. Norton, unpublished results): CLN7-expressing oocytes display a strong inward current upon application of cysteine. Mixes of acidic, basic, non-polar and polar amino acids at 1 mM pH 5.0 were applied to EGFP CLN7 LLAA, EGFP CLN7 LLAA G429D, EGFP CLN7 LLAA T294K and Sialin LLGG expressing oocytes. When an inward current was identified upon application of the polar mix to the CLN7 LLAA oocytes, each individual polar amino acid was applied at 10 mM. The source of the current change was identified to be cysteine. 10 mM of cysteine was also applied. The same flux after cysteine application was not observed in Sialin LLGG expressing oocytes.

However, the specificity of the cysteine-evoked current carried by EGFP-CLN7-LLAA could be questioned in two ways.

First, CLN7 constructs harbouring a presumable loss-of-function pathogenic mutation (G429D, T294K) showed about the same response to application of cysteine. These mutants are sorted normally to lysosomes^{130,135}, which suggests instead that the molecular activity of CLN7 is impaired. This suggested that the cysteine-evoked current may not be linked to the

molecular function of CLN7 (although we could not exclude more complex pathological effects of the mutations such as, for instance, the loss of an important protein interaction).

Secondly, the shape of the cysteine-evoked currents was rather unusual: the inward current persisted even after full washout of the applied cysteine (see next paragraph), suggesting an indirect mechanism between cysteine and the observed current rather than a genuine electrogenic transport of cysteine.

These two aspects led me to perform new controls to examine further the specificity and the relevance of this cysteine-evoked current.

So, I applied the same protocol to oocytes expressing EGFP-fused sialin LLGG or CLN7 LLAA, but as well other transporters expressed at the plasma membrane: PepT1, a secondary active proton-dependent transporter of oligopeptides of the epithelial membrane of enterocytes; PQLC2 LLAA, a lysosomal transporter of basic amino acids and DIRC2 LLAA, a putative lysosomal transporter. The PQLC2 and DIRC2 constructs used were mutated in their sorting motif to redirect them to the plasma membrane.

Unfortunately, currents observed with these new constructs were similar to those previously observed with CLN7 LL/AA: cysteine evoked an inward current continuing even after its wash-out from the perfused medium. (see Fig 18) However, maximum intensities varied a lot from one transporter to another. In particular, PQLC2-expressing oocytes displayed stronger cysteine-evoked currents compared to CLN7-expressing ones (see Fig 18).

These results suggested that, when transporters are overexpressed at the plasma membrane of *Xenopus* oocytes, they often upregulate an endogenous inward current which is activated by cysteine. This ability varies from one transporter to another, possibly depending on the availability of disulphide bonds on the extracellular face of oocytes. Cysteine could indeed reduce them and cause leak currents. Whatever the mechanism, the cysteine-evoked seems unrelated to the transport activity of the transporter, since PQLC2 displayed the strongest response to cysteine, but it has a narrow selectivity for cationic amino acids, not cysteine ²³.

To conclude, the hypothesis that this cysteine-induced current was characteristic of CLN7 activity seemed very unlikely, and other approaches were necessary to unravel this function.

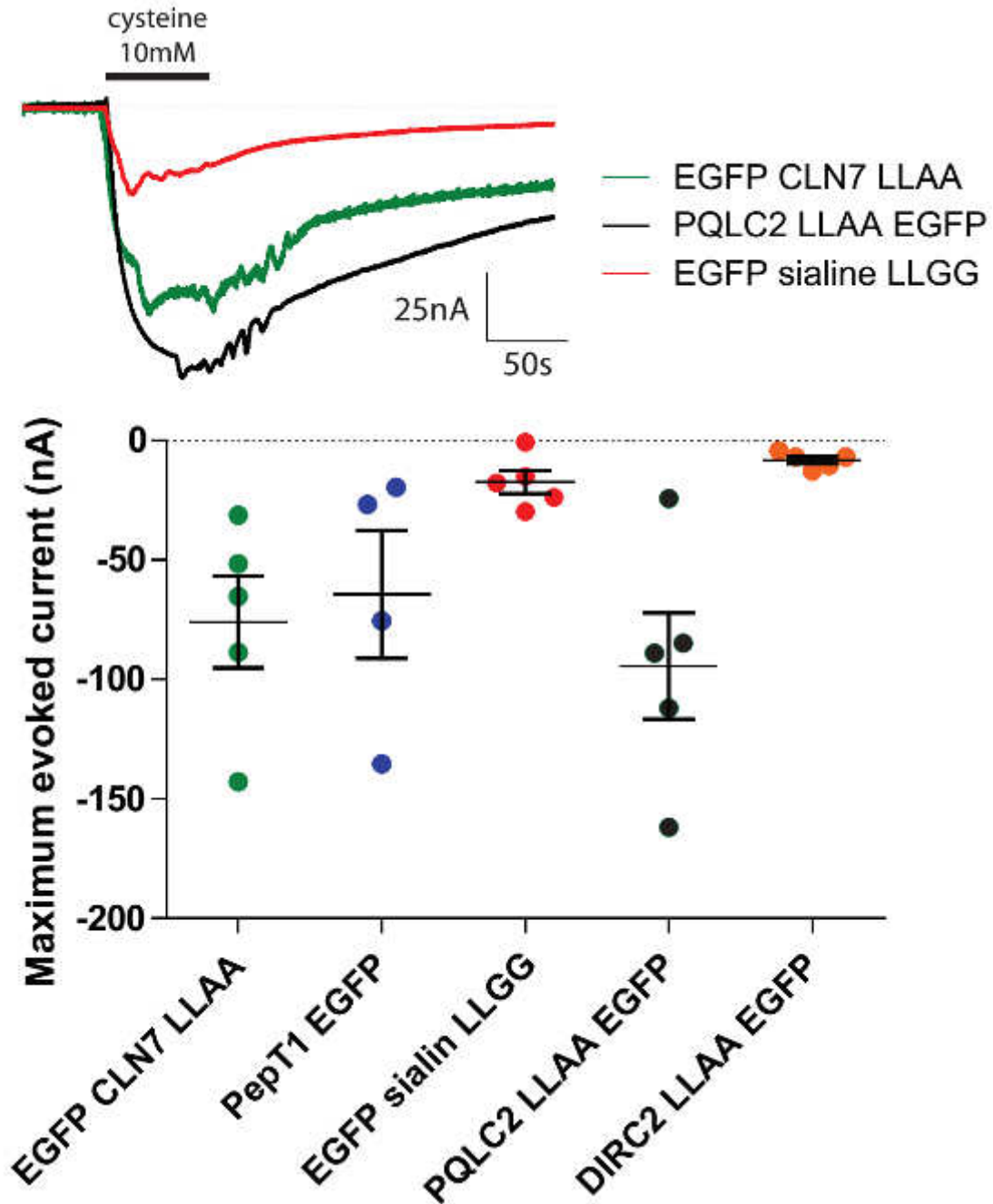


Fig 18: Cysteine-induced current are not specific of CLN7 expression.

Upper panel: representative TEVC traces of sialin-, PQLC2- and CLN7- expressing oocytes upon application of cysteine at 10 mM at pH 5.0.

Lower panel: quantification of the maximum intensity of the inward current observed upon application of 10mM of cysteine at pH 5.0 observed in CLN7-, PepT1-, sialin-, PQLC2- and DIRC2-expressing oocytes. CLN7-expressing oocytes display about the same current as PepT1-expressing oocytes and less current than PQLC2-expressing oocytes.

3. Lysosomal proteolysis is impacted by CLN3 malfunction

3.1 Metabolomics of *Cln3* KI mice

CLN3 function remains unclear, since extensive literature has linked this protein to many cellular mechanisms. It is likely that all cell mechanisms eventually become defective during cell degeneration, making it difficult to decipher between what is due to CLN3 primary function and what is due to general cell death.

It has been claimed for a long time by the group of D.A. Pearce that CLN3 is a lysosomal/vacuolar arginine transporter based on studies in budding yeast (for instance,¹²³) and human lysosomes¹²⁴. This statement is even circulated as established knowledge in several reviews on lysosomes. However, the published data is rather indirect, and, to date, they have not been replicated, including in our own lab. Moreover, our lab and the group of Xiaochen Wang in Beijing have identified the lysosomal arginine transporter as another protein, PQCL2^{23,89}.

However, on the other hand, another yeast group had reported altered cellular levels of arginine, lysine, as well as histidine, ornithine and citrulline in fission yeasts lacking the orthologue of CLN3¹³⁶. Therefore the possibility remained that CLN3 dysfunction induces alterations of amino acids, or other metabolites, at the cellular level or, as initially suggested by Pearce and co-workers, at the lysosomal level through some indirect, poorly characterized mechanism. To address this possibility in a comprehensive manner, without prior hypothesis on specific biochemical pathways, we decide to perform metabolomics analyses of (i) whole tissues and (ii) lysosomal fractions lacking, or not, the CLN3 protein.

To get the biological material for these analyses, we took advantage of one of the mouse models for juvenile Batten disease (courtesy of Dr. Susan Cotman, Harvard Medical School, USA). This mouse is a knock-in model, displaying the most common patient mutation in CLN3: a one kilobase deletion, which results in the expression of a truncated protein. The model displays accumulation of autofluorescent pigments in neurons and gliosis, which resembles the human pathology^{137,138}.

To characterize the impact of CLN3 genetic inactivation on cellular (whole tissue) or subcellular (lysosomal) metabolomes, we selected liver as the best organ for our studies since it represents a well characterized, easy source of purified lysosomes.

Lysosomes were thus purified by Corinne Sagné and me from the livers of wild-type and *Cln3* KI mice according to a classical protocol used for rats¹³⁹. Pieces of livers were kept as well for to characterize the metabolome at the level of whole cells. Lysosomes were enriched firstly by differential centrifugation and next by an isopycnic centrifugation on a discontinuous gradient of Nycodenz. To scale the protocol accordingly to that established for rat, 8 mice were used per purification. In each experiment, WT and *Cln3* KI mice were used. Due to the necessity of having a large number of mice of three months old, which Dr. Cotman suggested was the age at which symptoms began. All mice were produced through homozygous crossing. Eight WT/KI pairs of biological replicates were prepared and the 6 best were selected for metabolomics analysis. Purification quality was tested using beta-galactosidase as a marker. Specific activity was measured. Enrichment from liver homogenates to purified fractions reached between 15 and 25 with 2 to 3% of recovery of total beta-galactosidase. In addition, latency was measured to confirm the integrity of the lysosomes in the purified fractions. Beta-galactosidase activity was measured on fractions treated or not with triton, which solubilises the lysosomal membrane without disturbing the activity of enzymes. Thus, the triton-sensitive fraction of beta-galactosidase represents the amount of enzymes enclosed within intact lysosomes. Latency was calculated as follows:

$$L (\%) = 100 \times \left(1 - \frac{\text{activity}_{\text{without triton}}}{\text{activity}_{\text{with triton}}} \right).$$

Most of the preparations had a latency between 40 and 60%, which is typical of this protocol and was reproducible from one experiment to another.

Paired WT/*Cln3* KI liver homogenates and lysosomal fractions were sent to Metabolon and their content in small molecules was analyzed both by gas chromatography coupled to mass spectrometry and liquid chromatography coupled to mass spectrometry.

Of note, and in contrast with the amino acid findings reported in yeast studies, no significant difference could be detected in the metabolite content of liver tissues from WT and KI mice, except for a lower level of free fatty acids and monoacylglycerols in KI livers.

Most metabolites were present at about the same concentration in WT and KI lysosomes, thus validating the homogeneity of preparation. However, strikingly, out of 18 amino acids and 26 dipeptides that were identified in the metabolomics fingerprints, respectively 12 and 17 were present in decreased quantities in KI lysosomal fractions. For these, reduction varied slightly from one preparation to another, apart from a few amino acids (not shown here). Yet differences were significant in most cases (see fig 19). On the other hand, most other metabolites had comparable levels in WT and *Cln3* KI lysosomes. (see fumarate, a typical mitochondrial metabolite, and galacticol, typically found in lysosomes for example in fig X).

The fact that so many dipeptides and amino acid are present in decreased quantities in lysosomes from KI mice did not support the hypothesis that CLN3 could be a lysosomal transporter.

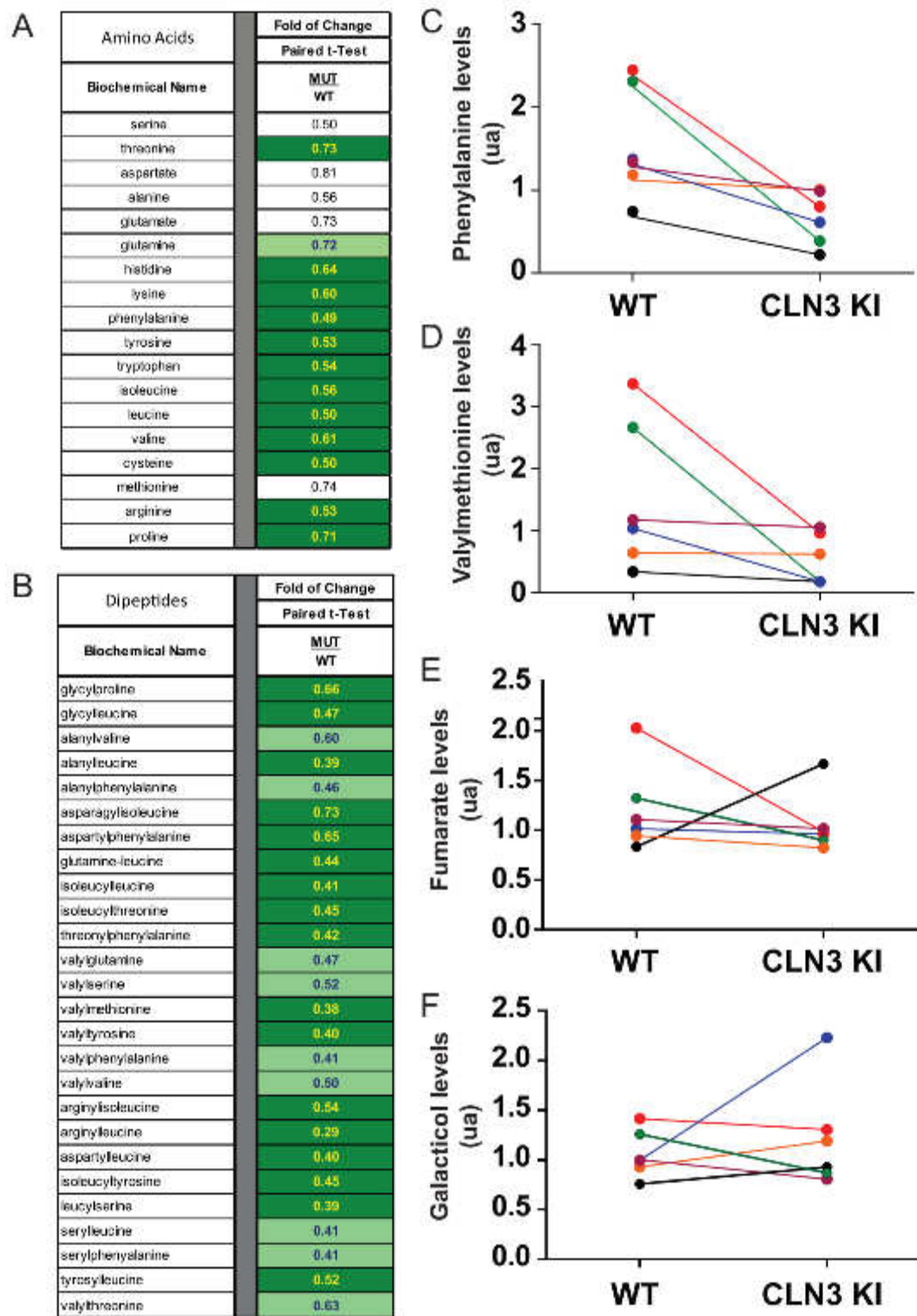


Fig 19: Lysosome fractions from KI mice have lower levels of proteolysis products. A: reduction of amino acid levels. The mean KI/WT ratio is shown for each amino acid. Green highlighting means $p < 0.05$ between WT and KI using paired t-test; light green $p < 0.1$ and white $p > 0.1$. B: same with dipeptides. Tripeptides and larger peptides were not included in the MS peak identification procedure. C: Levels of phenylalanine in lysosomal fractions shown as WT/KI pair plots for the 6 biological replicates. Each colour represents a separate experiment. D: same with valylmethionine. E: same with fumarate. F: same with galacticol.

This decrease in intralysosomal amino acid and dipeptide levels in the KI lysosome-enriched lysosomal fractions can be explained in several ways:

- Fewer protein cargos may reach lysosomes for degradation. This could be caused by reduced endocytosis or autophagy. However, both increase and decrease of autophagy and endocytosis have been documented in CLN3-defective cells in the literature, making this hypothesis rather unlikely¹⁴⁰⁻¹⁴³.

- Export of amino acids and dipeptides from lysosomes may be increased. Because of the diversity of amino acids affected in KI lysosomal fractions and, therefore, of the diversity of lysosomal transporters involved, such a mechanism would be possible only if CLN3 regulated a general parameter influencing these transporters such as the lysosomal pH or the transmembrane electrochemical H⁺ gradient.

- Lysosomal proteolysis may be decreased. Although somewhat unexpected for a lysosomal transmembrane protein, this hypothesis is very attractive because 4 other genetic forms of NCLs are caused by primary deficiency of lysosomal proteases (CLN2/TPP1, CLN10/CTSD, CLN13/CTSF) and or of a lysosomal enzyme cleaving off palmitoyl groups from proteins (CLN1/PPT1).

This latter hypothesis may suggest the existence of a converging pathological mechanism involving defective lysosomal proteolysis between enzymatic forms of NCLs and at least one non-enzymatic form, CLN3, caused by a primary membrane defect. We thus focused our efforts on testing this hypothesis, although we cannot exclude a contribution of the remaining two hypotheses to our metabolomics findings.

In summary, our metabolomics analyses revealed a decrease in amino acids and dipeptides associated with CLN3 dysfunction which is selective at two levels: first, this decrease is observed in lysosome-enriched fractions, but not in liver tissue; secondly, other type of metabolites were not significantly altered in KI lysosomal fractions (except for a higher levels of glutathione and cysteine-glutathione disulfides; data not shown). These differences could be due to a proteolysis defect of CLN3-defective lysosomes.

However, this metabolomic evidence remained indirect and the lysosomal selectivity was not rigorously established because of the presence of contaminating organelles in purified lysosomal fractions and of the high sensitivity of mass spectrometry. Some

metabolites of our 'lysosomal' metabolome may in fact be predominantly mitochondrial. We thus aimed to confirm, or not, these conclusions with more direct approaches.

3.2 Evaluation of proteolysis in neurons of *Cln3* KI mice

Since neuronal ceroid lipofuscinoses are neurodegenerative diseases, we wanted to examine first if lysosomal proteolysis was decreased in *Cln3* KI neurons. Hippocampal neurons were prepared from a heterozygous breeding of the *Cln3* KI mouse line according to usual protocols to minimize variability between neurons from different mice embryos. Neurons from each embryo were kept separately.

During the preparation of neurons, fibroblasts from embryonic skin were prepared as well to allow genotyping of preparations and produce another CLN3 deficient cell model.

Neurons were kept for 13 (data not shown, consistent results with below) or 17 (see below) days after preparation in medium previously conditioned by primary rat glial cells. Then, to analyze proteolysis, DQ-red-BSA, a fluorogenic probe for monitoring lysosomal proteolysis, was used. It consists of BSA coupled to a heavy amount of Bodipy-TR-X dyes. The fluorescence of the dyes, being very close from one another, is thus quenched. Fluorescence of Bodipy is only revealed when BSA is degraded, which considerably reduces the noise of this probe. DQ-red-BSA applied extracellularly to live cells is internalized by fluid-phase endocytosis and ultimately delivered to lysosomes, thus providing a way to monitor in situ lysosomal proteolysis. Interestingly, the fluorescence of Bodipy-TR-X is insensitive to pH within physiological ranges (even from 3.5 to 11), which is helpful to monitor proteolysis in acidic compartments such as lysosome, which pH ranges between 4.5 and 5.

DQ-red-BSA was applied at 50µg/mL to neurons for 6, 12 or 24h in conditioned medium. This way, DQ-red-BSA entered cells by endocytosis and could only be degraded by lysosomes and not by proteasome, which is in the cytosol. Neurons were fixed and, to discriminate between healthy and unhealthy neurons, stained using Hoechst 33258. Additionally, MAP2 was revealed by immunofluorescence. Only neurons characterized by unfragmented nucleus and unfragmented MAP2 staining were selected for further analysis.

Most of the DQ-red-BSA-associated fluorescence was indeed noticeable in circular structures mostly in the soma of neurons, suggesting that most of BSA proteolysis occurred in lysosomes (see Fig 20), as reported in former studies¹³⁰.

DQ-red-BSA fluorescence was comparable in neurons from both genotypes after 6h of incubation. However, after 12 or 24h of incubation, it was about 50% lower in neurons derived from *Cln3* KI mice (see Fig 20).

This suggested lysosomal proteolysis was strongly reduced in neurons derived from CLN3 KI mice, thus confirming our metabolomics results and providing direct evidence for a lysosomal proteolysis defect.

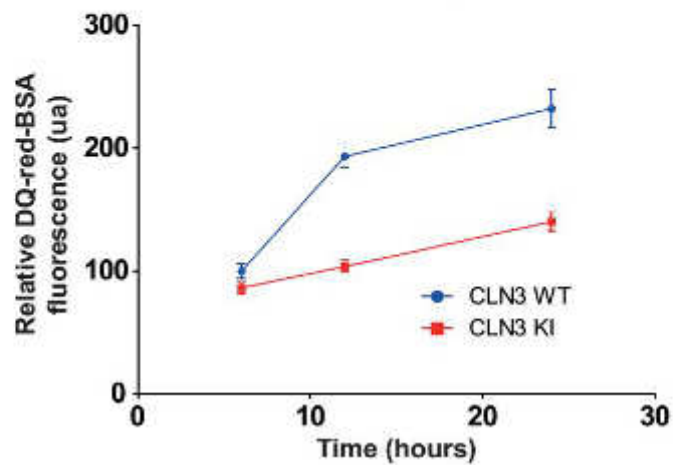
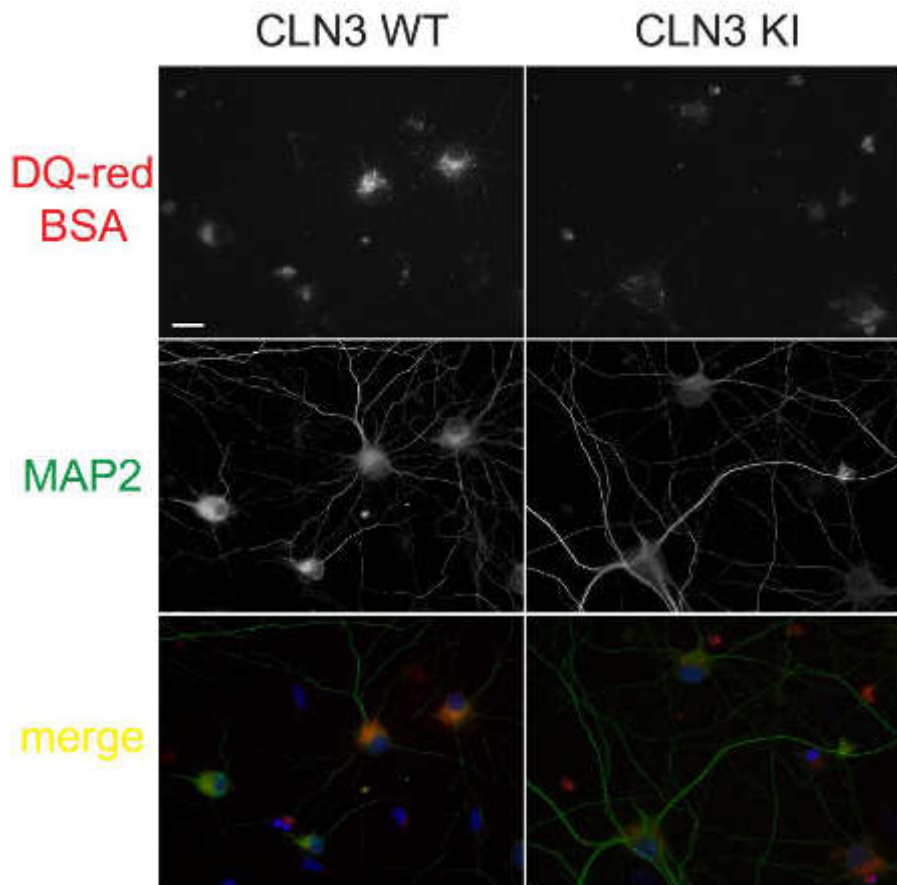


Figure 20: Decrease of lysosomal proteolysis in *Cln3* KI hippocampal neurons
 Scheme: Principle of the experiment. DQ-red-BSA is a BSA coupled to lots of Bodipy fluorophores quenching themselves due to proximity. When BSA is degraded, Bodipy molecules are released and emit fluorescence.
 Pictures: hippocampal neurons of *Cln3* WT and KI mice show DQ-red-BSA staining after 12h of incubation (upper pictures). MAP2 was revealed by immunofluorescence (middle pictures). DQ-red-BSA staining is much reduced in *Cln3* KI neurons (bar: 10 μ m).
 Graph: Quantification from 10 pictures per condition (approx. 40 neurons).

3.3 Measure of long-lived protein degradation in *Cln3* WT and KI primary fibroblasts

Using DQ-red-BSA only provides an indirect measurement of lysosomal proteolysis. The previous results were thus independently tested using a direct measurement of lysosomal proteolysis of long-lived cellular proteins by a pulse-chase method¹⁴⁴. In addition to its quantitative nature, this assay also offered a way to test proteolysis of cargos delivered to lysosomes by autophagy rather than endocytosis, thus minimizing the contribution of altered cargo delivery to our lysosomal proteolysis studies.

This pulse-chase experiment required:

- numeral washes and serum deprivation,
- a vast amount of material for significant signals,

For all these reasons, neurons seemed a poor model. Thus, we switched to primary mouse fibroblasts, which were prepared at the same time as neurons by Cécile Jouffret.

This method is based on radiolabelling of proteins with tritiated valine. Cells were firstly loaded for 24h with tritiated valine (pulse) which was incorporated in proteins during synthesis. Pulse lasted 24h to enable the sorting of proteins to compartments, which are the target of autophagy, and, thus, of lysosomal degradation. Cells were then washed to remove the radioactive tracer and incubated for one hour in medium with 10mM valine for pre-chase, to remove the contribution of short-lived proteins (degraded by the proteasome) to our measurements. This medium was depleted in serum to activate macroautophagy and enhance lysosomal proteolysis. At the end of pre-chase, cells were washed, initiating the chase step to monitor the degradation of long-lived proteins, which is mediated by autophagy and lysosomes.

In one well, proteins were precipitated using trichloroacetic acid (TCA, 10% in water) to measure how much radioactivity remained in long-lived proteins after pre-chase. The rest of cells was put in new medium without serum once again. This time point was considered the beginning of chase, which lasted from 2 to 12h. At the end of chase, proteins were precipitated using TCA and radioactivity in the pellet quantified, enabling to monitor the decrease of radioactivity in long-living proteins.

Protein degradation was thus calculated as follows:

$$\%_{\text{protein degradation}} = 100 \times \left(1 - \frac{\text{radioactivity after chase}}{\text{radioactivity before chase}}\right)$$

Percentage of protein degradation reached 30 to 35% in WT cells after 2h, 4h or 6h of chase, remaining quite stable. However, proteolysis was much slower during these first hours in KI fibroblasts: it reached 8% after 2h of chase, 17% after 4h and 22% after 6h, showing that lysosomal proteolysis was significantly impaired in CLN3 KI fibroblasts (Fig 21). For longer times of chase, percentage of lysosomal proteolysis increased rather linearly over times in both cell types, which can possibly be considered the beginning of cell death consecutively to serum depletion, as the morphology and the ability to adhere to plates of cells seemed altered.

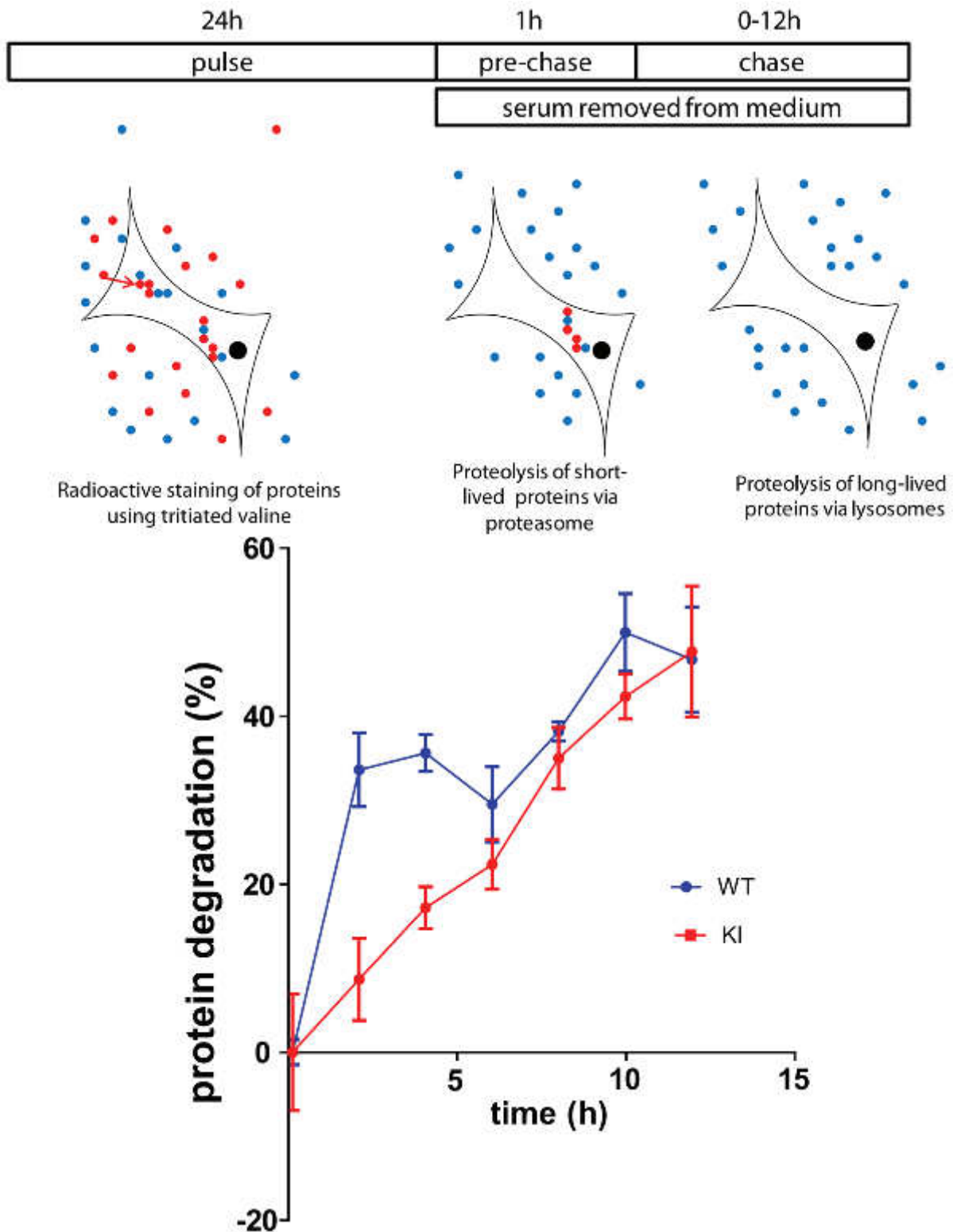


Figure 21: Lysosomal proteolysis is impaired in CLN3 KI primary fibroblasts. Upper panel: principle of the pulse-chase test. Primary fibroblasts were incubated for 24h in complete medium supplemented with tritiated valine. They were then washed and incubated in medium without serum supplemented with 10mM valine for the degradation of short-lived proteins by proteasome. Then, they were washed and incubated in the same medium to trigger the degradation of long-lived proteins by lysosomes. Lower panel: quantification of protein degradation in WT and CLN3 KI fibroblasts. For shorter times of chase, lysosomal proteolysis was significantly impaired in CLN3 KI cells. Cells were looking damaged for longer times.

3.4 Rescue of lysosomal proteolysis by CLN3 overexpression

Lysosomal proteolysis was shown to be defective in primary MEF cultures from two distinct *Cln3* KI embryos.

To confirm this defect was indeed due to CLN3 malfunction and not to some variability across primary MEF cultures, rescue experiments were performed by overexpressing human CLN3 in the mouse cellular models. Rescue was performed using transitory transfection. However, primary cells are very difficult to transfect with good efficiency. Thus, new CLN3 KI cell models were developed: immortalized fibroblasts.

Murine fibroblasts were immortalized from the previous primary fibroblasts by Cécile Jouffret by successive passage in 25cm² flasks. Primary fibroblasts division drastically slows down after 3 to 5 passages. Growth resumes after 15 to 20 passages, when a dividing clone overruns the rest of the cellular population. By doing so, four lineages were obtained: two WT, two *Cln3* KI. These cell lines had very different morphologies, from only slight modifications as compared to primary fibroblasts (very elongated cells) to HeLa cell-like morphologies.

Since transfection never succeeds in 100% of the cellular population, the former pulse-chase approach could not be used to monitor lysosomal proteolysis, since it would have been impossible to discriminate transfected from non-transfected cells in this test. To bypass this difficulty, EGFP-tagged proteins were transiently expressed, which allowed discriminating between transfected and non-transfected cells by flow cytometry (FACS), based on cells' green fluorescence. Flow cytometry enabled at the same time to measure of DQ-red-BSA intracellular proteolysis in a large number of cells.

DQ-red-BSA was used in a pulse-chase approach on MEFs. They were incubated half an hour in 50µg/mL DQ-red-BSA in serum- and antibiotics-free medium, and then washed. Chase was performed afterwards in complete medium for 2h. Cells were then fixed and analysed by FACS.

First, before performing rescue experiments, the four non-transfected cell lines were analysed using this new protocol to check whether it could detect a reduction in lysosomal proteolysis in the *Cln3* KI models.

DQ-red-BSA signals were very variable. Clone 140212-1 and 140212-8, being respectively CLN3 KI and WT, had about the same DQ-red-BSA signal, whereas clone 130605-2 (WT) displayed about 50% more DQ-red-BSA proteolysis and clone 141212-1 (*Cln3* KI) about 25% less (see Fig 22).

This was presumably due to cellular volume differences between the MEF clones. Interestingly, flow cytometry enables to measure cell morphological parameters such as diameter, thus offering a way to test this prediction. Since cells are rather spherical when in suspension, cellular volume could be estimated ($V = \frac{4}{3}\pi(\frac{d}{2})^3$). Volume varied from one to two between all four cell lines (see Fig 22), which probably impacted the number of lysosomes per cell and, consequently, the DQ-red-BSA signal. However, we chose not to correct DQ-red-BSA proteolysis data by cellular volumes since there was no evidence that the number of lysosomes would vary linearly with the size of cells.

As a result, it seemed that comparing different immortalized MEF cell lines together was not relevant, due to the vast changes in the morphology of cells. However, this difficulty did not prevent us from proceeding with the rescue experiments if we could avoid comparing distinct MEF clones. Therefore, an internal control for each lineage was designed. To do so, MEFs were transiently transfected 48h prior to experiment to express the following EGFP-tagged proteins: human CLN3 and, as a negative control, human sialin-P334R. Human sialin P334R is a pathogenic mutant of lysosomal transport sialin which transport activity is almost completely abolished, thus being a good control for the expression of lysosomal membrane proteins²⁵.

This protocol was performed on two MEF clones: 141212-1 (*Cln3* KI) and 140212-8 (WT), for they were the only ones that could be transfected with a sufficient efficiency.

In WT MEFs, overexpressing CLN3 had very little effect (-10%) on lysosomal DQ-red-BSA proteolysis as compared to overexpressing sialin P334R. In striking contrast, it doubled DQ-red-BSA proteolysis in *Cln3* KI cells (see fig 22).

In summary, despite the variability of shapes and volumes of our MEF clones which hindered analysis in this cell model, it seemed that *Cln3* KI clones have insufficient lysosomal proteolysis, since proteolysis was increased by overexpressing WT human CLN3 in *Cln3* KI, but not WT, clones.

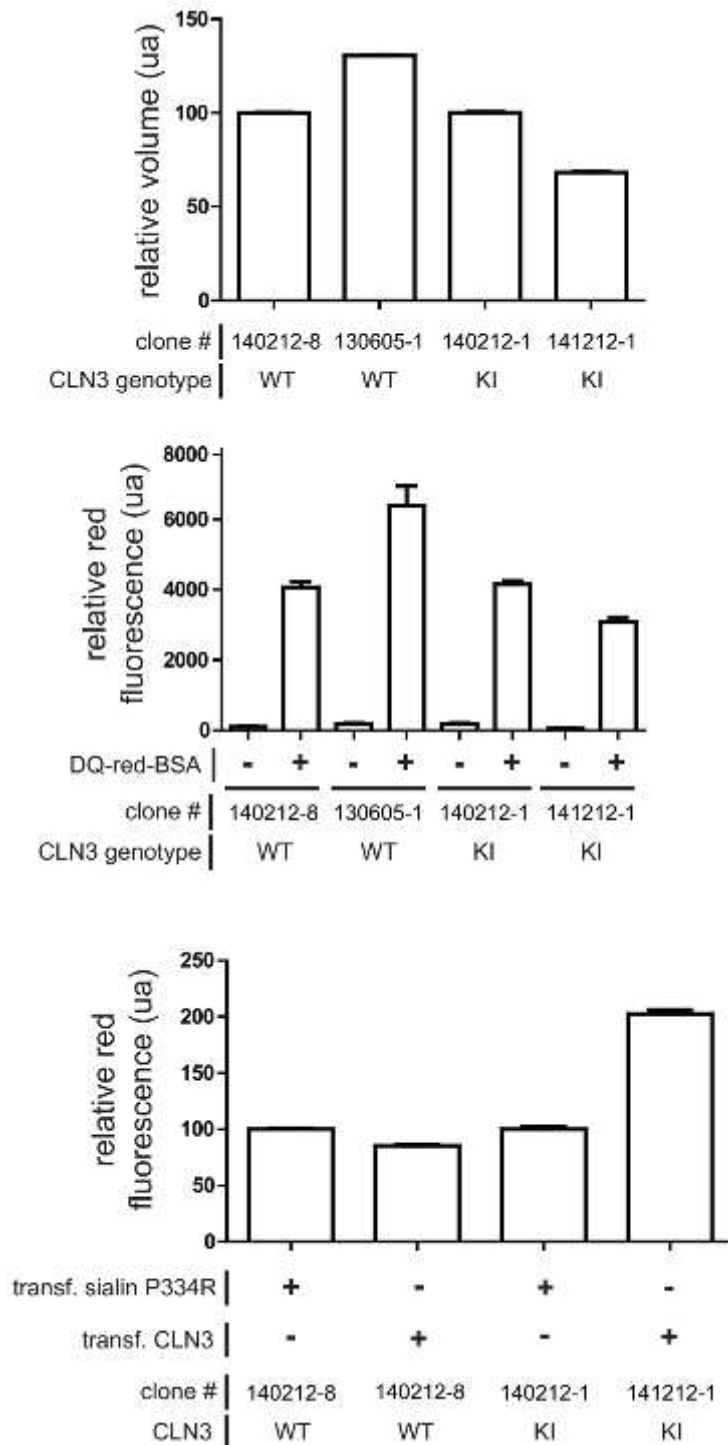


Figure 22: Lysosomal proteolysis in murine *Cln3* KI immortalized MEFs is increased by overexpression of human *CLN3*

Upper panel: volume of cell lineages used in this experiment, estimated from the diameter measured by flow cytometry.

Middle panel: Immortalized MEFs were treated with DQ-red-BSA and their red fluorescence measured. Red fluorescence signals strongly correlate with estimated volumes of cells.

Lower panel: MEFs were transiently transfected to express human sialin-P334R (control) or human *CLN3*. DQ-red-BSA assays were then performed. *CLN3* overexpression had little effect on WT immortalized MEFs but it doubled DQ-red-BSA proteolysis in *CLN3* KI MEFs.

4. Conclusion

4.1 Other approaches to identify CLN7 substrate(s)

Several approaches may be considered for pursuing our quest for CLN7 molecular function.

4.1.1 Widening the electrophysiological screen

The electrophysiological screen of putative CLN7 substrates led to the discovery of an artefact induced by cysteine on oocytes overexpressing several proteins at the plasma membrane. Contrary to what was firstly believed, the response of CLN7 oocytes to application of cysteine is thus most probably independent of CLN7 function. Yet, only amino acids were tested in this assay. It could be interesting to widen this screen by using sugars, catabolites of lipids or of nucleic acids.

4.1.2 Checking for amino acid transport using other techniques.

Like with all screenings using TEVC, it is impossible to exclude that CLN7 could be electroneutral and thus invisible in this technique. Our TFEB-based screen (Chapters 1 and 3) could provide an alternative approach to address this possibility. In addition, most amino acids are available in a radiolabelled form in my host laboratory, so direct uptake experiments could be systematically performed on amino acids. This could help to conclude whether CLN7 is a transporter for amino acids, or not.

4.1.3 Enriching oocytes with CLN7 substrate

Another approach was developed in my host laboratory on *Xenopus* oocytes to attempt identifying CLN7 substrates. *Xenopus* oocytes expressing CLN7 at the plasma membrane were incubated in a metabolite 'soup' (Bacto-Yeast Extract, an autolysate of yeast). Our assumption was that CLN7 may select its substrate from this soup and accumulate it into oocytes. It would thus have been accumulated in CLN7-expressing oocytes as compared to controls. To measure this putative accumulation, a metabolomic approach using mass-spectrometry was used.

This technique had previously been tested on LYAAT-1, a lysosomal transporter for small neutral amino acid, and oocytes expressing LYAAT-1 were indeed selectively enriched in proline and alanine identified by Principal Component Analysis, thus validating this novel approach. However, no clear enrichment in particular metabolites could be shown in CLN7-expressing oocytes (data not shown, obtained in collaboration with the group of Christophe Junot, CEA Saclay).

In our first implementation of this approach, the presence of endogenous oocyte metabolites may have prevented detection of accumulated exogenous metabolites if the latter have a mass identical or close to an abundant endogenous metabolite. The sensitivity and selectivity of this technique may be improved using metabolite extracts from bacteria or yeast grown on a carbon or nitrogen source labelled by a stable isotope (^{13}C , ^{15}N). This would help discriminating endogenous metabolites from exogenous ones imported by the transporter of interest.

4.1.4 Metabolomic profiling of CLN7 KO mice

Another approach to 'fish' CLN7 substrates could be to repeat our metabolomics analyses of lysosomal fractions from *Cln3* KI mice with a mouse model knock-out for *Cln7*. Such a model is already available (145 and unpublished data). Thus, its substrate(s) should accumulate in lysosomes of KO mice if, as most lysosomal transporters do, CLN7 exports hydrolysis products from the lysosome.

4.2 Relevance of the lack of lysosomal proteolysis in the pathophysiology of Batten disease

Although our metabolomic profiling of lysosomes could not provide any clue about CLN3 molecular function, it strongly suggested that CLN3 malfunction strongly impacted lysosomal proteolysis. Since four other genetic forms of NCL are caused by a primary defect in lysosomal protein degradation, these results suggests that defective lysosomal proteolysis, either primary or secondary, is a converging mechanism in the cellular pathophysiology of ceroid neuronal lipofuscinoses.

The decreased lysosomal proteolysis revealed in our metabolomics *Cln3* KI data was tested with three methods on diverse cell models derived from the KI mice, which, although each of them had its own limitations, all confirmed our findings and the suggested underlying mechanism. In addition, it should be noted that these biochemical and cellular assays confirmed the existence of a lysosomal proteolysis defect with both exogenous (BSA) and endogenous delivered to lysosomes by endocytosis or macroautophagy.

4.2.1 Checking further the selectivity of the proteolysis defect

To confirm that the lack of proteolysis is indeed due to CLN3 deficiency and associated to CLN3 (unknown) molecular function, two additional controls could prove useful.

First, overexpressing CLN3 in deficient cell models rescued lysosomal proteolysis. It could prove interesting to show that pathogenic mutants are unable to do so. Signals are variable between MEF clones. Corrections of factors indirectly influencing the proteolysis signals could help making these data more reliable. Cellular volumes seem to vary a lot from one cell clone to another, so probably the overall lysosomal volume per cell as well. Using lysosomal probes, such as internalized dextrans, could enable to normalize our proteolysis signals to the amount of lysosomes per cell.

The second possible control concerns the biochemical selectivity of the lysosomal hydrolysis defect revealed by our metabolomics data. Hydrolysis of proteins, but not polysaccharides, nor lipids, is affected. Similar biochemical or, if appropriate tools are available, cell biological experiments should be performed on our cell models to examine the degradation of sugars and lipids.

Better characterization of the proteolysis defect should as well aim at understanding if this defect is a general defect, impacting all lysosomal proteases, or if some proteases are more impacted than other by CLN3 deficiency. Addressing this issue could prove difficult, since the activity of lysosomal enzymes should be studied in situ, in lysosomes. However, there are a few enzyme-specific substrates that can be used on whole cells, such as Magic Red for cathepsin B (Immunochemistry Technologies), to test a small subset of lysosomal proteases but a wider screen of lysosomal proteases seems challenging.

Knowing which proteases are impacted by the defect of CLN3 could prove interesting to make hypotheses on a molecular mechanism that would link CLN3 malfunction and

lysosomal proteolysis. If the defect of lysosomal proteolysis is due to a decreased activity of all lysosomal proteases, it would suggest a general lysosomal problem, such as an increase in pH, for instance (but this would not explain why the hydrolysis of other macromolecules is affected, if this aspect is confirmed). On the other hand, if only a few lysosomal proteases are impacted, studying potential molecular interactions between CLN3 and these enzymes could help unravel CLN3 function.

4.2.2 A need for a better model to study CLN3 dysfunction

Although corrections and controls might help confirming the specificity of the defect of lysosomal proteolysis in current *Cln3* KI cell models, cells derived from clonal selections, such as immortalized MEFs or cells derived from CRISPR/Cas9 method, are quite variable, even in size or division rate. Thus, comparing between WT and KI models is made more difficult, for it is difficult to tell which differences are due to CLN3 dysfunction and which are due to other differences between cell models.

As a result, to be able to compare results between WT and KI cells models, inducible knock-out models of CLN3 could prove helpful. For instance, human cell lines with a modified *CLN3* could be designed: by putting two *Lox* sites around an exon of *CLN3*, expression of CLN3 could be abolished by transitorily expressing Cre recombinase. An inducible gene encoding small interfering RNAs against *CLN3* expression could as well be integrated in the genome on cells. Either way, WT controls and KO cells would originate from the same cell line, thus making comparisons much easier.

In addition, an inducible model KO for *CLN3* could be very useful to dissect the chronology of events due to *CLN3* dysfunction, and could help determine whether the decrease of lysosomal proteolysis occurs earlier or later than the diverse cellular defects already reported in the literature on CLN3.

4.2.3 Generalization to other NCLs?

NCL share common clinical and physiopathological features, in particular the accumulation of lipofuscin inside lysosomes and qualitatively similar clinical signs, thus suggesting that CLN proteins could play a role in a common pathway. The pathological convergence between enzymatic forms of NCLs and Batten disease (CLN3) revealed by our

study thus prompt us to ask whether defective lysosomal proteolysis occur in other genetic forms of NCL.

In my host laboratory, mice models knock-out for *Cln6* and *Cln7* are available. Further studies in these models could tell whether lysosomal proteolysis is the main cellular pathway controlled by CLN proteins.

4.2.4 Increasing lysosomal proteolysis: a potential therapeutic target?

If the lysosomal proteolysis defect revealed by our study is central and causative to the pathology of CLN3-deficient cells, increasing proteolysis would open a promising therapeutic strategy to counteract this deficiency. In this instance, understanding the molecular function of CLN3 might not be necessary to start developing therapies.

Pharmalogical activation of cathepsins has already been documented. Weak cathepsin B and L inhibitor PADK can be used as a molecular scaffold to develop activators¹⁴⁶. Ceramide was also been shown to activate cathepsin D in vitro¹⁴⁷.

Should a few proteases be specifically affected by the defect of CLN3, enzyme replacement therapy of those lysosomal proteases could as well be experimented (see p28). These therapies consist in delivering mannose-6-phosphate-coupled lysosomal enzymes directly in patients' blood. These enzymes can be taken up by M6P receptor at the plasma membrane, thus delivering functional lysosomal enzymes directly into patients' lysosomes. The blood-brain barrier is a severe issue for these approaches, NCL being mostly neurological disorders. However, intrathecal administration of gene therapy vectors could be considered. Of note, delivery of recombinant TPP1 protein directly into the brain using an Ommaya reservoir (a technique developed for chemotherapy of brain tumours) has proven a successful technique for treating children with a CLN2 disease (unpublished clinical trial).

The study of common neurodegenerative disorders like Parkinson or Alzheimer diseases is especially complex, since they seem to be multifactorial disorders, both due to genetic predispositions and environmental stimuli. Still, the importance of the endo-lysosomal system in these diseases has received increasing attention recently, being probably impacted early in the development of these diseases at the cellular level¹⁴⁸. NCLs are as well neurodegenerative disorders with an important role of the dysfunction of endolysosomes; but, contrary to more common diseases, they are monogenic and little

environmental factors seem to modulate the gravity of symptoms. In addition, some NCL genes are directly linked to other neurodegenerative disorders: for instance mutations of *ATP13A2* (*CLN12* gene) causes Kufor-Rakeb / PARK9 syndrome, a juvenile-onset form of parkinsonism, or a NCL ¹⁴⁹. Parkinson disease is also much more frequent in Gaucher disease, suggesting a possible convergence in the physiopathologies of these diseases ⁶⁵. Thus, studying the physiopathology of NCLs could be an easier way to gain insight into more common diseases due to the accumulation of abnormally degraded material.

Chapter 3: Identification of SNAT7 as a lysosomal glutamine transporter essential to the opportunistic nutrition of cancer cells

1. Introduction

SNAT7 (SLC38A7) was identified in our proteomic screen for new lysosomal membrane proteins. In this paper ¹⁵⁰, I expressed it in HeLa cells and showed that it was sorted to lysosomes, thus confirming this localization (see chapter 1).

1.1 The SLC38 family

The SLC38 family comprises eleven members (SLC38A/SNAT 1-11). Among them, 6 members have been functionally characterized as secondary active amino acid transporters: SNAT1-5 and SNAT9 ^{58,151,152}. They are characterized by ten or eleven transmembrane segments.

SNAT1, 2 and 4 are amino acid transporters with broad substrate selectivity. They are expressed at the plasma membrane. In polarized cells, the expression of these three proteins seems restricted to apical domains. SNAT1 and 2 are expressed in an ubiquitous manner whereas SNAT4 is only expressed in the liver and bladder. They have been referred to as system A transporters, a term based on early biochemical studies of amino acid transport ¹⁵³, which means they are able to transport small neutral amino acids, like alanine or proline. In addition, they can as well transport glutamine, asparagine, cysteine or histidine ¹⁵¹. All three are dependent on sodium for transport, which they co-transport with amino acids. They have been studied in more detail using electrophysiology ^{154,155}. SNAT1 and SNAT2 seem to share a similar mechanism, but SNAT4 has been described as voltage dependent, although the physiological relevance of this property, if any, is unclear.

All three transporters have been shown to have an important role in the exchange of amino acids in placenta, being expressed in apical membranes. Their expression is tightly regulated there ¹⁵⁶. The biological role of SNAT2 has been more extensively studied:

- It has been shown to be upregulated in a MAPK-dependent way during lymphocyte T activation, providing glutamine to sustain the growing metabolism ¹⁵⁷.
- It is also overexpressed in type-2 diabetes in beta cells of the pancreas. In these cells, insulin becomes inefficient leading to an upregulation of the production of insulin in the pancreas. It causes an increase of protein synthesis, which leads to ER stress. In response to ER stress, strangely, SNAT2 has been shown to be overexpressed, providing more amino acids and thus further increasing ER stress, which eventually can cause apoptosis of beta-cells ^{158,159}.
- MAPK-dependent upregulation of SNAT2 has been documented under deprivation of amino acid or hormonal activation, but in certain cell lines only including cancer cells. ^{160,161}

SNAT 3 and 5 have narrower substrate selectivity, transporting mostly glutamine, arginine and histidine. Thus, they are functionally described as system N. They are as well symporters of amino acids and sodium. The two proteins have distinct tissue expression profile: for instance, neurons and glial cells express mostly SNAT3 and kidney cells SNAT5 ¹⁵¹. Although SNAT3 activity can be monitored using electrophysiology, its transport activity turned out to be electroneutral, the current signal representing in fact an uncoupled current carried by protons ¹⁶². In contrast to SNAT 1, 2 or 4, which are importers of amino acids under physiological conditions because of their exclusive coupling to Na⁺, SNAT3 ion-coupling properties are quite particular: it co-transportes one Na⁺ and one amino acid in exchange for one proton. Because of this additional proton coupling, SNAT3 is more prone to reverse direction and depending on the organ and the membrane, it can either import or export amino acids from the cell.

SNAT1 and SNAT3 have an important role in the glutamate-glutamine cycle between astrocytes and neurons. Glutamate and GABA are respectively excitatory and inhibitory neurotransmitters which concentrations have to be very tightly regulated in the extracellular space to guarantee the spatial and temporal accuracy of synaptic transmission. In the case of glutamate, the uptake from extracellular medium by plasma membrane also prevents the inherent toxicity of this neurotransmitter. Indeed, upon release, glutamate can activate NMDA receptors. These ionotropic receptors, when open, trigger the entry of Ca²⁺ into the postsynaptic cell. Excess of glutamate can increase the intracellular concentration of calcium too excessive levels, leading to apoptosis. Moreover, glutamate triggers neuronal activation and further glutamate release from excitatory neurons, thus creating a dangerous feed-

forward loop. This phenomenon is called excitotoxicity and is implied in many neurodegenerative disorders ¹⁶³.

After release from synaptic vesicles, GABA and glutamate are taken up by astrocytes using EAAT transporters and GAT3, respectively. Both transmitters are then metabolized into glutamine in astrocytes, directly in the case of glutamate, and indirectly through the TCA cycle in the case of GABA. Glutamine is then exported from astrocytes by SNAT3 to the outer medium, taken up by adjacent neurons through SNAT1 and metabolized to glutamate or GABA in these neurons, before being loaded back again into synaptic vesicles ¹⁶⁴. Although other transporters can be implicated in this process, SNAT1 and SNAT3 are the main ones (see Fig 23).

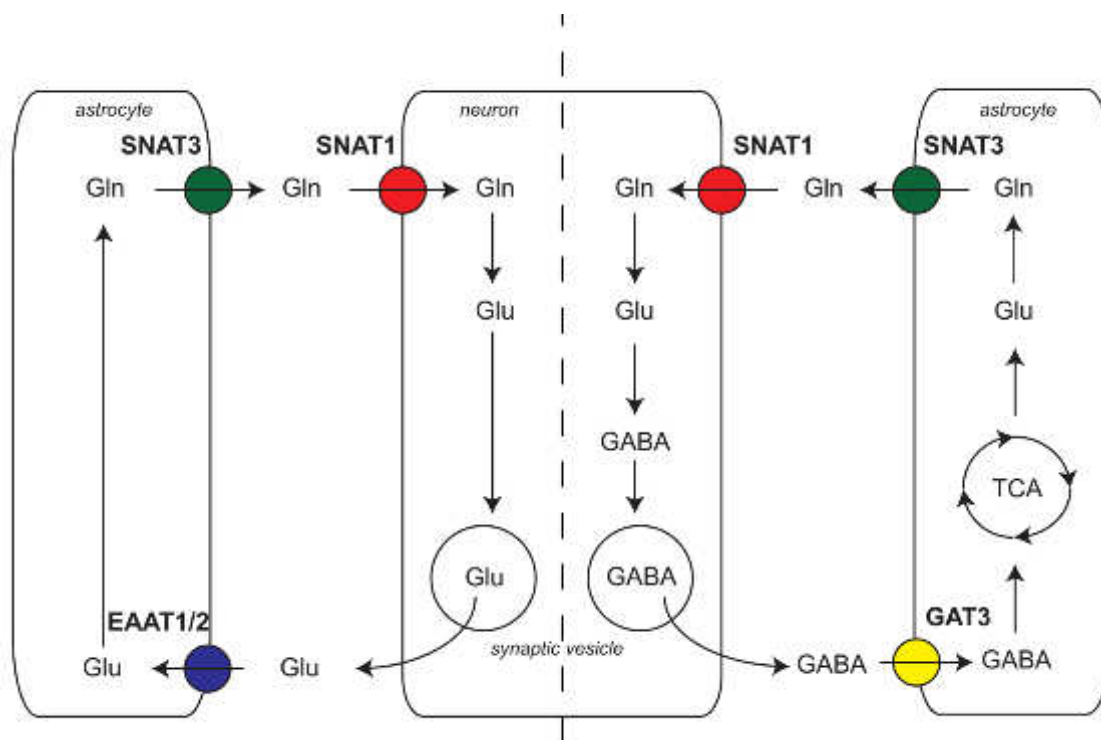


Figure 23: glutamate-glutamine cycle. Glutamate and GABA are release by neurons upon stimulus. They are taken up by astrocytes and metabolized into glutamine, which is exported by SNAT3 mainly. Neurons take up glutamine thanks to SNAT1 and can resynthesize GABA and glutamate. Co-transported ions are not figured.

SNAT8 was studied in the CNS by immunohistochemistry. It is expressed in most regions of the brains and both in astrocytes and neurons. Its role as transporter was studied in *Xenopus oocytes*. It was described there as a transporter for amino acid with low selectivity, transporting mostly alanine, glutamine, glutamate and serine. However, signal-to-noise ratio was rather low and confirmation of these results might be required, as authors suggested. SNAT8 could thus play a role in the glutamate-glutamine cycle.

SNAT9 was characterized during my PhD by three different teams as a key component of amino acid sensing at the lysosomal membrane^{58,152,165}. Moreover, two studies provided evidence for a lysosomal transporter function. However, its selectivity is not well assessed, since these two teams partially disagree in this respect, but glutamine and arginine seem the main substrates. Arginine is transported with a very low affinity (39 mM!). The main functional feature of SNAT9, documented by the three studies, is its ability to act as a signalling protein. It is part of a signalling platform at the lysosomal membrane, the Ragulator complex, which regulates mTORC1 activity. mTORC1 is the kinase that regulates most signalling pathway implied in cell growth and metabolism. SNAT9 may thus signal to mTORC1 about the metabolic state of lysosomes (see p25).

1.2 About SNAT7

1.2.1. Results from Hägglung et al

One study focusing on SNAT7 was published as well during my PhD¹⁶⁶. Its authors showed that SNAT7 was strongly and widely expressed in neurons, but not astrocytes.

In addition, they presented transport experiments done in *Xenopus* oocytes without mutating any putative sorting motif, thus implicitly suggesting that the protein operates at the plasma membrane under physiological conditions. Based on these experiments, the authors claimed that that SNAT7 mediates the transport of glutamine, alanine and arginine in a sodium dependent-manner, but the transport signals were exceedingly small.

1.2.2. SNAT7 could still be a lysosomal transporter

Although the authors focused extensively on role at the plasma membrane, they showed that SNAT7 was also expressed intracellularly in neurons. This suggested that SNAT7 localization at the plasma membrane could not be the only one.

Concerning transport experiments, SNAT7 was described as a transporter for glutamine mostly and histidine and alanine marginally, yet the best transport signal shown in the figures was obtained with arginine. These experiments also had a very low signal-to-noise ratio (as pointed out by¹⁵¹ and colleagues). Moreover the pH dependency of the transport activity was not studied, which could have unraveled a typical characteristic of

lysosomal transporters. Most lysosomal transporters have indeed been described to highly depend on the lysosomal proton gradient for their activity^{25,95,167}. Yet, Hägglung and colleagues did not mimic the lysosomal gradient in their experiment by incubating *Xenopus* oocytes in acidic buffers. This could explain why transport activity seemed weak in their article.

Concerning the small signals at plasma membrane, in my host laboratory, lysosomal transporters are typically studied by mutating their sorting motif to delocalize proteins at plasma membrane. However, before this method was applied, our lab had already characterized LYAAT-1, a lysosomal transporter of proline and alanine. To do so, this transporter had been strongly overexpressed in COS-7 cells, thus overflowing sorting machineries in the Golgi and resulting in a leak of proteins to plasma membrane⁹⁵. Thus, in experiments from Hägglung and colleagues, it is possible that some proteins may have reached the plasma membrane due to the overexpression, but SNAT7 may mainly act as a lysosomal transporter.

Altogether, a few signs in this article prompted us to examine the role of SNAT7 at the level of lysosomes:

- SNAT7 seemed to localize mostly inside cells and not at plasma membrane in neurons.
- Transport assays had low signal-to-noise ratio, suggesting the function had not been studied in the best conditions, in particular concerning pH.
- Lysosomal transporters can reach plasma membrane when overexpressed, which could explain why Hägglung and colleagues still observed some signal.

2. SNAT7 is a lysosomal transporter for glutamine and asparagine

2.1 Radioactive uptake in *Xenopus* oocytes

Hägglung and colleagues described a weak uptake of tritiated glutamine¹⁶⁶ from *Xenopus* oocytes expressing SNAT7, which suggested that, when SNAT7 was

overexpressed in *Xenopus* oocytes by injection of mRNAs, a fraction of the newly synthesized proteins was able to reach plasma membrane by overloading sorting machineries in the Golgi. However, their experiments were performed at neutral pH. Thus, we hypothesized that reproducing their experiment in acidic buffers could result in stronger uptake signals if our hypothesis about a lysosomal role of SNAT7 was correct (see p56. for a scheme of transport uptake at plasma membrane).

To do so, we synthesized in vitro mRNAs encoding an untagged murine SNAT7 and injected them in *Xenopus* oocytes (50ng per oocyte). We used an untagged version of SNAT7 since we did not know if fusion with EGFP at the N-terminal end could impact the activity of SNAT7 (we otherwise often use EGFP-tagged constructs because it allows selecting the best expressing oocytes under a fluorescence microscope prior to the functional measurements). Transport experiments were performed 48h after injection for proteins to be synthesized and sorted.

At that time, all antibodies against SNAT7 were poorly characterized, so we could not check for SNAT7 expression at plasma membrane using techniques such as surface biotinylation (see p83 for an example on CLN7).

Oocytes were incubated for at least 1h in transport buffer at pH7.0 for equilibration of ionic concentrations (buffer ND100, see materials and methods). They were then incubated for uptake at room temperature for 15 minutes in transport buffer supplemented with 1 μ M glutamine and 1 μ Ci [³H]-glutamine (5 oocytes per condition). This uptake mix was at pH 5.0 to create a proton gradient across the plasma membrane, and thereby activate lysosomal transporters. Oocytes were then washed four times in ice-cold pH7.0 transport buffer and individually broken down in SDS 10%. Radioactivity was then counted in each oocyte lysate.

Results varied greatly for one experiment to another (see fig 24). In some experiments (5 out of 13), a selective uptake of glutamine was observed in a pH-dependent manner (data not shown), whereas, in most of the experiments (8 out of 13), no difference could be observed between unspecific uptake in control oocytes (which expressed EGFP) and uptake in SNAT7-expressing oocytes.

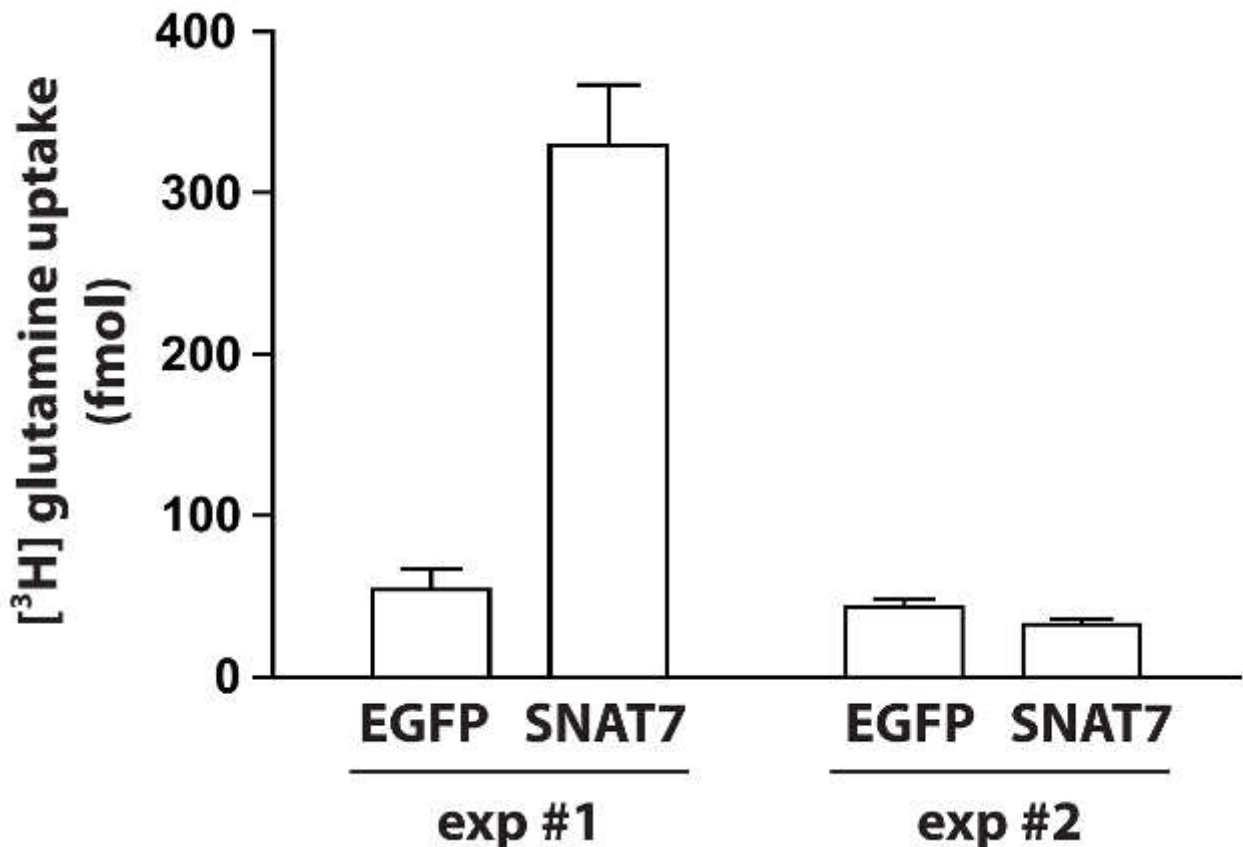


Fig 24: variable uptake tests on Xenopus oocytes expressing SNAT7
 Oocytes were injected with mRNA encoding EGFP or SNAT7 48h prior to experiment. They were incubated in pH 5.0 buffer with 1 μ M glutamine and 1 μ Ci [3H]-glutamine for 15 minutes and washed. Radioactivity was then counted in each oocyte. In some experiments, like exp #1, SNAT7-expressing oocytes took up far more glutamine than controls, whereas in some experiments like exp #2, the uptake was similar.

This could be explained by variable processing of SNAT7 mRNAs: Injection of mRNA triggers a burst in protein synthesis. On the one hand, some oocytes could have a “fast” Golgi apparatus that is able to sort all newly synthesized proteins to lysosomes, which leads to no proteins at plasma membrane, so no signal. On the other hand, some oocytes could have “slower” sorting machineries, which lets some of the vast amount of newly-synthesized proteins due to the injection of mRNA leak to the cell surface, enabling signal monitoring. Such variability could as well been explained in a similar manner by variations in the ability of synthesize proteins or to degrade exogenous mRNA from one oocyte preparation to another.

In addition, since SNAT7 was expressed untagged in oocytes, it is possible that many oocytes tested for transport did not express the protein properly.

Whichever phenomenon made the results of this transport assay variable, in the end this system was too unreliable to perform functional studies of SNAT7.

2.2. Sorting of SNAT7

To try and improve the expression of SNAT7 at plasma membrane to monitor reliable transport, I tried the misrouting approach which has been extensively mentioned in this dissertation (see p55 for more details).

The primary sequence of SNAT7 was screened for putative lysosomal motifs in predicted cytosolic loops. Four putative motifs corresponded to these criteria in the mouse sequence: 21 ERARLL, 115 YQEV, 203 YASF and 355 YKGM. The first two motifs seemed the most promising, as they were well conserved in many species. The two last ones were only poorly conserved. For instance, 203 YASF becomes 203 YASS in the rat protein.

To screen for the most important motif for the sorting of SNAT7, plasmids encoding for the fusion of EGFP and mutated form of SNAT7 were generated. Tyrosine residues were mutated into alanine residues (Y115A for example) and leucines into alanines (LL(25/26)AA for example) to impair putative motifs interaction with adaptors. HeLa cells were then transfected to transiently express the mutated forms of SNAT7. Subcellular localizations of mutated SNAT7 proteins were observed after 48h.

The mutation of tyrosine residues at positions 203 and 355 resulted in the localization of EGFP-SNAT7 in the ER, suggesting a strong destabilization of the protein 3D structure, making it impossible to pass through quality control in the ER (data not shown) (see fig 25).

The mutation of the two remaining motifs (LLAA and Y 115A) did not alter the subcellular localization of EGFP-SNAT7 when compared to WT. Both proteins colocalized very well with LAMP-1, a resident protein of the lysosome membrane which was revealed by immunofluorescence (see Fig 25). This suggested that none of these motifs was necessary for lysosomal sorting.

MAQVSINSDY SEWASSTDAG **ERARLLQ**SPC VDVVPKSEGE ASPGDPDSGT TSTLGAVFIV VNACLGAGLL NFFPAAFSTAG
 81
GVAAGIALQM GMLVFTISGL VILAYCSQAS NERT**YQEVVW** AVCGKLTGVL CEVAIAVYTF GTCIAFLIII GDQQDKIIAV
 163
MSKEPDGASG SPWYTDKRFI ISLTAFLFIL PLSIPKEIGF QKYASFLSVV GTWYVTATII IKYIWPDKEM RPGDILTRPA
 243
SWMAVFNAME TICFGFQCHV SSVPFVNSMR QPEVKTWGGV VTRAMVIALA VYMGTGICGF LTRGAAVDPD VLRSYPSDEV
 321
AVAVARAFII LEVLTSYPIL HFCGRAVVEG LWLRYKGMPV EEDVGRERRR RVLQTLVWFL LPIILLALFIP DIGKVISVIG
 401
GLAACFIFIF PGLCLIQAKL SEMEEVKP**RS** NWALVSYGVL LVTLGAFIFG QTTANAIFVD LLA

transmembrane domain
 lysosomal domain
 conserved putative lysosomal sorting motif

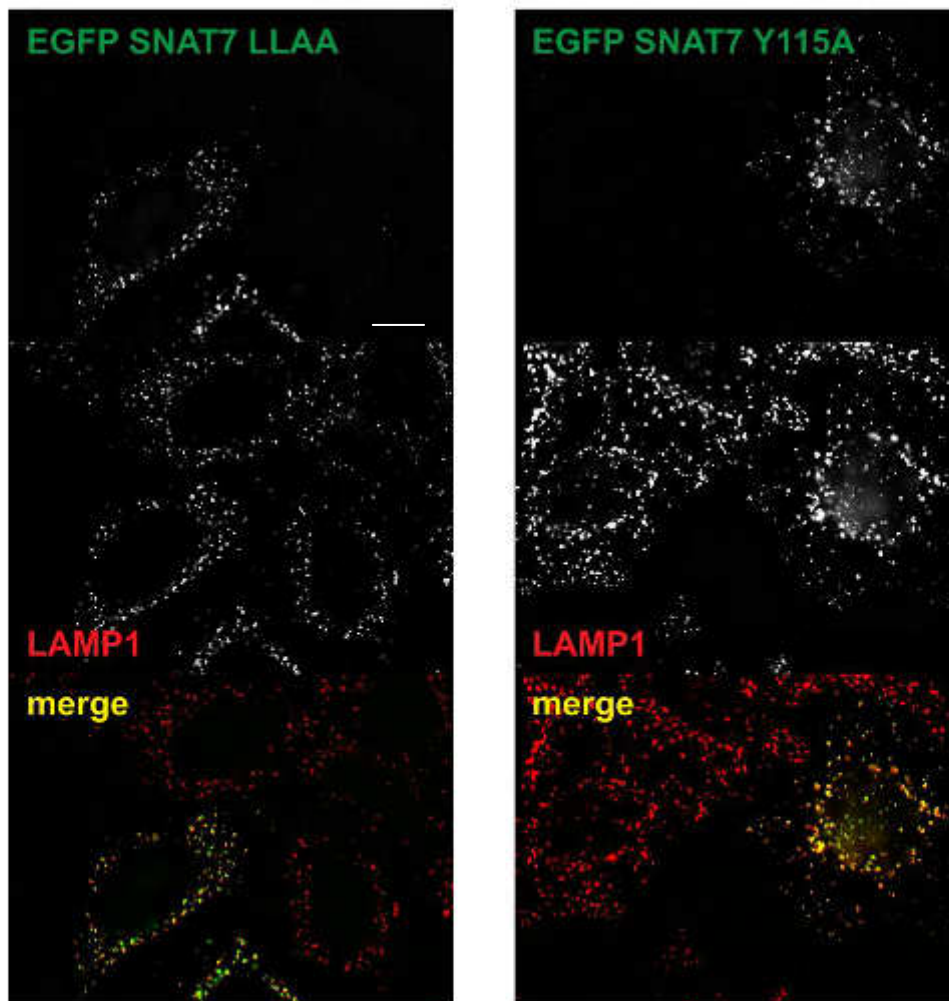


Fig 25: SNAT7 is not sorted to lysosomes thanks to a canonical motif.
 Upper panel: primary sequence of SNAT7. Two sorting lysosomal motifs were studied extensively (in blue).
 Lower panel: HeLa cells transiently expressing EGFP-SNAT7 LLAA or Y115A were fixed 48h after transfection.
 LAMP-1 was revealed by immunofluorescence. Both mutated forms of SNAT7 colocalized nicely with LAMP-1,
 suggesting that nor 21ERARLL nor 115 YQEV are not the main sorting motifs.
 Bar: 10µm

To check whether the two latter motifs could play redundant roles, a plasmid encoding the double-mutant protein (SNAT7 LLAA Y115A) was generated and expressed. However, the double mutant also localized to lysosomes (data not shown), thus suggesting that none of the two motifs was critical for lysosomal sorting.

As a result, the main sorting motifs important for localizing SNAT7 to lysosomes could not be identified. This could be due to several reasons:

- SNAT7 is targeted to lysosomes when overexpressed in HeLas for degradation purposes. We could however show in fractionation experiments (see p127) that endogenous SNAT7 was expressed at the lysosomal membrane, in agreement with our comparative proteomic data. Yet, it is still possible that overexpression results in an overload of newly-synthesized proteins which are targeted to lysosomes for degradation thanks to another mechanism than motif-specific sorting (autophagy of the ER, for instance).
- Motifs 203 YASF and 355 YKGM are critical for the lysosomal sorting of SNAT7. However, since their mutation critically destabilizes the architecture of SNAT7, this hypothesis is difficult to confirm. In addition, these motifs are not conserved in the human form of SNAT7, which we could show was sorted to lysosomes, suggesting a minor role for these motifs, if any. Whichever these motifs are important or not, expression of SNAT7 at plasma was not possible by mutating them.
- SNAT7 is sorted to lysosomal membranes thanks to a non-canonical motif. This has already been described for some lysosomal membrane proteins, such as CLN3¹²⁰. In its last two cytosolic loops, SNAT7 contains indeed acidic clusters (glutamate residues, see fig 25) which have been shown to be potentially important for lysosomal sorting⁴¹
- SNAT7 is sorted to lysosomes thanks to a durable interaction with another lysosomal protein with canonical sorting motifs. This has been documented in the case of Ostm1, which is sorted to lysosomes thanks to its interaction with the lysosomal chloride channel Clc7⁶⁹.

We did not aim at understanding the mechanisms of SNAT7 sorting, but rather at generating a suitable model for functional studies. However, it could be interesting to study them more extensively in the future by, for instance, expressing only domains of SNAT7 instead of the full protein to try and understand which loop is responsible for lysosomal sorting.

2.3 Sending SNAT7 to plasma membrane by activating lysosomal exocytosis

Because it seemed difficult to induce expression of SNAT7 at the plasma membrane either by mutating its sorting motif or merely by overexpressing it, we tried to force the exocytosis of lysosomes to the plasma membrane to make SNAT7 amenable to transport assays in whole cells.

The discovery of autophagy and the implication of lysosomes in the processing of antigens in immunity cells have shown that lysosomes are more dynamic than thought previously. Lysosomes have now been shown to be secreted in several cellular contexts, the two best described being:

- Immunity cells. Among all these cells, secretory lysosomes have mostly been described in two cell types: firstly, cytotoxic T cells, which are able to secrete toxic proteins via specialized lysosomes: lytic granules¹⁶⁸. Secondly, dendritic cells secrete lysosomes at the immunological synapse with B-cells, which takes part to antigen processing and presentation¹⁶⁹.
- In the context of damaged plasma membrane. A wound in plasma membrane typically results in a strong increase in extracellular calcium levels, the cytosol being usually deprived of Ca^{2+} by pumps. This increase is detected at the lysosomal membrane by synaptotagmin VII, which activates calcium release from lysosomes by mucolipin 1, which in turn triggers lysosomal exocytosis, thus patching the wound¹⁷⁰. This mechanism has been shown to be present in many cell types, which encouraged us to try to trigger lysosomal exocytosis in cell models suitable for transport assays, such as HEK293T.

In both cases, cytosolic Ca^{2+} seemed to be the critical trigger for lysosomal exocytosis. We hoped to be able to trigger lysosomal exocytosis using calcium without wounding plasma membrane, since our functional assays were based on the cellular uptake of a soluble compound in the cytosol from the outer medium, thus requiring plasma membrane integrity.

In addition, the homeostasis of endocytic compartments has been described to regulate the rates of exocytosis as well. For example, dynasore, a drug blocking the influx of membrane into the endocytic compartments by blocking dynamin, which is necessary for the scission of endocytic vesicles from plasma membrane, has been shown to increase the exocytosis of post-Golgi granules¹⁷¹. Thus, blocking endocytosis could prove helpful when trying to induce lysosomal exocytosis.

To test functional approaches based on lysosomal exocytosis, we used HEK293T cells, which have routinely been used in my host laboratory for transport assays of lysosomal transporters, in addition to *Xenopus* oocytes. Before trying to monitor SNAT7 activity, the proof of principle of this method was investigated using sialin, a well-known lysosomal transporter for sialic acids previously characterized in my host laboratory²⁵. Cells transiently expressed EGFP-sialin, which is expressed on lysosomal membranes, or EGFP-sialin-LLGG, which is mutated at the sorting motif and misrouted to the plasma membrane. Cells were treated with uptake buffer at pH 7.0 (MOPS, see material and methods) for 30 min with 5 mM calcium chloride and 20 μ M ionomycin, an ionophore for calcium, to increase the cytosolic concentration of calcium. In addition, cells were treated at the same time with 80 μ M dynasore to block endocytosis.

Immediately afterwards, a transport assay was performed. Cells were treated for 15 minutes with uptake buffer at pH 5.0 (MES, see material and methods) containing 0.5 μ Ci per well of [³H]N-Acetylneuraminic acid (Neu5Ac), one of the best substrates of sialin. Cells were washed with ice-cold pH 7.0 buffer twice and lysed with NaOH. Radioactivity in lysates was finally counted.

Untreated cells expressing sialin LLGG (at the plasma membrane) displayed much more uptake of [³H]Neu5Ac than untreated cells expressing WT sialin (at lysosomal membranes). This showed that both transfected proteins were functional.

However, cells treated with the Ca²⁺ ionophore and dynasore showed little uptake of the radiolabelled substrate of sialin, independently of the overexpressed protein (see fig 26). This suggests that the treatment probably damaged the cells, maybe resulting in wounding the plasma membrane and creating a leak of the radioactive compound from the cytosol.

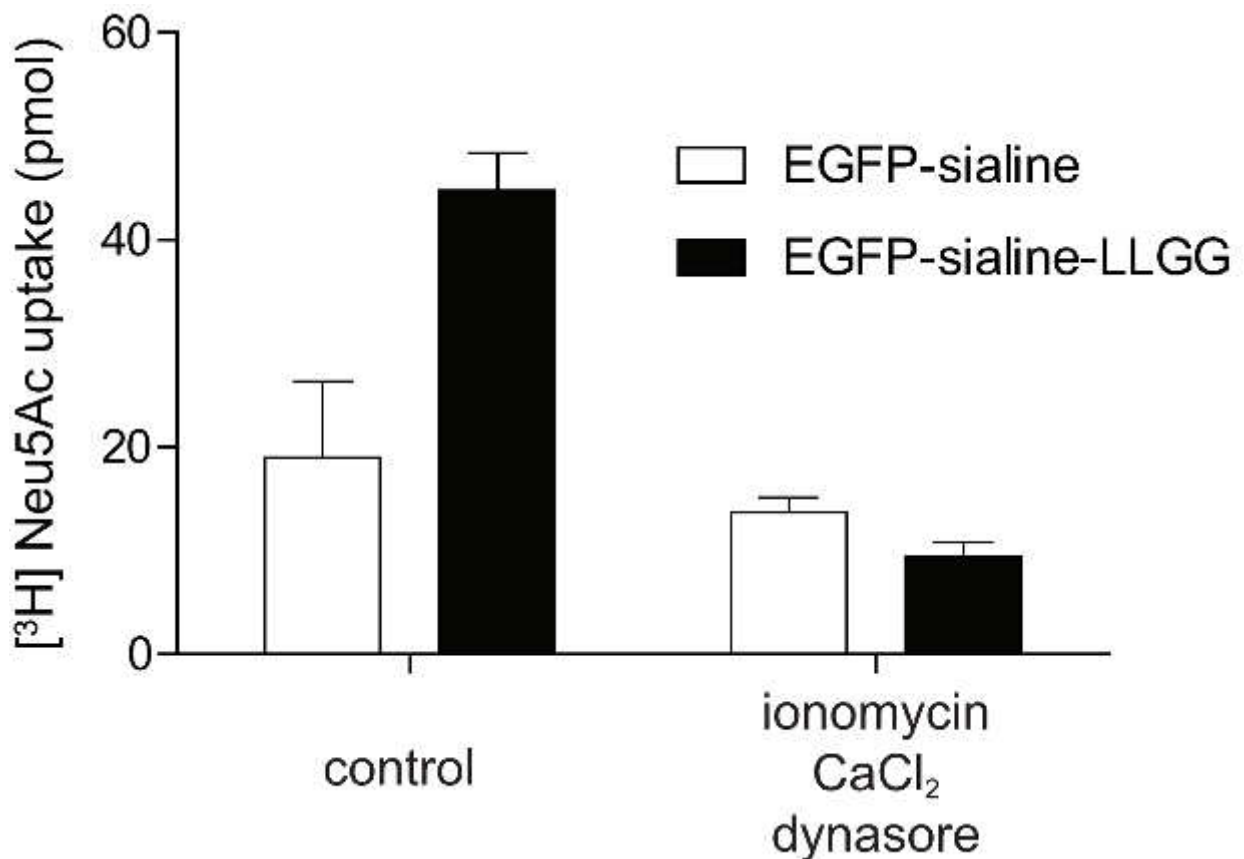


Figure 26: Trying to trigger lysosomal exocytosis for transport assays in HEK293T cells. Cells were transfected to transiently expressed EGFP sialin (at the lysosomal membrane) or EGFP-sialin-LLGG (at plasma membrane) 48h prior to experiment. They were treated with ionomycin, calcium chloride and dynasore (or control buffer) for 30 minutes. They were washed and incubated in pH5 buffer containing [³H]Neu5Ac for 15 minutes. They were eventually lysed and radioactivity of lysates counted. This treatment completely impaired sialin activity in HEK293T cells.

Milder conditions were tried as well, with shorter periods of incubation or lower concentrations, resulting in either the same damaging effect or no effect at all (data not shown). This suggests that, depending on the concentration, the treatment either did not have a strong effect on lysosomal exocytosis, or damaged cells in a way incompatible with transport measurements.

Protocols wounding plasma membrane a longer time before uptake could be considered, yet they would be challenging, since one would have to master the dynamics of lysosomal exocytosis and wound repair on the one hand, and of internalization by endocytosis of proteins of interest on the other hand.

2.4 Confirming SNAT7 function as lysosomal transporter for glutamine by developing an indirect assay

2.4.1 Principle of the test

Because it seemed impossible to express SNAT7 at the plasma membrane, more time-consuming techniques such as lysosome purification or reconstruction in liposomes seemed necessary to functionally characterize SNAT7 as a lysosomal transporter. Before doing so, an indirect assay was designed, which was much easier to handle and which could be re-used for other candidates.

This assay enables to measure indirectly transport activity at the lysosomal level, and not at the plasma membrane, in intact cells. It was performed on HeLa cells exposed to amino acid esters. Because of their being more hydrophobic than regular amino acids, these esters are able to diffuse through membranes. However, lysosomes are the major organelles containing hydrolases, which are able to catalyse the cleavage of the ester bond and thus generate the free amino acid. Once inside lysosomes, non-modified amino acids are trapped and their efflux through transporters is slow, hence creating a strong overload inside lysosomes. It should be pointed out that other organelles, such as ER, contain hydrolases as well, but most of the accumulation occurs inside lysosomes¹⁷².

We speculated that this overload could be reduced when a transporter able to export some of the overloaded amino acid was overexpressed. Eventually, control cells expressing a mock construct should display high levels of the accumulated amino acid, whereas cells expressing a transporter able to export the overloaded amino acid should have a smaller accumulation. (see Fig 27) The level of lysosomal amino acid overload should thus reflect transport activity of the tested protein.

To detect lysosomal overload, we used the transcription factor TFEB, which controls most of the genes implicated in autophagy and lysosome biogenesis. Under normal conditions, TFEB usually is localized in cytosol, but it is targeted to the nucleus in case of lysosomal overload⁶⁰. Thus, in cells with no overexpressed transporter, overload should be quite strong and TFEB quite dramatically translocated to the nucleus, whereas this translocation should be milder in cells overexpressing the corresponding transporter.

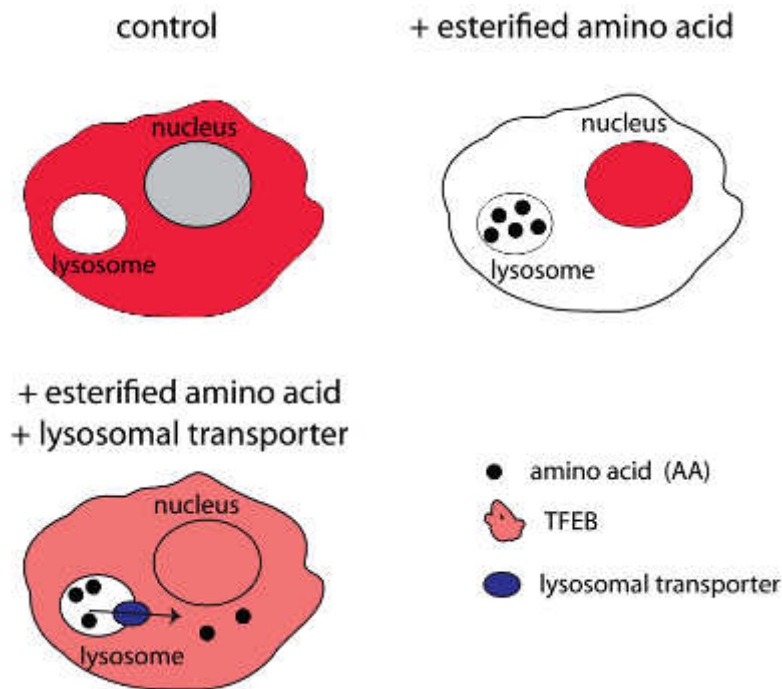


Figure 27: principle of the indirect test for lysosomal amino acid transporters. Under normal conditions, TFEB is inactive and localized in the cytosol in most cells. When lysosomes are overloaded with amino acids, TFEB is activated and translocated to the nucleus. However, if a lysosomal transporter able to export the amino acid is overexpressed, overload is reduced and TFEB is redistributed in cytosol.

2.4.2 Quantification method and determination of the optimal ester concentration

To follow TFEB localisation by epifluorescence, a plasmid encoding mRFP-TFEB was generated and transfected into HeLa cells. Indeed, despite a few publications, antibodies against endogenous TFEB are not highly specific and precise localisation is difficult to assess.

On the other hand, an antibody against TFE3 was available. TFE3 belongs, like TFEB, to the MiT family (microphthalmia family of transcription factors)¹⁷³. In the same way as TFEB, TFE3 is supposedly translocated to nucleus under lysosomal stress. Using immunofluorescence, we confirmed this result in HeLa cells but signal-to-noise ratio was rather low and mRFP-TFEB was used as our method of choice.

It is important to point out that HeLa cells used for the following experiments were used 48h after transfection, as transfection results in lysosomal stress (especially with lipofectants which accumulate into lysosomes) and, consequently, in TFEB translocation. 24h after transfection, TFEB was indeed almost always fully translocated to nuclei in HeLa cells. Besides, electroporation was favoured over lipofection, for lysosomal stress was

noticed to be much milder then. In the end, 48h after electroporation, mRFP-TFEB was mostly localized in cytosol of HeLa cells (see Fig 28).

Eleven different amino acid esters (see Fig 28) were shown to trigger TFEB translocation after 2h at 37°C with no or little toxic side effects at the concentration used. However, a few trials have been unsuccessful: arginine methyl-ester and glutamine methyl-ester were not able to cause noticeable translocation of TFEB without toxicity on cells. This is why glutamine tert-butyl-ester was used instead of the methyl-ester one. We do not fully understand why these differences occur, but it could however be hypothesised that different ester groups are taken up differently by cytosolic, ER or lysosomal hydrolases, hence resulting in different activation thresholds of TFEB. Similarly, all esters do not trigger TFEB translocation at the same concentration, possibly for similar reasons.

For quantification, at least 50 cells per condition were classified in three groups depending on TFEB localisation: TFEB mainly in cytosol, here after “C” group, TFEB mainly in nucleus, “N” group, or mixed localisation, “M” group. A few counts were replicated by different people in my host laboratory in a blind manner to avoid subjective interpretation. To deal with variability, experiments were replicated three times.

To determine the optimal dose of esters for our experiments, we hypothesised the following. To be reversed by transporters, overload of lysosomes with amino acids should not be too strong; otherwise it would not be possible to reduce lysosomal concentrations of amino acids back to tolerable levels and thus to translocate TFEB back to cytosol. We thus selected for each ester the concentration that induce 45% nuclear/nuclear + mixed distribution of TFEB for subsequent experiments with the lysosomal transporter constructs. All optimal concentrations are listed in Materials and Methods.

In all experiments, sucrose was used as a positive control since (i) it has been shown to enter lysosomes by endocytosis and (ii) lysosomes have no invertase to hydrolyse it, nor any transporter to export it. It has thus been documented for a long time as an easy way to trigger lysosomal overload^{2,60}. Interestingly, in our system, only about 50% of cells treated with sucrose displayed mixed or nuclear localisation of TFEB, suggesting a mild overload at the concentration used.

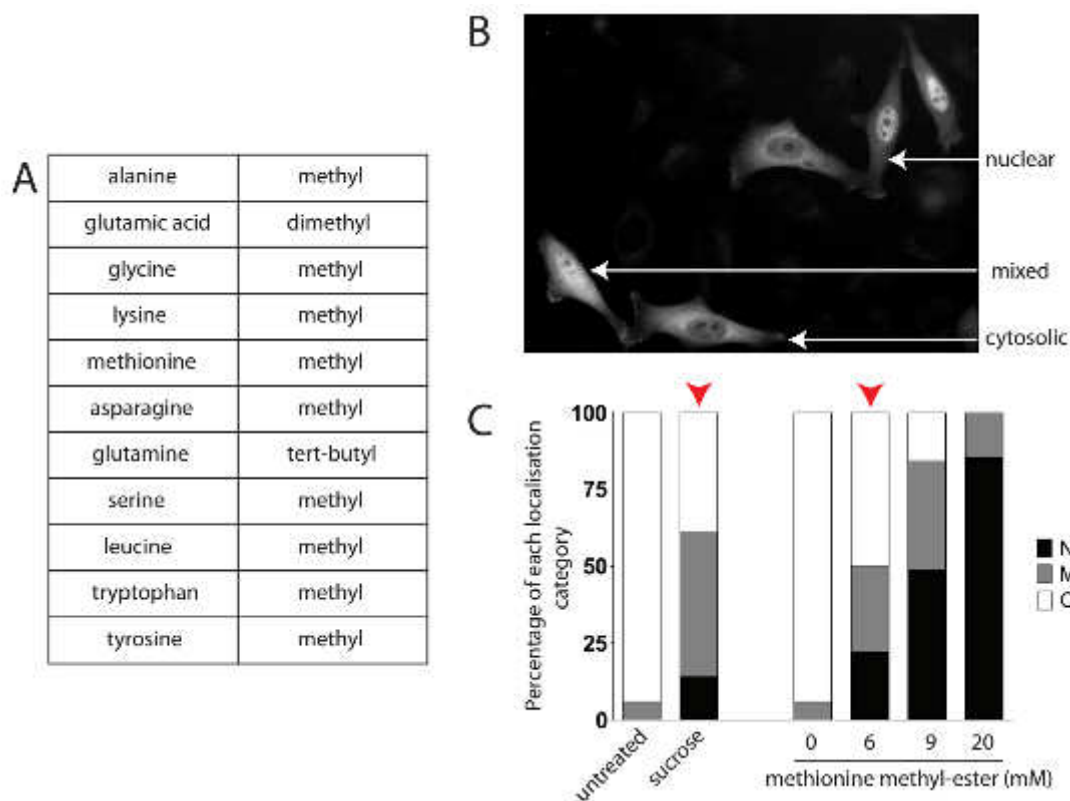


Figure 28: modalities of the lysosomal amino acid overload assay.

A: List of all esterified amino acid used and of corresponding ester groups. Ester groups were carried by amino acid carboxylic acid functions.

B: HeLa cells expressing mRFP-hTFEB. TFEB localisation was classified in three different groups: cells with TFEB mainly in nucleus ("N"), cells with TFEB mainly in cytosol ("C"), and cells with mixed localisation ("M").

C: Dose response of TFEB to methionine methyl-ester in HeLa cells. Cells were treated for two hours with control medium or medium containing 100 mM sucrose or various concentrations of methionine methyl-ester. Localisation of mRFP-TFEB was classified as in point B for at least 50 cells per bar. Here for example, for further experiments, 6mM of methionine methyl-ester were applied, since TFEB translocation level is comparable to the one induced by sucrose (see red arrows).

2.4.3 Proof of principle

To prove its efficiency in detecting lysosomal transporter activity in intact cells, the TFEB-AA ester assay was firstly applied to two amino acid lysosomal transporters well characterised in my host laboratory: PQLC2, a transporter of cationic amino acids and LYAAT1, a transporter of small neural amino acids. Sialin P334R was used as a negative control (see Chapter 2, p XX).

Cells expressing these transporters (identified thanks to an EGFP tag) were exposed to two esters: lysine methyl-ester and alanine methyl-ester. Lysine is a substrate of PQLC2 and alanine a substrate of LYAAT-1. In sialin-expressing cells TFEB was translocated to the nucleus in about 50% of cells when exposed to sucrose or any of the two esters. However,

PQLC2-expressing cells were resistant to lysine methyl-ester-induced translocation of TFEB, suggesting PQLC2 reduces the lysine lysosomal overload induced by the ester application. Similarly, LYAAT-1 cells displayed little translocation of TFEB when their lysosomes were overloaded with alanine, suggesting again that the overexpressed transporter reduced the lysosomal overload induced by the corresponding ester.

Thus, this test could have helped identify PQLC2 as a lysosomal lysine transporter and LYAAT-1 as an alanine lysosomal transporter if the substrate selectivity of these transporters were unknown, confirming the efficiency and relevance of our assay (see Fig 29).

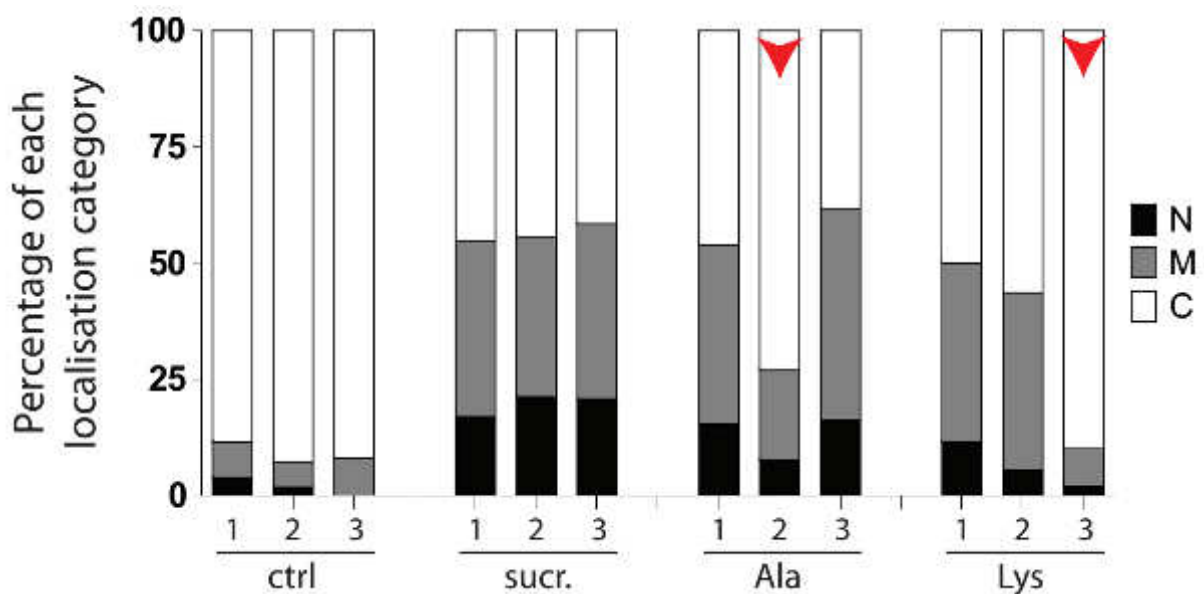


Figure 29: proof of principle of the TFEB-AAE assay
 48h before experiments, HeLa cells were transfected to co-express mRFP-TFEB and: 1: EGFP-hsialin-P334R, 2: EGFP-rLYAAT1, 3: rPQLC2-EGFP.
 They were treated for two hours with medium supplemented, or not, with sucrose, alanine methyl-ester or lysine methyl-ester. Cells were fixed and TFEB localisation was assessed as previously.
 LYAAT1-expressing cells are resistant to the lysosomal overload response induced by alanine methyl-ester and PQLC2-expressing cells to lysine methyl-ester (see red arrows).

2.4.4 Application of the TFEB-AAE assay to SNAT7

This paragraph and the following ones summarize part of the draft of a paper in preparation, to which I contribute as first author.

When overexpressed in HeLa cells fused to EGFP, SNAT7 was sorted to lysosomes. Thus, we used our *TFEB-AAE* assay to characterize the amino acid selectivity of SNAT7.

PQLC2-EGFP was used as a control, like previously. As expected, TFEB is translocated to nucleus in about 50% of PQLC2-expressing cells in all conditions but when they were treated with lysine-methyl-ester, confirming its function of lysosomal lysine transporter. Similarly, EGFP-SNAT7 had no effect on the nuclear distribution of TFEB except when cells were treated with glutamine and asparagine esters, which suggested SNAT7 is a lysosomal transporter selective for glutamine and asparagine (see Fig 30)

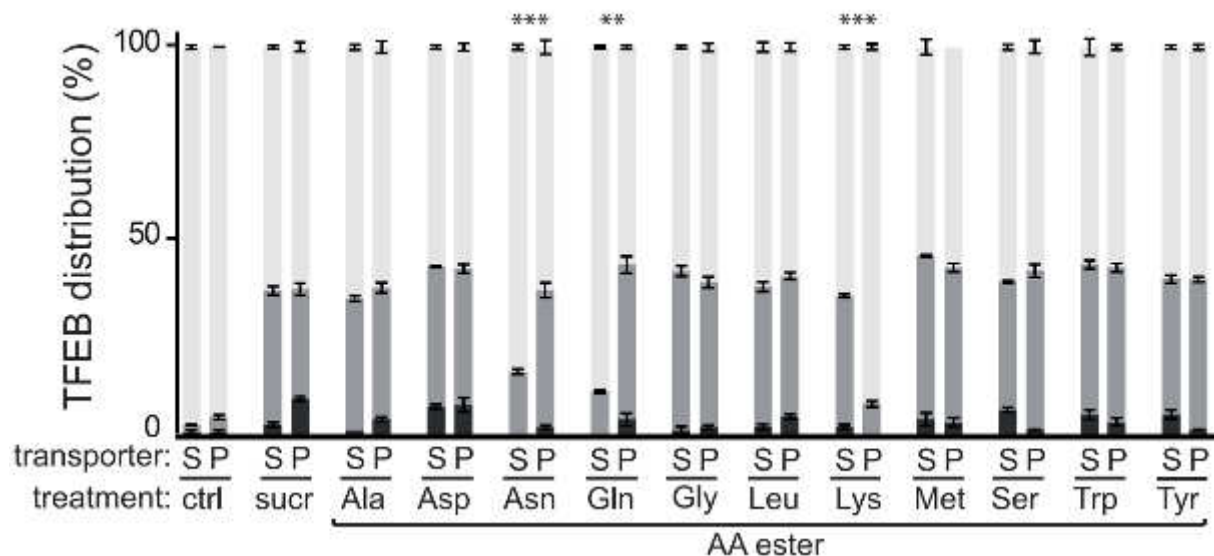


Figure 30: TFEB-AAE screening of amino acids suggests SNAT7 is a transporter selective for glutamine and asparagine.

The same protocol as p125 was applied to EGFP-SNAT7-overexpressing and PQLC2-EGFP-overexpressing HeLa cells.

Black: cells displaying TFEB in nucleus. Light grey: TFEB in cytosol. Dark grey: in between localization. S: EGFP-SNAT7-overexpressing HeLa cells. P: PQLC2-EGFP-overexpressing HeLa cells.

2.4.5 Localization of endogenous SNAT7

Our fluorescence microscopy and TFEB-AAE assay data provided strong morphological and functional evidence for the lysosomal localization of recombinant SNAT7. In the case of native SNAT7, our proteomics data provided strong indirect evidence for a lysosomal localization since peptides assigned to SNAT7 were only detected in lysosome-enriched, but not lysosome-depleted, fractions. To strengthen this conclusion, we aimed to get more direct evidence for the localization of native SNAT7.

Firstly, Christopher Ribes and I characterized an antibody against human SNAT7, recognizing the first 53 amino acids (see material and methods for more details). The specificity of this antibody was assessed by Western Blot on cellular lysates of WT HeLa

cells or SNAT7 KO HeLa cells, which were generated using the CRISPR/Cas-9 method ¹⁷⁴. This antibody recognized a 40 kDa band in WT cells, but no in SNAT7 KO cells. Other bands recognized by this antibody were present in both types of cell (see Fig 31). This band had an apparent mass lower than the predicted mass of human SNAT7 (50kDa), but this phenomenon often happens for highly polytopic proteins due to an excessive binding of SDS compared to less hydrophobic proteins. This suggested that our antibody was specific for SNAT7 and that only the band at 40 kDa should be considered.

To determine the subcellular localization of native SNAT7, WT HeLa cells were fractionated by Marielle Boonen (Université de Namur, Belgium) into five fractions by differential centrifugations. She measured the activity of beta-galactosidase, a lysosomal marker, in each fraction. Beta galactosidase was mostly found in fraction L, with a little amount in fractions M and P. She measured as well the activity of other enzymes representative for other compartments: cytochrome oxidase for mitochondria, alkaline phosphodiesterase for plasma membrane, alkaline α -diesterase for ER and catalase for peroxysomes. Most enzymes were not enriched in the same fractions as beta-galactosidase, except perhaps for phosphodiesterase, the marker for plasma membrane, although it was much less enriched in fraction L (see Fig 31).

Then, these fractions were analysed by Christopher Ribes and I by Western Blot using our SNAT7 antibody. We obtained a very similar profile to the one of beta-galactosidase: most of SNAT7 was found in fraction L, a little in fractions P and M. The strong enrichment in fraction L correlated much better with the distribution of beta-galactosidase (lysosomal enzyme) than with the one of phosphodiesterase (plasma membrane enzyme). The fact that beta-galactosidase and SNAT7 had a similar behaviour along this fractionation strengthened the hypothesis of a lysosomal localization of endogenous SNAT7 (see Fig 31).

For a further confirmation, Marielle Boonen pooled fractions M and L and loaded them onto a sucrose gradient, which helped separating organelles further. After isopycnic centrifugation, she obtained eleven fractions of different densities. She quantified beta-galactosidase activity in each fraction, in addition to other enzymes representative for other compartments. Beta galactosidase was mostly found in fractions 7 and 8, around a density of 1.15, whereas almost all other markers, such as cytochrome oxidase, the enzyme marker for mitochondria, were found in denser fractions, around 1.2. Only the plasma membrane marker, alkaline phosphodiesterase, was found in the same fractions as beta-galactosidase,

consistently with other studies using isopycnic centrifugations to purify lysosomes, in which plasma membrane was a typical contaminant.

Then, Christopher Ribes and I analysed these isopycnic centrifugation fractions by Western Blot. Most of SNAT7 could be found in fractions 7 and 8, similarly to beta-galactosidase and phosphodiesterase. (see Fig 31).

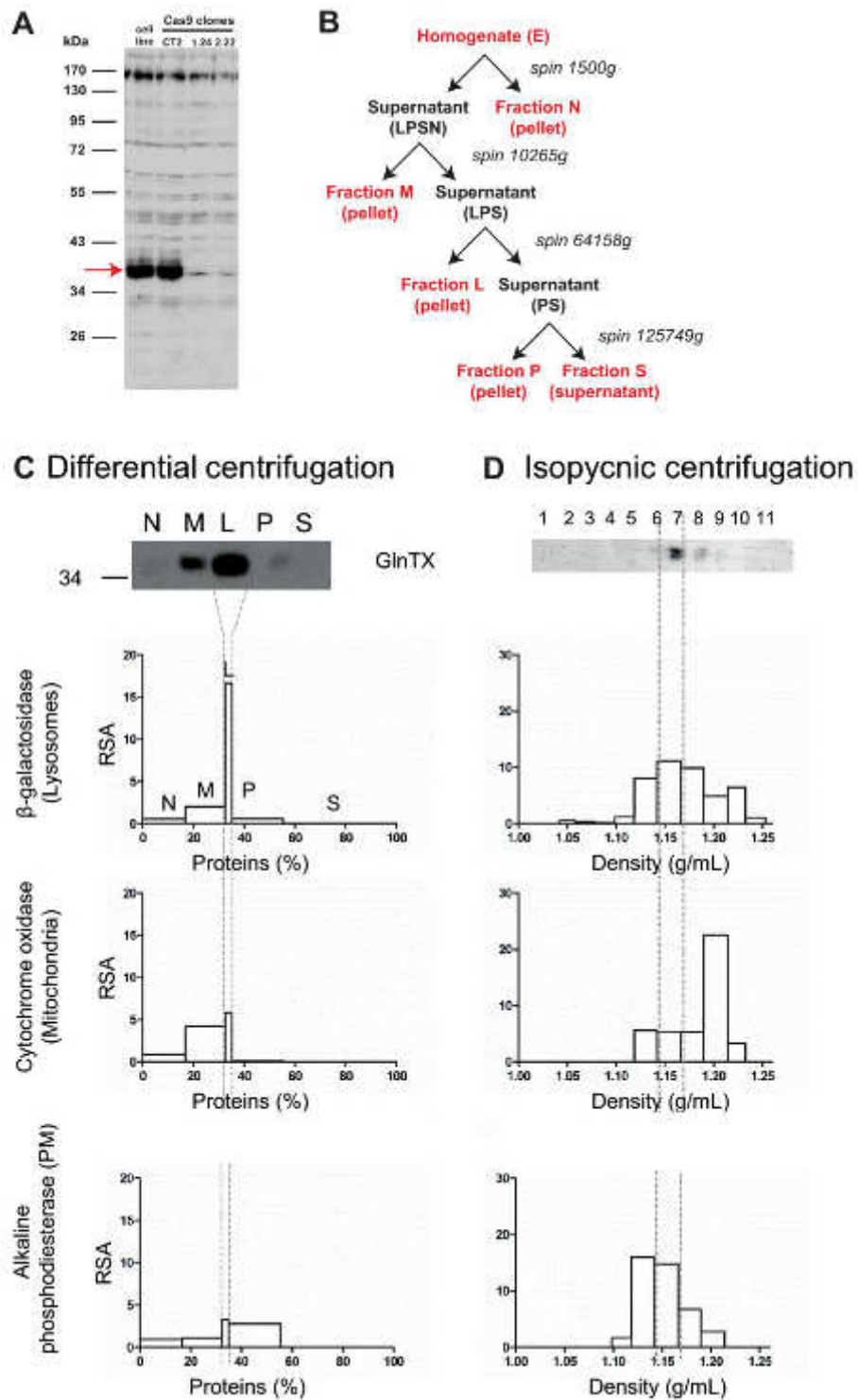


Figure 31: Native SNAT7 localizes to lysosomes
 A: Western Blot on lysates from HeLa cells WT or KO for SNAT7 (generated by CRISPR/Cas9). A specific band can be detected at 40kDa.
 B: Scheme of cellular fractionations. Graphs were designed by Marielle Boonen.
 C: Analysis of cellular fractionations. Picture: Western Blot using an antibody against SNAT7 on each fraction. Graphs: distribution of marker enzymes in each fraction. RSA: Relative specific activity. This represents the relative activity of enzymes in each fraction normalized by the activity in homogenate.
 D: Analysis of isopycnic centrifugations. Same as C.

In summary, the distribution of SNAT7 in the differential centrifugation fractions correlated exclusively with that of the lysosomal marker. The same was observed with isopycnic centrifugation, but the distribution of SNAT7 was as well similar to the one of phosphodiesterase. These results strongly supported that SNAT7 is an endogenous lysosomal protein, but we cannot exclude that a few SNAT7 proteins can as well be sorted to plasma membrane.

2.4.6 Direct measurement of SNAT7 transport activity

These encouraging results prompted to testing by a more direct assay if SNAT7 was a lysosomal transporter for asparagine and glutamine. Endogenous SNAT7 is localized in the lysosomal membrane. Thus, to be able to manipulate the cytosolic side of lysosomal membranes, lysosome-enriched fractions were prepared according to Harms and colleagues¹⁷⁵ with slight modifications (see material and methods). Cells were lysed in a syringe in a high concentration suspension. Lysates were then centrifuged several times at increasing speeds to discard nucleus and mitochondria. Then, they were centrifuged at high speed to pellet lysosomes, but not lighter membranes. When compared to cell homogenate, enrichment in lysosomal beta-galactosidase varied between 4 and 9 in these fractions, with about 20% recovery.

These crude lysosomal fractions should provide better sensitivity to detect SNAT7 transport activity. However, a technical difficulty remained regarding the topology of the membrane vesicles. Indeed, as most lysosomal transporters do and consistently with its effect in our TEFB-AAE assay, SNAT7 exports amino acids from the lysosome. Yet only the cytosolic side of the organelle is accessible to the experimenter in our preparations. To address this difficulty, we took advantage of long-known hallmark of transporters: their ability, when their activity is followed by adding a substrate on one side of the membrane (*cis* side), to be stimulated by the presence of substrates on the other side of the membrane (*trans* side). This property, known as trans-stimulation or counter-transport, is directly linked to the conformational changes (alternate access mechanism) required for the translocation of substrates across the membrane in an active ('uphill') manner (see Introduction).

We thus artificially loaded these isolated lysosomes with specific amino acids using an ester precursor and then exposed them to radiolabelled amino acids to exploit this property and measure the counter-transport activity of SNAT7.

More precisely, the following steps were followed to perform this counter-transport assay: (see Fig 32)

- Load lysosomes, or not, with unlabelled glutamine.
- Expose the loaded and unloaded lysosomes to radiolabelled glutamine to measure their capacity to accumulate this radiotracer.

For the first step, lysosomal fractions were loaded with glutamine by taking advantage once again of amino acid esters, like in the TFEB-AAE assay (see p122). This made very advanced purifications of lysosomes unnecessary, since the treatment with esters selectively loads lysosomes but not, or poorly, contaminating organelles.

The dose of glutamine tert-butyl-ester used for loading (3.75mM) was chosen to avoid damaging lysosomes using a latency test (see p90).

For the second step, after treatment with the ester, lysosomal fractions were centrifuged, washed and incubated with radiolabelled glutamine. Based on the expected trans-stimulation property of SNAT7, prior loading with unlabelled glutamine should stimulate accumulation of radiolabelled glutamine into the lysosomes if this amino acid is translocated by SNAT7. After uptake, fractions were filtered and the accumulated radioactivity quantified.

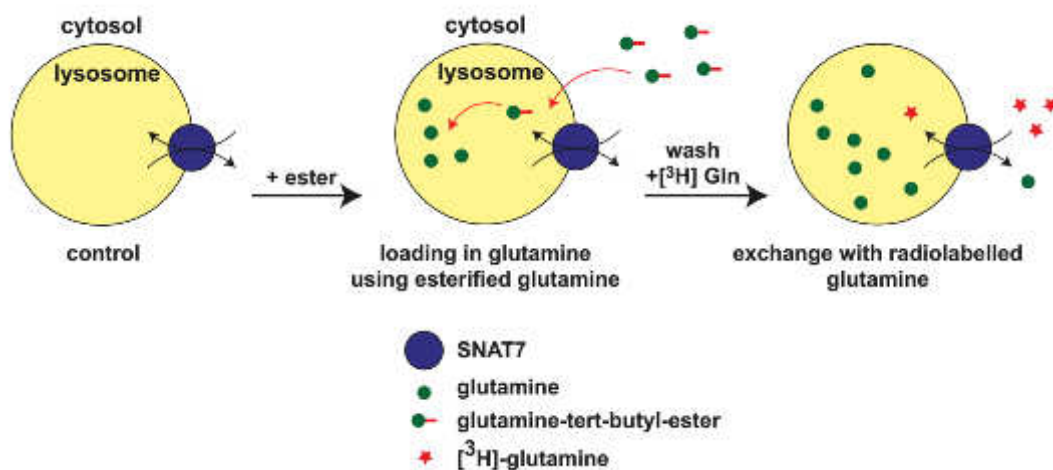


Fig 32: principle of the counter-transport assay. Lysosomal fractions were loaded with unlabeled glutamine using glutamine tert-butyl ester (upper right). They were then washed and incubated with radiolabelled glutamine (lower left). SNAT7 trans-stimulation by luminal glutamine should result in an uptake of radioactive glutamine into the lysosome.

This assay was applied to WT HeLa cells and to a SNAT7 KO HeLa cell clone obtained using the CRISPR/Cas-9 method. Accumulated radioactivity was measured over

time for 30 minutes. After 30 minutes, lysosomes were specifically lysed using 100mM of glycine methyl-ester. This compound can as glutamine tert-butyl-ester enter lysosomes and be cleaved to generate glycine. However, at this concentration, its accumulation is so fast that it creates an hypo-osmotic shock. Other compartments are not or little affected, which allows discriminating between lysosomal uptake and uptake into contaminating organelles.

Lysosomal fractions from WT cells took up far more radiolabelled glutamine than fractions from KO cells, in which very little uptake was detectable, proving that SNAT7 is indeed a lysosomal transporter for glutamine. Moreover, the marginal accumulation observed into KO lysosomes shows that SNAT7 represents the predominant glutamine pathway across the lysosomal membrane. When lysosomes were lysed, almost this entire uptake was lost, showing that this uptake took place in lysosomes and not in another compartment (see Fig 33).

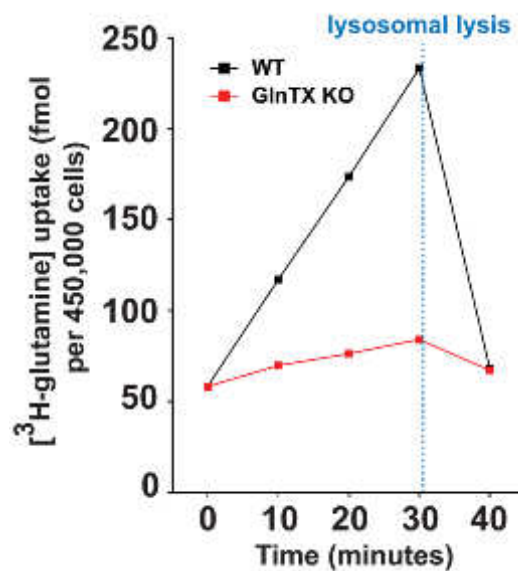


Figure 33: SNAT7 is the main lysosomal transporter for glutamine. Lysosomal fractions were loaded with glutamine using an ester precursor. They were then washed and incubated with [³H]-glutamine. The uptake of radiolabelled glutamine is almost completely abolished in SNAT7 KO subcellular fractions. This uptake was lysosomal, since lysosomal lysis using glycine methyl-ester completely released the radioactivity.

To confirm and strengthen this result, SNAT7 KO cells were transiently transfected by electroporation with a plasmid encoding EGFP-mSNAT7. This expression partially restored the ability of lysosomal fractions to take up radiolabelled glutamine by counter-transport, confirming that SNAT7 is a transporter for glutamine (see Fig 34).

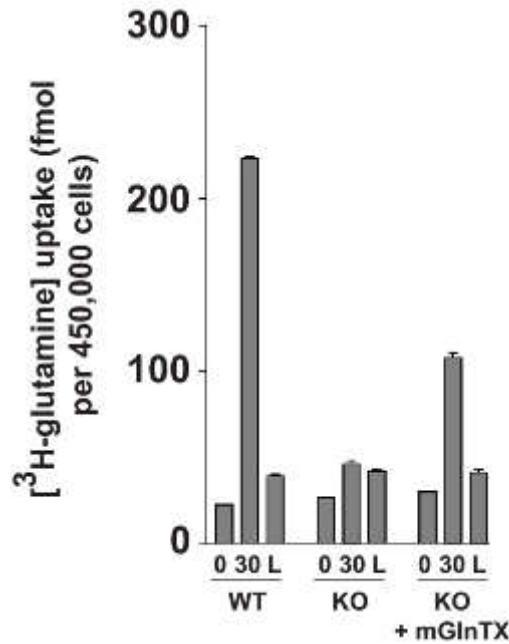


Figure 34: Rescue of SNAT7 activity in SNAT7 KO lysosomal fractions. HeLa cells were transiently transfected with a plasmid encoding EGFP-SNAT7 and the uptake experiment was repeated as in Fig33. 0: Unspecific binding to chilled membranes before uptake at 25°C. 30: Maximum uptake after 30 minutes of incubation. L: Remaining uptake after lysis of lysosomes by glycine-methyl-ester.

2.4.7. Control experiment: are lysosomes from SNAT7 KO cells more fragile?

In the former experiments, lysosomes in fractions prepared from SNAT7 KO cells took up less glutamine than fractions from WT cells, suggesting that SNAT7 was a lysosomal transporter for glutamine. However, this lack of uptake could as well be due to lysosomes breaking down during the uptake due to a higher fragility caused by SNAT7 inactivation.

To investigate this hypothesis, lysosomal fractions from WT or KO cells were treated with increasing concentrations of glycine-methyl-ester in uptake buffer. Like all amino acid esters, it can go through the lysosomal membrane. There, lysosomal esterases generate the corresponding amino acid, which is trapped inside. If concentrations of ester are too high, this creates an osmotic shock, resulting in the breakdown of the lysosomal membrane. If lysosomes from KO cells are more fragile than lysosomes from WT cells, the dose-response curve should be shifted to the left.

The integrity of lysosomes was measured by a latency assay using beta-galactosidase (see p90 for detailed explanations). The principle of this assay is the following: beta-galactosidase activity is measured in fractions treated or not with Triton X-100, a detergent. In presence of the detergent, all beta-galactosidase can access to substrate. Without it, beta-galactosidase in intact lysosomes cannot react with the substrate.

Subtracting both activities thus gives access to how much of beta-galactosidase is inside intact lysosomes.

For both fractions from WT and KO cells, the latency of beta-galactosidase decreased with higher concentrations of glycine methyl-ester (see Fig 35). They did so in a similar manner, indicating that SNAT7-defective lysosomes are not more sensitive to osmotic shock.

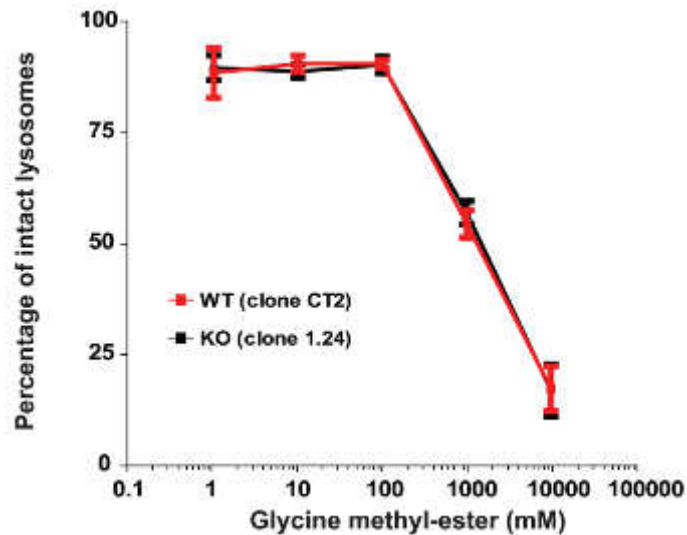


Figure 35: sensitivity of lysosomes to hypo-osmotic shock. Lysosomal fractions from WT and KO cells were incubated with various concentrations of glycine-methyl-ester to induce increasing levels of osmotic stress. Their integrity was then measured by a latency test based on beta-galactosidase. Fractions from both cell types had the same sensitivity to glycine-methyl-ester.

As lysosomal fractions from WT and KO cells seemed to be similarly resistant to osmotic shock, indicating that the differences observed in the counter-transport assay are probably due to SNAT7 activity and not to a differential lysis of lysosomes along the experiment.

2.4.8 Further characterization of SNAT7 activity

The activity of SNAT7 was further studied with the same counter-transport assay as in paragraph 2.4.6 to address the following questions:

- - Is SNAT7 an active transporter?
- - Does SNAT7 depend on the lysosomal pH gradient and/or on the lysosomal potential gradient?
- - How specific is SNAT7 for glutamine or other amino acids?
- - Is this substrate specificity the same on both sides of SNAT7?

As an active transporter, SNAT7 would require energy, directly or indirectly, which is usually brought by ATP. Normal uptake buffer contained 5 mM ATP. So, for the first question, the former experiment was replicated while removing ATP from the uptake buffer. This resulted in a strong decrease in the counter-transport of glutamine into lysosomes, suggesting that SNAT7 strongly depends on the activity of the V-type H⁺-ATPase of the lysosomal membrane (see Fig 36)

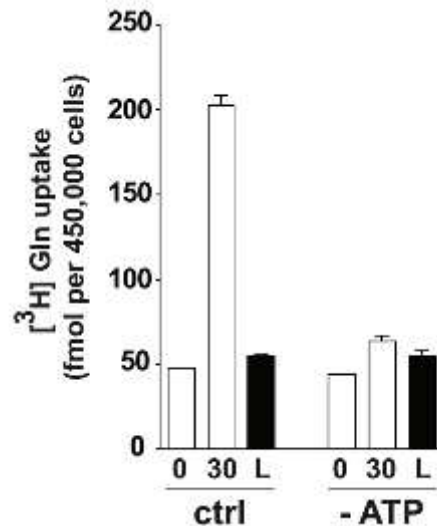


Figure 36: SNAT7 is dependent on ATP. The same protocol as figure X was replicated with or without 5mM ATP in the uptake buffer. The absence of ATP strongly inhibits SNAT7 activity.

By translocating protons into the lysosome, the V-ATPase generates both a concentration (pH) gradient and a potential gradient, since protons carry a positive charge. To examine which components of the proton electrochemical gradient 'drive' SNAT7, we applied three ionophores (5 μM) to the uptake buffer:

- FCCP, which abolishes both components of the gradient, since it is a proton ionophore.
- Nigericin, which abolishes the pH gradient, but not the potential gradient by exchanging protons for K⁺ in an electroneutral manner.
- Valinomycin, which abolishes the potential gradient only by letting K⁺ exit lysosomes.

FCCP completely abolished the uptake of glutamine inside lysosomal fractions, confirming that SNAT7 activity depends on the v-ATPase and the proton electrochemical gradient. Interestingly, only nigericin, and not valinomycin, replicated this effect. This suggested that SNAT7 depended on the pH gradient and not on the potential gradient for its

activity (see Fig 37). However, we cannot exclude that under physiological conditions (i.e. net glutamine export) SNAT7 could be modulated by the lysosomal potential, in contrast with the presumably electroneutral glutamine/glutamine exchange monitored in our artificial counter-transport assay.

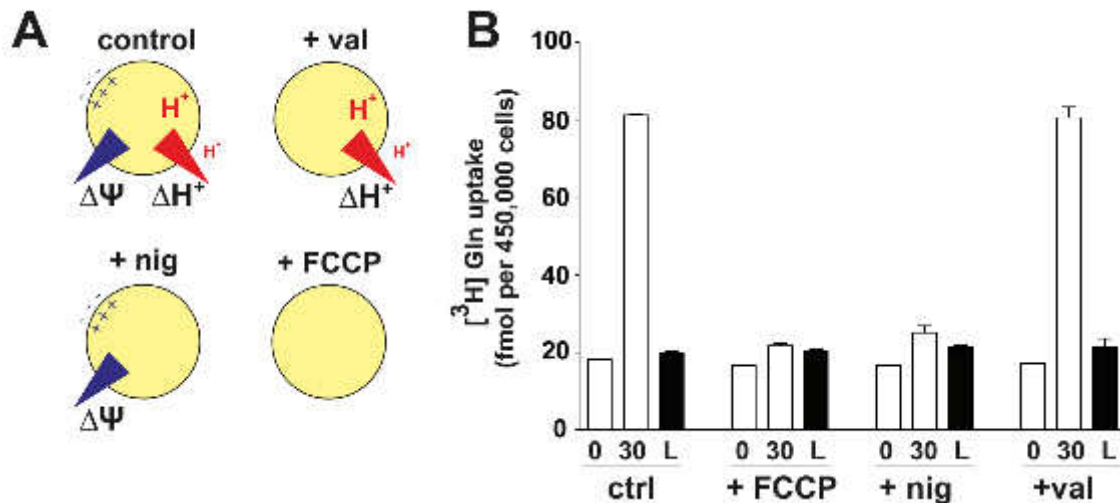


Figure 37: effect on ionophores on SNAT7 activity. The same protocol as fig 33 was applied while adding ionophores to uptake buffer.

A: Scheme of the effect of each ionophore on the pH and the potential gradients across the lysosomal membrane.
B: Uptake experiments with ionophores. FCCP and valinomycin abolished transport, but not valinomycin.

The selectivity for amino acids was addressed in two steps, using the same countertransport assay. First, to study the selectivity of SNAT7 on the luminal side, lysosomal fractions were treated with different amino acid esters to load them with different amino acids in their lumen. In addition to glutamine-tert-butyl-ester, alanine-methyl-ester, asparagine-methyl-ester, serine-methyl-ester and glutamate-dimethyl-ester were used. The side chain of these amino acids have distinct chemical natures to sample what family of amino acids could be transported by SNAT7. On the cytosolic side, radiolabelled glutamine was added like in former experiments.

Results are shown in Fig 38. In addition to glutamine, only asparagine, but not alanine, serine or glutamate, could trigger SNAT7 countertransport activity on the luminal side,. This suggested that SNAT7 is quite specific for asparagine and glutamine on its luminal side, although not all amino acids could be tested (see Fig 38).

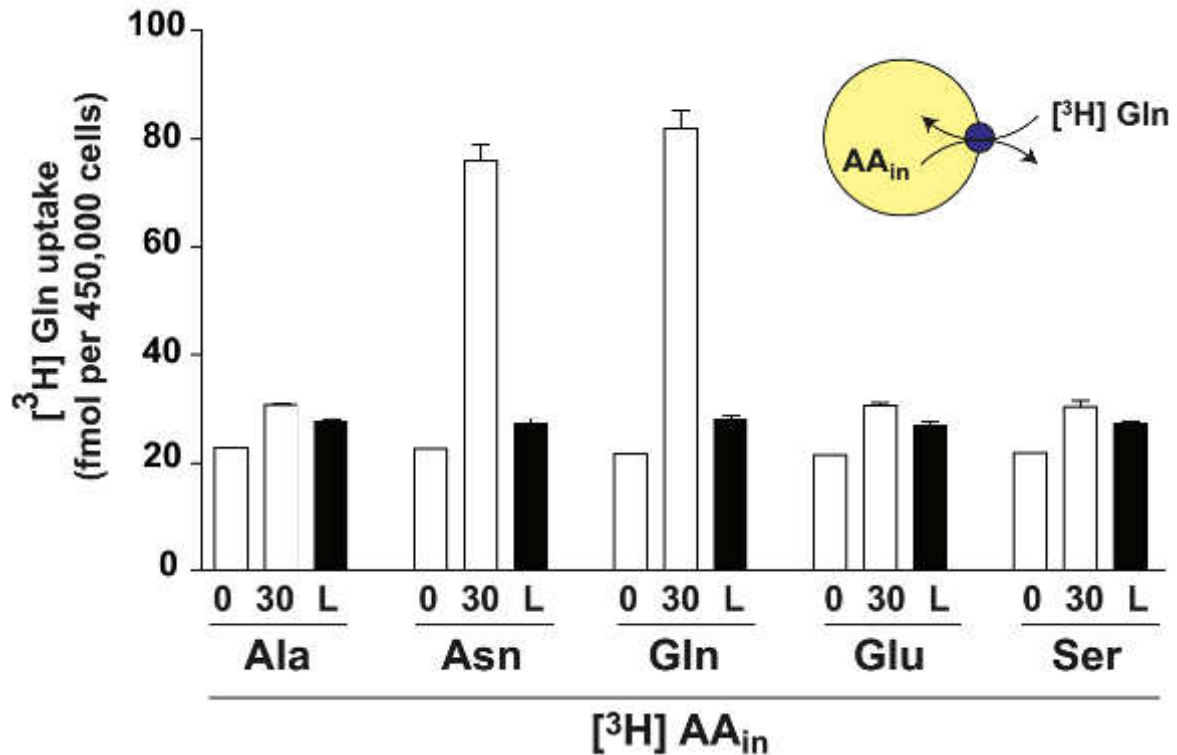


Fig 38: selectivity of SNAT7 on its luminal side. The experiment of fig 33 was repeated with different amino acid esters, thus loading lysosomes with different amino acids. Only loading with glutamine and asparagine could activate SNAT7 countertransport activity, suggesting it is selective for these two amino acids on its luminal side.

Concerning the selectivity on the cytosolic side, the same experiment was done; but, instead of switching amino acids inside lysosomes by switching esters, lysosomes were loaded with glutamine while lysosomal fractions were incubated in various tritiated amino acids, which uptake was quantified. Nine amino acids were tested: alanine, arginine, asparagine, aspartate, glutamate, histidine, phenylalanine, proline and serine. Similarly to the previous experiment, these amino acids were selected to be representative samples of diverse chemical classes of amino acids.

Again, in addition to glutamine, only asparagine could be taken up into lysosomes. All 8 other amino acids showed no specific uptake. Yet, for alanine and valine, a high uptake was observed into lysosomal fractions. However, this uptake was insensitive to glycine-methyl-ester, indicating that contaminating organelles were responsible for this uptake (see fig 39).

Finally, the same test was used with asparagine-methyl-ester, to load lysosomes with asparagine, but fractions were then incubated with radiolabelled asparagine. An uptake of

radiolabelled asparagine could be observed (data not shown). This showed that SNAT7 can counter-transport both asparagine and glutamine in either direction.

Altogether, these results indicate that SNAT7 has the same selectivity on its cytosolic side and luminal sides: it is highly selective for asparagine and glutamine, and do not transport other amino acids, in particular arginine, in striking contrast with the broader substrate selectivity reported by Hägglung et al ¹⁶⁶.

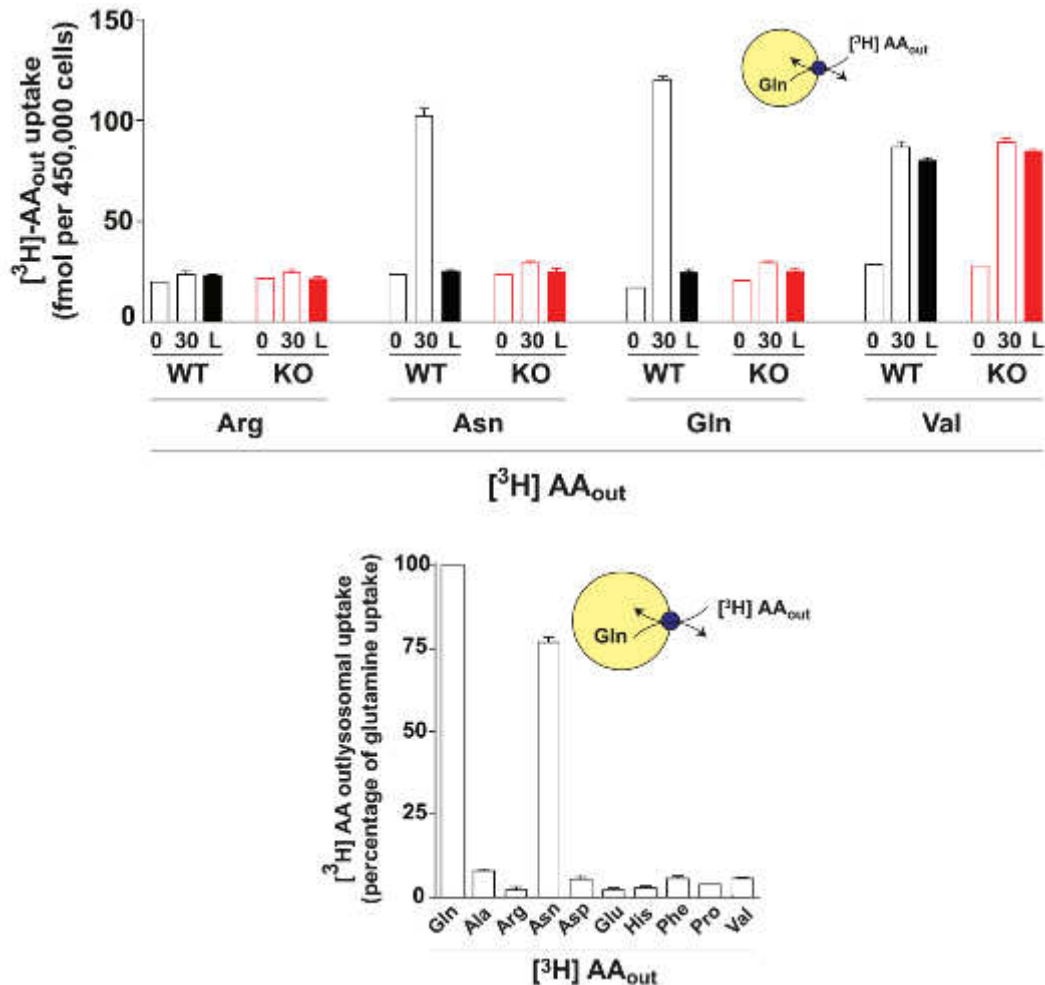


Figure 39: Selectivity of SNAT7 on its cytosolic side. The experiment of fig 33 was repeated, but with various radiolabelled amino acids applied to lysosomes loaded with glutamine. Upper panel: representative experiment. Arginine is not accumulated in fractions. Asparagine and glutamine are accumulated into lysosomes, since lysosomal lysis with glycine methyl-ester (L) abolishes the uptake. Valine is accumulated to high level into a non-lysosomal compartment, since glycine-methyl-ester (L) has not effect on the uptake. Lower panel: lysosomal uptake for each amino acid across 2 independent experiments. Specific transport was calculated as follows:

$$\% \text{ uptake}_{\text{amino acid}} = 100 \times \frac{\text{uptake } 30 \text{ min}_{\text{amino acid}} - \text{uptake } L_{\text{amino acid}}}{\text{uptake } 30 \text{ min}_{\text{Gln}} - \text{uptake } L_{\text{Gln}}}$$

Only glutamine and asparagine were transported by SNAT7 from the cytosolic side.

3. Does SNAT7 play a role in the nutrition of cancer cells?

3.1 Glutamine and cancer cells

Finding a lysosomal transporter for glutamine at the lysosomal membrane with a high specificity is of much interest. It could indeed provide new insights on nutrition pathways depending on lysosomes in cancer cells.

Glutamine is indeed important to all cell types: it is the most abundant amino acid in blood and can be easily incorporated in many cellular metabolic pathways. However, it plays an especially important role in cancer cells. Because of rapid anabolic processes, cancer cells have higher nutritional need than normal cells.

To fulfil these needs, they mostly rely on glucose and free glutamine, but glutamine has a special role as it brings nitrogen as well as carbon and energy, contrary to glucose. Nitrogen is necessary for the anabolism of both proteins and nucleobases¹⁷⁶ and glutamine is an important intermediate of these metabolic pathways. Up to some extent, glutamine is necessary for cancer cell survival and depriving cancer cells from glutamine is a promising axis in the development of new therapies¹⁷⁷. This however seems to depend on the type of cancer.

Glutamine can be obtained through the overexpression of glutamine transporters, for instance SNAT2¹⁷⁸ or ATB0+/SCL6A14. However, angiogenesis in tumours is often untidy, leading to parts of tumours to be badly irrigated by blood in oxygen, but as well in nutrients¹⁷⁹, so the overexpression of plasma membrane transporters can in some cases prove insufficient.

Glutamine can as well be synthesized by glutamine synthetase, which has been proved as an important actor of cancer cell metabolism¹⁸⁰.

Recently, cancer cells have also been shown to rely on the degradation of proteins to meet their needs in glutamine. These can be intracellular proteins coming from autophagic processes (for survival under nutrient deficiency rather than cell growth;¹⁸¹) or extracellular proteins obtained by macropinocytosis¹⁸². This last process is especially important in the

nutrition of K-Ras activated cancer cells. This is of particular interest since these are the types of cancers that have a particularly bad prognosis today, such as pancreatic carcinoma.

In these latter contexts, lysosomal transporters for glutamine could play an important role. Proteolysis-dependent pathways to obtain glutamine all converge indeed to lysosomes, but most metabolic pathways take place in the cytosol or in distinct organelles such as mitochondria. As a result, lysosomal transporters for glutamine appear necessary for glutamine to be used. Blocking them could result in starving cancer cells (see fig 40). In addition, since these pathways are upregulated in cancer cells and since normal cells can obtain glutamine through their plasma membrane transporters, blocking lysosomal transporters could result in a few side-effects on normal cells.

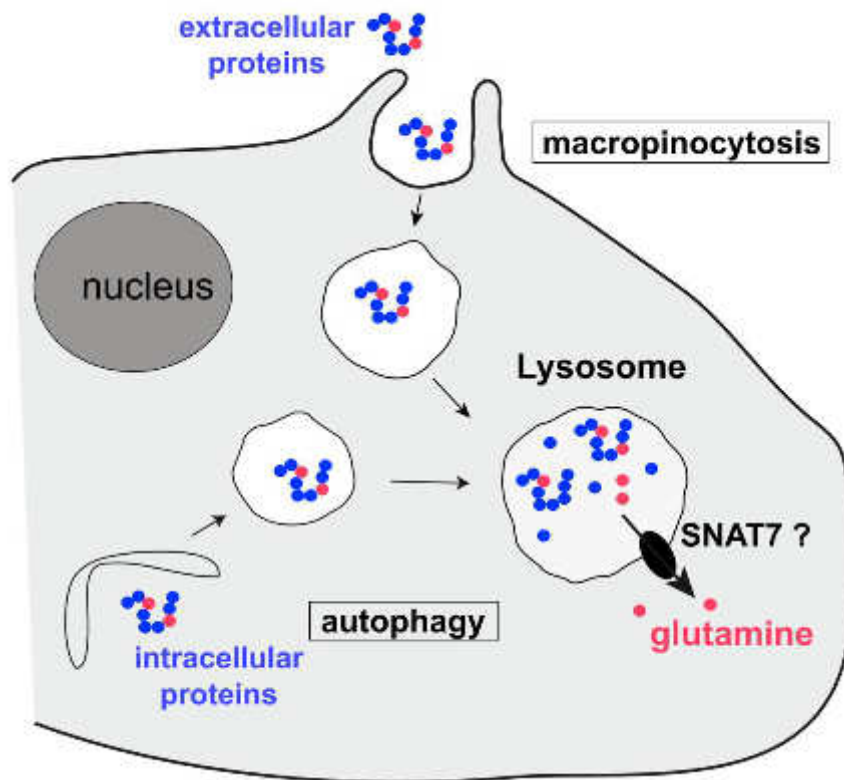


Figure 40: Obtaining glutamine from autophagy and macropinocytosis
Macropinocytosis and autophagy result in an uptake or sequestration, respectively, of proteins into lysosomes. Lysosomal proteases generate glutamine from these proteins, but glutamine must be exported to be used by cellular metabolic processes, which take place in the cytosol or other organelles such as mitochondria.

These considerations prompted us to examine the role of SNAT7 in the nutrition of some cancer cell types.

3.2 SNAT7 is required for extracellular protein-dependent proliferation of cancer cells in low free glutamine environment

3.2.1 BSA can be used as a source of glutamine.

To study the nutrition of cancer cells, MIA-PaCa2 cells were used. This cell line derives from a human pancreatic carcinoma. It is activated by K-Ras and it was used by Commisso and colleagues¹⁸², who proved this cell line to be especially dependent on macropinocytosis to meet its need in free glutamine-restricted conditions.

First, the dependency of MIA-PaCa2 to glutamine was assessed at low concentrations. Cells were seeded at a fixed concentration of glutamine. They grew for five days and were counted, out of which their average number of mitosis was calculated.

Half of the cells were as well supplemented with delipidified BSA to check whether extracellular proteins could help cells cope better with the lack of glutamine by providing glutamine through the macropinocytosis pathway.

MIA-PaCa2 division rate is heavily affected by the concentration of glutamine in the medium (see Fig 41). However, division rates were increased at low glutamine concentration when BSA was added to the medium. At high concentrations of glutamine, it had however no effect, suggesting that the growth stimulation effect of extracellular BSA is mediated by the supply of glutamine, in agreement with earlier results from Commisso and colleagues (see fig 41)¹⁸²

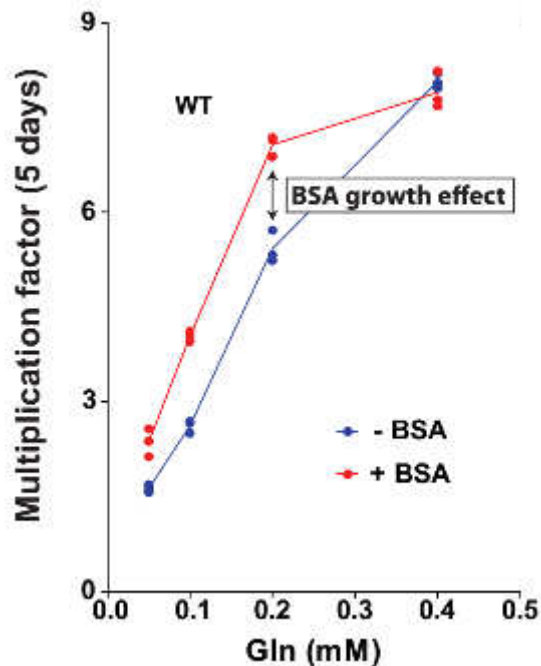


Figure 41: MIA-PaCa2 cells can obtain glutamine from BSA to sustain cell proliferation. MIA-PaCa2 cells grew for 5 days in medium with controlled concentrations of glutamine, with (red) or without (blue) BSA. At lower concentrations, when the cellular division rate was slowed by the lack of glutamine, BSA accelerated cell division. But, when glutamine was sufficient in the medium, it had no effect.

3.2.2. SNAT7 is critical for BSA-dependent proliferation of cancer cells

Since BSA could be used as a source of glutamine and since it had been shown that lysosomes were important in this process, SNAT7 was expected to be important to export glutamine from lysosomes after the degradation of BSA. Thus, SNAT7 expression was reduced by RNA interference and the impact of BSA on MIA-PaCa2 proliferation rate measured.

The importance of SNAT7 to sustain BSA-dependent proliferation was then measured at 0.2 mM glutamine, the concentration with the higher BSA effect. Human SNAT7 expression was reduced in MIA-PaCa2 cells using dsRNAs targeting three different regions of SNAT7 mRNAs. In addition, a rescue was performed with the murine form of SNAT7. This form was insensitive to silencing.

The reduction of expression due to silencing was checked at the level of the protein. I generated cell lysates and Christopher Ribes analysed them by Western Blot using our

antibody against SNAT7. The same growth protocol was then applied to these cells and the BSA-dependent proliferation was calculated (see Fig 42).

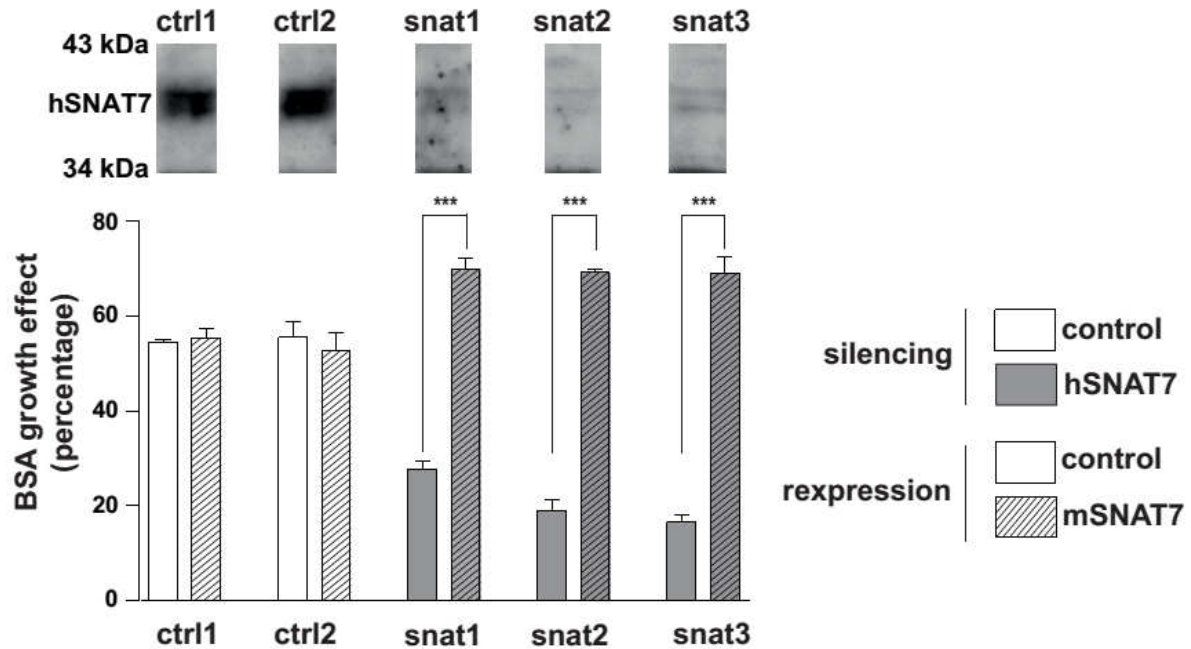


Figure 42: SNAT7 is necessary for to sustain BSA-dependent growth in low free glutamine environment. Upper picture: Lysates of MIA-PaCa2 cells transfected with dsiRNAs were analysed by Western Blot using an antibody against SNAT7. dsiRNAs snat1, 2 and 3 drastically reduced levels of SNAT7 when compared to controls.

Lower graph: SNAT7 expression was reduced in MIA-PaCa2 with three different dsiRNAs (snat 1, 2, 3; dark grey) or control dsiRNAs (ctrl1, 2; white) and rescued with a plasmid encoding either mSNAT7 (stripes) or a negative control (sialin P334R, no stripes). Cells were seeded in control medium with 0.2 mM glutamine with or without BSA. The BSA-dependent growth was calculated after 3 days. Silencing SNAT7 significantly reduces BSA effect on cellular proliferation.

DsiRNAs were quite efficient to reduce the expression of SNAT7, as shown in Western Blot. Concerning the proliferation assays, in negative controls, BSA increased cell proliferation by 50%. However, when SNAT7 was silenced, BSA had significantly lower effect left on cell proliferation (25, 20 and 17% for each dsiRNA respectively), showing that SNAT7 to sustain BSA-dependent growth, presumably by supplying lysosome-derived glutamine to the cell.

Similar results were obtained with another cell line: A2780 (data not shown). These cells are derived from a human breast carcinoma. Interestingly, they are not activated by K-Ras, suggesting that the supply of glutamine through macropinocytosis and lysosomal degradation of extracellular proteins when free glutamine is insufficient could be a more generic response to nutritional stress than previously anticipated.

DsiRNAs only induce a reduction in the expression of target genes. To confirm the former results and get clearer responses, the same protocol was applied to MIA-PaCa2 cells KO for SNAT7 generated using the CRISPR/Cas-9 technique: the loss of expression was analysed by Western Blot by Christopher Ribes and me, and I analysed the effect of BSA on the growth of these cells under a limiting concentration of glutamine.

The Western Blot confirmed that no residual expression of SNAT7 could be observed in KO models. In these cells, strikingly, the genetic inactivation of SNAT7 abolished the BSA-dependent growth, showing that SNAT7 is the main, if not only, transporter supplying glutamine for growth from the macropinocytosis/lysosomal pathway (see Fig 43).

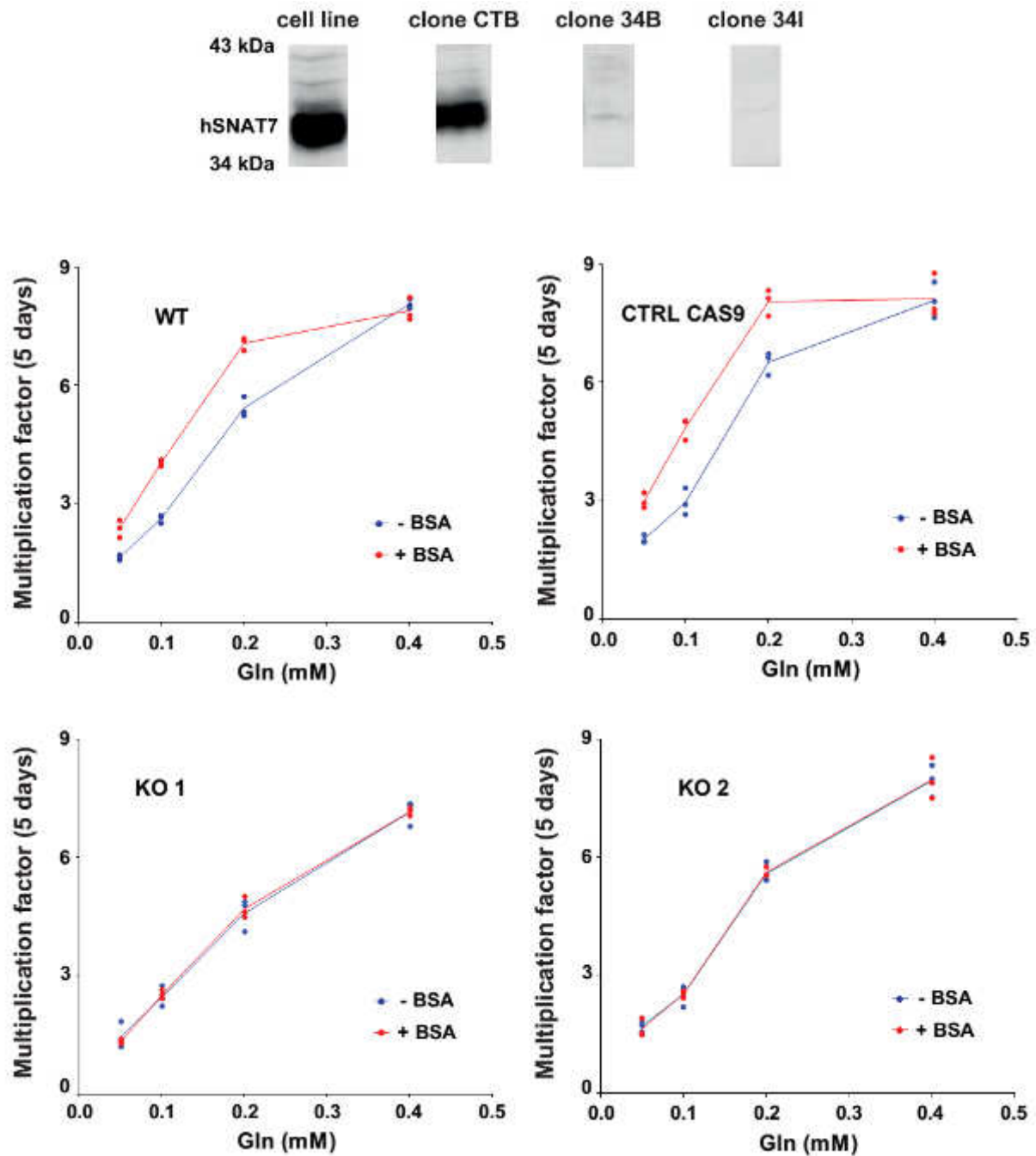


Figure 43 Genetic inactivation of SNAT7 in MIA PaCa-2 cells abolishes their BSA-dependent proliferation in low free glutamine environment

Upper picture: lysates from WT cells or cells KO for SNAT7 were analysed by Western Blot using an antibody against SNAT7. No SNAT7 can be detected in lysates of KO cells.

Lower graph: The same protocol as Fig 41 (blue, without BSA; red, with BSA) was repeated on four different MIA-PaCa2 clones: WT, two clones KO for SNAT7 generated using CRISPR/Cas9 and a WT clone (positive control) which was transfected with Cas9 but the nuclease did not target the SNAT7 locus. At low concentrations of glutamine, BSA rescued the proliferation of control cells, but it had no effect on KO cells, showing that SNAT7 is absolutely required for BSA-dependent growth of cancer cells.

3.2.3 Control experiment: is BSA degraded properly in SNAT7 deficient cells?

In both SNAT7-deficient models (silenced MIA-PaCa2 and KO cells), BSA failed to compensate the lack of glutamine in the medium. This could be due to the absence of SNAT7-mediated lysosomal export. However, an alternative interpretation could be a deficient degradation of BSA in SNAT7-defective lysosomes.

Thus, lysosomal proteolysis was evaluated in SNAT7 deficient cells generated by silencing. To do so, after silencing, cells were treated with DQ-red-BSA, a low-noise fluorescent probe for lysosomal proteolysis (see p94 for more details). DQ-red-BSA signals were measured by flow cytometry.

DQ-red-BSA was well degraded in MIA-PaCa2 (signal was about ten times stronger than autofluorescence). Despite small differences, there was no strong effect of dsiRNAs on DQ-red-BSA signal. In particular, there was no difference in DQ-red-BSA processing between cells treated with control dsiRNAs and cells treated with dsiRNAs inhibiting the expression of *SNAT7* (see fig 44).

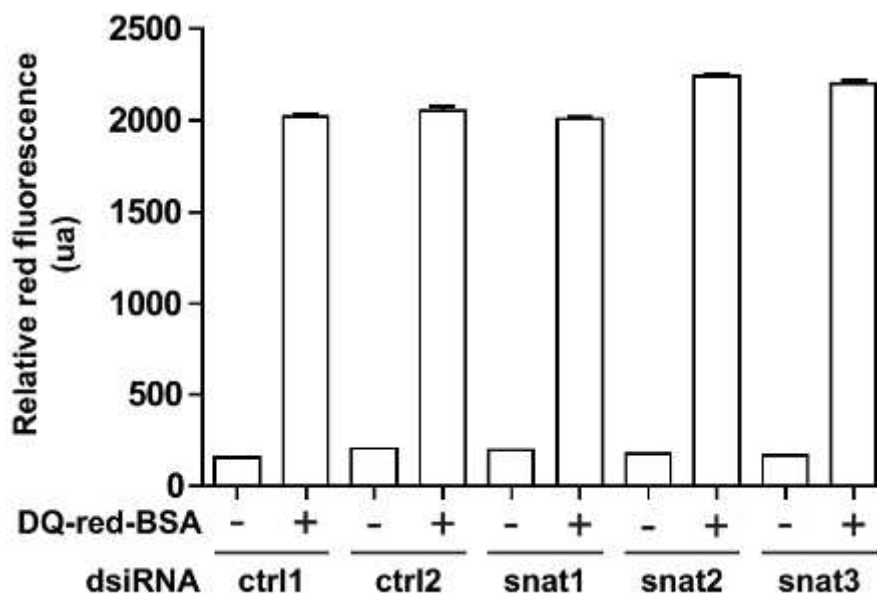


Figure 44: lysosomal proteolysis is not affected by the silencing of SNAT7 in MIA-PaCa2 cells. Cells were transfected with five different dsiRNA, three of them targeting SNAT7 (*snat1*, 2 and 3) and two controls (*ctrl 1* and 2). They were treated with DQ-red-BSA and the fluorescence generated by DQ-red-BSA degradation was quantified by flow cytometry. DsiRNAs had little effect on the proteolysis of DQ-red-BSA.

Overall, these results suggested that lysosomal proteolysis was normal in MIA-PaCa2 cells with reduced expression of SNAT7.

The simplest explanation for the effect of SNAT7 silencing or inactivation on the BSA-dependent proliferation of MIA-PaCa2 cells is thus most probably the lack or reduction in the transport activity of SNAT7 and not to a side-effect of the absence or reduction of SNAT7.

4. Conclusion

4.1. SNAT7 is a lysosomal transporter for glutamine and asparagine

SNAT7 is sorted to lysosomes through an unknown mechanism, which made its study challenging. An indirect test based on TFEB and the application of amino acid esters showed it could be an interesting candidate for lysosomal transporter for glutamine. Since such a transporter might have a great interest to attempt blocking the metabolism, and growth, of cancer cells, its transport activity was characterized more directly on purified lysosomal fractions. SNAT7 is a very selective lysosomal transporter for glutamine and asparagine, in agreement with the TFEB-AAE data, and its activity is strongly dependent on the lysosomal pH gradient. These results suggest that its main function is at the lysosomal membrane, although it is possible that, in some cell types, a few proteins go to plasma membrane and could play a significant biological role.

Although it appears from our results that SNAT7 is the main lysosomal transporter responsible for lysosomal glutamine and asparagine export, other transporters might play a role in these processes. This could be the case of SNAT9 for instance, which, to date, is the only other lysosomal protein characterized as a transporter for glutamine in the literature^{58,152}. However, its low affinity and wide specificity seems more adapted to a predominant function in signalling processes. Another transporter, SNAT4, was found in our proteomic study and could be another interesting candidate.

4.2. Role of SNAT7 in cancer cell nutrition

4.2.1 Role of SNAT7 in in vivo cancer models

When SNAT7 is absent, cancer cells can hardly obtain glutamine from macropinocytosis of extracellular proteins. In addition, both autophagy and macropinocytosis require lysosomal enzymes to generate glutamine out of proteins. Thus, targeting the lysosomal recycling of glutamine could prove more efficient than blocking either macropinocytosis (to impair cell growth) or autophagy (to impair cell survival under nutrient deficiency).

To confirm the impact that blocking SNAT7 could have on tumour growth, in vivo experiments are currently run. Nude mice were injected subcutaneously with WT MIA-PaCa2 or SNAT7-deficient MIA-PaCa2, and the growth rate of tumours is being followed. If SNAT7 is really important for the nutrition of cancer cells in this more complex environment compared to our 'reductionist' in vitro assays, KO cells should divide more slowly.

Another approach is being considered for further experiments: subcutaneous tumours could be generated in nude mice. Then, these tumours could be treated with viruses blocking *SNAT7* expression or dsRNAs against *SNAT7* expression. The growth rate of tumours before and after treatment would be followed as a read-out.

4.2.2 Relevance of macropinocytosis in the nutrition of cancer cells

Glutamine can be acquired from four sources: synthesis, lysosomal proteolysis, proteasome proteolysis or import through the plasma membrane. Although all these ways seem to play an important role in cancer cell nutrition, it remains unclear which way plays the strongest role from a quantitative point of view.

It had been suggested that the activation of macropinocytosis, which leads to use lysosomes as an important source for glutamine, was specific for some cancer cells, in particular those activated by K-Ras. However, MIA-PaCa2 and A2780 cells seemed to both be able to use extracellular BSA as a source of glutamine, although the first cells are activated by K-Ras and the latter are not. Thus, it could be interesting to evaluate in the

context of cancer and in a quantitative way, for instance using metabolic tracers, which mechanism to obtain glutamine is critical for the survival of cancer cells.

4.2.3 Advantages and development of a SNAT7-based anti-cancer therapy

Reducing *SNAT7* expression had no effect on cell proliferation in glutamine-sufficient conditions. In vivo, supplies of glutamine are mostly insufficient in the context of untidy tumour angiogenesis. Thus, blocking SNAT7 could have a much stronger impact on cancer cells than on normal cells.

Other proteins have been suggested as potential targets to block glutamine uptake by cells, such as SNAT2, ATB0+ or glutamine synthetase. However, these proteins seem to have a major role in other processes. SNAT2 has been implicated in numerous different cellular mechanisms (see p112), and, for example, glutamine synthetase is necessary for the synthesis of glutamate in glutamatergic neurons (see p112). Inhibiting these proteins could, as a result, lead to important side-effects.

Thus, SNAT7 seems like a better target to block the metabolism of glutamine in cancer cell: blocking it could prove a selective therapy against cancer and could have only little impact on healthy cells.

To develop such a therapeutic approach, two of our tests could be used in large-scale screening of putative inhibitors of SNAT7. Firstly, growth tests are already used to screen for anti-cancer drugs, and the present test could be adapted quite quickly.

Secondly, the indirect transport assay using TFEB and amino acid esters could prove useful to narrow down the selection of inhibitors from the first screen, or could be used in the first line using high content screening (HCS), since the direct transport assay on isolated lysosomes is challenging and time-consuming. HCS imaging techniques has developed extensively and it could be possible to screen putative inhibitors based on the localization of TFEB¹⁸³ by using a marker for nucleus as a reference. Then, direct transport assays could be used to confirm and characterize inhibitors.

4.3 Importance of SNAT7 in other mechanisms

Glutamine is a key metabolite in all cells, but it has been shown to play a more specific role in several cell types, in particular in neurons (see p109 for a detailed scheme). In excitatory glutamatergic neurons, after exocytosis at the synapse, glutamate is taken up by astrocytes and metabolized into glutamine. Glutamine is then secreted, taken up by neurons and used as a glutamate precursor. Using metabolic tracers, this cycle has been shown to be accountable for about 60% of glutamate synthesis in neurons ¹⁸⁴.

Interestingly, SNAT7 has been reported to be expressed at high levels in neurons ¹⁶⁶. In this context, SNAT7 could play two roles:

- If SNAT7 is partially expressed at plasma membrane, it could help taking up glutamine when it is secreted by astrocytes. However, this possibility appears unlikely considering the strong pH dependence of SNAT7 activity observed in our experiments.
- It could provide glutamine from another source than plasma membrane uptake: lysosomal proteolysis.

Neurons have been shown to be able to take up proteins by macropinocytosis in the context of protein aggregates often implicated in neurodegenerative disorders ^{185,186}. Macropinocytosis has been as well documented in neurons during development of the growth cone ¹⁸⁷, but its role in healthy functional neurons remains unclear. These data and our own studies lead us to raise the provocative hypothesis that macropinocytosis of extracellular proteins, lysosomal degradation and amino acid export through SNAT7 could be another source of glutamine for the synthesis of glutamate in glutamatergic neurons and of GABA in inhibitory neurons.

Finally, glutamine plays an important role in innate immunity. Macrophages are produced as M0, and, when exposed to stimuli, they undergo polarization. There are two types of polarization, depending on which receptor is activated and to which cytokines M0 are exposed. They can become two different types of macrophages: M1 or M2, which both experiment metabolic switches ¹⁸⁸. The balance between M1 and M2 is strictly regulated.

M2 have high phagocytic capacities. They are believed to have anti-inflammatory properties, for instance in wounds. However, when overactivated, they could trigger allergic

reactions ¹⁸⁹. Thus, inhibiting differentiation into M2 could help reduce allergic symptoms in some cases. The shift from M0 to M2 has been shown to be glutamine dependent. In vitro, glutamine deprivation reduced the differentiation from M0 to M2 by about 50% ¹⁹⁰.

Since M2 are highly phagocytic cells, they probably engulf many extracellular proteins. Thus, it is likely that lysosomal degradation is an important source of glutamine for them. SNAT7 could thus prove critical for polarization from M0 to M2.

Conclusion: emerging roles for lysosomal membrane proteins

Lysosomes have first been characterized as terminal degradative organelles, thus having few functions other than degradation. Studies on lysosomes typically focused on their degradative machineries: the v-ATPase, hydrolases and transporters¹⁹¹. Thus, lysosomal membrane proteins were firstly described as important for degradation and recycling.

The characterization of autophagy has led to reconsider how cargos reach lysosomes and have highlighted the importance of lysosomal membrane proteins in the control of fusion of lysosomes (in the case of macroautophagy) or direct import of cargo (in the case of chaperone-mediated autophagy).

Lysosomal membrane proteins have other roles in lysosomal homeostasis: they can regulate the luminal concentrations of ions (ion channels), they participate to lysosomal degradation (lysosomal membrane protease) or they protect the lysosomal membrane against enzymes. However, maybe the main change in the understanding of the lysosomal function is that it was shown to interact through its membrane with other cellular compartments and that it played an essential role in various cellular mechanisms (see Fig 45) such as:

- Nutrition: some nutrients, mostly those coupled to carrier proteins such as iron or vitamin B12, have to transit through lysosomes to be taken up by cells, thus implying lysosomal transporters.
- Maintenance of cell membrane integrity: the lysosomal membrane can be used to help repair wounds of the plasma membrane. Upon membrane damage, through calcium signaling, lysosomes can be fused to the plasma membrane by exocytosis, thanks to SNARE proteins, thus providing necessary membrane to help repair the wound.
- Control of cell death. During apoptosis, necrosis or other cell death programs, the lysosomal membrane can be permeabilized, thus releasing enzymes and

accelerating cell death. Lysosomal membrane permeabilization is controlled by lysosomal membrane proteins, such as LAMPs or the v-ATPase.¹⁹²

- Signaling: Lysosomes are able to send signal concerning the metabolic state of the cell to mTORC1, which controls many metabolic and signaling pathway and cell growth. The lysosomal membrane, in particular, is an integration platform of signals from different origins: cytosolic signaling pathways (through Rheb) and inside-out lysosomal signals (through the Ragulator complex), such as the ones provided by lysosomal transporters such as SNAT9 and cystinosin.
- Redox control: lysosomes are believed to be reductive compartments, although no direct evidence supports this hypothesis¹⁹³. An impairment of the redox state of lysosomes could be due to generally impairing lysosomal degradative function. Cysteine contains a reductive thiol group. Thus, the lysosomal importer of cysteine, by depleting cytosol of reductive species and accumulating it inside lysosomes, could play an important role in regulated the redox potential, both of lysosomes and of cytosol.

During my PhD, I have characterized two lysosomal membrane proteins which function was previously unclear. CLN3 is a lysosomal membrane protein which is mutated in a neurodegenerative lysosomal storage disorder: Batten disease. Although CLN3 molecular function remains unclear, it seems that its impairment leads to a decrease of lysosomal proteolysis. Thus, CLN3 may have a primarily regulatory role of lysosomal function and may only be indirectly linked to other cellular mechanisms reported in the literature. However, addressing this proposal and characterizing better the link between CLN3 and lysosomal proteolysis requires further studies.

On the other hand, SNAT7 is the main lysosomal membrane transporter for glutamine and asparagine, at least in HeLa and MIA-PaCa2 cells. Thus, it is probably important in many cell types to recycle glutamine and asparagine molecules produced by the degradation of proteins inside lysosomes. In addition, SNAT7 plays a critical role in the nutrition of cancer cells. Some types of cancer cells become highly dependent on glutamine, which is often insufficiently supplied by blood. Glutamine is alternatively obtained by internalization of extracellular proteins by macropinocytosis, which are eventually degraded in lysosomes. Then, glutamine is exported to the cytosol through SNAT7. Our cell proliferation data showed

that this transporter is a central player in such opportunistic nutrition pathway which is specific to cancer cells.

Overall, lysosomal membrane proteins have an extensive variety of roles. Lysosomes were firstly described by du Duve's original paper as physically very heterogeneous organelles. Similarly, lysosomes could be as well functionally heterogeneous. This idea has already been suggested by a few authors, and it has been proven in the case of chaperone-mediated autophagy, which is mediated by only a fraction of lysosomes¹⁹⁴. Other lysosomal subpopulations could be, for instance, specialized in long-term storage of material, or in signaling.

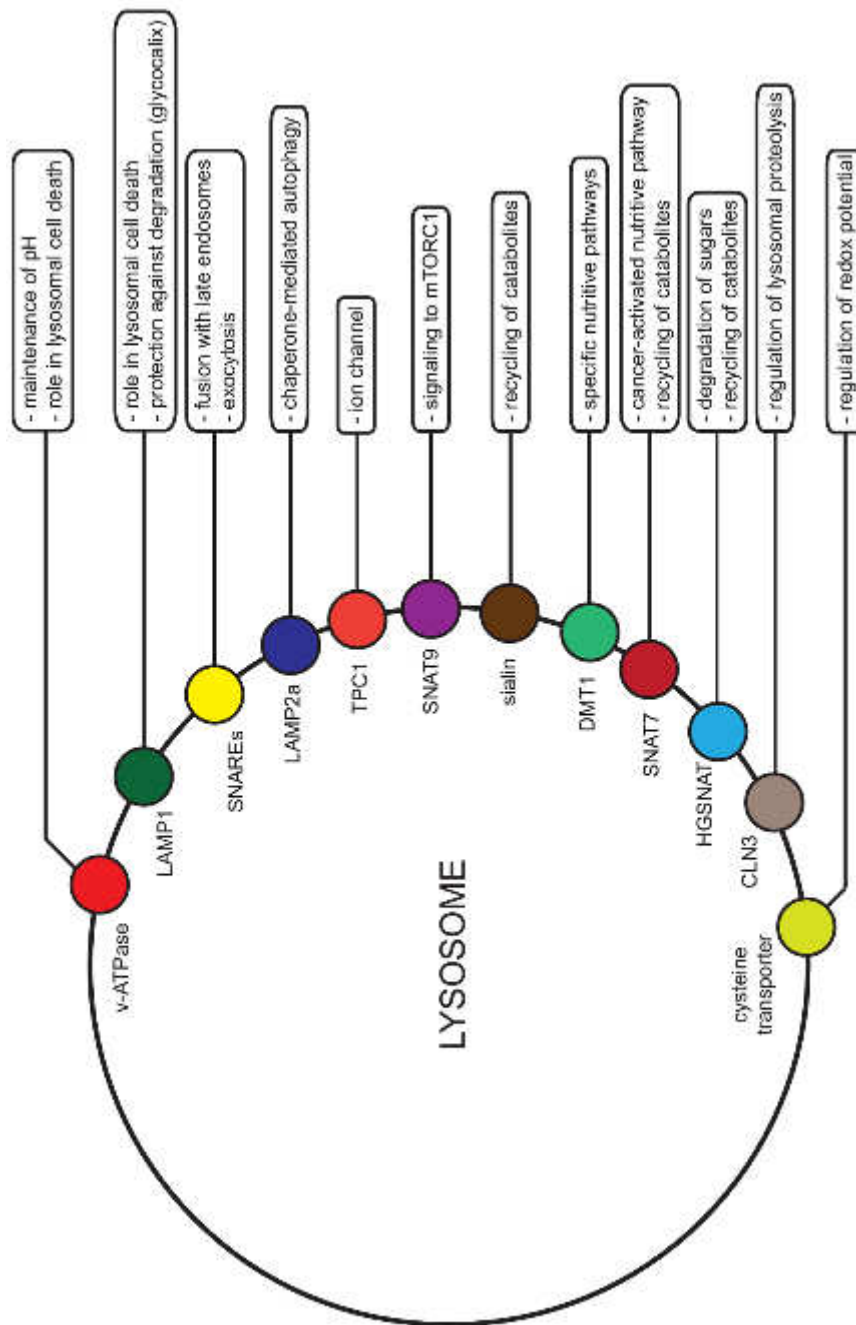


Fig 46: functions of lysosomal membrane proteins. The v-ATPase pumps protons inside lysosomes. LAMP-1 is the most abundant protein of the lysosomal membrane; its molecular function is still unclear. SNAREs are complexes implied in fusion between membranes. LAMP2a associates in tetramers that can internalize unfolded proteins into lysosomes. TPC1 is a sodium channel. SNAT9 is a transporter for arginine and glutamine interacting with the mTORC1 pathway to sense and signal the availability of amino acids. Sialin is the lysosomal transporter for sialic acids. DMT1 is the lysosomal transporter for Fe^{2+} . SNAT7 is a lysosomal transporter for glutamine and asparagine, implied in cancer cell nutrition, as demonstrated during my PhD thesis. HGSNAT is a lysosomal membrane enzymes, catalyzing the degradation of heparan sulfate. CLN3 is mutated in Batten disease. Its dysfunction induces a decrease of lysosomal proteolysis. An unknown transporter imports cysteine into lysosomes.

Material and methods

DNA and RNA constructs.

All constructs were designed in pOX(+) vector (Addgene), pEGFP-C2 vector (Addgene), pEGFP-N1 vector (Addgene) or pcDNA6.2 C-EmGFP-TOPO vector (Invitrogen, shortened in pcDNA EmGFP further). Most constructs and corresponding primers are already listed in the Mol Cell Proteomics paper (see p34).

In addition, the following constructs were already available in my host laboratory: all sialin constructs, all CLN3 constructs, all CLN7 constructs, all PQLC2 constructs.

Other constructs were generated by two methods according to the manufacturer's instruction: direct cloning using Phusion polymerase and restriction enzymes (all from NEB), or Q5-mutagenesis kit (NEB).

Primers are listed in the following table:

plasmid	method	sequence	restriction site
pcDNA EmGFP Spinster	cloning	ATTAGAATTCGCCACCATGGCCGGGTCCGACACCGCG	EcoRI
		ATTAGAATTCGATGAGCACACTGGCCACGGG	EcoRI
pcDNA EmGFP Spinster Y408A	mutagenesis	CATTCTGCTGGCTGTGGTGATCCCTACCCGACGCTC	
		TCGGCCACGATGGCCAG	
pcDNA EmGFP Spinster E164K	mutagenesis	TAGCTATTCCACCATCGCGCCCACTC	
		GCCTTCCGACCCCAACAGGCC	
pcDNA EmGFP MFS1 LLA	mutagenesis	CTGGGGCCGCGCGAGGCGG	
		CTGCCGCCGATCTTCCCATCCTCGTCCTCC	
pOX MFS1 LLA EGFP	cloning	AAGGTACCGCCACCATGGAGGACGAGGATGGGGAG	KpnI
		TGAGGTTCAATTCAGTGTG	SpeI
pcDNA EmGFP TTY3 LIA	mutagenesis	CTGTGAGAACACCCCGCGGCTGGGGCGGAGTCCCC	
		GGGGACTCGCGCCAGCCGCGGGGTGTTCTCACAG	
pEGFP-C2-TMEM104 LLA	mutagenesis	GCCTCAGACAGTGACGCCGCTAGCCAAGACAACACTAC	
		GTAGTTGCTTGGCTAGCGGCTCACTGTCTGAGGC	
pcDNA EmGFP SLC37A2 iso2	mutagenesis	AATCAATTGACCATGCGGTCTCCCTGGCTC	
		CGACAATTGCTGGTGGGTTAGGACCATAC	
pEGFP-C2-SNAT7 Y115A	mutagenesis	CAGCAATGAGAGGACCGCTCAGGAGGTGGTGTGG	
		CCACACCACCTCTGAGCGGTCCTCTCATTGCTG	
pEGFP-C2-SNAT7 LLA	mutagenesis	TGGGGAGCGGGCCCGGGCGGCCAAAGTCCCTGTGTG	
		CACACAGGGACTTTGGGCCGCCGGGCCCGCTCCCAG	
pOX SNAT7	cloning	AACTAGTGCCACCATGGTGAGCAAG	EcoRI
		AACTAGTGCCACCGCCAGGTCAGCATCAACAGTG	SpeI

Dsi RNAs were used to reduce the expression of Snat7 in mice. The sequences are the following:

- DsiRNA #1:

rArGrCrArCrArGrArArGrUrArGrCrCrCrArArArCrUrCrUTC

rGrArArGrArGrUrUrUrGrGrGrCrUrArCrUrUrCrUrGrUrGrCrUrGrG

- DsiRNA #2:

rCrCrArUrArGrCrUrArArUrArGrArCrArUrUrUrCrCrCrAGG

rCrCrUrGrGrGrArArArUrGrUrCrUrArUrUrArGrCrUrArUrGrGrGrA

-DsiRNA #3:

rCrArGrGrUrCrUrArArUrGrUrUrUrArCrArArArCrGrGrUGC

rGrCrArCrCrGrUrUrUrGrUrArArArCrArUrUrArGrArCrCrUrGrGrU

Antibodies

Antibodies used for Western Blot or immunofluorescence assays are listed in the following table:

target	coupled to	name	from	mono/polyclonal	made in	dilution
hIAMP1	-	H4A3	Abcam	monoclonal	mouse	1:2000
hSNAT7	-	HPA041777	Atlas	polyclonal	rabbit	1:500
mMAP2	-	AP20	EMD Millipore	monoclonal	mouse	1:1000
EGFP	-	clone 13,1	Roche	monoclonal	mouse	1:10000
IG rabbit	HRP	-	Sigma	polyclonal	goat	1:30000
IG mouse	HRP	-	Sigma	polyclonal	goat	1:30000
IG mouse	CY3	-	Jackson Immuno Research	polyclonal	donkey	1:1000
IG mouse	Alexa 488	-	Molecular Probes	polyclonal	donkey	1:1000

Expression of proteins in Xenopus oocytes

Ovarian lobes were extracted from *Xenopus laevis* females under anesthesia and oocyte clusters were incubated on a shaker in OR2 medium (85 mM NaCl, MgCl₂ 1 mM, 5 mM Hepes-K⁺ pH 7.6) containing 2 mg/mL of collagenase type II (GIBCO) for 1 h at room temperature. De-folliculated oocytes were sorted and kept at 19 °C in Barth's solution (88 mM NaCl, 1 mM KCl, 2.4 mM NaHCO₃, 0.82 mM MgSO₄, 0.33 mM Ca(NO₃)₂, 0.41 mM CaCl₂, 10 mM Hepes-Na⁺ (pH 7.4), supplemented with 50 µg/mL of gentamycin.

Capped cRNAs were synthesized in vitro from linearized pOX(+) plasmids using mMessage-mMachine T7 and SP6 kits (Ambion), respectively. Oocytes were injected with 50 ng of cRNA using a nanoliter injector (World Precision Instruments). Expression of EGFP-tagged constructs at the oocyte surface was verified under an Eclipse TE-2000

epifluorescence microscope (Nikon) with a 4x objective lens and used to preselect oocytes with highest expression levels for radioactive uptake or electrophysiological recording. Epifluorescence micrographs were acquired with a CCD camera (Coolsnap) and processed using ImageJ.

Uptake of glutamine in oocytes

Radiotracer flux analysis was performed in 100 mM NaCl, 2 mM KCl, 1 mM MgCl₂, and 1.8 mM CaCl₂ buffered with 5 mM HEPES to the required pH with NaOH (ND100 solution). Groups of five oocytes per condition were incubated in ND100 with 0.5 µCi of [³H]Gln and 1 µM of the same nonradiolabeled compound. Incubation time was fixed to 30min. Uptake was stopped by four ice-cold ND100 washes at pH 7.0. Intracellular radioactivity was counted individually for each oocyte, after lysis in SDS 10%, using a Tri-Carb 2100 TR liquid scintillation analyzer (Packard).

Cell-surface biotinylation

All the protocol was done at 4°C. Two days after injection with mRNAs, oocytes were washed in PBS (5 oocytes per well, 500µL solution per well). They were then incubated in PBS supplemented with 2.5 mg/mL sulfo-NHS-SS-biotin (Pierce) for 20 minutes. They were washed 6 times in PBS and lysed by pipetting in lysis buffer (NaCl 150 mM, EDTA 5 mM, Tris(HCl) 50 mM, 0.1% SDS, 1% Triton-X-100, protease inhibitors cocktail 1X (Pierce)).

Lysates were clarified by centrifugation at 14000 g for 10 minutes and the supernatant was incubated for 2h with 150 µL streptavidin-agarose beads (Fluka). Supernatants were kept and beads washed three times with lysis buffer. Bound material was then eluted with 50µL Laemmli buffer. Supernatants and eluted fractions were analyzed by Western Blot.

Electrophysiological recordings

Electrophysiological recording was performed at room temperature usually two days after mRNA injection. Voltage clamp was applied using an OpusXpress 6000A workstation

(Molecular Devices) and two borosilicate-glass microelectrodes filled with 3 M KCl (0.3–2 MΩ tip resistance) and an Ag/AgCl reference electrode located close to the oocyte. Currents were recorded using a Digidata 1320 interface and the pClamp software (Molecular Devices).

Oocytes were perfused with ND100 solutions (100 mM NaCl, 2 mM KCl, 1 mM MgCl₂, 1.8 mM CaCl₂, 5 mM HEPES or MES adjusted to the required pH with NaOH) supplemented, or not, with tested compounds (all from Sigma).

Steady-state currents were recorded using the automated OpusXpress 6000A workstation and robotic compound delivery from 96-well plates. Traces acquired at a constant holding potential (-40 mV) were filtered at 5 Hz and sampled at 200 Hz. Blank application of ND100 buffer from the OpusXpress liquid handler generated a small outward-current artefact that was subtracted from evoked currents in subsequent data analysis.

Cell culture and transfection

All cells but neurons were kept at 37°C in 5%CO₂ and in glucose rich DMEM supplemented with 100 units/mL penicillin, 100 µg/mL streptomycin and 10% fetal bovine serum.

For electroporation of HeLa cells, a GHT 1287 electroporator (Jouan) was used. 2000000 cells were resuspended in 50 µL ice-cold PBS supplemented with 5-10 µg DNA. Immediately after mixing, cells were subjected to ten square pulses (200 V, 3ms) at 1Hz with 5mm-spaced electrodes. Cells were then resuspended and distributed in fourteen wells (24-wells plate).

For lipofection of HEK-293T and MEFs, for each well, 150µL DMEM were mixed with 0.8 µg DNA. In parallel, 150 µL DMEM were mixed with 2 µL Lipofectamine2000 (Invitrogen). Both mixes rested 5minutes at RT and were then mixed together. After 20 minutes at RT, the medium of cells was substituted for the transfection mix for 4-5 hours.

For lipofection of Mia-PACA2, for each well, 50 µL DMEM were mixed with 5pmol dsRNA or 2.5 pmol dsRNA and 0.4 µg DNA. In parallel, 50 µL DMEM were mixed with 2 µL Lullaby (Ozbiosciences). Both mixes rested 5 minutes at RT and were then mixed together.

After 20 minutes at RT, the medium of cells was changed for 400 μ L fresh complete medium. Then, the transfection mix was dispatched over the top and left overnight.

Western Blot

Cells samples in 24 wells plates were rinsed with ice-cold PBS++ (PBS supplemented with 0.1 mM $MgCl_2$ and 0.1 mM $CaCl_2$). They were resuspended in Laemmli buffer at 1,250,000 cells per mL. The equivalent of 250,000 cells was analyzed by SDS-Page (10% gel)

Separated proteins were electrotransferred onto nitrocellulose. The membrane was blocked for 1 h in PBS supplemented with 5% non-fat-milk, then incubated in the primary antibody (see “antibodies”) for 1h in PBS supplemented with Tween20 0.05% and milk 5%. After three rinse of 5 minutes in PBS+Tween, the membrane was incubated with horseradish-conjugated secondary antibody in PBS+Tween+milk for 1h, and then rinsed three times. Immune complexes were detected using Lumi Light Plus (Roche) and images acquired using an Image Quant LAS 4000 (GE). Images were analyzed using Image J.

Immunofluorescence

In 24 wells plates, cells were rapidly washed with PBS++ (PBS supplemented with 0.1 mM $CaCl_2$ and 0.1 mM $MgCl_2$). They were then incubated for 10 minutes in paraformaldehyde 4% in PBS. Then, paraformaldehyde was quenched by a 15 minutes-incubation in 50mM NH_4Cl (in PBS). Cells were then washed three times, 5 minutes every time, in PBS++. Samples were then blocked and permeabilized with blocking buffer (0.05% saponin, 0.2% BSA in PBS++) for 15 minutes. Coverslips were then incubated for 1h with the primary antibody (see antibodies) in blocking buffer, and then rinsed with PBS++ for 5 minutes each times. They, they were treated for 1h with the secondary antibody in blocking buffer. They were rinsed three times like previously once again, then once with water and then mounted onto glass slides with 5 Fluoromount-G (Southern Biotechnology Associates).

This protocol has been used while skipping blocking and antibodies when no immunofluorescence was required.

This protocol was modulated for mice neurons. After fixation with PFA, coverslips were rinsed three times with PBS++ for 10 min. They, cells were permeabilized with PBS++ supplemented with triton-X100 0.2% for 10 minutes. Then, they were washed once, for 10 minutes, with PBS++ and then incubated with PBS++ supplemented with anti-MAP2 (see antibodies), BSA 3%, normal donkey serum (NDS) 2% and normal goat serum (NGS) 2%. After 3 washes of 10 minutes with PBS++, they were incubated in PBS with anti-rabbit-A488 1:1000, NDS 2%, NGS 2%, BSA 3%.

Images were acquired under a 40X or a 100X objective lens with an Eclipse TE-2000 microscope (Nikon) equipped with a CCD camera (Coolsnap). Images were analyzed using Metamorph (Universal Imaging Corporation) and ImageJ.

TFEB test

HeLa cells were electroporated with DNA encoding mRFP-TFEB and EGFP-fused transporters and seeded onto coverslips 48 h prior to experiment. Cells were treated for 2h with complete medium supplemented with 100 mM sucrose or esters: alanine methyl-ester, 3 mM; glutamate dimethyl-ester 10 mM, glycine methyl-ester 4.5 mM, lysine methyl-ester 40 mM, leucine methyl-ester 1.7 mM, methionine methyl-ester 6 mM, asparagine methyl-ester 27 mM, glutamine tert-butyl-ester 3.75 mM, serine methyl-ester 3.7 mM, tyrosine methyl-ester 7 mM. They were then fixed (see immunofluorescence).

For each condition, 50 cells were observed using a 40X objective with an Eclipse TE-2000 (Nikon) and divided in three categories depending on TFEB localization: C (cytosolic, N (nuclear), M (mixed).

CRISPR-Cas9

We used the protocol from ¹⁷⁴[¹⁷⁴¹⁷³¹⁷³\(Ran et al. 2013\)](#). pSpCas9n(BB)-2A-Puro was used. This plasmid encodes a mutated form of Cas9 that catalyzed simple-strand breaks. To trigger deletion-insertions in the target gene, two sites are selected that are close enough from one another. This helps reduce the number of off-targets. Sites were selected using www.crispr.mi.edu. Two regions were targeted, both in exon 1 of *SNAT7*: 151-194 (clones named 26) and 129-194 (clones named 34).

Clones were validated by PCR on genomic DNA of cells and by Western Blot.

Sialic acid uptake

HEK-293 cells expressing sialin constructs were washed twice with 500µl of uptake buffer A (5 mM D-glucose, 140 mM NaCl, 1 mM MgSO₄ and 10 mM Mops, pH 7.0) and incubated for 15 min at room temperature in 200µl of uptake buffer A or B (identical to buffer A, but adjusted to pH 5.0 with MES buffer) containing 0.1 µCi of N-acetyl-[6-³H]neuraminic acid (20 Ci/mmol; American Radiolabeled Chemicals). Uptake was stopped by aspiration of the medium, followed by two brief washes with 500 µl of ice-cold uptake buffer A. Cells were lysed in 200 µL of 0.1 M NaOH and the accumulated radioactivity was counted in Emulsifier-Safe cock-tail (Packard) using a Tri-Carb 2100 TR liquid scintillation analyzer (Packard).

Mice models

Cln3(Δ ex7/8) KI mice were generously provided by Susan Cotman (Harvard Medical School, USA) ¹⁹⁵

Preparation of hippocampal neurons

Hippocampi were dissected out in pre-chilled (4°C) Neurobasal medium (Gibco) using a stereomicroscope, and the meninges carefully removed. Hippocampi were washed twice with pre-chilled HBSS (Gibco), and incubated for 10–12 min in 2.5% trypsin in EDTA with 2.5% DNase diluted in HBSS in a 37°C water-bath. The cells were then dissociated by trituration, and plated at a density of 50 000/2CM² onto glass coverslips previously coated with poly-L-Lysine (100 µg/ml) (Falcon, Thermo Fischer Scientific). Plating culture medium consisted of Neurobasal medium supplemented with 2% B27 (Life Technologies, Gaithersburg, MD), 2 mM GlutaMAXTM-I (Invitrogen), and penicillin 2.5 U/ml-streptomycin 2.5 mg/ml (Gibco). Cells were maintained at 37°C in 5% CO₂. After 2 to 24 hours in vitro, plating medium was replaced by glial cell-conditioned medium (CM). The conditioned medium was not replaced over the time of the hippocampal culture.

Primary cultures of glial cells were prepared from PND4 Sprague-Dawley rats (Janvier Labs). Cortices were dissected out and processed as previously described¹⁹⁶. Cells were plated in 75 cm² flasks in Dulbecco's Modified Eagle Medium with 4.5 g/L glucose and glutamine (DMEM High glucose GlutaMAXTM-I, Invitrogen) supplemented with 10% fetal calf serum and 0.1% penicillin-streptomycin (Gibco). Cells were let to grow until they were sub-confluent (80%) and passaged to 1:2 in same medium. Further passages #1 and #2 were used to prepare conditioned medium as followed: DMEM medium was replaced by pre-warmed Neurobasal medium supplemented with 2% B27, GlutaMAXTM-I and 0.1% penicillin-streptomycin for 24 h to 48 h, then filtered and used to feed primary hippocampal neurons.

DQ-red-BSA uptake

For neurons, at DIV 13 or 17, cells were kept in 1000µL conditioned medium. For DQ-red-BSA (Molecular Probes) uptake, 500 µL of medium was removed. It was supplemented with 100 µg/mL DQ-red-BSA and then added back onto neurons for 6, 12 or 24 hours. Neurons were then fixed (see immunofluorescence).

For MEFs, cells were incubated for 30 minutes in DMEM supplemented with 50µg/mL DQ-red-BSA. They were then washed three times with PBS++ (PBS supplemented with 0.1 mM CaCl₂ and MgCl₂) and incubated for two hours in complete, fresh medium.

Flow cytometry

Cells were prepared in the dark. They were dissociated using trypsin. They were then centrifuged at 300 g. Then, they were washed with PBS supplemented with EDTA 5mM, and centrifuged again. The pellet was resuspended in 150 µL PBS+EDTA. Then, 150µL PFA% in PBS was added. Cells were gently mixed for 10 minutes in PFA before being analyzed or kept at 4°C overnight.

Cells were analyzed at the Service commun de cytométrie en flux (CUSP, Université Paris Descartes, France) using a Canto II BD. If necessary, cells were diluted with PBS+EDTA.

Lysosomal proteolysis measures in primary fibroblasts

Primary fibroblasts were seeded in 6-well plates at 50,000 cells per well in complete medium one day prior to experiment. The protocol from ¹⁴⁴ was then used using tritiated valine (Perkin Helmer, 50 Ci/mmol).

Cellular fractionation

This paragraph was written by our collaborator, Marielle Boonen (Université de Namur, Belgium).

HeLa cells were fractionated by differential centrifugation essentially as described by de Duve et al ². This allows a partial separation of the different cellular organelles into six fractions: E, Extract or post-nuclear supernatant; N, Nuclear fraction; M, Heavy mitochondrial fraction; L, Light mitochondrial fraction; P, microsomal fraction and S, Soluble fraction. Note that in our adapted protocol, all ultracentrifugation steps were conducted at 4°C using a 70.1Ti rotor and that the M fraction (3.5 mL per tube) was pelleted at 10000 rpm for 3'15", then washed (2 mL final volume), and re-centrifuged for 2'24" at 10000 rpm. A M + L pooled fraction was then centrifuged in a linear sucrose density gradient as described previously ¹⁹⁷. Enzyme activities of lysosomal β -galactosidase, mitochondrial cytochrome oxidase, peroxisomal catalase, plasma membrane alkaline phosphodiesterase, and of the endoplasmic reticulum marker alkaline α -glucosidase were measured as described ^{85,198}.

Transport assay on lysosomal preparations

22,500,000 HeLa cells were dissociated with trypsin and centrifuged 10min at 300g. They were washed twice in 1.125 mL purification buffer (250 mM sucrose, 10 mM triethanolamine, 10 mM CH₃COOH, 1mM EDTA, 2.5mM KCl, 5mM MgATP, Pierce protease inhibitor cocktail 1X, adjusted at pH7.60). Unless mentioned, all the rest of this protocol is done at 4°C. Cells were passed 50 times in a 0.25 mM needle using a syringe for lysis.

Lysates (fraction L) were centrifuged at 750 g for 10 min. Supernatants were kept and pellets resuspended in 1.125 mL purification buffer. Pellets were centrifuged again in the same way and supernatants from both centrifuges pooled (fraction S1). Pellets (C1) were discarded. S1 was centrifuged at 1500 g for 15 minutes. Pellets (C2) were discarded and

supernatants (S2) centrifuged at 20000 g for 15 minutes. Supernatants (S3) were discarded and Pellets (C3) resuspended in 125 μ L purification buffer.

For transport, C3 fractions were supplemented with amino acid esters (same concentrations as in TFEB test) and incubated for 15 minutes at 25°C. They were split into 5 tubes and centrifuged at 20000 g for 15 minutes. Supernatants were discarded. Each tube was resuspended in 400 μ L purification buffer supplemented with 1.27 μ Ci of radioactive amino acids (Perkin-Elmer, 50 Ci/mmol). Each tube was then split into seven hemolysis tubes (50 μ L per tube). One tube was immediately filtered. Three tubes were filtered after 30 minutes at 25°C. The last three tubes were supplemented with 100mM glycine methyl-ester at 30 minutes and filtered at 40 minutes.

Lysosomal suspensions were filtered on vacuum using 0.45 μ m nitrocellulose filters (Millipore). First, 3 mL ice-cold PBS were added to lysosomal suspensions, and then filtered. Tubes were then rinsed twice with 3mL ice-cold PBS and the rinsing liquid was filtered onto the same filter. Radioactivity on filters was counted in Emulsifier-Safe cocktail (Packard) with a Tri-Carb 2100 TR liquid scintillation analyser (Packard).

Latency test

C3 lysosomal fractions were diluted 5 times in purification buffer (see transport assay on lysosomal fractions). Reaction was mixed at 4°C as follows: sample: 20 μ L; methyl-umbelliferyl-galactoside-N-acetyl-galactoside 40 mM 2.5 μ L; triton X-100: 0 or 5 μ L; NaCl 0.4M 25 μ L; NaCH₃COO 0.2M pH 5.0 50 μ L, water 97.5 or 102.5 μ L respectively. Samples were incubated at 37°C for 10 minutes. The reaction was then stopped by adding 1.7 mL ice-cold Na₂CO₃ 0.5 M + glycine 0.5 M pH 10.5. Fluorescence was analyzed using a Fluorescence Spectrophotometer F-7100 (Hitachi) (excitation at 350nm, emission 450nm).

Growth assays

For growth assays, MP2 or A2780 cells were seeded at respectively 15,000 and 25,000 cells per well in 24-wells plates in glutamine-free DMEM (Gibco), supplemented with dialyzed fetal serum (Gibco, 10%), penicillin (100 units/mL) and streptomycin (100 μ g/mL), glutamine (Sigma) and delipidified BSA (Calbiochem). Medium was changed daily.

Cells were dissociated after growth using trypsin and resuspended in complete medium.
They were finally counted using a Coulter Z2.

References

1. PALADE, G. E. Intracellular localization of acid phosphatase; a comparative study of biochemical and histochemical methods. *J. Exp. Med.* **94**, 535–48 (1951).
2. DE DUVE, C., PRESSMAN, B. C., GIANETTO, R., WATTIAUX, R. & APPELMANS, F. Tissue fractionation studies. 6. Intracellular distribution patterns of enzymes in rat-liver tissue. *Biochem. J.* **60**, 604–17 (1955).
3. Luzio, J. P., Pryor, P. R. & Bright, N. A. Lysosomes: fusion and function. *Nat. Mol Cell Bio* **8**, 622–632 (2007).
4. NOVIKOFF, A. B., BEAUFAY, H. & DE DUVE, C. Electron microscopy of lysosomerich fractions from rat liver. *J. Biophys. Biochem. Cytol.* **2**, 179–84 (1956).
5. Schröder, B. A., Wrocklage, C., Hasilik, A. & Saftig, P. The proteome of lysosomes. *Proteomics* **10**, 4053–76 (2010).
6. Fan, X. *et al.* Identification of the gene encoding the enzyme deficient in mucopolysaccharidosis IIIC (Sanfilippo disease type C). *Am. J. Hum. Genet.* **79**, 738–44 (2006).
7. Mellman, I., Fuchs, R. & Helenius, A. Acidification of the endocytic and exocytic pathways. *Annu. Rev. Biochem.* **55**, 663–700 (1986).
8. Mindell, J. A. Lysosomal acidification mechanisms. *Annu. Rev. Physiol.* **74**, 69–86 (2012).
9. Steinberg, B. E. *et al.* A cation counterflux supports lysosomal acidification. *J. Cell Biol.* **189**, 1171–86 (2010).
10. Cang, C., Aranda, K., Seo, Y., Gasnier, B. & Ren, D. TMEM175 Is an Organelle K(+) Channel Regulating Lysosomal Function. *Cell* **162**, 1101–12 (2015).
11. Frese, M.-A., Schulz, S. & Dierks, T. Arylsulfatase G, a novel lysosomal sulfatase. *J. Biol. Chem.* **283**, 11388–95 (2008).
12. Gowrishankar, S. & Ferguson, S. M. Lysosomes relax in the cellular suburbs. *J. Cell Biol.* **212**, 617–9 (2016).
13. Kolter, T. & Sandhoff, K. Principles of lysosomal membrane digestion: stimulation of sphingolipid degradation by sphingolipid activator proteins and anionic lysosomal lipids. *Annu. Rev. Cell Dev. Biol.* **21**, 81–103 (2005).
14. Sagné, C. & Gasnier, B. Molecular physiology and pathophysiology of lysosomal membrane transporters. *J. Inherit. Metab. Dis.* **31**, 258–66 (2008).
15. Neiss, W. F. A coat of glycoconjugates on the inner surface of the lysosomal membrane in the rat kidney. *Histochemistry* **80**, 603–8 (1984).

16. Ruivo, R., Anne, C., Sagné, C. & Gasnier, B. Molecular and cellular basis of lysosomal transmembrane protein dysfunction. *Biochim. Biophys. Acta* **1793**, 636–49 (2009).
17. Winchester, B. G. Lysosomal membrane proteins. *Eur. J. Paediatr. Neurol.* **5 Suppl A**, 11–9 (2001).
18. Wang, X. *et al.* TPC proteins are phosphoinositide- activated sodium-selective ion channels in endosomes and lysosomes. *Cell* **151**, 372–83 (2012).
19. Dong, X. *et al.* PI(3,5)P(2) controls membrane trafficking by direct activation of mucolipin Ca(2+) release channels in the endolysosome. *Nat. Commun.* **1**, 38 (2010).
20. Gahl, W. a, Bashan, N., Tietze, F., Bernardini, I. & Schulman, J. D. Cystine transport is defective in isolated leukocyte lysosomes from patients with cystinosis. *Science* **217**, 1263–5 (1982).
21. Pisoni, R. L., Flickinger, K. S., Thoene, J. G. & Christensen, H. N. Characterization of carrier-mediated transport systems for small neutral amino acids in human fibroblast lysosomes. *J. Biol. Chem.* **262**, 6010–7 (1987).
22. Pisoni, R. L., Thoene, J. G. & Christensen, H. N. Detection and characterization of carrier-mediated cationic amino acid transport in lysosomes of normal and cystinotic human fibroblasts. Role in therapeutic cystine removal? *J. Biol. Chem.* **260**, 4791–8 (1985).
23. Jézégou, A. *et al.* Heptahelical protein PQLC2 is a lysosomal cationic amino acid exporter underlying the action of cysteamine in cystinosis therapy. *Proc. Natl. Acad. Sci. U. S. A.* **109**, E3434–43 (2012).
24. Sakata, K. *et al.* Cloning of a lymphatic peptide/histidine transporter. *Biochem. J.* **356**, 53–60 (2001).
25. Morin, P., Sagné, C. & Gasnier, B. Functional characterization of wild-type and mutant human sialin. *EMBO J.* **23**, 4560–70 (2004).
26. Augustin, R., Riley, J. & Moley, K. H. GLUT8 contains a [DE]XXXL[LI] sorting motif and localizes to a late endosomal/lysosomal compartment. *Traffic* **6**, 1196–212 (2005).
27. Gunshin, H. *et al.* Cloning and characterization of a mammalian proton-coupled metal-ion transporter. *Nature* **388**, 482–8 (1997).
28. Graves, A. R., Curran, P. K., Smith, C. L. & Mindell, J. a. The Cl⁻/H⁺ antiporter CIC-7 is the primary chloride permeation pathway in lysosomes. *Nature* **453**, 788–92 (2008).
29. Baldwin, S. A. *et al.* Functional characterization of novel human and mouse equilibrative nucleoside transporters (hENT3 and mENT3) located in intracellular membranes. *J. Biol. Chem.* **280**, 15880–7 (2005).
30. Pisoni, R. L., Acker, T. L., Lisowski, K. M., Lemons, R. M. & Thoene, J. G. A cysteine-specific lysosomal transport system provides a major route for the delivery of thiol to

- human fibroblast lysosomes: possible role in supporting lysosomal proteolysis. *J. Cell Biol.* **110**, 327–35 (1990).
31. Pisoni, R. L. & Thoene, J. G. The transport systems of mammalian lysosomes. *Biochim. Biophys. Acta* **1071**, 351–73 (1991).
 32. Kalatzis, V., Cherqui, S., Antignac, C. & Gasnier, B. Cystinosis, the protein defective in cystinosis, is a H(+)-driven lysosomal cystine transporter. *EMBO J.* **20**, 5940–9 (2001).
 33. Huotari, J. & Helenius, A. Endosome maturation. *EMBO J.* **30**, 3481–500 (2011).
 34. Pryor, P. R. & Luzio, J. P. Delivery of endocytosed membrane proteins to the lysosome. *Biochim. Biophys. Acta* **1793**, 615–24 (2009).
 35. Bonifacino, J. S. & Traub, L. M. Signals for sorting of transmembrane proteins to endosomes and lysosomes. *Annu. Rev. Biochem.* **72**, 395–447 (2003).
 36. Schindler, C., Chen, Y., Pu, J., Guo, X. & Bonifacino, J. S. EARP is a multisubunit tethering complex involved in endocytic recycling. *Nat. Cell Biol.* **17**, 639–50 (2015).
 37. Reczek, D. *et al.* LIMP-2 is a receptor for lysosomal mannose-6-phosphate-independent targeting of beta-glucocerebrosidase. *Cell* **131**, 770–83 (2007).
 38. Sando, G. N. & Neufeld, E. F. Recognition and receptor-mediated uptake of a lysosomal enzyme, alpha-l-iduronidase, by cultured human fibroblasts. *Cell* **12**, 619–27 (1977).
 39. Kan, S.-H. *et al.* Delivery of an enzyme-IGFII fusion protein to the mouse brain is therapeutic for mucopolysaccharidosis type IIIB. *Proc. Natl. Acad. Sci. U. S. A.* **111**, 14870–5 (2014).
 40. Laurent-Matha, V., Derocq, D., Prébois, C., Katunuma, N. & Liaudet-Coopman, E. Processing of human cathepsin D is independent of its catalytic function and auto-activation: involvement of cathepsins L and B. *J. Biochem.* **139**, 363–71 (2006).
 41. Braulke, T. & Bonifacino, J. S. Sorting of lysosomal proteins. *Biochim. Biophys. Acta* **1793**, 605–14 (2009).
 42. Hennigar, S. R., Seo, Y. A., Sharma, S., Soybel, D. I. & Kelleher, S. L. ZnT2 is a critical mediator of lysosomal-mediated cell death during early mammary gland involution. *Sci. Rep.* **5**, 8033 (2015).
 43. Klionsky, D. J. & Codogno, P. The mechanism and physiological function of macroautophagy. *J. Innate Immun.* **5**, 427–33 (2013).
 44. Jung, C. H., Ro, S.-H., Cao, J., Otto, N. M. & Kim, D.-H. mTOR regulation of autophagy. *FEBS Lett.* **584**, 1287–95 (2010).
 45. Ding, W.-X. & Yin, X.-M. Mitophagy: mechanisms, pathophysiological roles, and analysis. *Biol. Chem.* **393**, 547–64 (2012).
 46. Li, W., Li, J. & Bao, J. Microautophagy: lesser-known self-eating. *Cell. Mol. Life Sci.*

- 69**, 1125–36 (2012).
47. Utani, A. Laminin alpha3 chain-derived peptide promotes keratinocyte migration and wound closure: clustering of syndecan-4 and integrin beta1. *Seikagaku*. **82**, 327–31 (2010).
 48. Sattler, T. & Mayer, A. Cell-free reconstitution of microautophagic vacuole invagination and vesicle formation. *J. Cell Biol.* **151**, 529–38 (2000).
 49. Chiang, H. L., Terlecky, S. R., Plant, C. P. & Dice, J. F. A role for a 70-kilodalton heat shock protein in lysosomal degradation of intracellular proteins. *Science* **246**, 382–5 (1989).
 50. Cuervo, A. M. & Wong, E. Chaperone-mediated autophagy: roles in disease and aging. *Cell Res.* **24**, 92–104 (2014).
 51. Goh, L. K. & Sorkin, A. Endocytosis of receptor tyrosine kinases. *Cold Spring Harb. Perspect. Biol.* **5**, a017459 (2013).
 52. Quadros, E. V, Nakayama, Y. & Sequeira, J. M. The protein and the gene encoding the receptor for the cellular uptake of transcobalamin-bound cobalamin. *Blood* **113**, 186–92 (2009).
 53. Freeman, S. A. & Grinstein, S. Phagocytosis: receptors, signal integration, and the cytoskeleton. *Immunol. Rev.* **262**, 193–215 (2014).
 54. Saint-Pol, A., Codogno, P. & Moore, S. E. Cytosol-to-lysosome transport of free polymannose-type oligosaccharides. Kinetic and specificity studies using rat liver lysosomes. *J. Biol. Chem.* **274**, 13547–55 (1999).
 55. Kurz, T., Eaton, J. W. & Brunk, U. T. Redox activity within the lysosomal compartment: implications for aging and apoptosis. *Antioxid. Redox Signal.* **13**, 511–23 (2010).
 56. Kukic, I., Kelleher, S. L. & Kiselyov, K. Zn²⁺ efflux through lysosomal exocytosis prevents Zn²⁺-induced toxicity. *J. Cell Sci.* **127**, 3094–103 (2014).
 57. Sancak, Y. *et al.* Ragulator-Rag complex targets mTORC1 to the lysosomal surface and is necessary for its activation by amino acids. *Cell* **141**, 290–303 (2010).
 58. Rebsamen, M. *et al.* SLC38A9 is a component of the lysosomal amino acid sensing machinery that controls mTORC1. *Nature* **519**, 477–81 (2015).
 59. Andrzejewska, Z. *et al.* Cystinosin is a Component of the Vacuolar H⁺-ATPase-Ragulator-Rag Complex Controlling Mammalian Target of Rapamycin Complex 1 Signaling. *J. Am. Soc. Nephrol.* **27**, 1678–88 (2016).
 60. Sardiello, M. *et al.* A gene network regulating lysosomal biogenesis and function. *Science* **325**, 473–7 (2009).
 61. Futerman, A. H. & van Meer, G. The cell biology of lysosomal storage disorders. *Nat. Rev. Mol. Cell Biol.* **5**, 554–65 (2004).

62. Platt, F. M., Boland, B. & van der Spoel, A. C. The cell biology of disease: lysosomal storage disorders: the cellular impact of lysosomal dysfunction. *J. Cell Biol.* **199**, 723–34 (2012).
63. Schiffmann, R. *et al.* Enzyme replacement therapy in Fabry disease: a randomized controlled trial. *JAMA* **285**, 2743–9 (2001).
64. Bennett, L. L. & Turcotte, K. Eliglustat tartrate for the treatment of adults with type 1 Gaucher disease. *Drug Des. Devel. Ther.* **9**, 4639–47 (2015).
65. Westbroek, W., Gustafson, A. M. & Sidransky, E. Exploring the link between glucocerebrosidase mutations and parkinsonism. *Trends Mol. Med.* **17**, 485–93 (2011).
66. Xu, H., Delling, M., Li, L., Dong, X. & Clapham, D. E. Activating mutation in a mucolipin transient receptor potential channel leads to melanocyte loss in varitint-waddler mice. *Proc. Natl. Acad. Sci. U. S. A.* **104**, 18321–6 (2007).
67. Medina, D. L. & Ballabio, A. Lysosomal calcium regulates autophagy. *Autophagy* **11**, 970–1 (2015).
68. Plans, V., Rickheit, G. & Jentsch, T. J. Physiological roles of CLC Cl(-)/H(+) exchangers in renal proximal tubules. *Pflügers Arch. Eur. J. Physiol.* **458**, 23–37 (2009).
69. Lange, P. F., Wartosch, L., Jentsch, T. J. & Fuhrmann, J. C. ClC-7 requires Ostm1 as a beta-subunit to support bone resorption and lysosomal function. *Nature* **440**, 220–3 (2006).
70. Kasper, D. *et al.* Loss of the chloride channel ClC-7 leads to lysosomal storage disease and neurodegeneration. *EMBO J.* **24**, 1079–91 (2005).
71. Vanier, M. T. Complex lipid trafficking in Niemann-Pick disease type C. *J. Inherit. Metab. Dis.* **38**, 187–99 (2015).
72. Infante, R. E. *et al.* NPC2 facilitates bidirectional transfer of cholesterol between NPC1 and lipid bilayers, a step in cholesterol egress from lysosomes. *Proc. Natl. Acad. Sci. U. S. A.* **105**, 15287–92 (2008).
73. Wang, M. L. *et al.* Identification of surface residues on Niemann-Pick C2 essential for hydrophobic handoff of cholesterol to NPC1 in lysosomes. *Cell Metab.* **12**, 166–73 (2010).
74. Xie, X. *et al.* Amino acid substitution in NPC1 that abolishes cholesterol binding reproduces phenotype of complete NPC1 deficiency in mice. *Proc. Natl. Acad. Sci. U. S. A.* **108**, 15330–5 (2011).
75. Whitehead, V. M. Acquired and inherited disorders of cobalamin and folate in children. *Br. J. Haematol.* **134**, 125–36 (2006).

76. Rutsch, F. *et al.* Identification of a putative lysosomal cobalamin exporter altered in the cblF defect of vitamin B12 metabolism. *Nat. Genet.* **41**, 234–9 (2009).
77. Coelho, D. *et al.* Mutations in ABCD4 cause a new inborn error of vitamin B12 metabolism. *Nat. Genet.* **44**, 1152–5 (2012).
78. Morgan, N. V. *et al.* Mutations in SLC29A3, encoding an equilibrative nucleoside transporter ENT3, cause a familial histiocytosis syndrome (Faisalabad histiocytosis) and familial Rosai-Dorfman disease. *PLoS Genet.* **6**, e1000833 (2010).
79. Geisel, M. H. *et al.* Update of the effect estimates for common variants associated with carotid intima media thickness within four independent samples: The Bonn IMT Family Study, the Heinz Nixdorf Recall Study, the SAPHIR Study and the Bruneck Study. *Atherosclerosis* **249**, 83–87 (2016).
80. Togawa, N., Miyaji, T., Izawa, S., Omote, H. & Moriyama, Y. A Na⁺-phosphate cotransporter homologue (SLC17A4 protein) is an intestinal organic anion exporter. *Am. J. Physiol. Cell Physiol.* **302**, C1652–60 (2012).
81. Mancini, G. M., Havelaar, A. C. & Verheijen, F. W. Lysosomal transport disorders. *J. Inherit. Metab. Dis.* **23**, 278–92 (2000).
82. Neufeld, E. F., Lim, T. W. & Shapiro, L. J. Inherited disorders of lysosomal metabolism. *Annu. Rev. Biochem.* **44**, 357–76 (1975).
83. Ruivo, R. *et al.* Mechanism of proton/substrate coupling in the heptahelical lysosomal transporter cystinosin. *Proc. Natl. Acad. Sci. U. S. A.* **109**, E210–7 (2012).
84. Sagné, C. & Gasnier, B. Molecular physiology and pathophysiology of lysosomal membrane transporters. *J. Inherit. Metab. Dis.* **31**, 258–66 (2008).
85. Della Valle, M. C. *et al.* Classification of subcellular location by comparative proteomic analysis of native and density-shifted lysosomes. *Mol. Cell. Proteomics* **10**, M110.006403 (2011).
86. Bagshaw, R. D., Mahuran, D. J. & Callahan, J. W. A proteomic analysis of lysosomal integral membrane proteins reveals the diverse composition of the organelle. *Mol. Cell. Proteomics* **4**, 133–43 (2005).
87. Schröder, B. *et al.* Integral and associated lysosomal membrane proteins. *Traffic* **8**, 1676–86 (2007).
88. Brojatsch, J. *et al.* A proteolytic cascade controls lysosome rupture and necrotic cell death mediated by lysosome-destabilizing adjuvants. *PLoS One* **9**, e95032 (2014).
89. Liu, B., Du, H., Rutkowski, R., Gartner, A. & Wang, X. LAAT-1 is the lysosomal lysine/arginine transporter that maintains amino acid homeostasis. *Science* **337**, 351–4 (2012).
90. Maleszka, R., Hanes, S. D., Hackett, R. L., de Couet, H. G. & Miklos, G. L. The

- Drosophila melanogaster* dodo (dod) gene, conserved in humans, is functionally interchangeable with the ESS1 cell division gene of *Saccharomyces cerevisiae*. *Proc. Natl. Acad. Sci. U. S. A.* **93**, 447–51 (1996).
91. Suzuki, K., Juni, N. & Yamamoto, D. Enhanced Mate Refusal in Female *Drosophila* Induced by a mutation in the spinster locus. *Appl. Entomol. Zool.* **32**, 235–243 (1997).
 92. Sabirov, R. Z., Merzlyak, P. G., Islam, M. R., Okada, T. & Okada, Y. The properties, functions, and pathophysiology of maxi-anion channels. *Pflügers Arch. Eur. J. Physiol.* **468**, 405–20 (2016).
 93. Jentsch, T. J. VRACs and other ion channels and transporters in the regulation of cell volume and beyond. *Nat. Rev. Mol. Cell Biol.* **17**, 293–307 (2016).
 94. Cang, C. *et al.* mTOR regulates lysosomal ATP-sensitive two-pore Na(+) channels to adapt to metabolic state. *Cell* **152**, 778–90 (2013).
 95. Sagné, C. *et al.* Identification and characterization of a lysosomal transporter for small neutral amino acids. *Proc. Natl. Acad. Sci. U. S. A.* **98**, 7206–11 (2001).
 96. Pan, Y., Robinett, C. C. & Baker, B. S. Turning males on: activation of male courtship behavior in *Drosophila melanogaster*. *PLoS One* **6**, e21144 (2011).
 97. Bartoloni, L. & Antonarakis, S. E. The human sugar-phosphate/phosphate exchanger family SLC37. *Pflügers Arch. Eur. J. Physiol.* **447**, 780–3 (2004).
 98. Abe, T. *et al.* Molecular characterization and tissue distribution of a new organic anion transporter subtype (oatp3) that transports thyroid hormones and taurocholate and comparison with oatp2. *J. Biol. Chem.* **273**, 22395–401 (1998).
 99. Huang, Y., Lemieux, M. J., Song, J., Auer, M. & Wang, D.-N. Structure and mechanism of the glycerol-3-phosphate transporter from *Escherichia coli*. *Science* **301**, 616–20 (2003).
 100. Nakano, Y. *et al.* Mutations in the novel membrane protein spinster interfere with programmed cell death and cause neural degeneration in *Drosophila melanogaster*. *Mol. Cell. Biol.* **21**, 3775–88 (2001).
 101. Sweeney, S. T. & Davis, G. W. Unrestricted synaptic growth in spinster—a late endosomal protein implicated in TGF- β -mediated synaptic growth regulation. *Neuron* **36**, 403–16 (2002).
 102. Dermaut, B. *et al.* Aberrant lysosomal carbohydrate storage accompanies endocytic defects and neurodegeneration in *Drosophila* benchwarmer. *J. Cell Biol.* **170**, 127–39 (2005).
 103. Rong, Y. *et al.* Spinster is required for autophagic lysosome reformation and mTOR reactivation following starvation. *Proc. Natl. Acad. Sci. U. S. A.* **108**, 7826–31 (2011).
 104. Conrad, M. *et al.* Nutrient sensing and signaling in the yeast *Saccharomyces*

- cerevisiae. *FEMS Microbiol. Rev.* **38**, 254–99 (2014).
105. Haltia, M. The neuronal ceroid-lipofuscinoses: from past to present. *Biochim. Biophys. Acta* **1762**, 850–6 (2006).
 106. Seehafer, S. S. & Pearce, D. A. You say lipofuscin, we say ceroid: defining autofluorescent storage material. *Neurobiol. Aging* **27**, 576–88 (2006).
 107. Lim, M. J. *et al.* Distinct patterns of serum immunoreactivity as evidence for multiple brain-directed autoantibodies in juvenile neuronal ceroid lipofuscinosis. *Neuropathol. Appl. Neurobiol.* **32**, 469–82 (2006).
 108. Palmer, D. N., Barry, L. A., Tynnelä, J. & Cooper, J. D. NCL disease mechanisms. *Biochim. Biophys. Acta* **1832**, 1882–93 (2013).
 109. Mole, S. E., Williams, R. E. & Goebel, H. H. Correlations between genotype, ultrastructural morphology and clinical phenotype in the neuronal ceroid lipofuscinoses. *Neurogenetics* **6**, 107–26 (2005).
 110. Cooper, J. D., Messer, A., Feng, A. K., Chua-Couzens, J. & Mobley, W. C. Apparent loss and hypertrophy of interneurons in a mouse model of neuronal ceroid lipofuscinosis: evidence for partial response to insulin-like growth factor-1 treatment. *J. Neurosci.* **19**, 2556–67 (1999).
 111. Bible, E., Gupta, P., Hofmann, S. L. & Cooper, J. D. Regional and cellular neuropathology in the palmitoyl protein thioesterase-1 null mutant mouse model of infantile neuronal ceroid lipofuscinosis. *Neurobiol. Dis.* **16**, 346–59 (2004).
 112. Warriar, V., Vieira, M. & Mole, S. E. Genetic basis and phenotypic correlations of the neuronal ceroid lipofuscinoses. *Biochim. Biophys. Acta* **1832**, 1827–30 (2013).
 113. Zhong, N. *et al.* Heterogeneity of late-infantile neuronal ceroid lipofuscinosis. *Genet. Med.* **2**, 312–8 (2000).
 114. Kollmann, K. *et al.* Cell biology and function of neuronal ceroid lipofuscinosis-related proteins. *Biochim. Biophys. Acta* **1832**, 1866–81 (2013).
 115. Ballabio, A. & Gieselmann, V. Lysosomal disorders: from storage to cellular damage. *Biochim. Biophys. Acta* **1793**, 684–96 (2009).
 116. Lyly, A. *et al.* Novel interactions of CLN5 support molecular networking between Neuronal Ceroid Lipofuscinosis proteins. *BMC Cell Biol.* **10**, 83 (2009).
 117. Verstegen, R. H., Theodore, M., van de Klerk, H. & Morava, E. Lymphatic edema in congenital disorders of glycosylation. *JIMD Rep.* **4**, 113–6 (2012).
 118. Hofmann, S. L., Das, A. K., Yi, W., Lu, J. Y. & Wisniewski, K. E. Genotype-phenotype correlations in neuronal ceroid lipofuscinosis due to palmitoyl-protein thioesterase deficiency. *Mol. Genet. Metab.* **66**, 234–9 (1999).
 119. Luiro, K., Kopra, O., Lehtovirta, M. & Jalanko, A. CLN3 protein is targeted to neuronal

- synapses but excluded from synaptic vesicles: new clues to Batten disease. *Hum. Mol. Genet.* **10**, 2123–31 (2001).
120. Storch, S., Pohl, S. & Braulke, T. A dileucine motif and a cluster of acidic amino acids in the second cytoplasmic domain of the batten disease-related CLN3 protein are required for efficient lysosomal targeting. *J. Biol. Chem.* **279**, 53625–34 (2004).
 121. Maruvada, P., Dmitrieva, N. I., East-Palmer, J. & Yen, P. M. Cell cycle-dependent expression of thyroid hormone receptor-beta is a mechanism for variable hormone sensitivity. *Mol. Biol. Cell* **15**, 1895–903 (2004).
 122. Cárcel-Trullols, J., Kovács, A. D. & Pearce, D. A. Cell biology of the NCL proteins: What they do and don't do. *Biochim. Biophys. Acta* **1852**, 2242–55 (2015).
 123. Kim, Y., Ramirez-Montealegre, D. & Pearce, D. A. A role in vacuolar arginine transport for yeast Btn1p and for human CLN3, the protein defective in Batten disease. *Proc. Natl. Acad. Sci. U. S. A.* **100**, 15458–62 (2003).
 124. Ramirez-Montealegre, D. & Pearce, D. A. Defective lysosomal arginine transport in juvenile Batten disease. *Hum. Mol. Genet.* **14**, 3759–73 (2005).
 125. Cooper, J. D., Russell, C. & Mitchison, H. M. Progress towards understanding disease mechanisms in small vertebrate models of neuronal ceroid lipofuscinosis. *Biochim. Biophys. Acta* **1762**, 873–89 (2006).
 126. Eliason, S. L. *et al.* A knock-in reporter model of Batten disease. *J. Neurosci.* **27**, 9826–34 (2007).
 127. Herrmann, J. E. *et al.* STAT3 is a critical regulator of astrogliosis and scar formation after spinal cord injury. *J. Neurosci.* **28**, 7231–43 (2008).
 128. Siintola, E. *et al.* The novel neuronal ceroid lipofuscinosis gene MFSD8 encodes a putative lysosomal transporter. *Am. J. Hum. Genet.* **81**, 136–46 (2007).
 129. Wheeler, R. B. *et al.* A new locus for variant late infantile neuronal ceroid lipofuscinosis-CLN7. *Mol. Genet. Metab.* **66**, 337–8 (1999).
 130. Sharifi, A. *et al.* Expression and lysosomal targeting of CLN7, a major facilitator superfamily transporter associated with variant late-infantile neuronal ceroid lipofuscinosis. *Hum. Mol. Genet.* **19**, 4497–4514 (2010).
 131. Saier, M. H. *et al.* The major facilitator superfamily. *J. Mol. Microbiol. Biotechnol.* **1**, 257–79 (1999).
 132. Miyaji, T. *et al.* Identification of a vesicular aspartate transporter. *Proc. Natl. Acad. Sci. U. S. A.* **105**, 11720–4 (2008).
 133. Morland, C. *et al.* Vesicular uptake and exocytosis of L-aspartate is independent of sialin. *FASEB J.* **27**, 1264–74 (2013).
 134. Herring, B. E., Silm, K., Edwards, R. H. & Nicoll, R. A. Is Aspartate an Excitatory

- Neurotransmitter? *J. Neurosci.* **35**, 10168–71 (2015).
135. Kousi, M. *et al.* Mutations in CLN7/MFSD8 are a common cause of variant late-infantile neuronal ceroid lipofuscinosis. *Brain* **132**, 810–9 (2009).
 136. Pears, M. R. *et al.* Deletion of btn1, an orthologue of CLN3, increases glycolysis and perturbs amino acid metabolism in the fission yeast model of Batten disease. *Mol. Biosyst.* **6**, 1093–102 (2010).
 137. Lerner, T. *et al.* Isolation of a novel gene underlying Batten disease, CLN3. The International Batten Disease Consortium. *Cell* **82**, 949–57 (1995).
 138. Herrmann, P. *et al.* Developmental impairments of select neurotransmitter systems in brains of Cln3(Deltaex7/8) knock-in mice, an animal model of juvenile neuronal ceroid lipofuscinosis. *J. Neurosci. Res.* **86**, 1857–70 (2008).
 139. Wattiaux, R., Wattiaux-De Coninck, S., Ronveaux-dupal, M. F. & Dubois, F. Isolation of rat liver lysosomes by isopycnic centrifugation in a metrizamide gradient. *J. Cell Biol.* **78**, 349–68 (1978).
 140. Codlin, S., Haines, R. L. & Mole, S. E. btn1 affects endocytosis, polarization of sterol-rich membrane domains and polarized growth in *Schizosaccharomyces pombe*. *Traffic* **9**, 936–50 (2008).
 141. Cao, Y. *et al.* Autophagy is disrupted in a knock-in mouse model of juvenile neuronal ceroid lipofuscinosis. *J. Biol. Chem.* **281**, 20483–93 (2006).
 142. Luiro, K. *et al.* Interconnections of CLN3, Hook1 and Rab proteins link Batten disease to defects in the endocytic pathway. *Hum. Mol. Genet.* **13**, 3017–27 (2004).
 143. Wavre-Shapton, S. T. *et al.* Photoreceptor phagosome processing defects and disturbed autophagy in retinal pigment epithelium of Cln3 Δ ex1-6 mice modelling juvenile neuronal ceroid lipofuscinosis (Batten disease). *Hum. Mol. Genet.* **24**, 7060–74 (2015).
 144. Roberts, E. A. & Deretic, V. Autophagic proteolysis of long-lived proteins in nonliver cells. *Methods Mol. Biol.* **445**, 111–7 (2008).
 145. Brandenstein, L., Schweizer, M., Sedlacik, J., Fiehler, J. & Storch, S. Lysosomal dysfunction and impaired autophagy in a novel mouse model deficient for the lysosomal membrane protein Cln7. *Hum. Mol. Genet.* **25**, 777–91 (2016).
 146. Viswanathan, K. *et al.* Nonpeptidic lysosomal modulators derived from z-phe-ala-diazomethylketone for treating protein accumulation diseases. *ACS Med. Chem. Lett.* **3**, 920–4 (2012).
 147. Heinrich, M. *et al.* Ceramide as an activator lipid of cathepsin D. *Adv. Exp. Med. Biol.* **477**, 305–15 (2000).
 148. Peric, A. & Annaert, W. Early etiology of Alzheimer's disease: tipping the balance

- toward autophagy or endosomal dysfunction? *Acta Neuropathol.* **129**, 363–81 (2015).
149. Park, J.-S., Blair, N. F. & Sue, C. M. The role of ATP13A2 in Parkinson's disease: Clinical phenotypes and molecular mechanisms. *Mov. Disord.* **30**, 770–9 (2015).
150. Chapel, A. *et al.* Article. *Mol. Cell. Proteomics* **12**, 1572–1588 (2013).
151. Bröer, S. The SLC38 family of sodium-amino acid co-transporters. *Pflügers Arch. Eur. J. Physiol.* **466**, 155–72 (2014).
152. Wang, S. *et al.* Metabolism. Lysosomal amino acid transporter SLC38A9 signals arginine sufficiency to mTORC1. *Science* **347**, 188–94 (2015).
153. Christensen, H. N. Role of amino acid transport and countertransport in nutrition and metabolism. *Physiol. Rev.* **70**, 43–77 (1990).
154. Reimer, R. J., Chaudhry, F. A., Gray, A. T. & Edwards, R. H. Amino acid transport system A resembles system N in sequence but differs in mechanism. *Proc. Natl. Acad. Sci. U. S. A.* **97**, 7715–20 (2000).
155. Gu, S., Adan-Rice, D., Leach, R. J. & Jiang, J. X. A novel human amino acid transporter, hNAT3: cDNA cloning, chromosomal mapping, genomic structure, expression, and functional characterization. *Genomics* **74**, 262–72 (2001).
156. Desforges, M. *et al.* The SNAT4 isoform of the system A amino acid transporter is functional in human placental microvillous plasma membrane. *J. Physiol.* **587**, 61–72 (2009).
157. Cantor, H. & Shinohara, M. L. Regulation of T-helper-cell lineage development by osteopontin: the inside story. *Nat. Rev. Immunol.* **9**, 137–41 (2009).
158. Back, S. H. & Kaufman, R. J. Endoplasmic reticulum stress and type 2 diabetes. *Annu. Rev. Biochem.* **81**, 767–93 (2012).
159. Krokowski, D. *et al.* Coordinated Regulation of the Neutral Amino Acid Transporter SNAT2 and the Protein Phosphatase Subunit GADD34 Promotes Adaptation to Increased Extracellular Osmolarity. *J. Biol. Chem.* **290**, 17822–37 (2015).
160. Mackenzie, B. & Erickson, J. D. Sodium-coupled neutral amino acid (System N/A) transporters of the SLC38 gene family. *Pflügers Arch. Eur. J. Physiol.* **447**, 784–95 (2004).
161. Gjymishka, A., Palii, S. S., Shan, J. & Kilberg, M. S. Despite increased ATF4 binding at the C/EBP-ATF composite site following activation of the unfolded protein response, system A transporter 2 (SNAT2) transcription activity is repressed in HepG2 cells. *J. Biol. Chem.* **283**, 27736–47 (2008).
162. Chaudhry, F. A. *et al.* Coupled and uncoupled proton movement by amino acid transport system N. *EMBO J.* **20**, 7041–51 (2001).
163. Lewerenz, J. & Maher, P. Chronic Glutamate Toxicity in Neurodegenerative Diseases-

- What is the Evidence? *Front. Neurosci.* **9**, 469 (2015).
164. Bröer, S. & Brookes, N. Transfer of glutamine between astrocytes and neurons. *J. Neurochem.* **77**, 705–19 (2001).
 165. Jung, J., Genau, H. M. & Behrends, C. Amino Acid-Dependent mTORC1 Regulation by the Lysosomal Membrane Protein SLC38A9. *Mol. Cell. Biol.* **35**, 2479–94 (2015).
 166. Hägglund, M. G. A. *et al.* Identification of SLC38A7 (SNAT7) protein as a glutamine transporter expressed in neurons. *J. Biol. Chem.* **286**, 20500–11 (2011).
 167. Jézégou, A. *et al.* Heptahelical protein PQLC2 is a lysosomal cationic amino acid exporter underlying the action of cysteamine in cystinosis therapy. *Proc. Natl. Acad. Sci. U. S. A.* **109**, E3434–43 (2012).
 168. van der Sluijs, P., Zibouche, M. & van Kerkhof, P. Late steps in secretory lysosome exocytosis in cytotoxic lymphocytes. *Front. Immunol.* **4**, 359 (2013).
 169. Yuseff, M.-I. *et al.* Polarized secretion of lysosomes at the B cell synapse couples antigen extraction to processing and presentation. *Immunity* **35**, 361–74 (2011).
 170. Andrews, N. W. Regulated secretion of conventional lysosomes. *Trends Cell Biol.* **10**, 316–21 (2000).
 171. Jaiswal, J. K., Rivera, V. M. & Simon, S. M. Exocytosis of post-Golgi vesicles is regulated by components of the endocytic machinery. *Cell* **137**, 1308–19 (2009).
 172. Novak, E. K., Baumann, H., Ovnicek, M. & Swank, R. T. Expression of egasyn-esterase in mammalian cells. Sequestration in the endoplasmic reticulum and complexation with beta-glucuronidase. *J. Biol. Chem.* **266**, 6377–80 (1991).
 173. Martina, J. A. *et al.* The nutrient-responsive transcription factor TFE3 promotes autophagy, lysosomal biogenesis, and clearance of cellular debris. *Sci. Signal.* **7**, ra9 (2014).
 174. Ran, F. A. *et al.* Genome engineering using the CRISPR-Cas9 system. *Nat. Protoc.* **8**, 2281–308 (2013).
 175. Harms, E., Kern, H. & Schneider, J. A. Human lysosomes can be purified from diploid skin fibroblasts by free-flow electrophoresis. *Proc. Natl. Acad. Sci. U. S. A.* **77**, 6139–43 (1980).
 176. Boroughs, L. K. & DeBerardinis, R. J. Metabolic pathways promoting cancer cell survival and growth. *Nat. Cell Biol.* **17**, 351–9 (2015).
 177. White, E. Exploiting the bad eating habits of Ras-driven cancers. *Genes Dev.* **27**, 2065–71 (2013).
 178. Bhutia, Y. D. & Ganapathy, V. Glutamine transporters in mammalian cells and their functions in physiology and cancer. *Biochim. Biophys. Acta* (2015).
doi:10.1016/j.bbamcr.2015.12.017

179. Folkman, J. & Shing, Y. Angiogenesis. *J. Biol. Chem.* **267**, 10931–4 (1992).
180. Cadoret, A. *et al.* New targets of beta-catenin signaling in the liver are involved in the glutamine metabolism. *Oncogene* **21**, 8293–301 (2002).
181. Strohecker, A. M. *et al.* Autophagy sustains mitochondrial glutamine metabolism and growth of BrafV600E-driven lung tumors. *Cancer Discov.* **3**, 1272–85 (2013).
182. Commisso, C. *et al.* Macropinocytosis of protein is an amino acid supply route in Ras-transformed cells. *Nature* **497**, 633–7 (2013).
183. Lo, E., Soleilhac, E., Martinez, A., Lafanechère, L. & Nadon, R. Intensity quantile estimation and mapping--a novel algorithm for the correction of image non-uniformity bias in HCS data. *Bioinformatics* **28**, 2632–9 (2012).
184. Lieth, E. *et al.* Nitrogen shuttling between neurons and glial cells during glutamate synthesis. *J. Neurochem.* **76**, 1712–23 (2001).
185. Münch, C., O'Brien, J. & Bertolotti, A. Prion-like propagation of mutant superoxide dismutase-1 misfolding in neuronal cells. *Proc. Natl. Acad. Sci. U. S. A.* **108**, 3548–53 (2011).
186. Tang, W. *et al.* Arf6 controls beta-amyloid production by regulating macropinocytosis of the Amyloid Precursor Protein to lysosomes. *Mol. Brain* **8**, 41 (2015).
187. Zeineddine, R. & Yerbury, J. J. The role of macropinocytosis in the propagation of protein aggregation associated with neurodegenerative diseases. *Front. Physiol.* **6**, 277 (2015).
188. McGettrick, A. F. & O'Neill, L. A. J. How metabolism generates signals during innate immunity and inflammation. *J. Biol. Chem.* **288**, 22893–8 (2013).
189. Sica, A. & Mantovani, A. Macrophage plasticity and polarization: in vivo veritas. *J. Clin. Invest.* **122**, 787–95 (2012).
190. Jha, A. K. *et al.* Network integration of parallel metabolic and transcriptional data reveals metabolic modules that regulate macrophage polarization. *Immunity* **42**, 419–30 (2015).
191. Appelqvist, H., Wäster, P., Kågedal, K. & Öllinger, K. The lysosome: from waste bag to potential therapeutic target. *J. Mol. Cell Biol.* **5**, 214–26 (2013).
192. Aits, S. & Jäättelä, M. Lysosomal cell death at a glance. *J. Cell Sci.* **126**, 1905–12 (2013).
193. Kurz, T., Eaton, J. W. & Brunk, U. T. Redox activity within the lysosomal compartment: implications for aging and apoptosis. *Antioxid. Redox Signal.* **13**, 511–23 (2010).
194. Cuervo, A. M., Dice, J. F. & Knecht, E. A population of rat liver lysosomes responsible for the selective uptake and degradation of cytosolic proteins. *J. Biol. Chem.* **272**, 5606–15 (1997).

195. Cotman, S. L. *et al.* Cln3(Deltaex7/8) knock-in mice with the common JNCL mutation exhibit progressive neurologic disease that begins before birth. *Hum. Mol. Genet.* **11**, 2709–21 (2002).
196. Kaech, S. & Banker, G. Culturing hippocampal neurons. *Nat. Protoc.* **1**, 2406–15 (2006).
197. WATTIAUX, R., WIBO, M. & BAUDHUIN, P. Effect of the injection of Triton WR 1339 on the hepatic lysosomes of the rat. *Arch. Int. Physiol. Biochim.* **71**, 140–2 (1963).
198. Puissant, E. *et al.* Subcellular trafficking and activity of Hyal-1 and its processed forms in murine macrophages. *Traffic* **15**, 500–15 (2014).

Synthèse de la thèse

Les lysosomes sont des compartiments présents dans toutes les cellules eucaryotes. Ils sont caractérisés par la présence dans leur lumen d'environ soixante hydrolases acides différentes, capables de dégrader une grande partie des macromolécules biologiques.

L'activité des enzymes lysosomales est fortement dépendante du pH et culmine à pH 5,0 pour la plupart d'entre elles. Or, le lysosome a un pH compris entre 4,5 et 5,0, alors que celui du cytoplasme est plutôt de 7,0. Ceci permet d'éviter que les enzymes lysosomales soient actives en dehors du lysosome, par exemple lors de leur synthèse. Le pH du lysosome est maintenu acide par une pompe à proton ATP-dépendante : l'ATPase vacuolaire lysosomale (voir fig 1).

Les substrats de la dégradation lysosomale parviennent généralement à ce compartiment par deux voies principales. La première, l'endocytose, permet la dégradation de molécules parvenant de l'extérieur de la cellule. Les substrats internalisés dans des endosomes de recyclage transitent à travers les endosomes précoces, puis les endosomes tardifs, jusqu'aux lysosomes. Le lysosome, dans ce cadre, permet ainsi une fonction de nutrition globale de la cellule. Cette voie est particulièrement importante pour la nutrition en certaines molécules, pour lesquelles le lysosome est un passage obligatoire. La vitamine B12, par exemple, parvient à la cellule couplée à une protéine, la transcobalamine, et ne peut donc être internalisée en l'état par des transporteurs plasmiques. Ce système de couplage permet d'éviter la dégradation de la vitamine B12 dans la circulation sanguine, car cette molécule est particulièrement rare et réactive. Une fois parvenue au lysosome, la transcobalamine est dégradée et la vitamine B12 libérée. Cette dernière est renvoyée au cytoplasme par un transporteur encore inconnu, où elle jouera un rôle de cofacteur obligatoire pour deux enzymes clés du métabolisme.

L'autophagie permet d'adresser aux lysosomes des molécules ou des compartiments intracellulaires, permettant ainsi l'évacuation des compartiments ou des protéines abîmés. Il existe trois types d'autophagie, la microautophagie, l'autophagie médiée par des chaperones et la macroautophagie. Cette dernière est la mieux connue. Elle consiste en l'enveloppement d'une partie de cytoplasme, contenant ou non des organites, par du réticulum endoplasmique, qui finit par former une vacuole double autour de la partie de cytoplasme à dégrader. Cette vacuole, l'autophagosome, fusionne ensuite avec des lysosomes pour former un autolysosome. La macroautophagie est essentielle à l'homéostasie de la cellule. Elle est ainsi régulée par le niveau métabolique de la cellule (particulièrement en acides aminés) et est activée lorsque les ressources extérieures sont insuffisantes.

La dégradation lysosomale joue un grand rôle dans l'homéostasie cellulaire car les produits de la dégradation des macromolécules par le lysosome peuvent être recyclés vers le cytoplasme et être réutilisés par les enzymes anaboliques qui y sont présentes afin de synthétiser de nouvelles molécules fonctionnelles. Cette fonction de recyclage est assurée par une batterie de transporteurs actifs secondaires appelés transporteurs lysosomaux. Ces transporteurs sont dépendants du gradient de proton et/ou du gradient de potentiel entre les deux faces de la membrane lysosomale. Certains, comme la cystinosine, le transporteur

lysosomal de cystine, sont directement couplés aux protons et fonctionnent en symport (voir fig 1).

Les substrats de la dégradation lysosomale parviennent généralement à ce compartiment par deux voies principales.

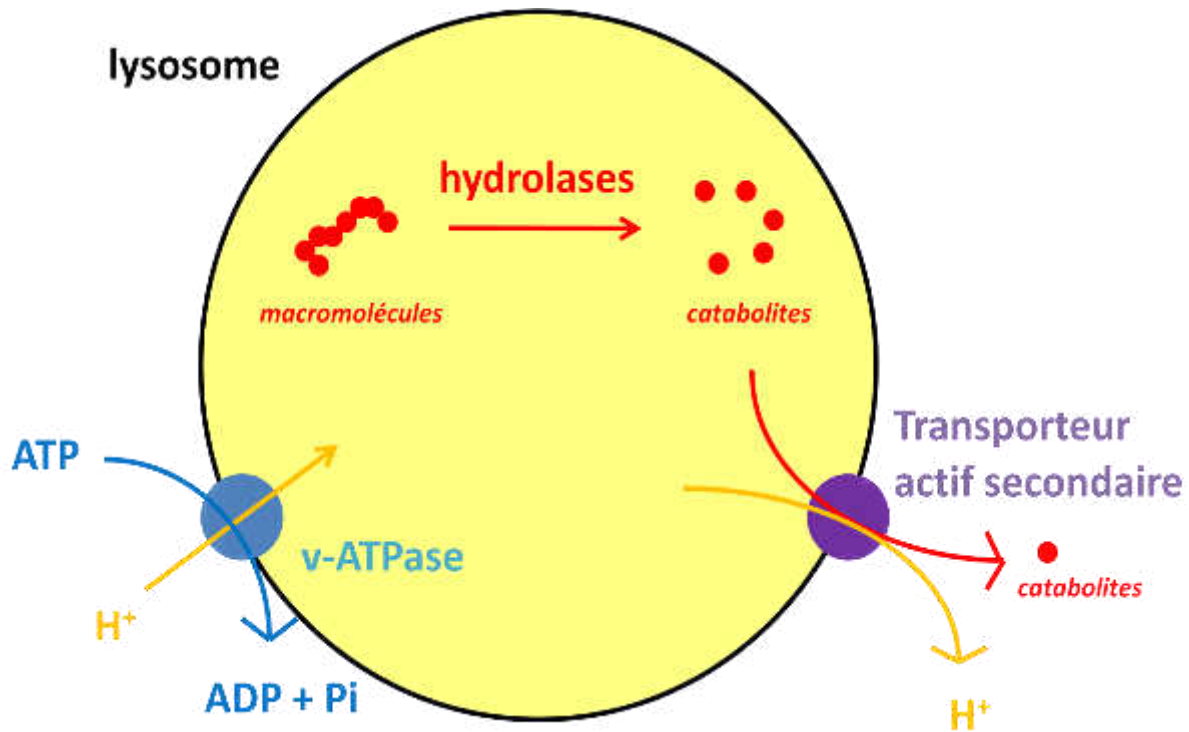


Figure 1 : Schéma du fonctionnement d'un lysosome Les hydrolases dégradent les macromolécules grâce au pH acide, maintenu par la v-ATPase. Le gradient de proton permet de fonctionnement de transporteurs actifs secondaires qui recyclent les produits de dégradation vers le cytoplasme.

Les lysosomes, longtemps considérés seulement comme des compartiments de dégradation, voient leur rôle considérablement élargi depuis quelques années par de nombreux auteurs. Ils sont ainsi impliqués dans de nouvelles voies. Les lysosomes semblent ainsi être impliqués dans le contrôle de la survie cellulaire via le mécanisme de mort cellulaire lysosomale (Lysosomal cell death, LCD). Ce mécanisme consiste en une perméabilisation contrôlée de la membrane lysosomale dépendante de signaux externes. Ce processus libère dans le cytosol diverses enzymes lysosomales, dont des protéases, qui à leur tour activent les caspases contrôlant l'apoptose, déclenchant ainsi un processus spécifique de mort cellulaire.

D'autre part, les lysosomes jouent un rôle de mieux en mieux établi de senseurs de l'état nutritionnel de la cellule et, de ce fait, contrôlent l'équilibre entre catabolisme et anabolisme. L'équilibre entre ces deux processus est principalement contrôlé par un complexe à activité kinase, mTORC1 (mammalian target of rapamycin 1), qui intègre un grand nombre de signaux intra- et extracellulaires. L'activation de mTORC1 favorise l'anabolisme aux dépens du catabolisme. Cette activation a lieu au niveau de la membrane lysosomale, où mTORC1

interagit avec plusieurs complexes, dont le Ragulator et Rheb, une petite GTPase. Or, ces complexes sont régulés par les niveaux d'acides aminés présents dans les lysosomes. Ainsi, lorsque les réserves lysosomales sont maigres, mTORC1 et donc la néosynthèse de macromolécules sont inhibés. On ignorait jusqu'à récemment les mécanismes précis de dialogue entre l'intérieur du lysosome et les complexes membranaires, mais il a été montré en 2015 que les transporteurs lysosomaux précédemment décrits pourraient interagir avec le Ragulator d'une façon dépendante de leur activité et des niveaux d'acides aminés dans le lysosome. SLC38A9, en particulier, a été le premier transporteur lysosomal fermement décrit comme faisant montre de pareille activité.

Ma thèse a été consacrée à la découverte et à la caractérisation de nouveaux transporteurs lysosomaux. En effet, si les enzymes lysosomales sont assez bien décrites dans la littérature, grâce à l'étude des nombreuses pathologies provoquées par leur mutation, les transporteurs restent encore un champ assez mal exploré de la biologie cellulaire en général. Ceci est probablement dû au fait que les méthodes d'études des transporteurs ont été pensées pour des transporteurs présents à la membrane plasmique et pas pour des transporteurs intracellulaires. Il est ainsi probable que différentes pathologies avec un problème de suraccumulation de matériel non dégradés dans les lysosomes mais encore incomprises d'un point de vue génétique soient dues à des dysfonctions de transporteurs lysosomaux inconnus.

Deux sources fournissent des protéines candidates au rôle de transporteurs lysosomaux : l'étude de maladies et la protéomique de la membrane du lysosome.

Dans la première partie de ma thèse, j'ai étudié un candidat, CLN3, dont la mutation provoque une maladie neurodégénérative appelée maladie de Batten ou céroïde lipofuscinose neuronale (CLN). Les CLN sont une famille de maladies rares neurodégénératives génétiques qui se déclenchent à des âges variés, de 0 à 20 ans en fonction du patient. Elles se caractérisent au niveau clinique par une neurodégénérescence comparable à celle provoquée par la maladie d'Alzheimer. Les principales régions affectées sont le cortex cérébral, le thalamus et l'hippocampe. Au niveau cellulaire, les CLN partagent une même caractéristique qui fonde cette appellation : dans les cellules des patients s'accumule en grande quantité au niveau des lysosomes un pigment autofluorescent normalement associé à l'âge, la lipofuscine.

La mutation de 14 gènes peut provoquer une CLN. De façon particulièrement surprenante, ces gènes codent pour des protéines très différentes, à la fois membranaires, sécrétées ou solubles. D'autre part, ces protéines, contrairement à ce que le défaut cellulaire suggère, ne sont pas toutes localisées au niveau du lysosome, bien que certaines d'entre elles soient présentes sur la membrane lysosomale ou soient des enzymes lysosomales. On comprend aujourd'hui mal pourquoi la probable dysfonction de protéines si différentes provoque des maladies très similaires. L'hypothèse la plus couramment acceptées dans le domaine est que ces protéines participent à une voie importante pour l'homéostasie du compartiment lysosomal et particulièrement importante pour la stabilité et la survie des neurones.

CLN3 est l'une des deux protéines CLN localisées dans la membrane lysosomale. Elle n'appartient à aucune famille connue. Sa mutation provoque une CLN juvénile (premiers symptômes vers 5-8 ans). La fonction moléculaire de CLN3 est particulièrement obscure. Une

littérature particulièrement abondante et parfois contradictoire l'a impliquée dans un très grand nombre de processus cellulaires, dont le trafic, la régulation du pH lysosomal ou le transport lysosomal par exemple, sans qu'un consensus se dégage dans la communauté sur ce qu'est la véritable fonction moléculaire de CLN3 et les conséquences tardives de son dysfonctionnement. En particulier, l'hypothèse de CLN3 comme transporteur lysosomal d'arginine, soutenue par des études de l'homologue de levure de CLN3 et une étude de la protéine humaine, semble ne pas refléter la véritable fonction de CLN3.

Afin d'obtenir un aperçu plus large de ce que pourrait être la véritable fonction moléculaire de CLN3, j'ai effectué pendant ma thèse une approche d'étude métabolomique de lysosomes déficients en CLN3. Pour cela, j'ai utilisé un modèle murin répliquant la mutation la plus courante de CLN3 chez les patients, généreusement fourni par le docteur S. Cotman (Harvard Medical School, Etats-Unis). Le Dr. Corinne Sagné et moi-même avons purifié les lysosomes issus du foie de souris CLN3 WT ou CLN3 KI (modèle muté) à l'aide de techniques de centrifugations différentielles puis isopycniques couramment utilisées dans la littérature. Huit préparations indépendantes ont été effectuées et leur qualité a été analysée par des méthodes biochimiques classiques. Les six meilleures ont été analysées par une entreprise américaine à l'aide d'une technique de spectrométrie de masse spécialement ajustée pour l'analyse de petites molécules : la métabolomique, fournissant ainsi une carte comparative du contenu en petites molécules des lysosomes des deux types de souris (WT et KI).

D'autre part, afin d'essayer d'identifier un défaut spécifique des lysosomes, potentiellement révélateur d'un défaut précoce dans la physiopathologie de la maladie, la même analyse a été menée sur des homogénats de foie complets.

Ces expériences ont donnés les résultats suivants :

- 1) Il n'y a de différence majeure de composition entre les foies des souris WT et des souris déficientes en CLN3 (CLN3 KI).
- 2) Les lysosomes des souris CLN3 KI ont significativement moins de produits de protéolyse que les lysosomes de souris WT. Cela était vrai pour environ la moitié (10) des acides aminés analysés et la plupart des dipeptides analysés. Les autres métabolites avaient un niveau comparable dans les deux types de lysosomes (voir fig 2)

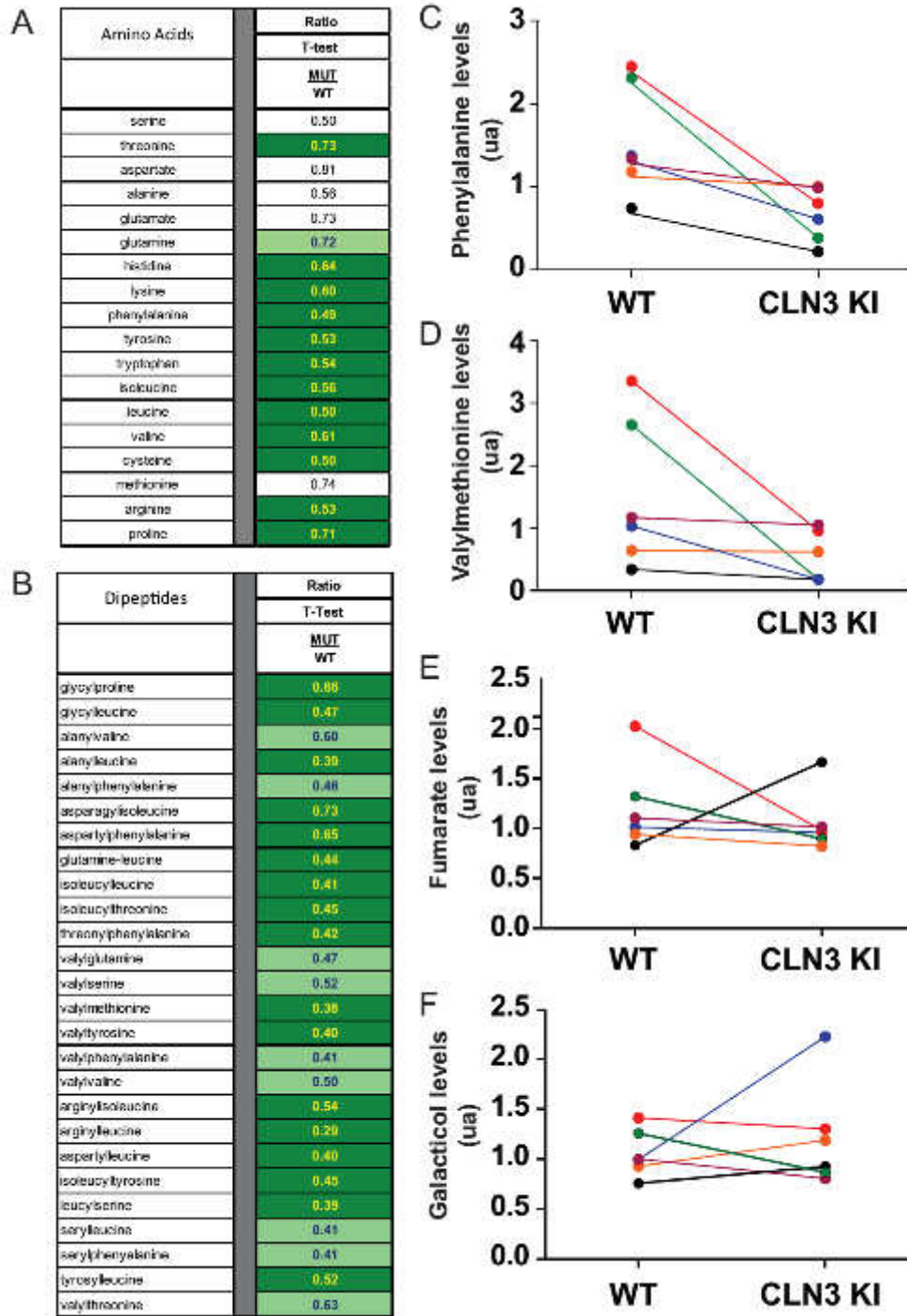


Figure 2 : analyse métabolomique des lysosomes de souris WT et CLN3 KI. Les tableaux donnent les ratios des contenus en acides aminés et dipeptides. Une couleur verte indique une différence significative en t-test. A droite, trois exemples de métabolites. Les préparations de lysosomes simultanées sont reliées par des traits.

Ces différences suggéraient un défaut exclusivement lysosomal, donc a priori assez tôt dans la cascade physiopathologique. Plusieurs hypothèses pouvaient être évoquées pour expliquer ces résultats :

- 1) Un problème d'endocytose, d'autophagie ou de trafic ralentissant l'adressage des substrats au lysosome.
- 2) Un problème d'export des acides aminés et dipeptides.
- 3) Un problème de protéolyse lysosomale.

La première hypothèse a été exclue car aucune différence n'était observée pour les autres espèces chimiques (sucres, lipides, etc). La seconde hypothèse suggérerait un transporteur très peu sélectif, ce qui n'a pas pu être mis en évidence dans la littérature. L'hypothèse étudiée ci-après était donc que CLN3 est nécessaire à la protéolyse lysosomale.

Ceci a été vérifié par trois techniques différentes. Dans la première, des neurones d'hippocampe de souris WT ou KI ont été préparés selon les techniques usuelles décrites dans la littérature. Ils ont ensuite été traités à la DQ-red-BSA. Cette seconde est constituée de BSA couplée à un très grand nombre de fluorophores Bodipy rouges. Ils sont cependant si nombreux qu'ils se quenchent entre eux. La BSA peut être endocytée et dégradée dans le lysosome, libérant alors les fluorophores et révélant la fluorescence. Cette sonde permet donc de mesurer spécifiquement la fluorescence lysosomale.

Dans les neurones, le signal lié au traitement à la DQ-red-BSA était significativement plus faible dans les neurones CLN3 KI, confirmant l'hypothèse d'un problème de protéolyse lysosomale dans ce modèle.

D'autre part, une méthode de mesure plus directe de la protéolyse lysosomale, indépendante du niveau d'endocytose d'une sonde, a été utilisée sur des fibroblastes WT ou CLN3 KI. Les protéines cellulaires ont été marquées avec de la valine tritiée. Ensuite, la radioactivité a été enlevée et le sérum retiré pour activer la macroautophagie. En précipitant les protéines à chaque point de temps, on peut mesurer la perte de radioactivité dans les protéines cellulaires, ce qui constitue une mesure de la protéolyse lysosomale. Cette technique est couramment utilisée dans la littérature.

Lors de temps courts (2-6h), la protéolyse lysosomale était significativement plus faible dans les fibroblastes déficients pour CLN3.

L'hypothèse d'un dysfonctionnement de la protéolyse lysosomale en l'absence de CLN3 a donc été confirmée. Ceci ouvre d'importantes perspectives thérapeutiques. On pourrait ainsi traiter pharmacologiquement la maladie de Batten à l'aide de drogues augmentant la protéolyse lysosomale sans chercher à éclaircir avec précision la fonction moléculaire de CLN3. Etant donné la similarité de la physiopathologie entre les différentes maladies de Batten, on pourrait envisager de toutes les traiter de la même façon, indépendamment du gène muté.

L'autre partie de ma thèse a porté sur une étude protéomique de la membrane lysosomale en collaboration avec Agnès Jourmet et Jérôme Garin, au CEA de Grenoble. L'objectif de cette étude était de découvrir de nouvelles protéines lysosomales pas impliquée dans une pathologie et donc pas encore étudiée, avec l'espoir d'y découvrir de nouveaux transporteurs.

Pour cela, des lysosomes de foie de rats ont été purifiés avec les méthodes usuelles et leurs membranes conservées. Les protéines hydrophobes, donc transmembranaires, cibles de l'étude, ont été extraites à l'aide de détergents et de solvants, puis analysées par HPLC et spectrométrie de masse. Celle-ci a permis d'identifier une liste de 134 protéines membranaires lysosomales, dont plusieurs déjà décrites mais aussi des protéines complètement inconnues.

J'ai participé à la validation de cette étude. J'ai exprimé dix candidats sélectionnés aléatoirement dans la nouvelle carte de la membrane lysosomale en les fusionnant à la GFP, puis j'ai examiné leur localisation subcellulaire. Dans neuf cas sur dix, les protéines étaient adressées au lysosome, ce qui validait la pureté des préparations et la qualité de la carte.

Dans cette étude, j'ai étudié plusieurs nouveaux candidats, dont l'un d'entre eux, GlnTX, s'est révélé le plus intéressant. Les méthodes d'étude classique d'étude des transporteurs lysosomaux se basent généralement sur un artifice d'adressage : si l'on mute la séquence d'adressage des transporteurs lysosomaux, ils sont adressés par défaut la membrane plasmique, ce qui facilite grandement leur adressage. Cette méthode n'a pas fonctionné avec GlnTX, qui est donc probablement adressé au lysosome par un mécanisme non canonique.

Un test indirect d'analyse de nouveaux transporteurs d'acides aminés a donc été développé pour essayer de mieux comprendre sa fonction avant de développer des tests fonctionnels proprement dits. Celui est basé sur la genèse d'une surcharge artificielle d'acides aminés dans les lysosomes en traitant des cellules entières avec des esters d'acides aminés. Cette technique, bien connue des biochimistes, repose sur le fait que les esters sont suffisamment hydrophobes pour traverser les membranes, contrairement aux acides aminés. Les esters diffusent donc jusqu'au lysosome, où ils sont en présence d'estérases, qui régénèrent l'acide aminé originel, alors piégé dans le lysosome. L'hypothèse de base de ce test était qu'on peut, de façon concomitante à ce traitement, forcer la surexpression d'un transporteur lysosomal d'acide aminé. Ce transporteur pourrait dériver une partie de la surcharge induite par les esters vers le cytoplasme, modérant ainsi la surcharge lysosomale. On aurait donc trois cas : une situation de base sans surcharge, un traitement induisant une forte surcharge et une surcharge modérée si on surexprime un transporteur d'acide aminé.

Pour détecter l'activité du transporteur, il suffit donc de détecter la surcharge. Pour cela, TFEB a été utilisé. TFEB est un facteur de transcription récemment décrit qui régule les gènes lysosomaux et d'autophagie. Lors que le compartiment lysosomal est stressé, TFEB est transloqué du cytoplasme au noyau, où il va induire la biogénèse de lysosomes. En situation de surcharge, TFEB est donc envoyé au noyau.

Des cellules HeLas ont donc été transfectées avec un transporteur de lysine, PQLC2, ou GlnTX. Elles ont été traitées avec de la lysine estérifiée, déclenchant une surcharge en lysine,

ou de la glutamine estérifiée, déclenchant une surcharge en glutamine. Comme prévu, les surcharges en acides aminés déclenchaient la translocation de TFEB. Dans les cellules exprimant fortement PQLC2, la surcharge en lysine était beaucoup moins efficace, confirmant l'efficacité du test. Or, les cellules surexprimant GlnTX étaient résistantes à la surcharge en glutamine, ce qui suggérait que GlnTX avait pour fonction d'être un exporteur lysosomal de glutamine.

Conforté par ces résultats, j'ai ensuite mis au point un test de transport direct pour mesurer l'activité de GlnTX. Celui-ci a été effectué sur des lysosomes purifiés à partir de cellules HeLa WT ou déficientes en GlnTX, générées par la méthode CRISPR/Cas9. Les lysosomes purifiés de ces cellules ont été chargés en glutamine à l'aide d'un ester de glutamine. Ensuite, les lysosomes ont été lavés, puis incubés dans de la glutamine tritiée. L'entrée de la glutamine tritiée au cours du temps a été mesurée.

Les lysosomes déficients pour GlnTX incorporent 90% de glutamine de moins que les lysosomes WT, suggérant une fonction de transporteur lysosomal de glutamine. Ceci a été confirmé par plusieurs approches :

- La lyse spécifique des lysosomes fait perdre tout signal, éliminant l'hypothèse qu'un contaminant pourrait accumuler la glutamine radiomarquée.
- La réexpression de GlnTX dans la lignée KO régénère une partie de l'activité d'incorporation de glutamine.
- Le traitement par la nigéricine (abolissant le gradient de proton) ou l'absence d'ATP (idem) inhibent très fortement l'incorporation de glutamine.

La sélectivité de GlnTX a également été étudiée par cette technique : GlnTX est un transporteur exclusif de glutamine et d'asparagine.

La découverte d'un transporteur lysosomal de glutamine a ensuite été intéressante pour l'étude du métabolisme de certaines cellules cancéreuses. En effet, un grand nombre de cellules cancéreuses voient leur métabolisme basculer pour utiliser la glutamine comme base à la place du glucose. La glutamine a l'avantage de pouvoir être utilisée comme source d'azote en plus de comme source d'énergie et de carbone, contrairement au glucose.

Les apports de glutamine libre en provenance du sang sont cependant souvent insuffisants dans les tumeurs à cause d'une angiogenèse mal organisée. Les cellules cancéreuses ont donc développé des stratégies d'adaptation au manque de glutamine, par exemple la surexpression de glutaminase ou de transporteurs plasmiques de glutamine. Dans les cellules activées par K-Ras, la macropinosome est activée. Celle-ci permet d'engloutir de grandes quantités de protéines extracellulaires. Le macropinosome ainsi formé fusionne avec le lysosome, dont les enzymes dégradent les protéines extracellulaires en acides aminés, dont la glutamine. La glutamine ainsi produite est recyclée vers le cytoplasme pour être utilisée par le métabolisme cellulaire (voir fig 3)

Dans ce contexte, le transporteur lysosomal pourrait être essentiel à la nutrition en glutamine. En effet, la sortie du macropinosome est essentielle à l'utilisation de la glutamine par les enzymes cytosoliques. Sans exporteur lysosomal de glutamine, cette dernière pourrait rester bloquée dans le macropinosome. Le rôle de GlnTX dans la nutrition des cellules cancéreuses dépendant des protéines extracellulaires pour leurs apports en glutamine a donc été étudié.

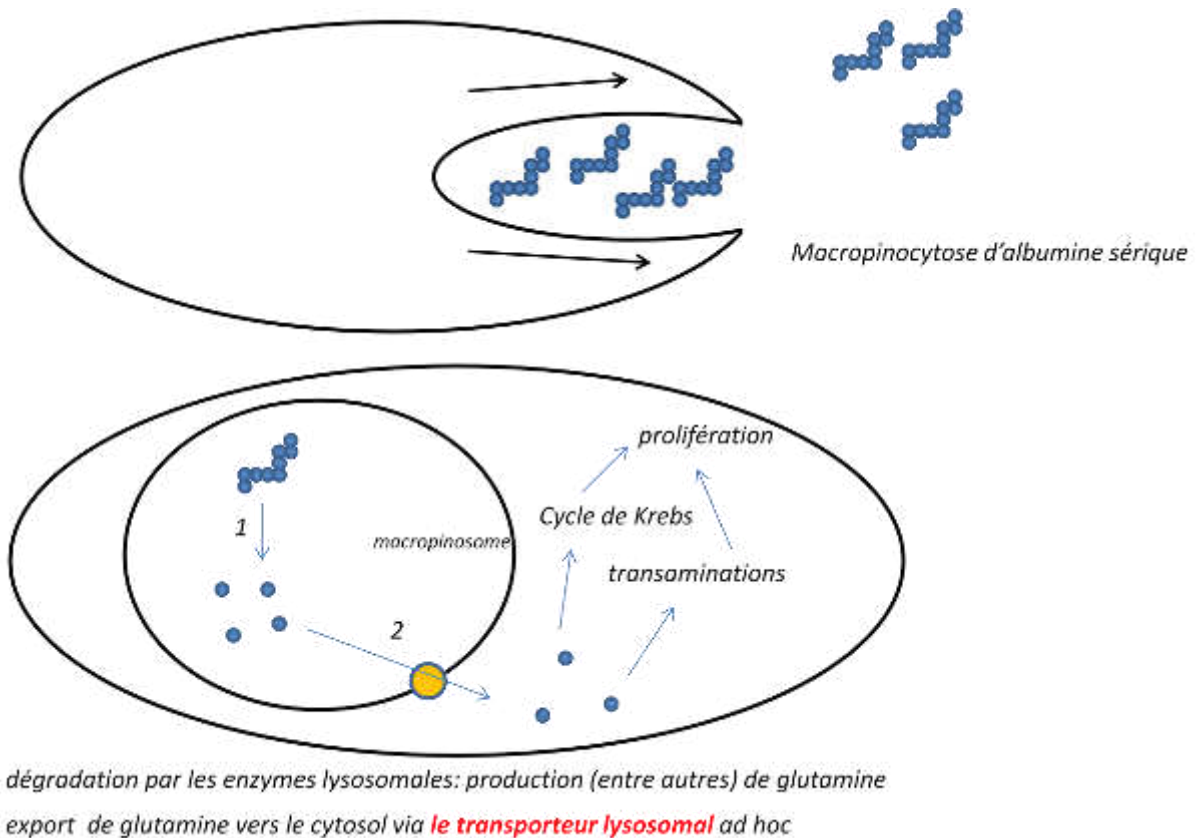


Figure 3 : rôle potentiel du transporteur lysosomal de glutamine dans la prolifération dépendante de la glutamine des cellules cancéreuses.

Pour ce faire, la dépendance à la glutamine de cellules dépendantes à la glutamine obtenue par macropinoctose, les Mia-PaCa2, a été étudiée. Comme attendu et décrit dans la littérature, ces cellules poussent moins quand la glutamine est moins présente dans le milieu. Cependant, lorsque de l'albumine est ajoutée dans le milieu, ce défaut de croissance est partiellement corrigé. C'est cet effet de l'ajout d'albumine qui a été étudié.

L'importance de GlnTX dans cet effet a été étudiée dans les Mia-PaCa2 dans deux modèles : un modèle de réduction de GlnTX par ARN-interférence et un modèle d'inactivation par CRISPR-Cas9. Dans le premier cas, la réduction de l'expression de GlnTX impacte très fortement l'effet correcteur de l'albumine sur la pousse. Dans le second cas, lorsque GlnTX est absent, l'effet de l'albumine sur la pousse disparaît complètement.

Ces résultats suggèrent que GlnTX est le principal transporteur de glutamine lysosomal important pour la nutrition des cellules cancéreuses. Ce projet est donc poursuivi sous deux angles :

- Confirmer l'importance de GlnTX in vivo, sur des modèles murins
- Rechercher des inhibiteurs de GlnTX à l'aide du test basé sur les esters.

Title : Towards the elucidation of orphan lysosomal transporters

Keywords : lysosome, transporter, lysosomal storage disorder, cancer, glutamine

Within lysosomes, about sixty different hydrolases degrade macromolecules. This degradation is dependent on the acidity of the lysosomal lumen, which pH ranges between 4.5 and 5.0. The lysosomal pH is maintained by the v-ATPase, a proton pump. Lysosomal degradation generates catabolites, which can be recycled to cytosol by secondary active transporters: lysosomal transporters.

The dysfunction of lysosomal proteins leads to lysosomal storage disorders (LSDs), rare inherited metabolic diseases characterised by accumulation of material inside lysosomes. Depending on the mutated gene, symptoms of LSDs vary greatly, although about half of LSD patients display some kind of neurodegenerative symptoms. Studying the physiopathology of LSDs has led to a good understanding of the function of lysosomal enzymes, but the knowledge of lysosomal transporters remain poor, since only a few LSDs has been shown to be linked with a mutation in a lysosomal transporter gene.

I focused on two proteins which dysfunction causes a special type of LSDs: CLN3 and CLN7. Mutations in *CLN3* and *CLN7* cause neuronal ceroid lipofuscinoses (NCLs), a special type of LSD which has mostly neurodegenerative symptoms and which is characterized by the accumulation of a specific pigment inside lysosomes: lipofuscin. There are fourteen NCL genes, but CLN3 and CLN7 are the two only proteins of the family which are resident proteins of the lysosomal membrane, suggesting they might be transporters.

Amino acids were screened as possible substrates for CLN7, but none could be shown to be transported. For CLN3, the content in metabolites of lysosomes from *Cln3*-deficient mice and from WT mice were compared by mass spectrometry, revealing a specific decrease in the amount of catabolites of proteins in lysosomes from *Cln3*-deficient mice. This suggested a lack of lysosomal proteolysis, which was checked in neurons, in primary fibroblasts and in immortalized fibroblasts. These results suggested that CLN proteins could take part to a metabolic pathway important for lysosomal proteolysis and, more generally, for neuronal health. These results could help improve the understanding of the early steps of NCL physiopathology.

To extend the number of candidates for lysosomal transporters, I took part to the validation step of an extensive proteomic study of the lysosomal membrane, which revealed forty-six new candidates for lysosomal transporters. I studied in more details TMEM104, SPINSTER, MFSD1, SLC37A2, TTYH3 and GLN1X Proteins were overexpressed in HeLa cells to check for lysosomal localization. Then, their putative sorting motifs were mutated to misroute their expression to plasma membrane and to enable their functional study. No function could elucidate for the first five candidates.

GLN1X could not be misrouted to plasma membrane, but, since it belonged to a family of transporters for glutamine, its function was studied by an indirect assay based on an artificial lysosomal overload in amino acids and a direct transport measure on lysosome-enriched cellular fractions, using radiolabelled substrates. Thus, GLN1X was shown to be a lysosomal transporter selective for glutamine and asparagine.

The function of GLN1X is the nutrition of cancer cells was then studied. Many cancer cells use glutamine as their main source of carbon, nitrogen and energy. Because of insufficient blood supply, they use macropinocytosis to uptake extracellular proteins, which degradation in lysosomes generates glutamine. Then, glutamine is recycled to the cytosol. GLN1X was shown to be critical in this process: in glutamine-dependent cancer cells, when *GLN1X* expression is reduced, cells cannot obtain glutamine from extracellular proteins. Thus, blocking GLN1X is a promising approach to target specifically the metabolism of cancer cells.

Title : Caractérisation fonctionnelle du transportome lysosomal

Keywords : lysosome, transporteur, maladie de stockage lysosomal, cancer, glutamine

Les lysosomes contiennent environ soixante hydrolases différentes, qui peuvent dégrader une grande variété de macromolécules. L'activité de ces enzymes est dépendante du pH, maintenu dans les lysosomes entre 4.5 et 5.0 par une pompe à protons : la v-ATPase. Les produits de dégradation sont recyclés dans le cytoplasme par des transporteurs actifs secondaires de la membrane des lysosomes.

Les maladies de surcharges lysosomales sont causées par des mutations de gènes codant pour des protéines lysosomales, souvent des enzymes. Elles sont caractérisées par un engorgement des lysosomes avec des agrégats ou des cristaux. Les symptômes associés à ces maladies sont variés, mais la moitié d'entre elles induisent des défauts neurologiques. L'étude de ces maladies a permis d'élucider la fonction de nombreuses enzymes, mais la connaissance des transporteurs lysosomaux reste parcellaire. Peu de ces transporteurs sont ainsi caractérisés au niveau moléculaire.

Je me suis intéressé à deux gènes dont la mutation provoque une maladie de surcharge particulière : *CLN3* et *CLN7*. Leur mutation provoque des céroïdes lipofuscinoses neuronales, des maladies de surcharge lysosomales caractérisées par une neurodégénérescence précoce et par l'accumulation dans les lysosomes d'un pigment autofluorescent, la lipofuscine. La mutation de 14 gènes différents cause une céroïde lipofuscinoïde neuronale. J'ai étudié *CLN3* et *CLN7* car ils codaient pour des protéines membranaires du lysosome, qui pourraient donc être des transporteurs.

Sur *CLN7*, j'ai effectué des tests de transport en utilisant les acides aminés comme substrats potentiels, sans résultats probants. Concernant *CLN3*, le contenu métabolique de lysosomes a été étudié par spectrométrie de masse dans des souris WT ou de souris où le gène *CLN3* était déficient. Les lysosomes des cellules déficientes contenaient moins de produits de la protéolyse, ce qui suggérait que *CLN3* était important pour la protéolyse lysosomale. Cela a été confirmé par des mesures plus directes sur des neurones et des fibroblastes primaires, et sur des fibroblastes immortalisés. Ces résultats pourraient aider à comprendre les premières étapes de la physiopathologie dans les cellules où des gènes *CLN* sont déficients.

Pour accroître le nombre de transporteurs lysosomaux potentiels, j'ai participé à la finalisation d'une étude par protéomique de la membrane lysosomale. Elle a révélé 46 transporteurs potentiels de fonction encore inconnue. Dans cette liste, j'ai étudié *TMEM104*, *SPINSTER*, *MFSD1*, *SLC37A2*, *TTYH3* et *SNAT7*. Pour ce faire, j'ai d'abord muté les motifs d'adressage de ces protéines pour les rediriger, lors de leur synthèse, vers la membrane plasmique, afin de faciliter leur étude. Aucune fonction claire n'a pu être identifiée par cette approche.

SNAT7 appartenait cependant à une famille de transporteurs de glutamine, ce qui était suffisamment encourageant pour envisager d'autres approches. Sa fonction a ainsi été étudiée en développant un nouveau test indirect basé sur la détection d'une surcharge artificielle des lysosomes en acides aminés. Un test fonctionnel plus direct a ensuite été mis au point sur des fractions enrichies en lysosomes en utilisant des acides aminés radiomarqués. Ces deux tests ont montré que *SNAT7* était un transporteur spécifique de l'asparagine et de la glutamine.

J'ai enfin étudié l'hypothèse suggérant que *SNAT7* pourrait jouer dans la nutrition de cellules cancéreuses. En effet, certaines utilisent la glutamine comme nutriment principal à la place du glucose ; mais les apports sanguins en glutamine, dans les tumeurs, sont parfois insuffisants. La glutamine est donc obtenue par macropinocytose de protéines extracellulaires et dégradation lysosomale de ces protéines, avant un recyclage vers le cytoplasme. J'ai montré qu'en l'absence de *SNAT7*, ce phénomène était bloqué. *SNAT7* est donc une cible thérapeutique intéressante pour tenter de bloquer l'approvisionnement des cellules cancéreuses en glutamine.